

Universita' degli Studi di Milano-Bicocca  
Doctorate School of Science



Ph.D. in Physics and Astronomy - XXII Cycle  
Coordinator: Prof. Claudio Destri

## Topics in SYM theories

- ★ *AdS/CFT* & Mesonic Spectra
- ★★ Superspace & Scattering Amplitudes

Ph.D. Dissertation of CarloAlberto Ratti  
Matr. 042667

Supervisor: Prof. Silvia Penati

Academic Years 2006–2009



# Contents

<b>1</b>	<b>Introduction</b>	<b>1</b>
<b>I</b>	<b>Flavors and mesons in marginal deformed <math>AdS/CFT</math></b>	<b>11</b>
<b>2</b>	<b><math>AdS/CFT</math> in short</b>	<b>13</b>
2.1	Generalities about $\mathcal{N} = 4$ SYM . . . . .	15
2.2	Generalities about $AdS/CFT$ . . . . .	16
2.3	Geometric construction of flavor symmetry . . . . .	20
<b>3</b>	<b>Mesons in marginally deformed <math>AdS/CFT</math></b>	<b>27</b>
3.1	Generalities on the three-parameter deformation of $AdS_5 \times S^5$ . . . . .	29
3.2	The embedding of D7-branes . . . . .	31
3.3	Probe fluctuations . . . . .	35
3.4	The mesonic spectrum . . . . .	39
3.4.1	The decoupled modes . . . . .	42
3.4.2	The coupled modes . . . . .	43
3.5	Analysis of the spectrum . . . . .	47
3.6	The dual field theory . . . . .	54
3.7	Conclusions . . . . .	59

<b>II</b>	<b>Scattering amplitudes in <math>\mathcal{N} = 4</math> SYM theory</b>	<b>63</b>
<b>4</b>	<b>General introduction to scattering amplitudes</b>	<b>65</b>
4.1	Quantum number analysis . . . . .	66
4.2	Unitarity techniques and recursive relations . . . . .	68
4.2.1	The BDS ansatz . . . . .	73
4.2.2	Dual conformal symmetry . . . . .	75
4.3	Why a direct computation . . . . .	77
<b>5</b>	<b>Superspace approach to scattering amplitudes in SYM theories</b>	<b>79</b>
5.1	The superamplitude . . . . .	81
5.1.1	The twistor formalism in superspace . . . . .	81
5.1.2	Color-ordered superamplitudes . . . . .	83
5.2	The supergraph approach . . . . .	84
5.2.1	Feynman rules in background field method . . . . .	85
5.3	From the effective action... . . . .	87
5.4	...to MHV scattering amplitudes . . . . .	89
<b>6</b>	<b>Two loop effective action in <math>\mathcal{N} = 4</math> SYM theory</b>	<b>93</b>
6.1	$\mathcal{N} = 4$ Lagrangian, vertices and vacuum diagrams . . . . .	94
6.1.1	$\mathcal{N} = 4$ SYM quantum vertices . . . . .	95
6.1.2	Vacuum graphs and combinatorics . . . . .	97
6.2	$\nabla$ -algebra for the two-loop contributions . . . . .	99
6.2.1	Diagrams with cubic vertices . . . . .	101
6.2.2	Diagrams with quartic vertices . . . . .	118
6.3	Cancellation of UV divergences . . . . .	120
6.3.1	Divergent terms revisited . . . . .	121
6.3.2	Double Divergent Graphs . . . . .	122
6.3.3	Single Divergent Graphs . . . . .	126

6.3.4	Tadpole divergent graphs . . . . .	134
<b>7</b>	<b>Towards the four point MHV amplitude</b>	<b>141</b>
7.1	Up to four points . . . . .	143
7.1.1	Two point covariant contributions . . . . .	144
7.1.2	Three point covariant contributions . . . . .	148
7.1.3	Four point covariant contributions . . . . .	151
7.2	The results . . . . .	153
<b>8</b>	<b>Conclusions</b>	<b>161</b>
<b>9</b>	<b>Acknowledgments</b>	<b>165</b>
<b>A</b>	<b>Basic conventions for Superspace</b>	<b>169</b>
<b>B</b>	<b>On-shell <math>\nabla</math>-algebra</b>	<b>171</b>
<b>C</b>	<b>Expansion of the covariant (anti)chiral propagators and their derivatives</b>	<b>173</b>
<b>D</b>	<b>Expansion of the covariant vector propagator and its derivatives</b>	<b>179</b>
<b>E</b>	<b>Color structures</b>	<b>185</b>
E.1	Color conventions . . . . .	185
E.2	Color structure and covariant effective action diagrams . . . . .	186
E.3	Four point color structures . . . . .	187
<b>F</b>	<b>Geometric Symmetries of the covariant supergraphs</b>	<b>191</b>
F.1	Up-Down Symmetry . . . . .	191
F.2	Left-Right Symmetry . . . . .	192
F.3	Consequences of geometric symmetries . . . . .	193

<b>G</b>	<b>Conventions in momentum space</b>	<b>195</b>
G.1	Fourier transform conventions . . . . .	195
G.2	Topologies for the scalar integrals . . . . .	197
<b>H</b>	<b>Scalar, vector and tensor integrals</b>	<b>199</b>
H.1	Symmetries of the scalar integrals . . . . .	199
H.2	Passarino–Veltman reduction . . . . .	201
H.2.1	Vector Integrals . . . . .	202
H.2.2	Tensor Integrals . . . . .	203
<b>I</b>	<b>Building up the pure vector diagram</b>	<b>205</b>
<b>J</b>	<b><i>Pierre</i></b>	<b>209</b>
J.1	PC can make your life easier . . . . .	209
J.2	<i>Pierre</i> 's dictionary . . . . .	210
J.3	Main routines . . . . .	212
J.3.1	Computing the master equation . . . . .	213
J.3.2	Computing the coefficients . . . . .	214
J.3.3	Computing the $n$ -point effective action . . . . .	214

# List of Figures

2.1	The relative displacements of D3 color branes (red) and D7 flavor branes (green) in the internal directions. . . . .	23
3.1	The Zeeman-splitting of the undeformed $8(l + 1)^2$ d.o.f. for $\hat{\gamma}_2 = \hat{\gamma}_3$ and $l$ even (left) or odd (right). . . . .	51
3.2	The Zeeman-splitting of the $\hat{\gamma}_2 = \hat{\gamma}_3 = \hat{\gamma}$ d.o.f. for $\hat{\gamma}_2 \neq \hat{\gamma}_3$ and $l$ even. The value of $\Delta M$ here appearing is pictured considering the case $\hat{\gamma}_3 < \hat{\gamma} < \hat{\gamma}_2$ . . . . .	52
3.3	The Zeeman-splitting of the $\hat{\gamma}_2 = \hat{\gamma}_3$ d.o.f. for $\hat{\gamma}_2 \neq \hat{\gamma}_3$ and $l$ odd. Once again $\hat{\gamma}_3 < \hat{\gamma} < \hat{\gamma}_2$ . . . . .	53
4.1	Massive and massless box, triangle and bubble one loop scalar integrals. . . . .	70
4.2	The addition of an extra internal (dashed) line allow to move from one loop to two loop integrals. . . . .	71
4.3	The rung rule. . . . .	72
4.4	Dual diagram for the one loop box integral . . . . .	75
5.1	Expansion of the $A, B, C$ coefficients up to two external fields. . . . .	87
5.2	Pure chiral two loop contribution to the gauge effective action . . . . .	89
6.1	Cubic vertex vacuum diagrams . . . . .	98
6.2	Tadpole-like vacuum diagrams . . . . .	99
7.1	Four point topologies for the $\mathcal{N} = 4$ SYM theory . . . . .	142
7.2	Tadpoles and triangleboxes can be written as doubleboxes and pentaboxes . . . . .	152
7.3	Examples of contributions to the four point effective action . . . . .	153

E.1	The three different color contraction for the tadpole vacuum diagrams . . .	187
E.2	Similar triangleboxes with different color factors . . . . .	188
E.3	General topology for a trianglebox . . . . .	189
F.1	Simplifications in the four point topologies induced by the UD and the LR symmetries . . . . .	194
G.1	Fourier transform of derivatives on internal and external lines . . . . .	196
G.2	Diagrammatic expression for the conservation of the momenta at the vertices	197
G.3	List of two loop scalar integrals . . . . .	198
J.1	Scheme of <i>Pierre</i> . . . . .	217



# List of Tables

2.1	Relative displacement of color and flavor branes preserving $\mathcal{N} = 2$ supersymmetry . . . . .	22
3.1	Degeneracy of states in the case $\hat{\gamma}_2 = \hat{\gamma}_3$ and $l \geq 2$ even. The degeneracy in the third column refers to every single value of $j$ . . . . .	50
3.2	Degeneracy of states in the case $\hat{\gamma}_2 = \hat{\gamma}_3$ and $l \geq 3$ odd. . . . .	50
3.3	Degeneracy of states in the case $\hat{\gamma}_2 \neq \hat{\gamma}_3$ and $l \geq 2$ even. The degeneracy in the fourth column refers to every single pair $(j, s)$ . . . . .	51
3.4	Degeneracy of states in the case $\hat{\gamma}_2 \neq \hat{\gamma}_3$ and $l \geq 3$ odd. . . . .	52
3.5	$U(1)$ charges of the chiral superfields. The corresponding antichirals have opposite charges. . . . .	56
6.1	Combinatoric for vacuum diagrams . . . . .	98
E.1	Color factors for four point topologies . . . . .	190
H.1	Basic symmetries of the scalar integrals . . . . .	200
J.1	Basic definitions of superspace objects in <i>Pierre's</i> language . . . . .	211
J.2	List of shell scripts for the extraction of a specific amplitude from a master equation. . . . .	216



# Chapter 1

## Introduction

*”At the present time there is no direct experimental evidence that supersymmetry is a fundamental symmetry of nature.” [1].*

At the present time this sentence was written 27 years ago, when I was 6 months old. 27 years later, the same sentence is still current and can be used as starting point for a Ph.D. thesis. This long interval of time could have produced negative feelings about the actual existence of supersymmetry in nature at some impatient researcher. However, it would be stupid to give up on the patient right now: LHC is now running and, likely, if I were simply few years younger, I should have found a different sentence to start my thesis.

Let us suppose for a while that LHC was out of our present technological possibilities. What would be our attitude with respect to supersymmetry? I mean, with respect to a symmetry that unifies objects that at our energy scales are very well distinct: Spacetime symmetries with internal symmetries, fermionic particles with bosons and, when promoted to be a local symmetry, gravity with matter.

A patient and trustful research would still be justified by the incredible variety of applications that supersymmetry has found through the years. Among the main results of supersymmetry, in fact, we can mention the solution of the hierarchy problem of the Standard Model, the proposal of a candidate for Dark Matter and the crucial role played by this symmetry in GUT theories.

These problems are spread over the whole frontier of modern, experimentally supported, theoretical description of nature and extend far beyond the original purposes that led to supersymmetry. Thus we can be reasonably confident that from supersymmetry other implications – at the moment unpredictable – for our future understanding of nature will follow.

Even though they play a crucial role, supersymmetry and symmetries in general are few of the ingredients of physical theories, which are definitely the principal elements of

our investigation of nature. The scientific method states in fact that a physical description of natural phenomena follows from few postulates that define the theories and from mathematically deduced predictions that can be falsified by empirical evidences. Unfortunately, given our present technological level, there are theories that have few chances to be checked by experiments. Nevertheless we can use towards these theories the same attitude that we have for supersymmetry: A theory becomes more and more intriguing as it touches a larger and larger set of problematics and suggests new ideas to solve them. From this point of view, a critical eye cannot be insensible to string theory and to the incredible multiplicity of ideas that this theory has produced in the past and still produces.

It is not the aim of this introduction to go along the historical path that led to the suggestion of string theory as a renormalizable quantum theory of gravity and as the ultimate theory of great unification of the fundamental forces, overcoming many unsatisfactory features of the Standard Model (the huge number of unfixed parameters and the unnatural smallness of some of them) and, at the same time, providing a consistent description of gravity where General Relativity breaks down (at black holes singularities and at the primordial stages of life of our universe). It is sufficient to note that up to now string theory is the only known consistent theory that has the potentials to solve all these problems at once. I would prefer to focus here on another remarkable peculiarity of strings: String theory, in fact, is a natural environment where old ideas can find solid physical basis, new ideas can be carried out and models can be built and applied in the most unexpected fields of high and low energy physics.

The idea of strings as a *solution–inspiring* theory becomes preeminent after the discovery of D–branes but some intuition of these potentialities can be found even before. The concept of extra dimensions is an illustrative example of this fact. Extra dimensional theories were developed before the formalization of string theory but they were confined into the sphere of mathematical speculations. On the contrary, a ten dimensional space-time became a mandatory request for the consistency of the superstring theory. As a consequence inside string theory extra dimensions got a concrete physical foundation. Starting from this renewed basis, extra dimensions has become more and more relevant for the research in high energy physics. In fact, even experiments at LHC have been set to catch possible signs of their presence.

An impressive improvement in the possibilities to build up models in the context of string theory followed from the discovery of D–branes. D–branes are dynamical non–perturbative objects of string theory. Their nature is twofold: 1) They interact with closed strings, so we can look at them as sources of mass and charge; 2) They are hyper–surfaces of various dimensionalities where open strings have their end points. Yang–Mills (YM) theories are localized on their worldvolume.

The properties of D–branes allow new descriptions of different physical systems inside string theory. Bound states of strings and D–branes have been used to build a microscopic description of the thermodynamic of Black Holes (BH). The degeneracy of these bound

states reproduces the Bekenstein area law for the entropy of a BH. The same models also replicate correctly the Hawking radiation rates from BHs and offer a perspective for the solution of the information paradox.

D-branes have been also used to build up cosmological models. These constructions give an explanation to the expansion of our universe and the presence of Dark Energy, responsible for the current acceleration in the expansion rate of the universe. At the same time, they give solutions to the horizon problem and the flatness puzzles alternative to inflation.

These models are tangible proofs of the descriptive potentialities of string theory. The only problem with them is an old issue of the string: The comparison with experiments is always a daunting enterprise, even for D-brane models. In recent years, however, string theory has started to overcome even the frontier of experimental testability: The *AdS/CFT* correspondence is the new idea that allows for covering this step.

The *AdS/CFT* correspondence is a consequence of the open-closed string duality built in the concept of D-branes. It states that YM theories in four dimensions are equivalent to string theories in curved higher dimensional backgrounds. At energies far below the string scale, this translates into a weak-strong duality between gauge theories and gravity theories. Strongly coupled gauge theories are dual to weakly coupled gravity theories and vice versa. Thus, string theory is not only the ultimate ultraviolet completion of YM gauge theories and of gravity at the Plank scale but, through the *AdS/CFT* correspondence, it becomes the theory that replaces Super-YM (SYM) theories, and hopefully QCD, in their non-perturbative regime.

The basic idea of the correspondence is however more general, suggesting that strongly coupled physical systems can be described by higher dimensional gravity models. These models can be directly linked to string and D-brane constructions (top-down approach) or can be stringy-inspired gravity models constructed *ad-hoc* for particular physical systems (bottom-up approach). In both cases, inside strongly coupled systems we can find signs of strings, or of ideas that they produce, at energies accessible by our technology.

Remarkably, we have in fact a couple of experimental checks: 1) Experiments on the Quark Gluon Plasma confirm the existence of a bound on the ratio between shear viscosity and entropy of strongly coupled plasmas which has been derived by general considerations in *AdS/CFT*; 2) Phase transition diagrams of superconductors have been exactly reproduced by gravity models.

These results are not the definitive answer on the validity of string theory but they confirm that it is a very prolific theory of ideas and solutions for many topics at the frontier of modern physics. Thus we can be reasonably confident that from string theory other implications – at the moment unpredictable – for our future understanding of nature will follow.

The same words have been previously referred to supersymmetry: Nowadays LHC can

reach the energy scales at which the existence of supersymmetry can be probed directly. It is likely that we will never be able to have experimental access to the energy regimes at which the stringy nature of the fundamental constituents of nature becomes manifest. However, this is not a limitation to string theory: In the spirit of the *AdS/CFT*, it seems plausible that in the future string theory will turn itself into something more easily accessible by our experimental inspections.

## This thesis

The results presented in this thesis set into the context of the *AdS/CFT* correspondence.

The thesis is divided in two parts: In the first part the *AdS/CFT* correspondence is considered on its gravity side. In a top–down approach some aspects of strongly coupled systems are investigated. In particular, results concerning the mass spectra of mesonic quark–antiquark bound states are presented.

In the second part, powerful methods based on superspace are developed for high precision perturbative computations of scattering amplitudes in SYM theories. The *AdS/CFT* correspondence predicts a lot of properties for these objects at strong coupling. There are evidences that they can be extended also at weak coupling. Our methods allow to perform direct and definitive checks of them.

## Part I: *AdS/CFT* & mesonic spectra

As previously mentioned, *AdS/CFT* opens new perspectives on the study of confined phases of YM theories and primarily of QCD. Recent progresses in this direction concern the inclusion in the correspondence of **flavor symmetry** and of **matter in the fundamental** representation of the gauge group.

The holographic description of flavored YM theories is obtained by considering the low energy limit of a **system of  $N$  D3 and  $N_f$  D7–branes**. In particular, the D3–branes span the usual four dimensional Minkowski spacetime and the D7 branes extend on these directions and wrap a  $S^3$  sphere in the internal ones. The  $SU(N)$  gauge symmetry is realized on the worldvolume of the D3–branes while the presence of D7–branes provides the  $SU(N_f)$  flavor symmetry.

In the stringy picture, the gluons of the theory are represented by open strings stretched between two D3–branes while the quarks by D3–D7 strings. The distance between the D3 and the D7 branes in their mutual orthogonal directions is directly proportional to the mass of the quarks. Open strings with the endpoints on the same D7–brane represent quark–antiquark  $q\bar{q}$  bound states, i.e. the **mesons** of the theory. Thus, it is possible to compute the mesonic mass spectrum by considering fluctuations of the flavor branes around their equilibrium configurations. These fluctuations satisfy a system of

second order differential equations often coupled between themselves.

The first study of mesonic spectra have been done for  $\mathcal{N} = 4$  SYM theory. The spectrum turns out to be discrete and with high degeneracy. After this first example, a lot of work has been done in the direction of studying more QCD-like theories (i.e. non-conformal theories, less supersymmetric theories, ...).

In the first part of the thesis I have extended the analysis to include **marginally  $\beta$ -deformations** of  $\mathcal{N} = 4$  SYM theory. The effect of these deformations is to break partly or completely supersymmetry. Unfortunately, these theories are still conformal symmetric, thus they cannot be used to give a realistic description of the RG flow of a gauge theory towards a confining phase. Nevertheless it is interesting to consider the effects of supersymmetry breaking on the D7-brane configurations and on the mesonic spectrum.

The results found show that the deformed spectrum has the same number of degrees of freedom of the undeformed case. The main effect of the deformation is the resolution of the huge degeneracy of the undeformed mass levels in a way that share a lot of similarities with the resolution of the degeneracy due to the Zeeman effect in the quantum mechanical description of the hydrogen atom.

These results follow from the study of a system of differential equations that is much more involved with respect to the undeformed  $\mathcal{N} = 4$  SYM case. Nevertheless, as in the undeformed case, it has been possible to solve it analytically. Together with the undeformed  $\mathcal{N} = 4$  SYM theory, this is the only case where solutions for the spectrum has been computed exactly, without using numerical computational techniques.

## Part II: Superspace & scattering amplitudes

In the last few years much attention has been payed to scattering amplitudes in gauge theories. There is, of course, an obvious phenomenological interest since the recent activity at the accelerators calls for highly precise theoretical results in YM theories. On the other hand, inside the *AdS/CFT* correspondence new interesting properties have been highlighted for scattering amplitudes in Super-YM theories.

The most intensive activity have been done in the study of the so called **color ordered Maximally Helicity Violating (MHV) amplitudes** i.e. amplitudes with two particles with the same helicity and the others with opposite helicity.

The most interesting results have been found in the context of  $\mathcal{N} = 4$  SYM theory. They are: A) the **BDS ansatz**, a recursive relation for the finite parts of the amplitudes that mimics and extends the recursive behavior of the IR poles. It was postulated that this ansatz would be valid to all loops and for an arbitrary number of gluons, but actually it fails at 2 loops and 6 particles and a correction is required; B) The **MHV amplitudes–Wilson loop duality**, i.e. the observation that the expectation values of Wilson loops

with a particular light-like contour are equivalent to MHV amplitudes. The validity of this equivalence has been demonstrated at strong coupling via *AdS/CFT*. All the perturbative level computations performed so far indicate that the equivalence should be valid also at weak coupling but a general proof is still missing; C) A new symmetry, called **dual superconformal symmetry**, that characterizes  $\mathcal{N} = 4$  scattering amplitudes. Once again this symmetry has been postulated on *AdS/CFT* indications.

The computational techniques employed to get these results, are based on the optical theorem and the reconstruction of the amplitudes from their infrared singularities. Their validity is based on two main assumptions: A) the **cut-constructibility**, i.e. the possibility to reconstruct the full amplitude by looking at its singularities at the cuts; B) the **no-bubble no-triangle hypothesis**, i.e. the absence of bubbles and triangles in any integral entering the final expression of an amplitude. Even if these hypothesis are in agreement with the dual conformal invariance and are supposed valid at any loop order, general proofs have been produced only at one loop and only for  $\mathcal{N} = 4$  SYM theory. Moreover, moving to less supersymmetric theories, these hypothesis are no more applicable and the computations become more and more involved.

From this point of view, an **assumption-free computational technique** at more than one loop is definitively necessary since it would give more insights on the consistency of these assumptions and would check the results and the properties found for the  $\mathcal{N} = 4$  SYM theory. The development of a direct perturbative technique is indeed the subject of the second part of this thesis.

The perturbative computation of a scattering amplitude can be reduced to the computation of the effective action. In fact an amplitude is constructed by composing trees of vertices and propagators given by 1PI Green functions. In particular a scattering amplitude involving  $n$  particles at  $\ell$  loops requires the evaluation of the effective action truncated at  $n$ -points at the same perturbative order.

Our computational strategy concentrates on the derivation of the complete all- $n$  point effective action at a fixed loop order. We provide a *master equation* from which it is in principle possible to derive any scattering amplitude at a given perturbative order. The method is based on a combined use of **background field method** and **superspace technologies** together with an appropriate use of the helicity and color informations of the interacting particles. It is important to stress that we work in  $\mathcal{N} = 1$  superspace, so the general set up we develop is suitable not only for  $\mathcal{N} = 4$  SYM but for **any SYM theory**.

In our method, the computation of the full effective action follows from the identification of a set of vacuum-like Feynman diagrams in superspace. The loop lines of these superdiagrams represent background covariant propagators. These propagators are given as power series in the external fields. Thus the covariant propagators make possible to incorporate inside the vacuum superdiagrams informations about interactions of any number of external fields in an extremely compact form. Each single contribution to the



effective action can be extracted from the vacuum superdiagrams by a suitable expansion of the propagators in the external fields.

The covariant  $D$ -algebra procedure (generally called  $\nabla$ -algebra) can be used to reduce the vacuum superdiagrams to sums of ordinary Feynman diagrams. To this end, we need to expand the covariant propagators in powers of covariant spinorial superspace derivatives, where the **coefficients** of the expansion are functions of the external fields. As such, they can be written as power series in the external fields. However the  $\nabla$ -algebra procedure can be worked out before the replacement of the coefficients with their power series so that the effective action turns out to be expressed in terms of the coefficients rather than their expansions. The advantage is evident: These formulas for the effective action are in fact **independent of the number**  $n$  of interacting particles and, potentially, of their helicity configurations. Thus the  $\nabla$ -algebra procedure and the use of the coefficients provide master equations for the all- $n$  effective action at a fixed loop order.

A generic contribution to the effective action corresponding to a fixed number  $n$  of external fields is then obtained by expanding the coefficients in power series only in a second step. Its form will be given by the product of a loop integral times a tensorial structure represented by a string of  $n$  fermionic and bosonic superfields. This second structure contains the informations about the scattered particles (their number, momentum, color and helicity).

The consistency of our superspace construction is supported by a set of non-trivial relations between the propagator coefficients. These identities follow straightforwardly from the basic algebraic relations satisfied by the covariant superspace derivatives. Their role in the computational process is twofold: They provide a lot of simplifications in the general expressions for the effective action and, at the same time, order by order in  $n$  they constitute highly non-trivial checks for the power series expansions of the coefficients.

The large number of terms involved in the computation of the effective action motivates the **automatization** of the computational procedure. A completely new program system, *Pierre*, has been developed. It is based on various program languages (mainly on FORM, a symbolic calculus language, and on *Mathematica*).

*Pierre* provides a complete automatization of the three key steps of the computational procedure for an  $n$  point scattering amplitude, that is the derivation of the complete effective actions, the power series expansion of the propagator coefficients and the extraction of the fixed  $n$ -point effective action from the full all- $n$  effective action.

*Pierre* is able to deal with both the tensorial and the loop structures of Feynman diagrams in superspace. The tensorial structure is controlled through a small set of basic superspace algebraic relations. The loop integrals are worked out with standard procedures like Passarino-Veltman reduction.

As a first application of our technology, we have computed the all- $n$  MHV effective action at two loop for  $\mathcal{N} = 4$  SYM theory. This expression turns out to be a linear

combination of Feynman diagrams written in terms of the propagator coefficients.

$\mathcal{N} = 4$  SYM theory is expected to be Ultraviolet (UV) finite. By power counting it is possible to distinguish the UV divergent contributions in the formula for the effective action and to separate them from the finite ones. Indeed, a careful analysis shows that all the UV divergent diagrams resum into UV finite ones. A key role in this resummation is played by the relations between the propagator coefficients.

Therefore the main result of the second part of this thesis is the following: We give a general expression for the two loop MHV effective action of  $\mathcal{N} = 4$  SYM theory that is manifestly UV-free and valid for any number of external particles. The cancellation of the UV divergences provides a highly non-trivial check of our results and, more generally, of the computational strategy adopted.

An immediate application of our results is the evaluation of the two loop four point amplitude. From the all- $n$  effective action it is possible to extract the four point MHV effective action and from there the four point MHV scattering amplitude. Partial results show that only 1PI diagrams contribute to this amplitude. The extrapolation of the four point scattering amplitude is work in progress.

In conclusion, it has been a common belief that a direct approach to scattering amplitudes in YM theories based on Feynman diagrams would be impossible, due to the large number of contributions that should be considered as soon as the number of loops and of interacting particles increases. Nevertheless, our computational method shows that non-trivial superspace techniques open the possibility of a direct computation in the context of SYM theories.

This thesis is the result of collaborations with M. Grisaru, S. Penati, M. Pirrone. It is based on the following publications and work in progress

- S. Penati, M. Pirrone and C. Ratti,  
“Mesons in marginally deformed AdS/CFT,”  
JHEP **0804** (2008) 037.
- S. Penati, M. Pirrone and C. A. Ratti,  
“On marginally deformed meson spectroscopy,”  
Fortsch. Phys. **56** (2008) 876.
- M. T. Grisaru, S. Penati and C. Ratti,  
“A superspace approach to scattering amplitudes,”  
in preparation.



# Part I

## Flavors and mesons in marginal deformed $AdS/CFT$



# Chapter 2

## *AdS/CFT* in short

One of the main challenges of elementary particle theoretical physics is the understanding of the low energy regime of confining theories, primarily QCD. Progress in this direction is expected in the context of the *AdS/CFT* correspondence [2] which allows for a dual description of Yang–Mills theories at strong coupling in terms of a perturbative string/supergravity theory.

The arguments that Yang–Mills theories are related to string theories are quite old and motivated at different levels.

The first argument has heuristic features. During the 60s, the nature of strong interactions at energies below the confinement/deconfinement transition phase was investigated with the aim of stringy like models. At that energies strong interactions are responsible for the formation of hadrons, i.e. bounded states of quarks, and can be modeled by color flux tubes extending between the quarks: These flux tubes can be described by strings.

In models like these mesons are described by strings that extend between a quark and an anti–quark and bind them. The mass of the mesons is in correspondence with the eigenvalues of the oscillatory modes of the flux tube strings. The study of the spectra of these oscillations led to a theoretical explanation of the the Regge behavior between the mass  $M$  and the total angular momentum  $J$ ,  $J \sim a + bM^2$ , observed in the mesonic spectra.

However, after the discovery of the asymptotically free nature of the strong interactions at distances below the Fermi scale, QCD came across as a more satisfactory description of the strong dynamics and the string like models were laid aside.

A more general argument in favor of a relation between YM and string theory is due to 't Hooft [3] and is valid for any  $SU(N)$  gauge theory. In the large  $N$  limit, a systematic expansion of physical quantities in powers of  $1/N$  is available. In order to keep finite self–energy diagrams while  $N \rightarrow \infty$ , one is forced to take at the same time the limit  $g \rightarrow 0$

on the gauge coupling constant in such a way that the product  $\lambda = g^2 N$  remains finite. This limit is called 't Hooft limit.

In the 't Hooft limit, it is possible to show that all possible graphs are finite. More remarkably, there exists an unambiguous correspondence between graph topologies in the field theory perturbative series and Riemann surfaces in two dimensions, classified by genus  $g$ . The general expression for the free energy takes this form

$$F = \sum_{g=0}^{\infty} N^{2-2g} f_g(\lambda) \quad (2.0.1)$$

This same perturbative expression is what one gets for the loop expansion of string theory with coupling constant  $g_s \equiv e^{\phi} = 1/N$ . This suggests that a more intimate relation between large  $N$  YM theories and string theory should exist.

The *AdS/CFT* conjecture is nowadays the most sophisticated and complete relation between these theories. It states that a gauge theory at strong coupling is describable as a string theory on a curved background in higher dimensions. Despite its name, explicit examples of the duality were found for non-conformal theories too: This is of primary importance in order to get eventually more insight into the confined phases of YM theories and, in particular, of QCD.

The first explicit example of gravitational dual of a YM field theory was found for the  $SU(N)$   $\mathcal{N} = 4$  SYM theory. It has been conjectured and largely tested that in the large  $N$  limit the strong coupling regime of this theory is described by type *IIB* superstring theory on curved  $AdS_5 \times S^5$  background.

This Chapter is primarily devoted to an introduction both to  $\mathcal{N} = 4$  SYM theory and to its gravitational dual. The goal is to provide the basic characteristics of the theory and to show how the correspondence works in this particularly simple case. The dictionary of the correspondence, valid for all the known examples of gravity duals of YM theories, is built by using the  $\mathcal{N} = 4$  SYM theory as an example. In the last Section we outline in which directions the original formulation of the correspondence should be extended to get more QCD-like models. In particular, we concentrate on the problem of flavor symmetry and of quarks inside *AdS/CFT*.

Beyond a natural theoretical interest in the development of these models, also very recent experimental activity asks for a better understanding of the behavior of physical systems at strong coupling. For example, we remember the results of the RHIC experiment at the Brookhaven National Laboratory, where for the first time a new, strongly coupled, state of matter, the quark-gluon plasma (QGP) was produced. Looking at the near future, the ALICE experiment at LHC, but CMS and ATLAS experiments too, promises to discover even newer aspects of QGP. On the theoretical side, all our present possibilities to give a description to the properties of strongly coupled systems are based on lattice simulations and on *AdS/CFT* correspondence. In this respect, all the efforts devoted to produce more realistic gravitational models are strongly motivated.



## 2.1 Generalities about $\mathcal{N} = 4$ SYM

The  $\mathcal{N} = 4$  SYM theory is the maximally extended global supersymmetric theory in 4 dimensions. This peculiarity made it one of the most studied supersymmetric gauge theories. The large amount of symmetry is the main reason of its many properties.

The physical content of the  $\mathcal{N} = 4$  vector multiplet in four dimensions is given by a spin-1 vector, 4 spin- $\frac{1}{2}$  Majorana spinors and 6 scalars [4, 5]. All these particles are massless and transforming in the adjoint representation of the gauge group  $SU(N)$ . In the  $\mathcal{N} = 4$  SYM theory the interactions are governed by the same coupling constant  $g$ . Thus, the theory presents two parameters: the coupling constant  $g$  and the number of colors  $N$ .

In principle the best description of the theory would have been in terms of  $\mathcal{N} = 4$  superfields since most of the symmetries of the theory would have been respected explicitly. Unfortunately, such a description has never been found. However, it has been discovered that a description in terms of unconstrained  $\mathcal{N} = 1$  superfields is available [6]. In fact, the field content of the  $\mathcal{N} = 4$  multiplet can be organized as an  $\mathcal{N} = 1$  vector superfield  $V$  and 3 chiral  $\mathcal{N} = 1$  superfields  $\Phi^i$ . The action with explicit off-shell  $\mathcal{N} = 1$  supersymmetry is

$$\begin{aligned} \mathcal{S} = & \int d^8z \operatorname{Tr} (e^{-gV} \bar{\Phi}_i e^{gV} \Phi_i) + \frac{1}{2g^2} \int d^6z \operatorname{Tr} W^\alpha W_\alpha \\ & + \frac{ig}{3!} \operatorname{Tr} \int d^6z \epsilon_{ijk} \Phi^i [\Phi^j, \Phi^k] + \frac{ig}{3!} \operatorname{Tr} \int d^6z \bar{z} \epsilon_{ijk} \bar{\Phi}^i [\bar{\Phi}^j, \bar{\Phi}^k] \end{aligned} \quad (2.1.1)$$

Here  $W_\alpha = i\bar{\nabla}^2 (e^{-gV} \nabla_\alpha e^{gV})$  is the gauge field strength,  $\nabla_\alpha$  ( $\bar{\nabla}_{\dot{\alpha}}$ ) is the (anti)chiral covariant superspace derivative,  $\Phi_i$  ( $\bar{\Phi}_i$ ) are covariant (anti)chiral fields

$$\begin{aligned} \nabla_\alpha &= e^{-V} D_\alpha e^V & \bar{\nabla}_{\dot{\alpha}} &= \bar{D}_{\dot{\alpha}} \\ \bar{\nabla}_{\dot{\alpha}} \Phi &= \nabla_\alpha \bar{\Phi} = 0 \end{aligned} \quad (2.1.2)$$

At the classical level the component action is invariant under superconformal transformations and  $SU(4)_R$   $R$ -symmetry transformations. On the other hand, the action (2.1.1) is manifestly invariant under global  $SU(3)_R \times U(1)_R$  transformations. These groups act respectively on the indices  $i, j, k$  of the superfields and on the phases of the superfields. Moreover, the action (2.1.1) is manifestly invariant under one of the four supersymmetry transformations too. The remaining three supersymmetries and the global  $Q_R = SU(4)_R / [SU(3)_R \times U(1)_R]$  symmetries are realized by these transformations

$$\delta\Phi^i = -(W^\alpha \nabla_\alpha \chi^i + c^{ijk} \bar{\nabla}^2 \bar{\chi}_j e^{-V} \bar{\Phi}_k e^V - i\bar{\nabla}^2 [(\nabla^\alpha \zeta) \nabla_\alpha \Phi^i])$$

(2.1.3)

$$\delta\nabla_\alpha = \nabla_\alpha \left[ i(\overline{\chi}_i \Phi^i - \chi_i e^{-V} \overline{\Phi}^i e^V) + (W^\beta \nabla_\beta + W^{\dot{\beta}} \overline{\nabla}_{\dot{\beta}}) \zeta \right]$$

The  $\chi_i$  and  $\zeta$  are chiral supermultiplets: The parameters for translations and central charge transformations, supersymmetry transformations and global  $Q_R$  transformations are encoded, respectively, in the  $\theta$ -independent, linear and quadratic components of these fields. The  $\chi_i$  transform in the fundamental representation of the  $SU(3)_R$  global group, while  $\zeta$  is invariant with respect to these global transformations.

Superconformal symmetry survives even at the quantum level at any order in the perturbation series. In general, it is expected that loop corrections introduce a mass scale that would eventually break conformality. However, explicit calculations [7, 8, 9], demonstrate that the  $\beta$ -function of the theory vanishes up to three loops. These results were extended at any loop order in the perturbation theory by using the light-cone superfield formalism [10, 11] and, alternatively, general power counting arguments [12]. Accordingly to these observations, it is a general statement to affirm that  $\mathcal{N} = 4$  SYM is a truly CFT at any loop order.

## 2.2 Generalities about *AdS/CFT*

The main motivations for the *AdS/CFT* correspondence come from the study of D-branes in string theory.

D $p$ -branes are solitonic objects in string theory. Their tension is inversely proportional to the string coupling constant  $g_s$ : This means that in the perturbative regime ( $g_s \ll 1$ ) they are objects much more massive than the other fundamental string theory objects. Furthermore, D-branes act as charge sources for RR supergravity fields. Both mass and charge contribute to the stress-energy tensor. Thus the presence of D-branes distorts spacetime geometry around them. In particular, very close to the surface of the brane the geometry develops a region of high negative curvature, the *AdS throat*, while away from the brane the geometry is asymptotically flat.

Although they are heavy objects, D-branes are dynamical objects as well. The concept of D-branes arises quite naturally in perturbation string theory as  $p$ -spatial extended hyperplanes on which an open string can have its endpoints [15, 16]. In the presence of only one brane, the massless modes of open strings with the endpoints on it describe  $U(1)$  gauge fields living along the brane as well as the fluctuations of the brane in its transverse directions around its equilibrium positions. In the presence of a stack of  $N$  branes placed one above the other, the low energy dynamics on the branes is described by a  $U(N)$  massless gauge field theory in  $p + 1$  dimensions.

Consider now string theory in presence of D-branes. There exists two kinds of light excitations in the spectrum. In addition to low energy open string excitations, we have to

consider also close string excitations away from the brane. In the low energy limit, in fact, they reproduce the massless supergravity degrees of freedom. The full spectrum includes then massive closed fields from both open and closed strings and fields that describe the interactions between them. However, at low energies all these modes can be integrated out and the effective action reduces to the two decoupled actions describing  $U(N)$  gauge theory on the brane and supergravity in ten dimensional flat space.

The correspondence is defined by matching these two theories with the light excitations of string theory in the throat-like curved background generated by the presence of the branes. In this curved space, for an observer sitting at infinity there are two kinds of low energy excitations: The massless modes of closed strings that live in the asymptotic flat region far from the D-branes and the the full spectrum of closed string modes that lives in the highly curved region close to the branes and that undergo gravitational red-shift. The first excitations are the same supergravity modes in flat ten dimensional spacetime we found in the descriptions of branes as dynamical objects. It is then natural to match the second modes, i.e. stringy closed modes in the throat region close to the D-branes, with the  $U(N)$  gauge theory sitting on the branes.

The reasoning described here above is applicable whatever is the dimensionality  $p$  of the stack of  $Dp$ -branes. However, since we are mainly interested in four dimensional field theories, the most relevant situation is for D3-branes. The field theory described along the worldvolume of a stack of  $N$  coincident D3-branes is, in fact, a  $3 + 1$   $SU(N)$  gauge theory. The stack of branes breaks a half of the supersymmetry present in the bulk, so, the theory is actually the  $\mathcal{N} = 4$  SYM theory.

On the other hand, the solutions to the supergravity equations of motion in presence of a stack of  $N$  D3-branes is [17]

$$\begin{aligned} ds^2 &= H^{-\frac{1}{2}} \eta_{\mu\nu} dx^\mu dx^\nu + H^{\frac{1}{2}} [du^2 + u^2 d\Omega_5] \\ F_5 &= (1 + *) dt dx_1 dx_2 dx_3 dH^{-1} \\ H &= 1 + \frac{R^4}{u^4}, \quad R^4 = 4\pi g_s \alpha'^2 N \end{aligned} \tag{2.2.1}$$

The branes extends in the four  $x^\mu$  directions and  $d\Omega_5$  is the metric of a five dimensional sphere  $S^5$ .  $F_5$  is the self dual field strength sourced by the branes:

$$\int_{S^5} F_5 = N \tag{2.2.2}$$

Branes are located at  $u = 0$ ,  $u \in (0, \infty)$  being a sort of radial coordinate in the transverse space to the branes. For  $u \gg R$ , i.e. far away from the branes, the space becomes asymptotically flat. On the other hand, by setting  $u \ll R$  we become more and more sensitive to the deformations induced by the presence of the D3-branes. In this limit the geometry becomes

$$ds^2 = \frac{u^2}{R^2} \eta_{\mu\nu} dx^\mu dx^\nu + \frac{R^2}{u^2} du^2 + R^2 d\Omega_5 \tag{2.2.3}$$

This metric describes an  $AdS_5 \times S^5$  space with radius  $R$ .

In the light of what was said before, the dual geometric description of the  $\mathcal{N} = 4$  SYM theory is given by type IIB string theory in the  $AdS_5 \times S^5$  curved background. More precisely the  $AdS/CFT$  correspondence states that there is a one to one map between observables in the two theories and a prescription that allows to compare physical quantities on the two sides of the duality.

The matching between observables comes from the observation that fields propagating in  $AdS_5$  act as sources for operators at the boundary of  $AdS$ . Since the boundary is four dimensional Minkowski space, it is natural to associate these operators to operators in the dual field theory and to match fields in  $AdS$  with the operators that they source in Minkowski. This connection is often found using symmetry: Natural couplings as

$$\int d^4x \sqrt{G} (g^{\mu\nu} T_{\mu\nu} + A_\mu J^\mu + \dots) \quad (2.2.4)$$

suggest that the the graviton in  $AdS$  is associated to the stress–energy tensor in CFT’s, gauge fields to currents etc..

Once a map between fields  $\phi(x^\mu, x)$  in  $AdS$  and operators  $\mathcal{O}(x^\mu)$  in CFT’s has been established, the prescription that matches observables on the two sides of the correspondence follows from this relation that connects the partition functions of the two theories

$$\langle e^{\int d^4x \phi_0(x^\mu) \mathcal{O}(x^\mu)} \rangle_{CFT} = \mathcal{Z}_{string} \left[ \phi(x^\mu, x)|_{x=0} = \phi_0(x^\mu) \right] \quad (2.2.5)$$

In particular, this equivalence occurs between the generating function of the correlation functions relative to the operator  $\mathcal{O}$  in conformal field theory (computed by taking functional derivatives with respect to  $\phi_0(x^\mu)$  and by setting  $\phi_0 = 0$ ) and the string theory partition function with boundary conditions for the field  $\phi$  fixed to be  $\phi_0$  at the boundary of  $AdS$ .

The predictonal limits of prescription (2.2.5) are built in the limits of the geometric construction (2.2.1): The metric (2.2.1) is derived in the supergravity approximation of string theory, i.e. by taking  $\alpha' \rightarrow 0$ . Thus, the near–horizon metric (2.2.3) suffers for the same limitations. In particular, that solution is valid as far as the string physical dimensions are smaller than the other length scales. In the solution (2.2.3), the only scale is given by  $R$ : Thus the gravitational dual description is valid when

$$1 \ll \frac{R^4}{\alpha'^2} \sim g_s N \sim g^2 N \quad (2.2.6)$$

In the last passages we have used the definition of  $R$  (2.2.1) and the relation between the string  $g_s$  and the Yang–Mills  $g$  couplings:  $g_s = g^2$ .

Equation (2.2.6) states that the gravity description of the  $\mathcal{N} = 4$  SYM theory is available at large ’t Hooft coupling, when the usual perturbative field theory description fails.

On the other hand perturbation theory is available when the theory is weakly coupled, i.e. when the supergravity solution (2.2.1) becomes unreliable. The two descriptions are not in competition but complete each other giving a different representation of the same physical theory at different coupling regimes.

This fundamental aspect of the correspondence is at the same time a problematic point for finding explicit proofs of it. In general, in fact, physical quantities usually depend on the coupling regime. So, quantities that can be computed in a coupling regime (for example in the perturbative regime for the field theory) cannot be computed in the other regime (i.e. at strong coupling) and vice versa. However, there are properties of a CFT (in our specific case of the  $\mathcal{N} = 4$  SYM theory) such as the global symmetries of the theory, the spectrum of chiral operators, the moduli space, etc. that are independent of the coupling constant and can be used to prove the validity of the correspondence. A comprehensive list of these properties and a discussion on their behavior in the two different regimes is given in [18]. For the purposes of this thesis it is sufficient to consider how the global symmetries of a YM theory are realized at strong coupling. For the moment we concentrate only on the  $\mathcal{N} = 4$  SYM case.

We have seen in Section 2.1 that the global symmetry groups of  $\mathcal{N} = 4$  theory are the  $SU(4)_R$  R-symmetry and the  $SO(2, 4)$  conformal symmetry. These are exactly the isometries of the  $S^5$  and  $AdS_5$  parts that form the dual geometric background of this theory.

The consequences of this observation are of primary importance. First of all, we have already discussed that the presence of the  $AdS$  geometry and of its flat boundary is crucial for the definition of the prescription (2.2.5) relating CFT's operators and string fields in the bulk. Since any four dimensional CFT has a  $SO(2, 4)$  conformal symmetry group, its dual must be in the form  $AdS_5 \times H_5$ , with  $H_5$  a generic five-dimensional compact manifold. Since  $H_5$  is compact, the string theory is effectively five dimensional. More generally, gravity duals of CFT's in  $d$  dimensions must be written in the form  $AdS_{d+1} \times H_{9-d}$ . Prescription (2.2.5) continues to be valid for all these extensions of the correspondence.

On the other hand, deforming the geometry on the gravity side would correspond to deform in some way the corresponding field theory. Deformations eventually break isometries of the original background and this corresponds on the field theory side to get less symmetric theories. The converse is true as well: Field theories with less symmetries have gravity duals with fewer isometries.

By considering the  $AdS_5 \times S^5$  geometry dual to the ( $\mathcal{N} = 4$ ) SYM theory, deformations that affect the  $S^5$  sphere would break part or completely the R-symmetry group and, with it, the supersymmetry of the theory. In the next Chapter one example of this kind of deformations, i.e. the Lunin-Maldacena background [19, 20], is discussed in details. Other examples of theories with reduced supersymmetry with known gravitational duals come out by replacing the  $S^5$  with other compact Sasaki-Einstein spaces such as the conifold

[21], the  $Y^{p,q}$  spaces [22, 23] and the  $L^{p,q,r}$  spaces [24, 25]. However, as far as the  $AdS_5$  factor stays untouched, the dual field theory is always a four dimensional CFT.

Breaking conformality means deforming the  $AdS_5$  factor. Examples of gravity duals of non-conformal theories have been found by considering different systems of branes [26, 27, 28] or by looking at  $\mathcal{N} = 4$  SYM theory at finite temperature [29]. In the first cases, the dual field theory has  $\mathcal{N} = 1$  supersymmetry while in the last example the temperature breaks all the supersymmetries explicitly.

These examples of non-conformal backgrounds are quite important: Even if the gravity dual of QCD is not yet known, however these models, sharing the same IR behavior of QCD can be used as toy models in order to give at least a qualitative description of real strongly coupled systems. Of course, the more the theory shares similarities with QCD, the more that our models become interesting.

From these point of view, a crucial step towards a more realistic model for QCD concerns the generalization of the AdS/CFT correspondence to include matter in the fundamental representation of the gauge group [30, 31]. Quarks in QCD are objects that transform in the fundamental representation of the gauge group and, at the same time, in the anti-fundamental representation of a global flavor symmetry group. Non-perturbative phenomena involving quarks in the real world are the formation of hadrons, the spontaneous chiral symmetry breaking, the scattering and the decay of pions, just mentioning the mains.

Quarks in QCD are strongly connected to the concept of flavor symmetry. In the gravity picture, a new symmetry is realized by the addition of a new stack of branes along which the symmetry gets realized. The degrees of freedom representing the quarks are given by the open strings that are stretched between this new set of branes and the branes that produces the original unflavored background.

The problem of constructing more QCD-like theories and to include quarks in them have been extensively studied in the literature (see [32] for a review) and led to discover gravitational duals for a rich variety of theories. The main results found allow to affirm that, beyond being a beautiful theoretical construction,  $AdS/CFT$  has much to say about real physical systems.

## 2.3 Geometric construction of flavor symmetry

The gravity description of a 4D supersymmetric Yang–Mills theory with fundamental matter can be obtained by considering a system of intersecting D3–D7 branes. Precisely, the near horizon geometry of a system of  $N$  D3–branes in the presence of  $N_f$  spacetime-filling D7–branes, in the large  $N$  limit and  $N_f$  fixed, gives the dual description of a  $\mathcal{N} = 4$   $SU(N)$  SYM theory living on the D3–branes with supersymmetry broken to  $\mathcal{N} = 2$  by

$N_f$  hypermultiplets in the fundamental representation of  $SU(N)$ . The field content of the hypermultiplets, i.e. quarks and squarks, is given by excitations of fundamental strings stretching between D3 and D7-branes. This analysis has been firstly accomplished in [30].

In  $\mathcal{N} = 1$  superspace language the  $\mathcal{N} = 2$  hypermultiplets are described by  $N_f$  chiral superfields  $Q^r$  transforming in the  $(N, \bar{N}_f)$  of  $SU(N) \times SU(N_f)$  plus  $N_f$  chirals  $\tilde{Q}_r$  transforming in the  $(\bar{N}, N_f)$ .

The lagrangian describing the theory is [30]

$$\begin{aligned} \mathcal{L} = & \int d^4\theta \left[ \text{Tr} \left( e^{-gV} \bar{\Phi}_i e^{gV} \Phi^i \right) + \text{tr} \left( \bar{Q} e^{gV} Q + \tilde{Q} e^{-gV} \bar{\tilde{Q}} \right) \right] + \frac{1}{2g^2} \int d^2\theta \text{Tr} (W^\alpha W_\alpha) \\ & + i \int d^2\theta \left[ g \text{Tr} (\Phi^1 [\Phi^2, \Phi^3]) + g \text{tr} (\tilde{Q} \Phi^1 Q) + m \text{tr} (\tilde{Q} Q) \right] + h.c. \end{aligned} \quad (2.3.1)$$

where the trace  $\text{Tr}$  is over color indices and  $\text{tr}$  is over the flavor ones. This action is  $\mathcal{N} = 2$  supersymmetric with  $(W_\alpha, \Phi_1)$  realizing a  $\mathcal{N} = 2$  vector multiplet and  $(\Phi_2, \Phi_3)$  an adjoint matter hypermultiplet. Note that by fixing  $Q^r = \tilde{Q}_r = 0$  we recover the  $\mathcal{N} = 4$  lagrangian (2.1.1). The coupling of  $\Phi_1$  with massive matter fields leads to a non-trivial vev  $\langle \Phi_1 \rangle = -m/g$ .

The theory has a  $SU(2)_\Phi \times SU(2)_R$  global invariance corresponding to a symmetry that exchanges  $(\Phi_2, \Phi_3)$  and to the  $\mathcal{N} = 2$  R-symmetry, respectively. In addition, for  $m = 0$ , there is a  $U(1)$  R-symmetry under which  $(Q^r, \tilde{Q}_r)$  and  $(\Phi_2, \Phi_3)$  are neutral, whereas  $\Phi_1$  has charge 2 and  $W_\alpha$  has charge 1 [65, 47]. Finally, the theory also possesses a  $U(1)$  baryonic symmetry under which only  $(Q^r, \tilde{Q}_r)$  are charged  $(1, -1)$ . This is a residual of the original  $U(N_f) = SU(N_f) \times U(1)$  invariance.

For  $m = 0$  and in the large  $N$  limit with  $N_f$  fixed the theory is superconformal invariant. In fact, the  $\beta$ -function for the 't Hooft coupling  $\lambda = g^2 N$  is proportional to  $\lambda^2 N_f/N$  and vanishes for  $N_f/N \rightarrow 0$ . On the other hand, for mass  $m \neq 0$  conformal symmetry is explicitly broken.

All these features are reproduced at strong coupling by a system of  $N$  color D3-branes and  $N_f$  flavor D7-branes.

We have already observed that the presence of extra stacks of branes introduces in the model extra symmetry groups localized on the worldvolume of the new branes. In principle, these symmetries are local symmetries. However, their coupling is given by  $\lambda_f = g_s N_f$  in the same way as the 't Hooft coupling for the D3-branes is  $\lambda = g_s N$ . So, by taking

$$N \gg N_f \quad (2.3.2)$$

we find in the 't Hooft limit that  $\lambda_f \rightarrow 0$  and the  $SU(N_f)$  symmetry turns to be a global symmetry. The limit (2.3.2) is called *quenching approximation* and it plays a crucial role in the construction of the geometric background.

In general, new sets of branes are new sources of charge and mass and this would backreact on the background generated by the  $N$  color branes. However, in the quenching approximation the backreaction of flavor branes on the background becomes negligible and flavor branes can be considered as probes in the geometry sourced by the color branes. On the field theory side, this corresponds to considering quarks as external fields that do not run in loops, neglecting in this way the quantum effects produced by fundamental fields.

The dynamics of probe branes is described by the DBI action. When  $N_f = 1$  we can use the abelian form for the DBI action

$$\begin{aligned} \mathcal{S}_{Dp} = & -\frac{\mu_p}{g} \int d^{p+1}\xi \left\{ e^{-\Phi} \sqrt{-\det [P (G - B)_{ab} + 2\pi\alpha' F_{ab}]} \right\} + \\ & + \mu_p \int P \left( \sum C_n e^{-B_2} \right) e^{2\pi\alpha' F_2} \end{aligned} \quad (2.3.3)$$

To be useful, the expression (2.3.3) requires to specify the dimensionality  $p$  of the flavor probe brane and how it is displaced inside the background geometry, i.e. the relative displacement of flavor and color branes.

There are various arguments that can be used to understand why  $p = 7$  is the correct choice for the flavor branes in backgrounds generated by D3-branes. In supersymmetric theories, the strongest motivations come from the study of systems of intersecting branes [33]. In that contest it is found that systems of  $Dp$  color branes and  $D(p+4)$ ,  $D(p+2)$  and  $Dp$  flavor branes are 1/4 BPS objects and so preserve  $\mathcal{N} = 2$  supersymmetry. Since they are BPS systems, they are stable configurations of branes. For  $p = 3$  this reduces the choice of flavor branes to D7, D5 and D3-branes. In Tab. 2.1 it is reported the disposition of flavor branes with respect to D3 color branes as it is required by supersymmetry.

	$x_0$	$x_1$	$x_2$	$x_3$	$X_1$	$X_2$	$X_3$	$X_4$	$X_5$	$X_6$
D3	<b>X</b>	<b>X</b>	<b>X</b>	<b>X</b>						
D7	<b>X</b>	<b>X</b>	<b>X</b>	<b>X</b>	<b>X</b>	<b>X</b>	<b>X</b>	<b>X</b>		
D5	<b>X</b>	<b>X</b>	<b>X</b>		<b>X</b>	<b>X</b>	<b>X</b>			
D3	<b>X</b>	<b>X</b>			<b>X</b>	<b>X</b>				

Table 2.1: Relative displacement of color and flavor branes preserving  $\mathcal{N} = 2$  supersymmetry

D7-branes are the only flavor branes that cover all the four dimensional Minkowski space  $\mathbb{M}_4$  spanned by the worldvolume directions  $x^\mu$  of the color D3-branes. The other sets of branes extent along subspaces of  $\mathbb{M}_4$  and the corresponding dual flavored theories are constrained to live on a lower dimensional spacetime. These theories, called defects theories [34], are more exotic and do not have an immediate phenomenological relevance.



So,  $\mathcal{N} = 2$  supersymmetry and the request to describe a four dimensional flavored field theory select the D7-branes as the correct candidate for flavor branes.

Let's go back to consider the flavored  $\mathcal{N} = 4$  SYM theory: The embedding of a probe D7 flavor brane displaced as prescribed in Tab. 2.1 inside the  $AdS_5 \times S^5$  background is

$$\begin{aligned}
 ds^2 &= \frac{L^2 + \rho^2}{R^2} \eta_{\mu\nu} dx^\mu dx^\nu + \frac{R^2}{L^2 + \rho^2} (d\rho^2 + \rho^2 d\Omega_3^2) \\
 u^2 &= L^2 + \rho^2 \quad L^2 = X_5^2 + X_6^2
 \end{aligned} \tag{2.3.4}$$

The parameter  $L$  determines the separation of the D3 and D7-branes along the mutual orthogonal directions  $(X_5, X_6)$  (see Fig. 2.1). When  $L = 0$  the branes overlaps and the

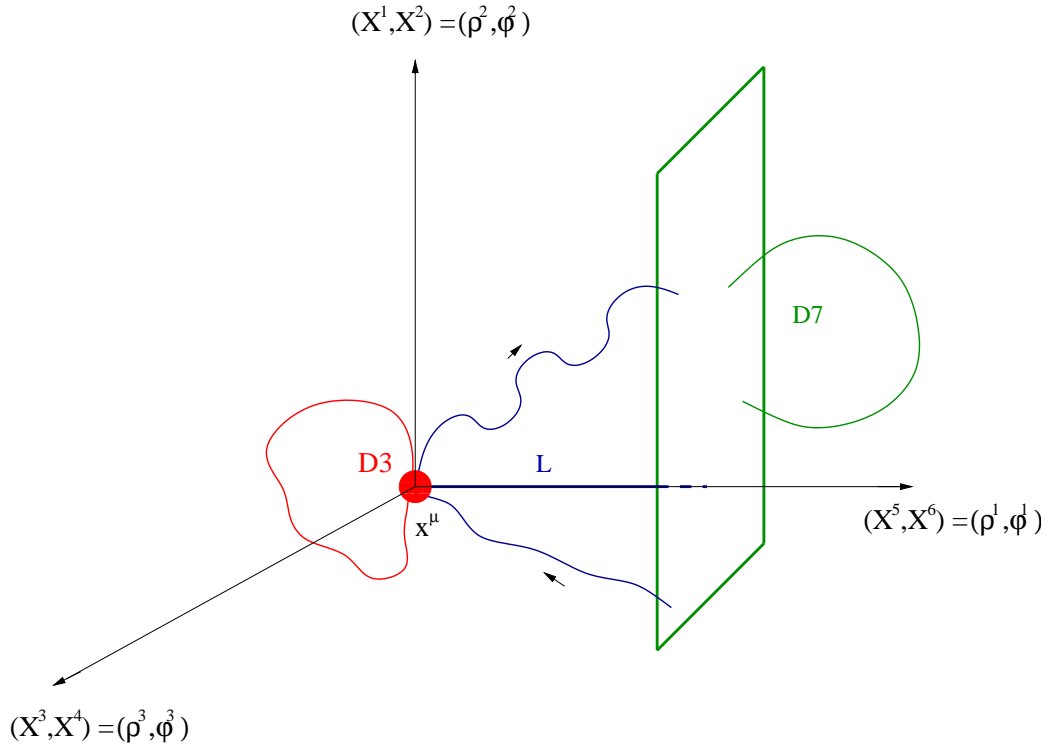


Figure 2.1: The relative displacements of D3 color branes (red) and D7 flavor branes (green) in the internal directions.

induced D7 metric (2.3.4) reduces to  $AdS_5 \times S^3$ . The isometries of the original  $AdS_5 \times S^5$

space filled with such flavor branes are

$$SO(2,4) \times SO(4) \times SO(2) = SO(2,4) \times SU(2) \times SU(2) \times U(1) \quad (2.3.5)$$

These symmetry groups come from the isometries of  $AdS_5$ ,  $S^3$  and rotations in the  $(X_5, X_6)$  plane respectively. They match exactly the symmetries of the lagrangian (2.3.1) when  $m = 0$ . On the other hand, when  $L \neq 0$  the isometry group gets reduced to just  $SO(4)$ : Both the isometries of  $AdS_5$  and of the plane  $(X_5, X_6)$  are broken explicitly by the presence of the flavor branes. Since in the lagrangian the presence of a non-zero mass induces exactly the same consequences, we are definitely led to identify the geometric parameter  $L$  in the gravity picture to the mass parameter  $m$  in the field theory picture. By dimensional reasons, the proportionality relation is  $m \propto L/R^2$ .

Intuitively the role of the parameter  $L$  can be understood in this way: Consider an oriented open string stretched between the color and the flavor branes. The corresponding operators transform, according with the orientation, in the fundamental or anti-fundamental of the color group and in the anti-fundamental or fundamental of the flavor group. Basically, the D3–D7 strings are the holographic description of quarks in field theory. When  $L \neq 0$  their minimum length is  $L$  and their tension is non-zero. So, the spectrum of their modes is massive, with mass proportional to  $L$ . This corresponds to massive quark states in field theory. On the other hand, when  $L = 0$  the minimum length string is tensionless and massless degrees of freedom can be found in the spectrum. These correspond to the massless quark states in field theory with  $m = 0$ .

As proposed in [31] (see also [35]), excitations of fundamental strings with both ends on the D7-branes represent bound quark–antiquark states with equal masses of the corresponding SYM field theory, i.e. mesonic  $q\bar{q}$  states. Thus, studying the fluctuations of the D7 probe branes allows for determining the mass spectrum of the mesonic excitations.

The spectrum can be computed by reducing the D7–worldvolume on  $S^3$ . For example, the scalar states are given by looking for regular and normalizable solutions of the equation of motion of the form

$$X_5 + iX_6 = L + \epsilon f(\rho) e^{ikx} \mathcal{Y}_l(S^3) \quad (2.3.6)$$

In this expansion,  $\mathcal{Y}_l(S^3)$  are the scalar spherical harmonics of  $S^3$  and the mass  $M^2 = -k^2$  is interpreted as the mass of the mesons. The equations of motion follow by expanding the DBI action (2.3.3) for the D7 brane at the second order  $\epsilon^2$  in the fluctuation. The problem in the  $AdS_5 \times S^5$  case is particularly simple and exactly solvable. The ansatz (2.3.6) reduces the equation of motion to an ODE for the function  $f(\rho)$

$$\partial_\rho^2 f(\rho) + \frac{3}{\rho} \partial_\rho f(\rho) + \left( \frac{\bar{M}^2}{(\rho^2 + L^2)} - \frac{l(l+2)}{\rho^2} \right) f(\rho) = 0 \quad (2.3.7)$$

where  $\bar{M}^2 = R^4 M^2 / L^2$ . A regular and normalizable solution to this equation is given in terms of hypergeometric functions

$$f(\rho) = \frac{\rho^l}{(\rho^2 + L^2)^{n+l+1}} F(-n-l+1, -n, l+2; -\rho^2/L^2) \quad (2.3.8)$$

In this expression, the principal quantum number  $n$  is related to the mass  $M$  of the mesons by

$$M^2 = \frac{4L^2}{R^4}(n+l+1)(n+l+2) \quad (n, l \in \mathbb{N}) \quad (2.3.9)$$

Thus, the spectrum turns out to be discrete, dependent on the  $S^3$  angular quantum number and with a mass gap [36]. Moreover, the mass of the mesons is directly proportional to the distance  $L$  between flavor and color branes, i.e. to the mass of its constituents. An unpleasant feature of the result is that at large  $l$  the mass is proportional to the angular momentum  $M \sim J$  and this violates the Regge behavior  $M \sim \sqrt{J}$ .

What we have shown here is just a sketch of what actually one has to do to compute the complete mesonic spectrum. The full description is postponed to the following Chapter, where we consider the embedding of a D7-brane in the Lunin–Maldacena–Frolov marginally deformed  $AdS_5 \times \tilde{S}^5$  background. Since this background is a continuous three parameter deformation of the undeformed  $AdS_5 \times S^5$  scenario, we can read the undeformed solutions in the deformed ones by turning off the deformation. We postpone to there any further comment.



# Chapter 3

## Mesons in marginally deformed *AdS/CFT*

Since the original proposal of inserting D7-branes in the standard  $\text{AdS}_5 \times \text{S}^5$  geometry, a lot of work has been done in the direction of finding generalizations to less supersymmetric and/or non-conformal backgrounds [37]–[51].

Among the formulations of the AdS/CFT correspondence with less supersymmetry, the one-parameter Lunin–Maldacena (LM) background [19] corresponding to  $\mathcal{N} = 1$   $\beta$ -deformed SYM theories plays an interesting role, being the field theory and the dual string geometry explicitly known. The gravitational background is  $\text{AdS}_5 \times \tilde{\text{S}}^5$  where  $\tilde{\text{S}}^5$  is the  $\beta$ -deformed five sphere obtained by performing a *TsT transformation* (consisting in a T-duality, a shift in the angles, and a second T-duality) on a 2-torus inside the  $\text{S}^5$  of the original background. This operation breaks the  $SO(6)$  symmetry group of the five sphere down to  $U(1) \times U(1) \times U(1)$ .

On the field theory side, this deformation corresponds to promoting the ordinary products among the fields in the  $\mathcal{N} = 4$  action to a  $*$ -product

$$\Phi_i \Phi_j \longrightarrow \Phi_i * \Phi_j = e^{i\pi\gamma(Q_i^a Q_j^b - Q_j^a Q_i^b)} \Phi_i \Phi_j \quad (3.0.1)$$

which depends on the charges  $Q^a, Q^b$  of the fields under  $U(1)_a \times U(1)_b$  global symmetry and allowing for the chiral coupling constant to be different from the gauge coupling. Consistently with what happens on the string side, these operations break  $\mathcal{N} = 4$  to  $\mathcal{N} = 1$  supersymmetry, as the third independent global  $U(1)$  inside the global  $SO(6)$  symmetry group corresponds to the R-symmetry. Further generalizations [20] lead to a dual correspondence between a non-supersymmetric Yang–Mills theory and a deformed LM background depending on three different real parameters  $\gamma_1, \gamma_2$  and  $\gamma_3$  <sup>\*</sup>.

A nice feature of these theories is that they are a continuous deformation of the  $\mathcal{N} = 4$

---

<sup>\*</sup>We use the standard convention to name *real* deformation parameters with  $\gamma$ .

SYM theory: This theory can always be recovered by switching off the deformation, i.e. by setting  $\gamma_i = 0$ .

All these models are (super)conformal invariant since the string geometry still has an AdS factor. As such they cannot be used to give a realistic description of the RG flow of a gauge theory towards a confining phase. However, it is interesting to investigate what happens if we insert D7-branes in these deformed backgrounds <sup>†</sup>. In particular, we expect to find a parametric dependence of the mesonic spectrum on  $\gamma_i$ 's which could then be used to fine-tune the results.

In what follows we accomplish this project by studying the effects of inserting D7-branes in the more general non-supersymmetric LM-Frolov background. In the probe approximation ( $N_f \ll N$ ), we first study the stability of the D3-D7 configuration. We find that, independently of the value of the deformation parameters, an embedding can be found which is stable, BPS and in the  $\gamma_1 = \gamma_2 = \gamma_3$  case it is also supersymmetric.

We then study fluctuations of a D7-brane around the static embedding which correspond to scalar and vector mesons of the dual field theory. We consider the equations of motion for the tower of Kaluza-Klein modes arising from the compactification of the D7-brane on a deformed three-sphere. The background deformation induces a non-trivial coupling between scalar and vector modes. However, with a suitable field redefinition, we manage to simplify the equations and solve them analytically, so determining the mass spectrum exactly.

The effects of the deformation on the mesonic mass spectrum and on the corresponding KK modes are the following: i) As in the undeformed case the mass spectrum is discrete and with a mass gap, but it acquires a non-trivial dependence on the deformation parameters. Precisely, it depends on the parameters  $\gamma_2, \gamma_3$  which are associated to  $TsT$  transformations along the tori with a direction orthogonal to the probe branes, whereas the parameter  $\gamma_1$  associated to the deformation along the torus inside the D7 worldvolume never enters the equations of motion for quadratic fluctuations and does not affect the mass spectrum. ii) Since the deformation breaks  $SO(4)$  (the isomorphisms of the three-sphere) to  $U(1) \times U(1)$  a Zeeman-like effect occurs and the masses exhibit a non-trivial dependence on the  $(m_2, m_3)$  quantum numbers associated to the two  $U(1)$ 's. The dependence is through the linear combination  $(\gamma_2 m_3 - \gamma_3 m_2)^2$  so that the mass eigenvalues are smoothly related to the ones of the undeformed case by sending  $\gamma_i \rightarrow 0$ . iii) The corresponding eigenstates are classified according to their  $SO(4)$  and  $U(1) \times U(1)$  quantum numbers. Expanding in vector and scalar harmonics on the three-sphere, we find Type I elementary fluctuations <sup>‡</sup> in the  $(\frac{l\mp 1}{2}, \frac{l\pm 1}{2})_{(m_2, m_3)}$  representations and Type II, Type III and scalar modes in the  $(\frac{l}{2}, \frac{l}{2})_{(m_2, m_3)}$ . For a given  $l$  the total number of degrees of freedom is  $8(l+1)^2$  as in the undeformed theory but, given the degeneracy breaking,

---

<sup>†</sup>Several works in the literature are devoted to the study of D-branes in this context [52, 53, 54, 55, 56, 57, 58].

<sup>‡</sup>We use the classification of [36].

they split among different eigenvalues. For any given triplet  $(l, m_2, m_3)$  we compute the degeneracy of the corresponding mass eigenvalue. We find that the splitting is different according to the choice  $\gamma_2 \neq \gamma_3$  or  $\gamma_2 = \gamma_3$  (which includes the  $\mathcal{N} = 1$  supersymmetric deformation). In the last case the spectrum exhibits a mass degeneracy between scalars and vectors which is remnant of the  $\mathcal{N} = 2$  supersymmetric, undeformed case.

The Chapter is organized as follows. In Section 3.1 we review the three-parameter deformation of the  $\text{AdS}_5 \times \text{S}^5$  by using a set of coordinates suitable for the introduction of D7-branes. In Section 3.2 we study the static embedding of a D7-brane and discuss its stability. In the  $\gamma_1 = \gamma_2 = \gamma_3$  case, we argue that our configuration is supersymmetric. We then find the equations of motion for the bosonic fluctuations of a D7-brane in Section 3.3 and solve them analytically in Section 3.4 determining the exact mass spectrum. In Section 3.5 we discuss the properties of the spectrum and analyze in detail the splitting of the mass levels and the corresponding degeneracy. Finally, in Section 3.6 we formulate the field theory dual to our configuration, whereas our conclusions, comments and perspectives are collected in Section 3.7.

The results exposed in this Chapter are based on the papers [125] and [126].

### 3.1 Generalities on the three-parameter deformation of $\text{AdS}_5 \times \text{S}^5$

Following [19, 20] we consider a type IIB supergravity background obtained as a three-parameter deformation of  $\text{AdS}_5 \times \text{S}^5$ . It is realized by three  $TsT$  transformations along three tori inside  $\text{S}^5$  and driven by three different real parameters  $\gamma_i$ . The corresponding metric is usually written in terms of radial/toroidal coordinates  $(\rho_i, \phi_i)$ ,  $i = 1, 2, 3$ ,  $\sum_i \rho_i^2 = 1$  on the deformed sphere, and in string frame it reads (we set  $\alpha' = 1$ )

$$ds^2 = \frac{u^2}{R^2} \eta_{\mu\nu} dx^\mu dx^\nu + \frac{R^2}{u^2} du^2 + R^2 \left[ \sum_i (d\rho_i^2 + G\rho_i^2 d\phi_i^2) + G\rho_1^2 \rho_2^2 \rho_3^2 \left( \sum_i \hat{\gamma}_i d\phi_i \right)^2 \right]$$

$$G^{-1} = 1 + \hat{\gamma}_3^2 \rho_1^2 \rho_2^2 + \hat{\gamma}_2^2 \rho_3^2 \rho_1^2 + \hat{\gamma}_1^2 \rho_2^2 \rho_3^2 \quad \hat{\gamma}_i \equiv R^2 \gamma_i \quad (3.1.1)$$

where  $R$  is the  $\text{AdS}_5$  and  $\text{S}^5$  radius. A further change of coordinates may be useful (we use the notation  $c_\xi \equiv \cos \xi$ ,  $s_\xi \equiv \sin \xi$  for any angle  $\xi$ )

$$\rho_1 = c_\alpha \quad , \quad \rho_2 = s_\alpha c_\theta \quad , \quad \rho_3 = s_\alpha s_\theta \quad (3.1.2)$$

leading to the description of this background in terms of Minkowski coordinates  $x^\mu$  plus the  $\text{AdS}_5$  coordinate  $u$  and five angular coordinates  $(\alpha, \theta, \phi_1, \phi_2, \phi_3)$ . The deformations correspond to  $TsT$  transformations along the three tori  $(\phi_1, \phi_2)$ ,  $(\phi_1, \phi_3)$ ,  $(\phi_2, \phi_3)$  and are parametrized by constants  $\hat{\gamma}_3$ ,  $\hat{\gamma}_2$  and  $\hat{\gamma}_1$  respectively.

This background is non-supersymmetric and it is dual to a non-supersymmetric but marginal deformation of  $\mathcal{N} = 4$  SYM (the deformation has to be exactly marginal since the AdS factor is not affected by  $TsT$ 's). The  $\mathcal{N} = 1$  supersymmetric background of [19] can be recovered by setting  $\hat{\gamma}_1 = \hat{\gamma}_2 = \hat{\gamma}_3$ .

With the aim of embedding D7-branes in this background we find more convenient to express the metric in terms of a slightly different set of coordinates. We describe the six dimensional internal space in terms of  $X^m \equiv \{\rho, \theta, \phi_2, \phi_3, X_5, X_6\}$  which are mapped into the previous set of coordinates by the change of variables

$$\rho = u s_\alpha \quad , \quad X_5 = u c_\alpha c_{\phi_1} \quad , \quad X_6 = u c_\alpha s_{\phi_1} \quad (3.1.3)$$

In string frame and still setting  $\alpha' = 1$ , we then have

$$ds^2 = \frac{u^2}{R^2} \eta_{\mu\nu} dx^\mu dx^\nu + \frac{R^2}{u^2} G_{mn} dX^m dX^n \quad (3.1.4)$$

where the non-vanishing components of the metric  $G_{mn}$  are

$$\begin{aligned} G_{\rho\rho} &= 1 & G_{\theta\theta} &= \rho^2 \\ G_{\phi_2\phi_2} &= G (1 + \hat{\gamma}_2^2 \rho_1^2 \rho_3^2) \rho_2^2 u^2 & G_{\phi_3\phi_3} &= G (1 + \hat{\gamma}_3^2 \rho_1^2 \rho_2^2) \rho_3^2 u^2 \\ & & G_{\phi_2\phi_3} &= G \hat{\gamma}_2 \hat{\gamma}_3 \rho_1^2 \rho_2^2 \rho_3^2 u^2 \\ G_{\phi_2 X_5} &= -G \hat{\gamma}_1 \hat{\gamma}_2 \rho_2^2 \rho_3^2 X_6 & G_{\phi_2 X_6} &= G \hat{\gamma}_1 \hat{\gamma}_2 \rho_2^2 \rho_3^2 X_5 \\ G_{\phi_3 X_5} &= -G \hat{\gamma}_1 \hat{\gamma}_3 \rho_2^2 \rho_3^2 X_6 & G_{\phi_3 X_6} &= G \hat{\gamma}_1 \hat{\gamma}_3 \rho_2^2 \rho_3^2 X_5 \\ G_{X_5 X_5} &= 1 - \frac{X_6^2}{u^2 \rho_1^2} [1 - G (1 + \hat{\gamma}_1^2 \rho_2^2 \rho_3^2)] & G_{X_6 X_6} &= 1 - \frac{X_5^2}{u^2 \rho_1^2} [1 - G (1 + \hat{\gamma}_1^2 \rho_2^2 \rho_3^2)] \\ & & G_{X_5 X_6} &= \frac{X_5 X_6}{u^2 \rho_1^2} [1 - G (1 + \hat{\gamma}_1^2 \rho_2^2 \rho_3^2)] \end{aligned} \quad (3.1.5)$$

where  $G$  is given in (3.1.1) and now

$$\rho_1^2 = \frac{X_5^2 + X_6^2}{u^2} \quad , \quad \rho_2^2 = \frac{\rho^2 c_\theta^2}{u^2} \quad , \quad \rho_3^2 = \frac{\rho^2 s_\theta^2}{u^2} \quad (3.1.6)$$

The constraint  $\sum_{i=1}^3 \rho_i^2 = 1$  is traded with the condition  $u^2 = \rho^2 + X_5^2 + X_6^2$ .

The LM-Frolov supergravity solution is characterized by a non-constant dilaton

$$e^{2\phi} = e^{2\phi_0} G \quad (3.1.7)$$

where  $\phi_0$  is the constant dilaton of the undeformed background related to the AdS radius by  $R^4 = 4\pi e^{\phi_0} N \equiv \lambda$ . For real deformation parameters  $\hat{\gamma}_i$  the axion field  $C_0$  is a constant and can be set to zero.



This background carries also a non-vanishing NS-NS two-form and R-R forms as well. In our set of coordinates they read

$$\begin{aligned}
B &= \frac{R^2 G}{u^2} \left( (X_5 dX_6 - X_6 dX_5) \wedge (\hat{\gamma}_3 \rho_2^2 d\phi_2 - \hat{\gamma}_2 \rho_3^2 d\phi_3) + \hat{\gamma}_1 \rho_2^2 \rho_3^2 u^2 d\phi_2 \wedge d\phi_3 \right) \\
C_2 &= 4R^2 e^{-\phi_0} \omega_1 \wedge \left( \hat{\gamma}_1 \frac{X_5 dX_6 - X_6 dX_5}{u^2 \rho_1^2} + \hat{\gamma}_2 d\phi_2 + \hat{\gamma}_3 d\phi_3 \right), \quad \omega_1 = \frac{\rho^4}{4u^4} c_\theta s_\theta d\theta \\
C_4 &= 4R^4 e^{-\phi_0} \left( \frac{u^4}{4R^8} dt \wedge dx_1 \wedge dx_2 \wedge dx_3 - G \omega_1 \wedge \frac{X_5 dX_6 - X_6 dX_5}{u^2 \rho_1^2} \wedge d\phi_2 \wedge d\phi_3 \right)
\end{aligned} \tag{3.1.8}$$

The corresponding field strengths are given by the general prescription  $\tilde{F}_q = dC_{q-1} - dB \wedge C_{q-3}$ .

The missing forms of higher degrees can be found by applying the ten-dimensional Hodge duality operator

$$\tilde{F}_7 = -\star \tilde{F}_3, \quad \tilde{F}_9 = \star \tilde{F}_1 \tag{3.1.9}$$

From the first identity and using the equation of motion for  $C_2$

$$d(\star \tilde{F}_3) = dC_4 \wedge dB, \tag{3.1.10}$$

it is easy to see that  $d(C_6 - B \wedge C_4) = 0$ , i.e.  $C_6 - B \wedge C_4 = dX$  for an arbitrary 5-form  $X$ . We make the gauge choice

$$C_6 = C_4 \wedge B \tag{3.1.11}$$

Finally, from the second identity in (3.1.9), by using (3.1.11) and taking into account that  $B \wedge B = 0$  and  $C_0 = 0$  we find  $\tilde{F}_9 = dC_8 = 0$ . Therefore, in what follows we set  $C_8 = 0$ .

The deformed background written in terms of the original internal coordinates  $(\rho, \alpha, \theta, \phi_1, \phi_2, \phi_3)$  has a manifest invariance under constant shifts of the toroidal coordinates  $(\phi_1, \phi_2, \phi_3)$  which correspond to three  $U(1)$  symmetries. With our choice of coordinates the invariance under  $\phi_{2,3} \rightarrow \phi_{2,3} + \text{const.}$  is still manifest, whereas the third  $U(1)$  associated to shifts of  $\phi_1$  is realized as a rotation in the  $(X_5, X_6)$  plane.

## 3.2 The embedding of D7-branes

We now study the embedding of  $N_f \ll N$  D7-branes in the deformed background described in the previous Section. For simplicity we consider the case of a single spacetime filling D7-brane ( $N_f = 1$ ) which extends in the internal directions  $(\rho, \theta, \phi_2, \phi_3)$  (we work in the static gauge where the worldvolume coordinates  $\sigma^a$  of the brane are identified with the appropriate ten dimensional coordinates). The  $X_5, X_6$  coordinates parametrize the mutual orthogonal directions of the intersecting system of  $N$  sources D3-branes and one flavor D7-brane.

The dynamics of bosonic degrees of freedom of the D7-brane is described by the action

$$S = S_{DBI} + S_{WZ} \quad (3.2.1)$$

where  $S_{DBI}$  is the abelian Dirac–Born–Infeld term (in what follows latin labels  $a, b, \dots$  stand for worldvolume components)

$$S_{DBI} = -T_7 \int_{\Sigma_8} d^8 \sigma e^{-\phi} \sqrt{-\det(g_{ab} + \mathcal{F}_{ab})} \quad (3.2.2)$$

whereas  $S_{WZ}$  is the Wess–Zumino term describing the coupling of the brane to the R-R potentials

$$S_{WZ} = T_7 \int_{\Sigma_8} \left\{ \frac{(2\pi\alpha')^3}{6} P[C_2] \wedge F \wedge F \wedge F + \frac{(2\pi\alpha')^2}{2} P[C_4 - C_2 \wedge B] \wedge F \wedge F \right\} \quad (3.2.3)$$

Here  $g_{ab} \equiv G_{MN} \partial_a X^M \partial_b X^N$  is the pull-back of the ten-dimensional spacetime metric (3.1.4, 3.1.5) on the worldvolume  $\Sigma_8$  and  $T_7$  is the D7-brane tension. The  $U(1)$  worldvolume gauge field strength  $F_{ab}$  enters the action through the modified field strength  $\mathcal{F}_{ab} = 2\pi\alpha' F_{ab} - b_{ab}$ , where  $b_{ab}$  is the pull-back of the target NS-NS two-form potential in (3.1.8),  $b_{ab} = B_{MN} \partial_a X^M \partial_b X^N$ . Moreover, in (3.2.3)  $P[\dots]$  denotes the pull-back of the R-R forms on  $\Sigma_8$ .

We look for ground state configurations of the D7-brane. These are static solutions of the equations of motion for  $X_5, X_6$  and  $\varepsilon F$  ( $\varepsilon \equiv 2\pi\alpha'$ ) derived from (3.2.1).

In the ordinary  $\text{AdS}_5 \times S^5$  background static embeddings (see for example [44]) can be found by setting  $X_6 = 0$ ,  $F = 0$  and  $X_5 = X_5(\rho)$  satisfying

$$\frac{d}{d\rho} \left( \frac{\rho^3}{\sqrt{1 + (\partial_\rho X_5)^2}} \frac{dX_5}{d\rho} \right) = 0 \quad (3.2.4)$$

with asymptotic behavior  $X_5(\rho) = L + \frac{c}{\rho^2}$  for  $\rho \gg 1$ . The mass solution  $X_5 = L$  is the only well-behaved solution and corresponds to fixing the location of the D7-brane in the 56-plane at  $X_5^2 + X_6^2 = L^2$ . This is a BPS configuration since the energy density turns out to be independent of  $L$  [59, 43].

In the deformed background we consider an embedding of the form

$$X^M = (x_\mu, \rho, \theta, \phi_2, \phi_3, X_5(\rho), X_6(\rho)) \quad , \quad F = F(X^M) \quad (3.2.5)$$

where, as in the ordinary case, we allow for a non-trivial dependence of the orthogonal directions on the non-compact internal coordinate  $\rho$ . Solving the equations of motion for  $X_5, X_6$  and  $F$  in the present case requires a bit of care since the non-vanishing NS-NS 2-form in (3.1.8) can act as a source for the field strength  $\varepsilon F$ .

We expand the action (3.2.1) up to second order in  $\varepsilon F$ . The WZ action is simply

$$S_{WZ} = \frac{T_7}{2} \int_{\Sigma_8} P[C_4 - C_2 \wedge B] \wedge \varepsilon F \wedge \varepsilon F \quad (3.2.6)$$

whereas the expansion of  $S_{DBI}$  gives

$$\begin{aligned} \mathcal{L}_{DBI} &= -T_7 \frac{\sqrt{-\det(g - b + \varepsilon F)}}{\sqrt{G}} \\ &= -T_7 \frac{\sqrt{-\det(g - b)}}{\sqrt{G}} \sqrt{\det(1 + Y)} \\ &= -T_7 \rho^3 s_\theta c_\theta \sqrt{\Omega_2} \left\{ 1 + \frac{1}{2} \text{Tr}(Y) - \frac{1}{4} \text{Tr}(Y^2) + \frac{1}{8} [\text{Tr}(Y)]^2 + \dots \right\} \end{aligned} \quad (3.2.7)$$

where we have defined

$$\begin{aligned} Y &\equiv (g - b)^{-1} \varepsilon F \\ \Omega_2 &\equiv 1 + (\partial_\rho X_5)^2 + (\partial_\rho X_6)^2 \end{aligned} \quad (3.2.8)$$

and set  $e^{\phi_0} \equiv 1$ .

The source for  $\varepsilon F$  comes from the term

$$\frac{1}{2} \text{Tr}(Y) = \frac{\varepsilon}{R^2 \Omega_2} [(X_5 \partial_\rho X_6 - X_6 \partial_\rho X_5)(\hat{\gamma}_2 F_{\rho\phi_3} - \hat{\gamma}_3 F_{\rho\phi_2}) - \hat{\gamma}_1 \Omega_2 F_{\phi_2\phi_3}] \quad (3.2.9)$$

In the abelian case the last term is a total derivative and, once integrated on the world-volume of the brane, it cancels. We are left with the first term which gives a non-trivial coupling between the scalars and the vectors. We note that these couplings are proportional to the deformation parameters and disappear for  $\hat{\gamma}_i = 0$ , consistently with the undeformed case.

Since all the  $F$  components except  $F_{\rho\phi_2}$  and  $F_{\rho\phi_3}$  satisfy homogeneous equations we can set them to zero and concentrate on the system of coupled equations of motion for  $X_5, X_6, F_{\rho\phi_2}$  and  $F_{\rho\phi_3}$ . It is easy to realize that a solution is still given by  $X_6 = 0$ ,  $F_{\rho\phi_2} = F_{\rho\phi_3} = 0$ , whereas  $X_5(\rho)$  satisfies eq. (3.2.4) and can be chosen as  $X_5 = L$ .

Therefore, even in the deformed case, the ground state of the probe brane is given by a static location at  $X_5^2 + X_6^2 = L^2$  with no  $F$  flux and absence of non-trivial quark condensate. The choice  $X_5 = L$  and  $X_6 = 0$  breaks the rotational invariance in the  $(X_5, X_6)$  plane.

This configuration is stable (BPS). In fact, the corresponding action

$$S = -T_7 \int_{\Sigma_8} d^8 \sigma \rho^3 s_\theta c_\theta \quad (3.2.10)$$

coincides with the one of the undeformed case and satisfies the no-force condition [59, 43].

Setting  $X_5^2 + X_6^2 = L^2$ , the induced metric on the D7-brane reads

$$\begin{aligned}
ds_I^2 &\equiv g_{ab} dX^a dX^b \\
&= \frac{L^2 + \rho^2}{R^2} (-dt^2 + dx_1^2 + dx_2^2 + dx_3^2) + \frac{R^2}{L^2 + \rho^2} (d\rho^2 + \rho^2 d\theta^2) \\
&+ \frac{R^2 G \rho^2}{(L^2 + \rho^2)} \left[ c_\theta^2 d\phi_2^2 + s_\theta^2 d\phi_3^2 + \frac{\rho^2 L^2 c_\theta^2 s_\theta^2 (\hat{\gamma}_2 d\phi_2 + \hat{\gamma}_3 d\phi_3)^2}{(L^2 + \rho^2)^2} \right] \tag{3.2.11}
\end{aligned}$$

where  $G$  in (3.1.1) takes the explicit form

$$G = \frac{(L^2 + \rho^2)^2}{(L^2 + \rho^2)^2 + \hat{\gamma}_1^2 \rho^4 s_\theta^2 c_\theta^2 + \hat{\gamma}_2^2 L^2 \rho^2 s_\theta^2 + \hat{\gamma}_3^2 L^2 \rho^2 c_\theta^2} \tag{3.2.12}$$

We note that, due to the particular embedding we have realized, the parameter  $\hat{\gamma}_1$  associated to the  $TsT$  transformation on the  $(\phi_2, \phi_3)$  torus inside the D7 worldvolume enters the metric differently from  $\hat{\gamma}_{2,3}$  which are instead associated to deformations on tori with one parallel and one orthogonal direction to the probe.

The different role played by  $\hat{\gamma}_1$  respect to  $(\hat{\gamma}_2, \hat{\gamma}_3)$  can be also understood by looking at the conformal case ( $L = 0$ ) or the UV limit ( $\rho \rightarrow \infty$ ) of the theory. In both cases the dependence on  $(\hat{\gamma}_2, \hat{\gamma}_3)$  disappears and the worldvolume metric reduces to the one for  $\text{AdS}_5 \times \tilde{S}^3$  where  $\tilde{S}^3$  is the deformed three-sphere with metric

$$\frac{ds_{\tilde{S}^3}^2}{R^2} = d\theta^2 + G(c_\theta^2 d\phi_2^2 + s_\theta^2 d\phi_3^2) \quad , \quad G = \frac{1}{1 + \hat{\gamma}_1^2 c_\theta^2 s_\theta^2} \tag{3.2.13}$$

Instead, for  $\rho$  finite and  $L \neq 0$  the  $\text{AdS}_5$  factor is lost, the theory is no longer conformal and a non-trivial dependence on all the deformation parameters appears.

The particular probe brane configuration we have chosen is smoothly related to the one of the undeformed case. In fact, sending  $\hat{\gamma}_i \rightarrow 0$  we recover the usual Karch-Katz [30] picture of flavor branes in  $\text{AdS}_5 \times S^5$ . As we have just proved, the stability of the D3-D7 system survives the deformation.

We have embedded flavor D7-branes in a deformed background. When the D7-brane is spacetime filling and wraps the  $(\phi_2, \phi_3)$  torus the configuration is stable and no worldvolume flux is turned on. Alternatively, we could have started with a configuration of D7-branes in the undeformed  $\text{AdS}_5 \times S^5$  background and perform the three  $TsT$  transformations as a second step. If the D7-branes were to be placed along the same directions as before, we would obtain exactly the same configuration of stable D7-branes in the deformed background with no flux turned on. In fact, along the directions  $(\phi_1, \phi_2, \phi_3)$  affected by  $TsT$  transformations the probe branes have Dirichlet-Neumann-Neumann (DNN) boundary conditions. Considering the proposal in [54] and according to the analysis of [56] a DNN configuration with no flux is mapped into the same configuration,

whatever is the  $TsT$  transformation we perform. Therefore, for the particular embedding we are analyzing the two operations i) Adding a probe to the deformed background and ii) Performing a  $TsT$  transformation on the undeformed brane scenario are equivalent processes. The stability of our brane configuration for any value of the deformation parameters then follows from the fact that  $TsT$  transformations do not affect the BPS nature of the original brane system [19] (see also [55]).

It is worth stressing that the possibility of applying equivalently prescriptions i) or ii) is peculiar of the particular brane configuration we have chosen. Had we considered different embeddings, the two procedures wouldn't have led necessarily to equivalent settings [54, 56]. Furthermore, the stability of the configuration would have become questionable.

When the deformation parameters  $\hat{\gamma}_i$  are all equal the  $\text{AdS}_5 \times \tilde{\text{S}}^5$  background has  $\mathcal{N} = 1$  supersymmetry. The question is whether our D7-brane embedding preserves supersymmetry. The standard way of finding supersymmetric configurations is to look at the  $\kappa$ -symmetry condition of the probes. However, since the  $\beta$ -deformed background can be described by an  $SU(2)$  structure manifold, it is more convenient to work using the formalism of G-structures [60] and Generalized Complex Geometry (GCG) [61]. In this framework the supersymmetry conditions for D-branes probing  $SU(2)$  structure manifolds have been established in [57]. For spacetime filling D7-branes a class of supersymmetric embeddings is given by  $z_1 \equiv X_5 + iX_6 = L$ , with  $z_2 \equiv X_1 + iX_2$  and  $z_3 \equiv X_3 + iX_4$  arbitrarily fixed and no worldvolume flux turned on. This embeddings break one of the  $U(1)$  global symmetries. Since our configuration belongs to this class we conclude that our embedding is supersymmetric.

### 3.3 Probe fluctuations

As proposed in [31, 35] D7-brane fluctuations around its ground state are dual to color singlets which may be interpreted as describing mesonic states of the four dimensional gauge theory. The mass spectrum of the mesons is given by the Kaluza-Klein spectrum of states which originate from the compactification of the D7-brane on the internal submanifold. In the ordinary undeformed scenario the spectrum is discrete and with a mass gap [36].

Our main purpose is to investigate probe fluctuations in the deformed background.

A generic vibration of the brane around its ground state can be described by

$$X_5 = L + \varepsilon \chi(\sigma^a), \quad X_6 = \varepsilon \varphi(\sigma^a) \quad (3.3.1)$$

together with a non-trivial flux  $\varepsilon F_{ab} = \varepsilon(\partial_a A_b - \partial_b A_a)$ . The fluctuations are functions of the worldvolume coordinates  $\sigma^a$  and  $\varepsilon$  is a small perturbation parameter.

We expand the action of the probe brane in powers of the small parameter

$$S = S_{DBI} + S_{WZ} = \int_{\Sigma_8} d^8\sigma \{ \mathcal{L}_0 + \varepsilon \mathcal{L}_1 + \varepsilon^2 \mathcal{L}_2 + \dots \} \quad (3.3.2)$$

and consider terms up to the quadratic order in  $\varepsilon$ .

We first concentrate on the DBI term

$$\mathcal{L}_{DBI} = -T_7 \frac{1}{\sqrt{G}} \sqrt{-\det(g - b + \varepsilon F)} \quad (3.3.3)$$

where we have written the dilaton field as in (3.1.7) with  $e^{\phi_0} \equiv 1$ .

We expand the various terms by writing

$$\begin{aligned} g &= g^{(0)} + \varepsilon g^{(1)} + \varepsilon^2 g^{(2)}, & b &= b^{(0)} + \varepsilon b^{(1)} + \varepsilon^2 b^{(2)} \\ \frac{1}{\sqrt{G}} &= G^{(0)} + \varepsilon G^{(1)} + \varepsilon^2 G^{(2)} \end{aligned} \quad (3.3.4)$$

Therefore, the determinant can be written as

$$\begin{aligned} \sqrt{-\det(g - b + \varepsilon F)} &= \sqrt{-\det(g^{(0)} - b^{(0)})} \sqrt{\det(1 + Y)} \\ &= \sqrt{-\det(g^{(0)} - b^{(0)})} \left[ 1 + \frac{1}{2} \text{Tr}(Y) - \frac{1}{4} \text{Tr}(Y^2) + \frac{1}{8} [\text{Tr}(Y)]^2 + \dots \right] \end{aligned} \quad (3.3.5)$$

where the matrix  $Y$  is given by

$$Y = (g^{(0)} - b^{(0)})^{-1} [\varepsilon (g^{(1)} - b^{(1)} + F) + \varepsilon^2 (g^{(2)} - b^{(2)}) + \dots] \quad (3.3.6)$$

At the lowest order the contribution  $g^{(0)}$  is easily read from (3.2.11), whereas for the pull-back of  $B$  from eq. (3.1.8) we find that the only non-vanishing component is  $b_{\phi_2\phi_3}^{(0)} = \hat{\gamma}_1 R^2 G \rho_2^2 \rho_3^2$ .

It is convenient to introduce the undeformed induced metric

$$\mathcal{G} = \text{diag} \left( -\frac{L^2 + \rho^2}{R^2}, \frac{L^2 + \rho^2}{R^2}, \frac{L^2 + \rho^2}{R^2}, \frac{L^2 + \rho^2}{R^2}, \frac{R^2}{L^2 + \rho^2}, \frac{R^2 \rho^2}{L^2 + \rho^2}, \frac{R^2 \rho^2 c_\theta^2}{L^2 + \rho^2}, \frac{R^2 \rho^2 s_\theta^2}{L^2 + \rho^2} \right) \quad (3.3.7)$$

the auxiliary metric  $\mathcal{C}$  defined by

$$\begin{aligned} d\hat{s}^2 &\equiv \mathcal{C}_{ab} d\sigma^a d\sigma^b \\ &= \frac{L^2 + \rho^2}{R^2} (-dt^2 + dx_1^2 + dx_2^2 + dx_3^2) + \frac{R^2}{L^2 + \rho^2} (d\rho^2 + \rho^2 d\theta^2) \\ &+ \frac{R^2 \hat{G} \rho^2}{L^2 + \rho^2} \left[ c_\theta^2 d\phi_2^2 + s_\theta^2 d\phi_3^2 + \frac{\rho^2 L^2 c_\theta^2 s_\theta^2 (\hat{\gamma}_2 d\phi_2 + \hat{\gamma}_3 d\phi_3)^2}{(L^2 + \rho^2)^2} \right] \end{aligned} \quad (3.3.8)$$

with

$$\hat{G} = \frac{(L^2 + \rho^2)^2}{(L^2 + \rho^2)^2 + \hat{\gamma}_2^2 L^2 \rho^2 s_\theta^2 + \hat{\gamma}_3^2 L^2 \rho^2 c_\theta^2} \quad (3.3.9)$$

and two deformation matrices  $\mathcal{T}$  and  $\mathcal{J}$  given by

$$\begin{aligned} \mathcal{T}^{\phi_2\phi_2} &= \hat{\gamma}_3^2 & \mathcal{T}^{\phi_3\phi_3} &= \hat{\gamma}_2^2 & \mathcal{T}^{\phi_2\phi_3} &= \mathcal{T}^{\phi_3\phi_2} = -\hat{\gamma}_2\hat{\gamma}_3 \\ \mathcal{J}^{\phi_2\phi_2} &= 0 & \mathcal{J}^{\phi_3\phi_3} &= 0 & \mathcal{J}^{\phi_2\phi_3} &= -\mathcal{J}^{\phi_3\phi_2} = \gamma_1 \end{aligned} \quad (3.3.10)$$

The metric  $\mathcal{C}$  is nothing but the induced metric (3.2.11) evaluated at  $\hat{\gamma}_1 = 0$ . Its inverse can be expressed as

$$\mathcal{C}^{-1} = \mathcal{G}^{-1} + \frac{L^2}{R^2(L^2 + \rho^2)} \mathcal{T} \quad (3.3.11)$$

It turns out that the matrix  $(g^{(0)} - b^{(0)})^{-1}$  in (3.3.6) can be written as

$$(g^{(0)} - b^{(0)})^{-1} = \mathcal{C}^{-1} + \mathcal{J} = \mathcal{G}^{-1} + \frac{L^2}{R^2(L^2 + \rho^2)} \mathcal{T} + \mathcal{J} \quad (3.3.12)$$

Since the whole dependence on the deformation parameters is encoded in  $\mathcal{T}$  and  $\mathcal{J}$ , the  $\hat{\gamma}_i \rightarrow 0$  limit is easily understood.

Now a long but straightforward calculation allows to determine the first order corrections  $g^{(1)}, b^{(1)}, G^{(1)}$  as well as the second order ones  $g^{(2)}, b^{(2)}, G^{(2)}$ . Inserting in  $\mathcal{L}_{DBI}$  we eventually find

$$\begin{aligned} \mathcal{L}_{DBI}^{(0)} &= -T_7 \rho^3 c_\theta s_\theta \\ \mathcal{L}_{DBI}^{(1)} &= T_7 \rho^3 c_\theta s_\theta \hat{\gamma}_1 F_{\phi_2\phi_3} / R^2 \\ \mathcal{L}_{DBI}^{(2)} &= -T_7 \rho^3 c_\theta s_\theta \left[ \frac{R^2}{2(L^2 + \rho^2)} \mathcal{C}^{ab} \partial_a \chi \partial_b \chi + \frac{R^2}{2(L^2 + \rho^2)} \mathcal{G}^{ab} \partial_a \varphi \partial_b \varphi \right. \\ &\quad \left. + \frac{1}{4} F_{ab} F^{ab} + \frac{L}{(L^2 + \rho^2)} (\hat{\gamma}_2 F_{a\phi_3} - \hat{\gamma}_3 F_{a\phi_2}) \mathcal{G}^{ab} \partial_b \varphi \right] \end{aligned} \quad (3.3.13)$$

where  $F^{ab} \equiv \mathcal{C}^{ac} \mathcal{C}^{bd} F_{cd}$  and  $\mathcal{C}^{ac}$  is given in (3.3.11). The first order Lagrangian is a total derivative since our embedding  $X_5 = L, X_6 = 0$  is an exact solution of the equations of motion.

The Wess–Zumino Lagrangian starts with a second order term in  $\varepsilon$  given by

$$\mathcal{L}_{WZ} = T_7 \frac{1}{2} P [C_4 - C_2 \wedge B] \wedge F \wedge F = T_7 \frac{(L^2 + \rho^2)^2}{R^4} \epsilon^{ijk} \partial_\rho A_i \partial_j A_k \quad (3.3.14)$$

where we use latin indices to indicate coordinates on the three–sphere parametrized by  $(\theta, \phi_2, \phi_3)$ ,  $A_i$  is the flux potential on it and  $\epsilon^{ijk}$  is the Levi–Civita tensor density ( $\epsilon^{\theta 23} = 1$ ). This term turns out to be independent of the deformation parameters since the

combination  $(C_4 - C_2 \wedge B)$  at lowest order gives exactly the 4-form of the  $\text{AdS}_5 \times \text{S}^5$  undeformed geometry.

Determining the equations of motion from the previous Lagrangian is now an easy task. Introducing the fixed vector

$$v^a = \hat{\gamma}_2 \delta_3^a - \hat{\gamma}_3 \delta_2^a \quad (3.3.15)$$

for the  $\chi$  and  $\varphi$  scalars we find

$$\partial_a \left[ \sqrt{-\det(\mathcal{G})} \left( \frac{R^2}{(L^2 + \rho^2)} \mathcal{G}^{ab} + \frac{L^2}{(L^2 + \rho^2)^2} v^a v^b \right) \partial_b \chi \right] = 0 \quad (3.3.16)$$

$$\partial_a \left[ \sqrt{-\det(\mathcal{G})} \frac{R^2}{(L^2 + \rho^2)} \mathcal{G}^{ab} \left( \partial_b \varphi + \frac{L}{R^2} v^c F_{bc} \right) \right] = 0 \quad (3.3.17)$$

whereas, using (3.3.17) the equations of motion for the gauge fields take the form

$$\begin{aligned} \partial_a \left[ \sqrt{-\det(\mathcal{G})} \mathcal{G}^{ac} \mathcal{G}^{bd} F_{cd} \right] - \frac{4\rho(L^2 + \rho^2)}{R^4} \epsilon^{bjk} \partial_j A_k \\ - \sqrt{-\det(\mathcal{G})} \frac{L}{(L^2 + \rho^2)} v^d \partial_d \left[ \mathcal{G}^{bc} \left( \partial_c \varphi + \frac{L}{R^2} v^f F_{cf} \right) \right] = 0 \end{aligned} \quad (3.3.18)$$

It is interesting to note that the equations of motion depend only on the deformation parameters  $\hat{\gamma}_2$  and  $\hat{\gamma}_3$  hidden in the vector  $v$ . In fact, at this order the dependence on the parameter  $\hat{\gamma}_1$  associated to the torus inside the D7 worldvolume completely cancels between the factors  $\sqrt{-\det(g - b + \varepsilon F)}$  and  $1/\sqrt{G}$ .

The scalar fluctuation  $\chi$  along the direction where the branes are located at distance  $L$  decouples from the rest. The scalar  $\varphi$ , instead, interacts non-trivially with the worldvolume gauge fields through terms proportional to the deformation parameters.

The vector  $v$  has non-vanishing components only on the three-sphere and selects there a fixed direction. As a consequence, the equations of motion (3.3.16 – 3.3.18) lose  $SO(4)$  invariance.

As a first application we consider the  $L = 0$  conformal case. The vibration of the brane is given by  $X_5 = \varepsilon \chi(\sigma^a)$  and  $X_6 = \varepsilon \varphi(\sigma^a)$ . The equations of motion reduce to

$$\begin{aligned} \partial_a \left[ \sqrt{-\det(\mathcal{G})} \frac{R^2}{\rho^2} \mathcal{G}^{ab} \partial_b \Psi \right] = 0 \\ \partial_a \left[ \sqrt{-\det(\mathcal{G})} \mathcal{G}^{ac} \mathcal{G}^{bd} F_{cd} \right] - \frac{4\rho^3}{R^4} \epsilon^{bjk} \partial_j A_k = 0. \end{aligned} \quad (3.3.19)$$

where  $\Psi \equiv (\varphi, \chi)$  and  $\mathcal{G}^{ab}$  is the inverse of the matrix (3.3.7) evaluated at  $L = 0$ . We see that the dependence on the deformation parameters disappears completely and the



equations of motion reduce to the ones of the undeformed case [36]. In particular, the scalar and gauge fluctuations decouple. Written explicitly, the scalar equations read

$$\frac{R^4}{\rho^4} \partial^\mu \partial_\mu \Psi + \frac{1}{\rho^3} \partial_\rho (\rho^3 \partial_\rho \Psi) + \frac{1}{\rho^2} \Delta_{S^3} \Psi = 0 \quad (3.3.20)$$

where

$$\Delta_{S^3} \Psi \equiv \frac{1}{c_\theta s_\theta} \partial_\theta (c_\theta s_\theta \partial_\theta \Psi) + \frac{1}{c_\theta^2} \partial_2^2 \Psi + \frac{1}{s_\theta^2} \partial_3^2 \Psi \quad (3.3.21)$$

is the Laplacian on the unit 3–sphere ( $\partial_2 \equiv \partial_{\phi_2}$ ,  $\partial_3 \equiv \partial_{\phi_3}$ ).

According to the results in [30, 36] the corresponding AdS<sub>5</sub> masses are above the Breitenlohner–Freedman bound [62]. This is a further check of the stability of our brane configuration.

### 3.4 The mesonic spectrum

We now concentrate on the more general situation  $X_5 = L + \varepsilon \chi(\sigma^a)$ ,  $X_6 = \varepsilon \varphi(\sigma^a)$  and solve the equations of motion (3.3.16 – 3.3.18) for scalar and vector modes. We write the abelian flux in terms of its potential one–form,  $F_{ab} = \partial_a A_b - \partial_b A_a$ , and choose the Lorentz gauge  $\partial_\mu A^\mu = 0$  on the spacetime components.

We find convenient to introduce covariant derivatives on the unit three–sphere ( $\theta, \phi_2, \phi_3$ ). Given its metric  $g = \text{diag}(1, c_\theta^2, s_\theta^2)$ , we have  $\nabla_i V^j = \partial_i V^j + \Gamma_{ik}^j V^k$  with the only non–vanishing components being  $\Gamma_{22}^\theta = -\Gamma_{33}^\theta = c_\theta s_\theta$ ,  $\Gamma_{2\theta}^2 = -\frac{s_\theta}{c_\theta}$  and  $\Gamma_{3\theta}^3 = \frac{c_\theta}{s_\theta}$ .

In order to simplify the equations we introduce the special operators

$$\begin{aligned} \mathcal{O}_{\hat{\gamma}} &\equiv \frac{R^4}{(L^2 + \rho^2)^2} \partial^\nu \partial_\nu + \frac{1}{\rho^3} \partial_\rho (\rho^3 \partial_\rho) + \frac{1}{\rho^2} \frac{1}{\sqrt{g}} \partial_i (\sqrt{g} \partial^i) + \frac{L^2}{(L^2 + \rho^2)^2} (\hat{\gamma}_2 \partial_3 - \hat{\gamma}_3 \partial_2)^2 \\ \tilde{\mathcal{O}}_{\hat{\gamma}} &\equiv \frac{R^4}{(L^2 + \rho^2)^2} \partial^\nu \partial_\nu + \frac{1}{\rho(L^2 + \rho^2)^2} \partial_\rho [\rho(L^2 + \rho^2)^2 \partial_\rho] + \frac{1}{\rho^2} \nabla_l \nabla^l \\ &\quad + \frac{L^2}{(L^2 + \rho^2)^2} (\hat{\gamma}_2 \partial_3 - \hat{\gamma}_3 \partial_2)^2 \end{aligned} \quad (3.4.1)$$

along with their undeformed versions  $\mathcal{O}_0 \equiv \mathcal{O}_{\hat{\gamma}}|_{\hat{\gamma}_2=\hat{\gamma}_3=0}$ ,  $\tilde{\mathcal{O}}_0 \equiv \tilde{\mathcal{O}}_{\hat{\gamma}}|_{\hat{\gamma}_2=\hat{\gamma}_3=0}$ .

Equation (3.3.16) for the  $\chi$  mode then takes the compact form

$$\mathcal{O}_{\hat{\gamma}} \chi = 0 \quad (3.4.2)$$

whereas equation (3.3.17) can be rewritten as

$$\mathcal{O}_0 \Phi - \frac{L}{R^2} (\hat{\gamma}_2 \partial_3 - \hat{\gamma}_3 \partial_2) \left[ \frac{1}{\rho^3} \partial_\rho (\rho^3 A_\rho) + \frac{1}{\rho^2} \nabla_l A^l \right] = 0 \quad (3.4.3)$$

where we have defined

$$\Phi \equiv \varphi + \frac{L}{R^2} v^a A_a = \varphi + \frac{L}{R^2} (\hat{\gamma}_2 A_3 - \hat{\gamma}_3 A_2) \quad (3.4.4)$$

Equations (3.3.18) for the vector modes come into three classes, according to  $b$  being in Minkowski, or  $b = \rho$  or  $b = i \equiv \{\theta, \phi_2, \phi_3\}$ . We list the three cases.

- $b$  in Minkowski: For  $b = \mu$  and expressing the  $F$  flux in terms of its one-form potential, equation (3.3.18) becomes

$$\mathcal{O}_{\hat{\gamma}} A_\mu - \partial_\mu \left[ \frac{1}{\rho^3} \partial_\rho (\rho^3 A_\rho) + \frac{1}{\rho^2} \nabla_l A^l + \frac{LR^2}{(L^2 + \rho^2)^2} (\hat{\gamma}_2 \partial_3 - \hat{\gamma}_3 \partial_2) \Phi \right] = 0 \quad (3.4.5)$$

with  $\Phi$  defined in (3.4.4).

We apply  $\partial^\mu$  to this equation and sum over  $\mu$ . Using  $[\partial^\mu, \mathcal{O}_{\hat{\gamma}}] = 0$  and Lorentz gauge, solutions corresponding to non-trivial dispersion relations ( $k^2 \neq 0$ ) satisfy

$$\left[ \frac{1}{\rho^3} \partial_\rho (\rho^3 A_\rho) + \frac{1}{\rho^2} \nabla_l A^l + \frac{LR^2}{(L^2 + \rho^2)^2} (\hat{\gamma}_2 \partial_3 - \hat{\gamma}_3 \partial_2) \Phi \right] = 0 \quad , \quad \mathcal{O}_{\hat{\gamma}} A_\mu = 0 \quad (3.4.6)$$

- $b = \rho$ : Again, expressing the flux in terms of the vector potential we obtain

$$\mathcal{O}_{\hat{\gamma}} A_\rho - \left[ \frac{1}{\rho^3} \partial_\rho (\rho^3 \partial_\rho A_\rho) + \frac{1}{\rho^2} \partial_\rho \nabla_l A^l + \frac{LR^2}{(L^2 + \rho^2)^2} (\hat{\gamma}_2 \partial_3 - \hat{\gamma}_3 \partial_2) \partial_\rho \Phi \right] = 0 \quad (3.4.7)$$

- $b = i$ : On the internal  $\tilde{S}^3$  sphere we have

$$\begin{aligned} \tilde{\mathcal{O}}_{\hat{\gamma}} A_j - \frac{1}{\rho^2} \left( \nabla_l \nabla_j A^l + \frac{4\rho^2}{L^2 + \rho^2} \frac{1}{c_\theta s_\theta} \epsilon_{jlm} \nabla^l A^m \right) \\ - \frac{1}{\rho(L^2 + \rho^2)^2} \partial_\rho [\rho(L^2 + \rho^2)^2 \partial_j A_\rho] - \frac{LR^2}{(L^2 + \rho^2)^2} (\hat{\gamma}_2 \partial_3 - \hat{\gamma}_3 \partial_2) \partial_j \Phi = 0 \end{aligned} \quad (3.4.8)$$

where we have used  $\frac{1}{\sqrt{g}} \partial_i (\sqrt{g} F^{ij}) = \nabla_i F^{ij} = \nabla_i \nabla^i A^j - \nabla_i \nabla^j A^i$ .

Now, collecting all the equations and using the first of (3.4.6) in (3.4.3) the system of coupled equations we need solve is

$$\begin{aligned} (0) \quad \mathcal{O}_{\hat{\gamma}} \chi = 0 \quad ; \quad \mathcal{O}_{\hat{\gamma}} A_\mu = 0 \\ (1) \quad \mathcal{O}_{\hat{\gamma}} \Phi = 0 \end{aligned} \quad (3.4.9)$$

$$(2) \quad \left[ \frac{1}{\rho^3} \partial_\rho (\rho^3 A_\rho) + \frac{1}{\rho^2} \nabla^l A_l + \frac{LR^2}{(L^2 + \rho^2)^2} (\hat{\gamma}_2 \partial_3 - \hat{\gamma}_3 \partial_2) \Phi \right] = 0$$

$$(3) \quad \mathcal{O}_{\hat{\gamma}} A_\rho - \left[ \frac{1}{\rho^3} \partial_\rho (\rho^3 \partial_\rho A_\rho) + \frac{1}{\rho^2} \partial_\rho \nabla^l A_l + \frac{LR^2}{(L^2 + \rho^2)^2} (\hat{\gamma}_2 \partial_3 - \hat{\gamma}_3 \partial_2) \partial_\rho \Phi \right] = 0$$

$$(4) \quad \tilde{\mathcal{O}}_{\hat{\gamma}} A_j - \frac{1}{\rho^2} \left( \nabla_l \nabla_j A^l + \frac{4\rho^2}{L^2 + \rho^2} \frac{1}{c_\theta s_\theta} \epsilon_{jlm} \nabla^l A^m \right) - \frac{1}{\rho(L^2 + \rho^2)^2} \partial_\rho [\rho(L^2 + \rho^2)^2 \partial_j A_\rho] - \frac{LR^2}{(L^2 + \rho^2)^2} (\hat{\gamma}_2 \partial_3 - \hat{\gamma}_3 \partial_2) \partial_j \Phi = 0$$

Equations (1)–(4) exhibit a non-trivial interaction between the scalar  $\Phi$  and the components of the vector potential along the internal directions. The modes  $\chi$  and  $A_\mu$  instead decouple.

It is convenient to search for solutions expanded in spherical harmonics on  $S^3$ . Scalar spherical harmonics are a complete set of functions  $\mathcal{Y}_l^{m_2, m_3}$  in the  $(\frac{l}{2}, \frac{l}{2})$  representation of  $SO(4)$  and with definite  $U(1) \times U(1)$  quantum numbers  $(m_2, m_3)$  satisfying  $|m_2 + m_3| = |m_2 - m_3| = l - 2k$ ,  $l, k = 0, 1, \dots$ . For fixed  $l$  the degeneracy is  $(l + 1)^2$ . Their defining equations are <sup>§</sup>

$$\begin{aligned} \Delta_{S^3} \mathcal{Y}_l^{m_2, m_3} &= -l(l + 2) \mathcal{Y}_l^{m_2, m_3} \\ \frac{\partial}{\partial \phi_{2,3}} \mathcal{Y}_l^{m_2, m_3} &= im_{2,3} \mathcal{Y}_l^{m_2, m_3} \end{aligned} \quad (3.4.10)$$

Vector spherical harmonics come into three classes. Choosing them to be also eigenfunctions of  $\frac{\partial}{\partial \phi_{2,3}}$  we have longitudinal harmonics  $\mathcal{H}_i = \nabla_i \mathcal{Y}_l^{m_2, m_3}$ ,  $l \geq 1$  which are in the  $(\frac{l}{2}, \frac{l}{2})$  representation of  $SO(4)$  with  $(m_2, m_3)$  ranging as before. Transverse harmonics are  $\mathcal{M}_i^+ \equiv \mathcal{Y}_i^{(l, m_2, m_3); +}$  with  $l \geq 1$  in the  $(\frac{l-1}{2}, \frac{l+1}{2})$  and  $\mathcal{M}_i^- \equiv \mathcal{Y}_i^{(l, m_2, m_3); -}$  with  $l \geq 1$  in the  $(\frac{l+1}{2}, \frac{l-1}{2})$ . Their degeneracy is  $l(l+2)$  and it is counted by  $|m_2 + m_3| = l \pm 1 - 2k$ ,  $|m_2 - m_3| = l \mp 1 - 2k$ . These harmonics satisfy

$$\begin{aligned} \nabla_i \nabla^i \mathcal{M}_j^\pm - R_j^k \mathcal{M}_k^\pm &= -(l + 1)^2 \mathcal{M}_j^\pm \\ \epsilon_{ijk} \nabla^j \mathcal{M}^{\pm; k} &= \pm \sqrt{g} (l + 1) \mathcal{M}_i^\pm \\ \nabla^i \mathcal{M}_i^\pm &= 0 \\ \frac{\partial}{\partial \phi_{2,3}} \mathcal{M}_i^\pm &= im_{2,3} \mathcal{M}_i^\pm \end{aligned} \quad (3.4.11)$$

where  $\sqrt{g} = c_\theta s_\theta$  is the square root of the determinant of the metric on  $S^3$ , whereas  $R_j^i = 2\delta_j^i$  is the Ricci tensor.

As in the undeformed case [36] we require the solutions to be regular at the origin ( $\rho = 0$ ), normalizable and small enough to justify the quadratic approximation. All these conditions are used to select the actual mass spectrum of the mesonic excitations.

<sup>§</sup>For their explicit realization see for instance [63, 53].

### 3.4.1 The decoupled modes

#### The scalar mode $\chi$

We start solving the equation for the decoupled scalar  $\chi$ . Using the general identity  $\frac{1}{\sqrt{g}}\partial_i(\sqrt{g}\partial^i s) = \nabla_i\nabla^i s$  valid for any scalar  $s$ , the equation  $\mathcal{O}_{\hat{\gamma}}\chi = 0$  reads explicitly

$$\frac{R^4}{(L^2 + \rho^2)^2}\partial^\nu\partial_\nu\chi + \frac{1}{\rho^3}\partial_\rho(\rho^3\partial_\rho\chi) + \frac{1}{\rho^2}\nabla_l\nabla^l\chi + \frac{L^2}{(L^2 + \rho^2)^2}(\hat{\gamma}_2\partial_3 - \hat{\gamma}_3\partial_2)^2\chi = 0 \quad (3.4.12)$$

We look for single-mode solutions of the form

$$\chi(\sigma^a) = r(\rho) e^{ikx} \mathcal{Y}_l^{m_2, m_3}(\theta, \phi_2, \phi_3) \quad (3.4.13)$$

Inserting in (3.4.12) we obtain an equation for  $r(\rho)$  that, after the redefinitions

$$\varrho = \frac{\rho}{L}, \quad \hat{\Gamma}^2 = -\frac{k^2 R^4}{L^2} - (\hat{\gamma}_2 m_3 - \hat{\gamma}_3 m_2)^2 = \bar{M}^2 - (\hat{\gamma}_2 m_3 - \hat{\gamma}_3 m_2)^2, \quad (3.4.14)$$

becomes

$$\partial_\varrho^2 r + \frac{3}{\varrho}\partial_\varrho r + \left[ \frac{\hat{\Gamma}^2}{(1 + \varrho^2)^2} - \frac{l(l+2)}{\varrho^2} \right] r = 0 \quad (3.4.15)$$

This has exactly the same structure of the equation found in the undeformed case [36]. The only difference is the presence of the deformation parameters in  $\hat{\Gamma}^2$  which in the undeformed case reduces simply to  $\bar{M}^2$ . Following what has been done in that case [36] we find that the general solution is

$$r(\rho) = \rho^l (L^2 + \rho^2)^{-\alpha} F(-\alpha, -\alpha + l + 1; l + 2; -\rho^2/L^2) \quad (3.4.16)$$

where  $F$  is the hypergeometric function and  $\alpha = \frac{-1 + \sqrt{1 + \hat{\Gamma}^2}}{2}$ . This solution satisfies the conditions of regularity and normalizability if the quantization condition

$$\hat{\Gamma}^2 = 4(n + l + 1)(n + l + 2) \quad n \in N, \quad n, l \geq 0 \quad (3.4.17)$$

is imposed. Using (3.4.14) and  $M^2 = -k^2$ , the mass spectrum of scalar mesons then follows

$$M_\chi(n, l, m_2, m_3) = \frac{2L}{R^2} \sqrt{(n + l + 1)(n + l + 2) + \left( \frac{\hat{\gamma}_2 m_3 - \hat{\gamma}_3 m_2}{2} \right)^2} \quad (3.4.18)$$

with  $n, l \geq 0$  and  $|m_2 + m_3| = |m_2 - m_3| = l - 2k$ ,  $k$  a non-negative integer.

We see that the deformation parameters induce a non-trivial dependence of the mass spectrum on the two  $U(1)$  quantum numbers  $(m_2, m_3)$ , so breaking the degeneracy of the undeformed case.

The mass spectrum is smoothly related to the one of the undeformed case for  $\hat{\gamma}_i \rightarrow 0$ .

## The Type II modes

We look for excitations of the form

$$A_\mu(\sigma^a) = \zeta_\mu Z_{II}(\rho) e^{ikx} \mathcal{Y}_l^{m_2, m_3}(\theta, \phi_2, \phi_3) \quad , \quad k \cdot \zeta = 0 \quad (3.4.19)$$

Following the classification introduced in [36] for the undeformed case we call them Type II modes. The equation  $\mathcal{O}_{\hat{\gamma}} A_\mu = 0$  in (3.4.9) yields to

$$\frac{R^4}{(L^2 + \rho^2)^2} \partial^\nu \partial_\nu A_\mu + \frac{1}{\rho^3} \partial_\rho (\rho^3 \partial_\rho A_\mu) + \frac{1}{\rho^2} \nabla_l \nabla^l A_\mu + \frac{L^2}{(L^2 + \rho^2)^2} (\hat{\gamma}_2 \partial_3 - \hat{\gamma}_3 \partial_2)^2 A_\mu = 0 \quad (3.4.20)$$

This is exactly the same equation as the one for the scalar mode  $\chi$ . Therefore, for each component  $A_\mu$  we follow the same strategy of subsection 5.1.1 and find the mass spectrum

$$M_{II}(n, l, m_2, m_3) = \frac{2L}{R^2} \sqrt{(n+l+1)(n+l+2) + \left( \frac{\hat{\gamma}_2 m_3 - \hat{\gamma}_3 m_2}{2} \right)^2} \quad (3.4.21)$$

with  $n, l \geq 0$  and  $|m_2 + m_3| = |m_2 - m_3| = l - 2k$ .

Even for this type of vector fluctuations the spectrum is smoothly related to the undeformed one for  $\hat{\gamma}_i \rightarrow 0$ .

## 3.4.2 The coupled modes

Having performed the field redefinition (3.4.4) we solve the coupled equations (1)–(4) by considering elementary fluctuations of  $\Phi$ ,  $A_\rho$  and  $A_i$ .

### The Type I modes

Being in a different representation the harmonics  $\mathcal{M}_i^\pm$  do not mix with the others. Therefore we can make the ansatz <sup>¶</sup>

$$\Phi = 0, \quad A_\rho = 0, \quad A_i(\sigma^a) = Z_I^\pm(\rho) e^{ikx} \mathcal{M}_i^\pm(\theta, \phi_2, \phi_3) \quad (3.4.22)$$

By using the identity  $\nabla_i A^i = 0$  as follows from (3.4.11), equations (1), (2) and (3) in (3.4.9) are identically satisfied whereas eq. (4) reads

$$\tilde{\mathcal{O}}_{\hat{\gamma}} A_j - \frac{1}{\rho^2} \left( \nabla_l \nabla_j A^l + \frac{4\rho^2}{L^2 + \rho^2} \frac{1}{c_\theta s_\theta} \epsilon_{jlm} \nabla^l A^m \right) = 0 \quad (3.4.23)$$

---

<sup>¶</sup>We note that if we were to follow closely the classification of [36] we would call Type I modes the elementary modes with  $\varphi = 0$ , i.e. with no fluctuations along the  $X^6$  coordinate. However, given the structure of the equations of motion, in our case we find the definition (3.4.22) more convenient. In any case, the two definitions coincide for  $\hat{\gamma}_i = 0$ .

Considering the explicit expression for the operator  $\tilde{\mathcal{O}}_{\hat{\gamma}}$  in (3.4.1) and using properties (3.4.11) we find that  $Z_I^\pm(\rho)$  is a solution of the equation

$$\frac{1}{\varrho} \partial_\varrho [\varrho(\varrho^2 + 1)^2 \partial_\varrho Z_I^\pm] + \left[ \hat{\Gamma}^2 - \frac{(\varrho^2 + 1)^2}{\varrho^2} (l + 1)^2 \mp 4(\varrho^2 + 1)(l + 1) \right] Z_I^\pm = 0 \quad (3.4.24)$$

where we have used the definitions (3.4.14). This is formally the same equation as the one of the undeformed case, except for the different definition of  $\hat{\Gamma}^2$ . Therefore, following the same steps [36] we find that the solutions are still hypergeometric functions

$$\begin{aligned} Z_I^+(\rho) &= \rho^{l+1} (\rho^2 + L^2)^{-\alpha-1} F(l + 2 - \alpha, -1 - \alpha; l + 2; -\rho^2/L^2) \\ Z_I^-(\rho) &= \rho^{l+1} (\rho^2 + L^2)^{-\alpha-1} F(l - \alpha, 1 - \alpha; l + 2; -\rho^2/L^2) \end{aligned} \quad (3.4.25)$$

where  $\alpha = \frac{-1 + \sqrt{1 + \hat{\Gamma}^2}}{2}$ . Requiring them to be regular at infinity we obtain the following quantization conditions

$$\begin{aligned} \hat{\Gamma}_+^2 &= 4(n + l + 2)(n + l + 3) \\ \hat{\Gamma}_-^2 &= 4(n + l)(n + l + 1) \end{aligned} \quad n \geq 0 \quad (3.4.26)$$

As a consequence the mass spectrum reads

$$\begin{aligned} M_{I,+} &= \frac{2L}{R^2} \sqrt{(n + l + 2)(n + l + 3) + \left( \frac{\hat{\gamma}_2 m_3 - \hat{\gamma}_3 m_2}{2} \right)^2} & \begin{cases} |m_2 + m_3| = l - 1 - 2k \\ |m_2 - m_3| = l + 1 - 2k \end{cases} \\ M_{I,-} &= \frac{2L}{R^2} \sqrt{(n + l)(n + l + 1) + \left( \frac{\hat{\gamma}_2 m_3 - \hat{\gamma}_3 m_2}{2} \right)^2} & \begin{cases} |m_2 + m_3| = l + 1 - 2k \\ |m_2 - m_3| = l - 1 - 2k \end{cases} \end{aligned} \quad (3.4.27)$$

where  $l \geq 1$  and  $k$  is a non-negative integer.

## The Type III modes

Finally, we consider the following fluctuations

$$\begin{aligned} \Phi(\sigma^a) &= X_{III}(\rho) e^{ikx} \mathcal{Y}_l^{m_2, m_3}(\theta, \phi_2, \phi_3) \\ A_\rho(\sigma^a) &= Y_{III}(\rho) e^{ikx} \mathcal{Y}_l^{m_2, m_3}(\theta, \phi_2, \phi_3) \\ A_i(\sigma^a) &= Z_{III}(\rho) e^{ikx} \nabla_i \mathcal{Y}_l^{m_2, m_3}(\theta, \phi_2, \phi_3) \equiv \nabla_i A(\sigma^a) \end{aligned} \quad (3.4.28)$$

with  $l \geq 1$ . We note that  $l = 0$  corresponds to having  $A_i = 0$ . We will comment on this particular case at the end of this Section.

Inserting in (3.4.9) and using the identities (3.4.10) for the scalar harmonics, after a bit of algebra the equations (1)–(4) can be rewritten as

$$\begin{aligned}
(1) \quad & \left[ \frac{R^4}{(L^2 + \rho^2)^2} \partial^\nu \partial_\nu + \frac{1}{\rho^3} \partial_\rho (\rho^3 \partial_\rho) - \frac{l(l+2)}{\rho^2} - \frac{L^2}{(L^2 + \rho^2)^2} (\hat{\gamma}_2 m_3 - \hat{\gamma}_3 m_2)^2 \right] \Phi = 0 \\
(2) \quad & \frac{1}{\rho^3} \partial_\rho (\rho^3 A_\rho) - \frac{l(l+2)}{\rho^2} A + i \frac{LR^2}{(L^2 + \rho^2)^2} (\hat{\gamma}_2 m_3 - \hat{\gamma}_3 m_2) \Phi = 0 \\
(3) \quad & \frac{R^4}{(L^2 + \rho^2)^2} \partial^\nu \partial_\nu A_\rho + \frac{1}{\rho^2} \partial_\rho \left( \frac{1}{\rho} \partial_\rho (\rho^3 A_\rho) \right) \\
& - \left[ \frac{l(l+2)}{\rho^2} + \frac{L^2}{(L^2 + \rho^2)^2} (\hat{\gamma}_2 m_3 - \hat{\gamma}_3 m_2)^2 \right] A_\rho \\
& + 2iLR^2 \frac{(L^2 - \rho^2)}{\rho(L^2 + \rho^2)^3} (\hat{\gamma}_2 m_3 - \hat{\gamma}_3 m_2) \Phi = 0 \\
(4) \quad & \frac{R^4}{(L^2 + \rho^2)^2} \partial^\nu \partial_\nu A + \frac{1}{\rho(L^2 + \rho^2)^2} \partial_\rho (\rho(L^2 + \rho^2)^2 \partial_\rho A) \\
& - \frac{L^2}{(L^2 + \rho^2)^2} (\hat{\gamma}_2 m_3 - \hat{\gamma}_3 m_2)^2 A - \frac{1}{\rho(L^2 + \rho^2)^2} \partial_\rho [\rho(L^2 + \rho^2)^2 A_\rho] \\
& - i \frac{LR^2}{(L^2 + \rho^2)^2} (\hat{\gamma}_2 m_3 - \hat{\gamma}_3 m_2) \Phi = 0 \tag{3.4.29}
\end{aligned}$$

It is worth mentioning that eq. (1) in (3.4.9) contains the operator  $\frac{1}{\sqrt{g}} \partial_i (\sqrt{g} \partial^i)$  which acts differently on scalars and spherical vectors. Therefore, when this operator is applied on  $\Phi = \varphi + \frac{L}{R^2} (\hat{\gamma}_2 A_3 - \hat{\gamma}_3 A_2)$ , in principle one should split it as acting on  $\varphi$  and  $A_i$  separately. However, since in the present case  $A_i = \nabla_i A$ , exploiting the algebra of covariant derivatives and the properties of scalar harmonics in (3.4.28), it is easy to show that

$$\frac{1}{\sqrt{g}} \partial_i (\sqrt{g} \partial^i \nabla_j A) = \nabla_i \nabla^i \nabla_j A - 2 \nabla_j A = -l(l+2) \nabla_j A \tag{3.4.30}$$

This is exactly the same relation satisfied by the scalar  $\varphi$ , so we are led to  $\frac{1}{\sqrt{g}} \partial_i (\sqrt{g} \partial^i \Phi) = -l(l+2) \Phi$ . This confirms that considering  $\Phi$  as an elementary scalar fluctuation is a consistent procedure.

Equations (3.4.29) are four equations for three unknowns  $X_{III}, Y_{III}, Z_{III}$  and lead to non-trivial solutions only if they are compatible. Indeed it turns out that equation (4) is identically satisfied once the others are. We then concentrate on the first three equations.

We first solve equation (1). By observing that it is identical to the equation for the scalar  $\chi$  (see eq. (3.4.12)) we immediately obtain

$$X_{III}(\rho) = \rho^l (L^2 + \rho^2)^{-n-l-1} F(-(n+l+1), -n; l+2; -\rho^2/L^2) \tag{3.4.31}$$

where the quantization condition (3.4.17) has been used. As a consequence, the mass spectrum is

$$M_{\Phi}(n, l, m_2, m_3) = \frac{2L}{R^2} \sqrt{(n+l+1)(n+l+2) + \left( \frac{\hat{\gamma}_2 m_3 - \hat{\gamma}_3 m_2}{2} \right)^2} \quad (3.4.32)$$

where  $n \geq 0$ ,  $l \geq 1$  and  $|m_2 + m_3| = |m_2 - m_3| = l - 2k$ .

Equation (2) can be used to express the mode  $A$  in terms of  $\Phi$  and  $A_{\rho}$ . Inserting the expressions (3.4.28) we obtain

$$Z_{III} = \frac{1}{l(l+2)} \left[ \frac{1}{\rho} \partial_{\rho} (\rho^3 Y_{III}) + i \frac{LR^2 \rho^2}{(L^2 + \rho^2)^2} (\hat{\gamma}_2 m_3 - \hat{\gamma}_3 m_2) X_{III} \right] \quad (3.4.33)$$

We then consider equation (3) which exhibits an actual coupling between  $X_{III}$  and  $Y_{III}$ . In order to solve for  $Y_{III}$  given the solution (3.4.31) for  $X_{III}$  we set

$$Y_{III}(\varrho) = \varrho^{l-1} (1 + \varrho^2)^{-\alpha} P(\varrho) \quad (3.4.34)$$

Using the definitions (3.4.14) together with the quantization condition (3.4.17) and defining  $y \equiv -\varrho^2$ , after some algebra the equation for  $P$  reads

$$\begin{aligned} y(1-y)P''(y) + [(l+2) + (2n+l)y]P'(y) - n(n+l+1)P(y) \\ = \eta \frac{(1+y)}{(1-y)^2} F(-(n+l+1), -n; l+2; y) \end{aligned} \quad (3.4.35)$$

where we have defined  $\eta \equiv i \frac{R^2}{2L^2} (\hat{\gamma}_2 m_3 - \hat{\gamma}_3 m_2)$ . This is an inhomogeneous hypergeometric equation whose source is a polynomial of degree  $n$ , solution of the corresponding homogeneous equation. The most general solution is then of the form

$$P(y) = c F(-(n+l+1), -n; l+2; y) + \bar{P}(y) \quad (3.4.36)$$

for arbitrary constant  $c$ , where  $\bar{P}$  is a particular solution of (3.4.35). Exploiting the general identity

$$\begin{aligned} (1-y)F'(-(n+l+2), -n; l+1; y) + (n+l+2)F(-(n+l+2), -n; l+1; y) \\ = \frac{(n+l+1)(n+l+2)}{(l+1)} F(-(n+l+1), -n; l+2; y) \end{aligned} \quad (3.4.37)$$

valid for hypergeometric functions with integer coefficients, it is easy to show that a solution is given by

$$\bar{P}(y) = \eta \frac{(l+1)}{(n+l+1)(n+l+2)} \frac{F(-(n+l+2), -n; l+1; y)}{1-y} \quad (3.4.38)$$



The general solution of equation (3) is then

$$Y_{III}(\rho) = \rho^{l-1}(L^2 + \rho^2)^{-n-l-2} \left[ c(L^2 + \rho^2) F(-(n+l+1), -n; l+2; -\rho^2/L^2) \right. \\ \left. + \eta \frac{(l+1)}{(n+l+1)(n+l+2)} F(-(n+l+2), -n; l+1; -\rho^2/L^2) \right] \quad (3.4.39)$$

This solution is regular at the origin and not divergent for  $\rho \rightarrow \infty$ . Due to the quantization condition (3.4.17) the corresponding mass spectrum is still given by

$$M_{III}(n, l, m_2, m_3) = \frac{2L}{R^2} \sqrt{(n+l+1)(n+l+2) + \left( \frac{\hat{\gamma}_2 m_3 - \hat{\gamma}_3 m_2}{2} \right)^2} \quad (3.4.40)$$

with  $n \geq 0$ ,  $l \geq 1$  and  $|m_2 + m_3| = |m_2 - m_3| = l - 2k$ .

Before closing this Section we comment on the particular  $l = m_2 = m_3 = 0$  mode. In (3.4.28) this corresponds to turn off  $A_i = \nabla_i A$  since  $A(\sigma^a)$  is independent of the three-sphere coordinates. Equation (2) reduces to  $\partial_\rho(\rho^3 A_\rho) = 0$  which, together with the condition of regularity at  $\rho = 0$ , sets  $A_\rho = 0$ . Equations (3) and (4) in (3.4.29) are then automatically satisfied, whereas eq. (1) provides a non-trivial solution for  $\Phi$  as given in (3.4.31) with mass (3.4.32) where we set  $l = m_2 = m_3 = 0$ .

As a slightly different attitude we can consider the configuration with all the vector modes turned off ( $Y_{III} = Z_{III} = 0$ ) and study only scalar  $\Phi$  fluctuations of the form (3.4.28). In this case  $\Phi$  is still solution of equation (1) but, as follows from the rest of equations, it is constrained by the further condition

$$(\hat{\gamma}_2 m_3 - \hat{\gamma}_3 m_2) \Phi = 0 \quad (3.4.41)$$

In general, for non-vanishing and distinct deformation parameters, non-trivial solutions can be found only for  $m_2 = m_3 = 0$ , i.e. only the  $U(1) \times U(1)$  zero-mode sector is selected and the fluctuations are independent of  $(\phi_2, \phi_3)$ . A greater number of solutions, corresponding to the modes  $m_2 = m_3$ , is instead allowed when  $\hat{\gamma}_2 = \hat{\gamma}_3$ , therefore in particular for the supersymmetric deformation. In any case, the mass spectrum is given by

$$M_\Phi(n, l) = \frac{2L}{R^2} \sqrt{(n+l+1)(n+l+2)} \quad n \geq 0 \quad l \text{ (even)} \geq 0 \quad (3.4.42)$$

and coincides with the undeformed mass.

### 3.5 Analysis of the spectrum

From the previous discussion it follows that the bosonic modes arising from the compactification of the D7-brane on the deformed  $\tilde{S}^3$  give rise to a mesonic spectrum which is given by

- 2 scalars and 1 vector in the  $(\frac{l}{2}, \frac{l}{2})$  with  $l \geq 0$ ,  $|m_2 \pm m_3| = l - 2k$  and mass

$$M_{\chi, \Phi, II}(n, l, m_2, m_3) = \frac{2L}{R^2} \sqrt{(n+l+1)(n+l+2) + \left(\frac{\hat{\gamma}_2 m_3 - \hat{\gamma}_3 m_2}{2}\right)^2}$$

- 1 scalar in the  $(\frac{l}{2}, \frac{l}{2})$  with  $l \geq 1$ ,  $|m_2 \pm m_3| = l - 2k$  and mass

$$M_{III}(n, l, m_2, m_3) = \frac{2L}{R^2} \sqrt{(n+l+1)(n+l+2) + \left(\frac{\hat{\gamma}_2 m_3 - \hat{\gamma}_3 m_2}{2}\right)^2}$$

- 1 scalar in the  $(\frac{l-1}{2}, \frac{l+1}{2})$  with  $l \geq 1$ ,  $|m_2 \pm m_3| = l \mp 1 - 2k$  and mass

$$M_{I,+}(n, l, m_2, m_3) = \frac{2L}{R^2} \sqrt{(n+l+2)(n+l+3) + \left(\frac{\hat{\gamma}_2 m_3 - \hat{\gamma}_3 m_2}{2}\right)^2}$$

- 1 scalar in the  $(\frac{l+1}{2}, \frac{l-1}{2})$  with  $l \geq 1$ ,  $|m_2 \pm m_3| = l \pm 1 - 2k$  and mass

$$M_{I,-}(n, l, m_2, m_3) = \frac{2L}{R^2} \sqrt{(n+l)(n+l+1) + \left(\frac{\hat{\gamma}_2 m_3 - \hat{\gamma}_3 m_2}{2}\right)^2}$$

for any  $n \geq 0$ . This matches exactly the bosonic content found in the undeformed case [36]. However, in this case the  $\gamma$ -deformation breaks  $SO(4) \rightarrow U(1) \times U(1)$  and induces an explicit dependence of the mass spectrum on the the quantum numbers  $(m_2, m_3)$  with a pattern similar to the Zeeman effect for atomic electrons where the constant magnetic field which breaks  $SU(2)$  rotational invariance down to  $U(1)$  induces a dependence of the energy levels on the azimuthal quantum number  $m$  <sup>||</sup>.

The dependence on the deformation parameters disappears completely in the  $m_2 = m_3 = 0$  sector (or for  $\hat{\gamma}_2 = \hat{\gamma}_3$  and  $m_2 = m_3$ ) and the mass eigenvalues coincide with the ones of the undeformed theory. When  $\hat{\gamma}_2 = \hat{\gamma}_3$  the mass spectrum acquires an extra symmetry under the exchange of the two  $U(1)$ 's and an extra degeneracy corresponding to  $m_2 \rightarrow m_2 + m$ ,  $m_3 \rightarrow m_3 + m$ ,  $m$  integer.

For any value of  $\hat{\gamma}_i$  there are no tachyonic modes, so confirming the stability of our configuration. Moreover, massless states are absent and the spectrum has a mass gap given by

$$M_{gap} = 2\sqrt{2} \frac{L}{R^2} \tag{3.5.1}$$

This is exactly the mass gap present in the undeformed theory [36].

---

<sup>||</sup>A similar effect has been observed in the case of backgrounds with  $B$  fields turned on in Minkowski [49, 64].

In order to analyze in detail the mass splitting induced by the deformation and study how the modes organize themselves among the different eigenvalues it is convenient to rewrite the mass of a generic eigenstate  $X$  as

$$M_X(n, l, m_2, m_3) = \sqrt{\left(M_X^{(0)}(n, l)\right)^2 + \frac{4L^2}{R^4} (\Delta M(m_2, m_3))^2} \quad (3.5.2)$$

where  $M_X^{(0)}$  is the undeformed mass, whereas

$$\Delta M(m_2, m_3) \equiv \left(\frac{\hat{\gamma}_2 m_3 - \hat{\gamma}_3 m_2}{2}\right) \quad (3.5.3)$$

is the Zeeman–splitting term.

Since for any  $l \geq 2$  the following mass degeneracy occurs

$$M_{\chi, \Phi, II}^{(0)}(n, l) = M_{III}^{(0)}(n, l) = M_{I,+}^{(0)}(n, l-1) = M_{I,-}^{(0)}(n, l+1) \quad (3.5.4)$$

for  $\hat{\gamma}_i = 0$  we have  $8(l+1)^2$  bosonic degrees of freedom corresponding to the same mass eigenvalue. For the particular values  $l = 0, 1$  the number of states is reduced since for  $l = 0$  modes  $A_{(I,+)}$  and  $A_{III}$  are both absent, whereas for  $l = 1$   $A_{(I,+)}$  is still absent. For any value of  $l$  they match the bosonic content of massive  $\mathcal{N} = 2$  supermultiplets [36].

In the present case mass degeneracy occurs among states which satisfy the above condition and have the same value of  $\Delta M(m_2, m_3)$ . Therefore, having performed the  $l$ -shift for the  $(I, \pm)$  modes as in (3.5.4), we concentrate on the degeneracy in  $\Delta M(m_2, m_3)$  for fixed values of  $(n, l)$ . It is convenient to discuss the  $\hat{\gamma}_2 = \hat{\gamma}_3$  and  $\hat{\gamma}_2 \neq \hat{\gamma}_3$  cases, separately.

$\hat{\gamma}_2 = \hat{\gamma}_3 \equiv \hat{\gamma}$ : This case includes the supersymmetric LM–theory. The deformation enters the mass spectrum only through the difference  $(m_2 - m_3)$  and the splitting term  $\Delta M$  depends only on a single integer  $j$

$$\begin{array}{ll} l \text{ even} & 2j \equiv |m_2 - m_3| = 0, 2, \dots, l & \Delta M(j) = \hat{\gamma} j \\ l \text{ odd} & 2j + 1 \equiv |m_2 - m_3| = 1, 3, \dots, l & \Delta M(j) = \hat{\gamma} \left(j + \frac{1}{2}\right) \end{array} \quad (3.5.5)$$

Excluding for the moment the  $l = 0, 1$  cases, for any given value of  $2j$  and  $2j + 1$  the degeneracies of the corresponding mass levels are listed in Table 3.1 and Table 3.2, respectively.

For any value of  $l \geq 2$  we observe Zeeman–like splitting as shown in Fig. 3.1. Precisely, the splitting occurs in the following way: For  $l$  even there are  $8(l+1)$  d.o.f. corresponding to  $j = 0$  and  $16(l+1)$  for each  $j \neq 0$ . Since we have  $l/2$  possible values of  $j \neq 0$ , the total number of states sum up correctly to  $8(l+1)^2$ . Analogously, for odd values of  $l$  the

State	$ m_2 - m_3  = 2j$	Degeneracy
$\chi, \Phi, A_{III}$	0	$l + 1$
	$2, 4, \dots, l$	$2(l + 1)$
$A_\mu$	0	$l + 1$
	$2, 4, \dots, l$	$2(l + 1)$
$A_{I,+}$	0	$l - 1$
	$2, 4, \dots, l$	$2(l - 1)$
$A_{I,-}$	0	$l + 3$
	$2, 4, \dots, l$	$2(l + 3)$

Table 3.1: Degeneracy of states in the case  $\hat{\gamma}_2 = \hat{\gamma}_3$  and  $l \geq 2$  even. The degeneracy in the third column refers to every single value of  $j$ .

State	$ m_2 - m_3  = 2j + 1$	Degeneracy
$\chi, \Phi, A_{III}$	$1, 3, \dots, l$	$2(l + 1)$
$A_\mu$	$1, 3, \dots, l$	$2(l + 1)$
$A_{I,+}$	$1, 3, \dots, l$	$2(l - 1)$
$A_{I,-}$	$1, 3, \dots, l$	$2(l + 3)$

Table 3.2: Degeneracy of states in the case  $\hat{\gamma}_2 = \hat{\gamma}_3$  and  $l \geq 3$  odd.

number of levels is  $(l + 1)/2$ , each of them corresponds to  $16(l + 1)$  d.o.f., so we still have  $8(l + 1)^2$  modes.

The  $l = 0$  case corresponds to  $m_2 = m_3 = 0$  ( $j = 0$ ). The deformation is then harmless and we are back to the bosonic content of the undeformed theory, that is three scalars  $\chi, \Phi, A_{(I,-)}$  and one vector with  $M^{(0)}(n, 0)$ . Similarly, for  $l = 1$  ( $j = 0$ ), excluding  $A_{(I,+)}$  we have three scalars and one vector in the  $(1/2, 1/2)$  of  $SO(4)$  and one scalar in the  $(3/2, 1/2)$ , all corresponding to  $M^2 = (M^{(0)}(n, 1))^2 + \hat{\gamma}^2 L^2 / R^4$ . These cases can be included in Tables 3.1 and 3.2 with the agreement to discharge modes which are not switched on.

We note that there is an accidental mass degeneracy which is remnant of the undeformed  $\mathcal{N} = 2$  theory. In particular, in the supersymmetric LM case this allows to organize the bosonic states in  $\mathcal{N} = 1$  supermultiplets.

In principle, this unexpected degeneracy could be related to the particular theories we are considering which are smooth deformations of their undeformed counterpart. In order to better understand  $\mathcal{N} = 2$  vs.  $\mathcal{N} = 1$  supersymmetry at the level of mesonic spectrum, the study of the fermionic sector is a mandatory requirement.

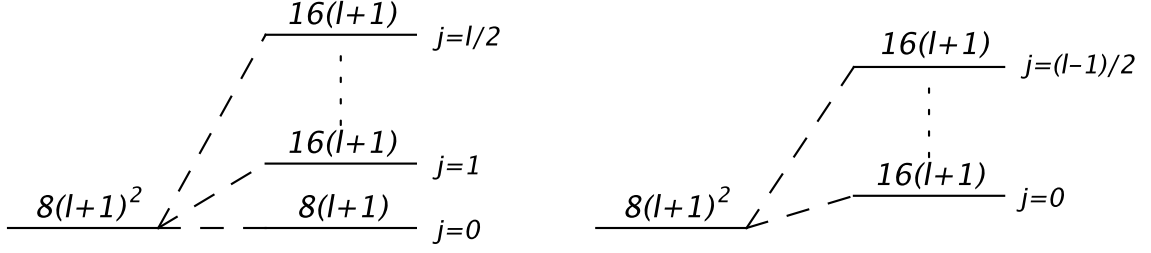


Figure 3.1: The Zeeman–splitting of the undeformed  $8(l+1)^2$  d.o.f. for  $\hat{\gamma}_2 = \hat{\gamma}_3$  and  $l$  even (left) or odd (right).

$\hat{\gamma}_2 \neq \hat{\gamma}_3$ : The splitting term  $\Delta M$  now depends on both  $m_{2,3}$  and no longer on their difference. In order to make the comparison with the  $\hat{\gamma}_2 = \hat{\gamma}_3$  case easier, for fixed  $l$  it is convenient to label  $\Delta M$  by two numbers  $j$  and  $s$

$$\begin{aligned}
l \text{ even} \quad \Delta M(j, s) &= \frac{(j+s)\hat{\gamma}_2 + (j-s)\hat{\gamma}_3}{2} \\
l \text{ odd} \quad \Delta M(j, s) &= \frac{(j+\frac{1}{2}+s)\hat{\gamma}_2 + (j+\frac{1}{2}-s)\hat{\gamma}_3}{2}
\end{aligned} \tag{3.5.6}$$

where  $j$  is still defined as before, whereas  $s$  is integer if  $l$  is even and half-integer if  $l$  is odd. Its range can be read in Tables 3.3 and 3.4.

State	$ m_2 - m_3  = 2j$	$s$	Degeneracy
$\chi, \Phi, A_{III}$	0	0	1
		$1, 2, \dots, \frac{l}{2}$	2
	$2, 4, \dots, l$	$-\frac{l}{2}, \dots, 0, \dots, \frac{l}{2}$	2
$A_\mu$	0	0	1
		$1, 2, \dots, \frac{l}{2}$	2
	$2, 4, \dots, l$	$-\frac{l}{2}, \dots, 0, \dots, \frac{l}{2}$	2
$A_{I,+}$	0	0	1
		$1, 2, \dots, \frac{l-2}{2}$	2
	$2, 4, \dots, l$	$-\frac{l-2}{2}, \dots, 0, \dots, \frac{l-2}{2}$	2
$A_{I,-}$	0	0	1
		$1, 2, \dots, \frac{l+2}{2}$	2
	$2, 4, \dots, l$	$-\frac{l+2}{2}, \dots, 0, \dots, \frac{l+2}{2}$	2

Table 3.3: Degeneracy of states in the case  $\hat{\gamma}_2 \neq \hat{\gamma}_3$  and  $l \geq 2$  even. The degeneracy in the fourth column refers to every single pair  $(j, s)$ .

State	$ m_2 - m_3  = 2j + 1$	$s$	Degeneracy
$\chi, \Phi, A_{III}$	$1, 3, \dots, l$	$-\frac{l}{2}, \dots, \frac{l}{2}$	2
$A_\mu$	$1, 3, \dots, l$	$-\frac{l}{2}, \dots, \frac{l}{2}$	2
$A_{I,+}$	$1, 3, \dots, l$	$-\frac{l-2}{2}, \dots, \frac{l-2}{2}$	2
$A_{I,-}$	$1, 3, \dots, l$	$-\frac{l+2}{2}, \dots, \frac{l+2}{2}$	2

Table 3.4: Degeneracy of states in the case  $\hat{\gamma}_2 \neq \hat{\gamma}_3$  and  $l \geq 3$  odd.

As appears in the Tables the degeneracy is almost completely broken. In fact, except for the  $m_2 = m_3 = 0$  case, only a residual degeneracy 2 survives due to the fact that the mass (3.5.2) is invariant under the exchange  $(m_2, m_3) \rightarrow (-m_2, -m_3)$ .

To better understand the level splitting it is convenient to compare the present situation with the previous one. In fact, fixing  $j$ , the degenerate degrees of freedom of the  $\hat{\gamma}_2 = \hat{\gamma}_3$  case further split according to the different values of  $s$ . If  $l$  is even and  $j = 0$ , the previous  $8(l+1)$  degenerate levels split in  $(l/2 + 2)$  new mass levels, while for  $j \neq 0$  the  $16(l+1)$  levels open up in  $(l+3)$  levels (see Fig. 3.2). If  $l$  is odd we find  $(l+3)$  different mass levels as drawn in Fig. 3.3.

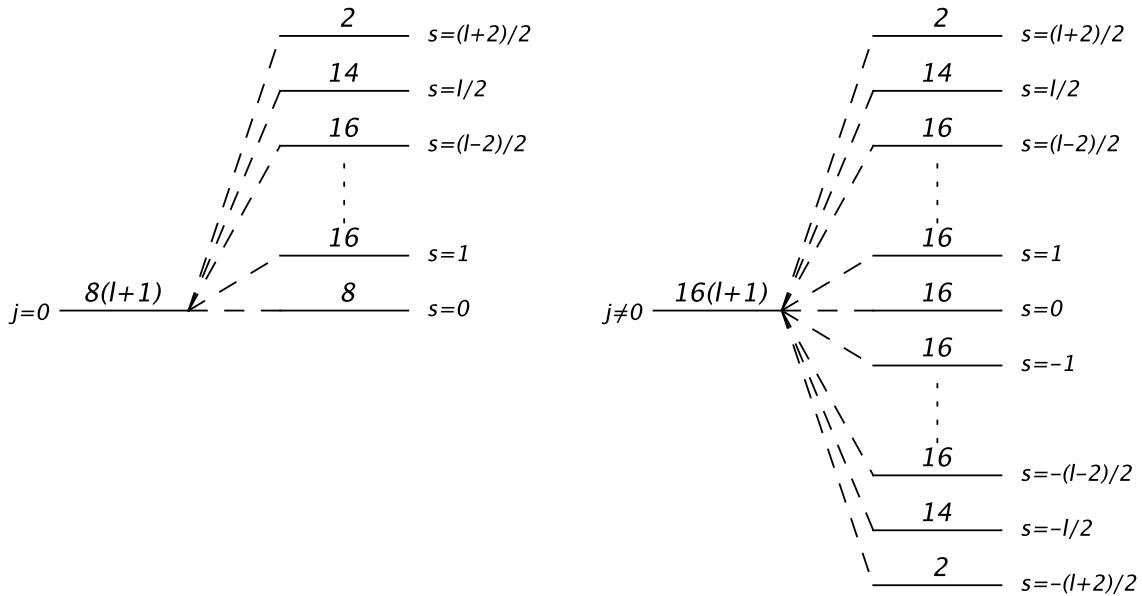


Figure 3.2: The Zeeman-splitting of the  $\hat{\gamma}_2 = \hat{\gamma}_3 = \hat{\gamma}$  d.o.f. for  $\hat{\gamma}_2 \neq \hat{\gamma}_3$  and  $l$  even. The value of  $\Delta M$  here appearing is pictured considering the case  $\hat{\gamma}_3 < \hat{\gamma} < \hat{\gamma}_2$ .

The particular cases  $l = 0, 1$  can be read from Tables 3.3 and 3.4 by discharging  $(A_{(I,+)}, A_{III})$  and  $A_{(I,+)}$ , respectively. For  $l = 0$  three modes  $\chi, \Phi$  and  $A_\mu$  correspond to

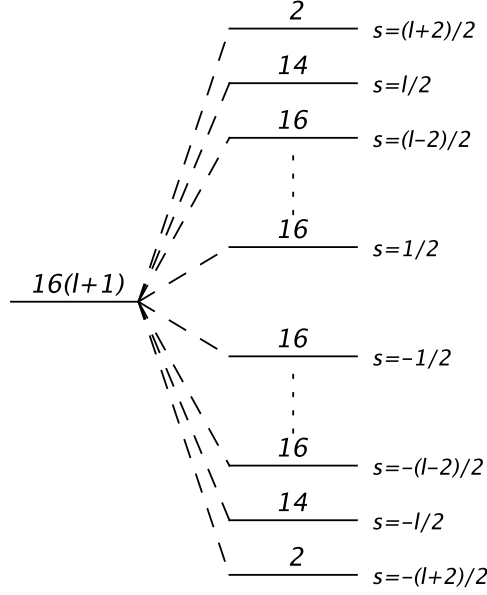


Figure 3.3: The Zeeman-splitting of the  $\hat{\gamma}_2 = \hat{\gamma}_3$  d.o.f. for  $\hat{\gamma}_2 \neq \hat{\gamma}_3$  and  $l$  odd. Once again  $\hat{\gamma}_3 < \hat{\gamma} < \hat{\gamma}_2$ .

$\Delta M = 0$  ( $j = s = 0$ ), whereas the three degrees of freedom of  $A_{(I,-)}$  split into one d.o.f. with  $\Delta M = 0$  ( $j = s = 0$ ) and two with  $\Delta M = \frac{\hat{\gamma}_2 - \hat{\gamma}_3}{2}$  ( $j = s = 1$ ). Already in the simplest  $l = 0$  case the  $SO(4)$  breaking is manifest. For  $l = 1$  ( $j = 0$ ) the four degrees of freedom of each mode  $\chi$ ,  $\Phi$ ,  $A_{III}$  and  $A_\mu$  now split into two states with  $\Delta M = \hat{\gamma}_2/2$  and two states with  $\Delta M = \hat{\gamma}_3/2$ . On the other hand, the 8 d.o.f. corresponding to  $A_{(I,-)}$  split into two states with  $\Delta M = \hat{\gamma}_2/2$ , two states with  $\Delta M = \hat{\gamma}_3/2$ , two states with  $\Delta M = (2\hat{\gamma}_2 - \hat{\gamma}_3)/2$  and two with  $\Delta M = (2\hat{\gamma}_3 - \hat{\gamma}_2)/2$ .

As discussed in [36] the undeformed spectrum exhibits a huge degeneracy in  $\nu \equiv n + l$  which can be traced back to a (non-exact)  $SO(5)$  symmetry. This originates from the fact that the induced metric on the D7-brane is conformally equivalent to  $E^{(1,3)} \times S^4$ . If in the quadratic action for the fluctuations the conformal factor can be re-absorbed by a field redefinition the corresponding equations of motion are invariant under  $S^4$  diffeomorphisms. Therefore, solutions can be found by expanding in spherical harmonics of  $S^4$  and the mass spectrum of the elementary modes depends only on the  $SO(5)$  quantum number  $\nu$ . This happens for instance for scalar modes and vectors which, for a given  $\nu$ , organize themselves into reducible representations  $(0, 0) \oplus (1/2, 1/2) \cdots \oplus (\nu/2, \nu/2)$  of  $SO(4)$ . This is indeed the decomposition of the highest weight representation  $[\nu, 0]$  of  $SO(5)$  in  $SO(4)$  representations.

In principle, the same analysis can be applied also to our case. Here the induced metric (3.2.11) is conformally equivalent to  $E^{(1,3)} \times \tilde{S}^4$  where  $\tilde{S}^4$  is the deformed four-sphere (set

$\varrho = \rho/L$ )

$$ds_{\mathbb{S}^4}^2 = \frac{R^4}{4L^2} \frac{4}{(1 + \varrho^2)^2} (d\varrho^2 + \varrho^2 d\tilde{\Omega}_3^2) \quad (3.5.7)$$

and

$$d\tilde{\Omega}_3^2 = d\theta^2 + G \left[ c_\theta^2 d\phi_2^2 + s_\theta^2 d\phi_3^2 + \frac{\varrho^2 c_\theta^2 s_\theta^2 (\hat{\gamma}_2 d\phi_2 + \hat{\gamma}_3 d\phi_3)^2}{(1 + \varrho^2)^2} \right] \quad (3.5.8)$$

is the deformed three–sphere.

It follows that a dependence on the  $SO(5)$  quantum number  $\nu = n + l$  still appears if the conformal factor  $(1 + \varrho^2)L^2/R^2$  can be compensated by a field redefinition and the action can be entirely expressed in terms of the metric of  $E^{(1,3)} \times \mathbb{S}^4$  plus deformations. A close look at the action (3.3.13) reveals that this is always the case for the decoupled modes  $\chi$ ,  $A_\mu$  and also for  $\Phi$ . Despite of the presence of the deformation terms which break explicitly the  $SO(5)$  invariance, we can still search for solutions expanded in spherical harmonics on  $\mathbb{S}^4$  and, consequently, the mass spectrum exhibits a dependence on  $n$  and  $l$  only in the combination  $n + l$ . In particular, in the zero–mode sector  $m_2 = m_3 = 0$  a degeneracy appears which is remnant of the  $SO(5)$  invariance. Of course, the eigenstates corresponding to degenerate eigenvalues never reconstruct the complete  $[\nu, 0]$  representation of  $SO(5)$ , being organized into a direct product of  $SO(4)$  representations with integer spins only  $(0, 0) \oplus (1, 1) \cdots ([\nu/2], [\nu/2])$ , since  $m_2 = m_3 = 0$  only occurs for even values of  $l$ .

## 3.6 The dual field theory

In this Section we construct the 4D conformal field theory whose composite operators are dual to the mesonic states just found.

As already discussed in Section 3.2, in the supergravity description the operations of  $TsT$  deforming the  $\text{AdS}_5 \times \mathbb{S}^5$  background and adding D7–branes commute. Since on the field theory side  $TsT$  deformations correspond to promoting all the products among the fields to be  $*$ –products [19], whereas the addition of D7–branes corresponds to adding interacting fundamental matter [30] we expect that in determining the action for the dual field theory the operations of  $*$ –product deformation and addition of fundamental matter commute. Therefore, in order to obtain the dual action we proceed by promoting to  $*$ –products all the products in the  $\mathcal{N} = 2$  SYM action with fundamental matter (2.3.1) corresponding to the undeformed Karch–Katz model.

Given  $N_f$  probe D7–branes embedded in the ordinary  $\text{AdS}_5 \times \mathbb{S}^5$  background with  $N$  units of flux,  $N \gg N_f$ , in the large  $N$  limit the dual field theory on the D3–branes consists of  $\mathcal{N} = 4$   $SU(N)$  SYM coupled in a  $\mathcal{N} = 2$  fashion to  $N_f$   $\mathcal{N} = 2$  hypermultiplets which contain new dynamical fields arising from open strings stretching between D3 and D7–branes.



The lagrangian has been given in the previous Chapter (see eq. (2.3.1)). For convenience, we report it here

$$\begin{aligned} \mathcal{L} = & \int d^4\theta \left[ \text{Tr} \left( e^{-gV} \bar{\Phi}_i e^{gV} \Phi^i \right) + \text{tr} \left( \bar{Q} e^{gV} Q + \tilde{Q} e^{-gV} \bar{\tilde{Q}} \right) \right] + \frac{1}{2g^2} \int d^2\theta \text{Tr} (W^\alpha W_\alpha) \\ & + i \int d^2\theta \left[ g \text{Tr} (\Phi^1 [\Phi^2, \Phi^3]) + g \text{tr} (\tilde{Q} \Phi^1 Q) + m \text{tr} (\tilde{Q} Q) \right] + h.c. \end{aligned} \quad (3.6.1)$$

According to the AdS/CFT duality the lowest components of the three chirals  $\Phi_i$  are in one-to-one correspondence with the three complex coordinates of the internal 6D space as (we use notations consistent with Section 2)

$$\begin{aligned} X^1 + iX^2 &\equiv u\rho_3 e^{i\phi_3} \rightarrow \Phi_3|_{\theta=\bar{\theta}=0} \\ X^3 + iX^4 &\equiv u\rho_2 e^{i\phi_2} \rightarrow \Phi_2|_{\theta=\bar{\theta}=0} \\ X^5 + iX^6 &\equiv u\rho_1 e^{i\phi_1} \rightarrow \Phi_1|_{\theta=\bar{\theta}=0} \end{aligned} \quad (3.6.2)$$

Since we are interested in non-supersymmetric deformations of this theory we need the Lagrangian (3.6.1) expanded in components. Given the physical components of the multiplets being

$$\begin{aligned} \Phi^i &= (a^i, \psi_\alpha^i) & Q^r &= (q^r, \chi_\alpha^r) \\ W_\alpha &= (\lambda_\alpha, f_{\alpha\beta}) & \tilde{Q}_r &= (\tilde{q}_r, \tilde{\chi}_{r\alpha}) \end{aligned} \quad (3.6.3)$$

after eliminating the auxiliary fields through their algebraic equations of motion, the Lagrangian (2.3.1) takes the form

$$\mathcal{L} = \mathcal{L}_{\mathcal{N}=4} + \mathcal{L}_b + \mathcal{L}_f + \mathcal{L}_{int} \quad (3.6.4)$$

where \*\*

$$\begin{aligned} \mathcal{L}_{\mathcal{N}=4} = & \text{Tr} \left( -\frac{1}{2} f^{\alpha\beta} f_{\alpha\beta} + i\lambda [\nabla, \bar{\lambda}] + \bar{a}_i \square a^i + i\psi^i [\nabla, \bar{\psi}_i] \right) \\ & + g^2 \text{Tr} \left( -\frac{1}{4} [a^i, \bar{a}_i] [a^j, \bar{a}_j] + \frac{1}{2} [a^i, a^j] [\bar{a}_i, \bar{a}_j] \right) \\ & + \left\{ ig \text{Tr} \left( [\bar{\psi}_i, \bar{\lambda}] a^i + \frac{1}{2} \epsilon_{ijk} [\psi^i, \psi^j] a^k \right) + h.c. \right\} \end{aligned} \quad (3.6.5)$$

is the ordinary  $\mathcal{N} = 4$  Lagrangian,

$$\begin{aligned} \mathcal{L}_b = & \text{tr} \left( \bar{q} (\square - |m|^2) q + \tilde{q} (\square - |m|^2) \bar{\tilde{q}} \right) \\ & - \frac{g^2}{4} \text{tr} \left( \bar{q} q \bar{q} q + \tilde{q} \bar{\tilde{q}} \tilde{q} \bar{\tilde{q}} - 2\bar{q} \tilde{q} \tilde{q} q + 4\tilde{q} \bar{\tilde{q}} \bar{q} q \right) + \frac{g^2}{2} \text{tr} \left( \bar{q} [a^i, \bar{a}_i] \tilde{q} - \bar{q} [a^i, \bar{a}_i] q \right) \\ & - \left\{ \text{tr} \left( g\bar{m} (\bar{q} a_1 q + \tilde{q} a_1 \bar{\tilde{q}}) + \frac{g^2}{2} (\bar{q} \bar{a}_1 a^1 q + \tilde{q} a^1 \bar{a}_1 \bar{\tilde{q}} + 2\tilde{q} [\bar{a}_2, \bar{a}_3] q) \right) + h.c. \right\} \end{aligned} \quad (3.6.6)$$

---

\*\*We use superspace conventions of [1]. When  $\psi\lambda$  indicates the product of two chiral fermions it has to be understood as  $\psi^\alpha\lambda_\alpha$ . The same convention is used for antichiral fermions.

describes the bosonic fundamental sector and its interactions with bosonic matter in the adjoint

$$\mathcal{L}_f = i \operatorname{tr} \left( \bar{\chi} \overrightarrow{\nabla} \chi - \tilde{\chi} \overleftarrow{\nabla} \tilde{\chi} \right) + \left\{ im \operatorname{tr} \left( \tilde{\chi} \chi \right) + h.c. \right\} \quad (3.6.7)$$

describes the free fermionic fundamental sector and

$$\mathcal{L}_{int} = ig \operatorname{tr} \left( \bar{\chi} \bar{\lambda} q - \tilde{q} \bar{\lambda} \tilde{\chi} + \tilde{q} \psi^1 \chi + \tilde{\chi} \psi^1 q + \tilde{\chi} a^1 \chi \right) + h.c. \quad (3.6.8)$$

contains the interaction terms between bosons and fermions.

The most general non-supersymmetric marginal deformation of this theory can be obtained by promoting all the products among the fields in the Lagrangian to be  $*$ -products according to the following prescription [66]

$$f g \longrightarrow f * g = e^{i\pi Q_i^f Q_j^g \epsilon_{ijk} \gamma_k} f g \quad (3.6.9)$$

where  $\gamma_k$  are the deformation parameters, whereas  $(Q_1, Q_2, Q_3)$  are the charges of the fields under the three  $U(1)$  global symmetries of the original  $\mathcal{N} = 4$  theory associated to the Cartan generators of  $SU(4)$ . On the dual supergravity side they correspond to angular shifts in (3.6.2). Accordingly, the charges of the chiral  $\Phi_i$  superfields are chosen as in Table 3.5 [66] with the additional requirement for the charges of the spinorial super-space coordinates to be  $(1/2, 1/2, 1/2)$ . This insures invariance of the superpotential term  $\int d^2\theta \operatorname{Tr}(\Phi^1[\Phi^2, \Phi^3])$  under the three  $U(1)$ 's. The charges for the matter chiral superfields are determined by requiring the superpotential term  $\int d^2\theta \operatorname{tr}(\tilde{Q}\Phi^1 Q)$  to respect the three global symmetries in addition to the condition for  $Q$  and  $\tilde{Q}$  to have the same charges.

	$\Phi^1$	$\Phi^2$	$\Phi^3$	$Q$	$\tilde{Q}$
$Q_1$	1	0	0	0	0
$Q_2$	0	1	0	$\frac{1}{2}$	$\frac{1}{2}$
$Q_3$	0	0	1	$\frac{1}{2}$	$\frac{1}{2}$

Table 3.5:  $U(1)$  charges of the chiral superfields. The corresponding antichirals have opposite charges.

The gauge superfield  $W_\alpha$  and the gaugino have charges  $(1/2, 1/2, 1/2)$ , whereas the gauge field strength  $f_{\alpha\beta}$  is neutral under the three  $U(1)$ 's.

In the absence of mass term in (3.6.1) the corresponding currents  $(J_{\phi_1}, J_{\phi_2}, J_{\phi_3})$  are conserved, whereas  $J_{\phi_1}$  fails to be conserved when  $m \neq 0$ . Moreover,  $(J_{\phi_2}, J_{\phi_3})$  are ABJ-anomaly free also in the presence of fundamental matter, whereas  $J_{\phi_1}$  is non-anomalous only in the quenching limit  $N_f/N \rightarrow 0$ .

As is well-known, the ordinary Lunin-Maldacena  $U(1) \times U(1)$  charges [19] are associated to  $(\varphi_1, \varphi_2)$  angular shifts after performing the change of variables (in our notations)

$$\varphi_1 = \frac{1}{3}(\phi_1 + \phi_2 - 2\phi_3), \quad \varphi_2 = \frac{1}{3}(\phi_2 + \phi_3 - 2\phi_1), \quad \varphi_3 = \frac{1}{3}(\phi_1 + \phi_2 + \phi_3), \quad (3.6.10)$$

Expressing the  $(J_{\varphi_1}, J_{\varphi_2})$  generators in terms of  $(J_{\phi_1}, J_{\phi_2}, J_{\phi_3})$  we easily find that the Lunin–Maldacena charges are given by

$$Q_1^{(LM)} = Q_2 - Q_3 \quad , \quad Q_2^{(LM)} = Q_2 - Q_1 \quad (3.6.11)$$

In the case of supersymmetric deformations the third linear combination  $Q_R \sim (Q_1 + Q_2 + Q_3)$  provides the R–symmetry charge.

We are now ready to derive the deformed action by using the prescription (3.6.9) in the original undeformed one.

We begin with the one–parameter deformation,  $\gamma_1 = \gamma_2 = \gamma_3$ . In this case  $\mathcal{N} = 1$  supersymmetry survives and we can work directly with the superspace action (3.6.1). Since only for  $m = 0$  the  $*$ –product is well–defined being the three U(1) charges conserved, the correct way to proceed is to deform the massless theory and then add the mass operator as a perturbation. Following this prescription and taking into account the superfields charges given in Table 3.5, the Lagrangian of the deformed theory is

$$\begin{aligned} \mathcal{L} = & \int d^4\theta \left[ \text{Tr} \left( e^{-gV} \bar{\Phi}_i e^{gV} \Phi^i \right) + \text{tr} \left( \bar{Q} e^{gV} Q + \tilde{Q} e^{-gV} \bar{\tilde{Q}} \right) \right] + \frac{1}{2g^2} \int d^2\theta \text{Tr} (W^\alpha W_\alpha) \\ & + ig \int d^2\theta \left[ \text{Tr} \left( e^{i\pi\gamma} \Phi_1 \Phi_2 \Phi_3 - e^{-i\pi\gamma} \Phi_1 \Phi_3 \Phi_2 \right) + \text{tr} \left( \tilde{Q} \Phi_1 Q \right) + m \text{tr} \left( \tilde{Q} Q \right) \right] \quad (3.6.12) \end{aligned}$$

We note that a non–trivial deformation appears in the superpotential only in the pure adjoint sector. The interaction and the mass terms involving flavor matter do not change, so that the vev for  $\Phi_1$  which is related to the D7–brane location through the dictionary (3.6.2) is the same as in the undeformed theory,  $\langle \Phi_1 \rangle = -m/g \equiv L$ . Since in the supergravity description we have chosen  $L$  to be real ( $X^5 = L$ ,  $X^6 = 0$ ) here and in what follows we restrict to real values of  $m$ .

As already stressed, for  $m \neq 0$  the  $Q_1$  charge is not conserved, neither is  $Q_2^{(LM)}$ . Therefore, this deformed theory possesses only one U(1) non–R–symmetry corresponding to  $Q_1^{(LM)}$ .

The action (3.6.12) has been obtained by  $*$ –product deforming the  $\mathcal{N} = 2$  SYM action (3.6.1). However, it could have been equivalently obtained by adding fundamental chiral matter to the  $\mathcal{N} = 1$   $\beta$ –deformed SYM theory of [19]. In particular, the appearance of the gauge coupling constant in front of the adjoint chiral superpotential insures that for  $m = 0$  and in the probe approximation the theory is superconformal invariant [67].

We now consider the more general non–supersymmetric case. We implement the  $*$ –product (3.6.9) in the action (3.6.4). Using the deformed commutator [66]

$$[X_i, X_j]_{M_{ij}} \equiv e^{i\pi M_{ij}} X_i X_j - e^{-i\pi M_{ij}} X_j X_i \quad (3.6.13)$$

where for  $X_i$  fermions

$$M_{\text{fermions}} \equiv B = \begin{pmatrix} 0 & \frac{1}{2}(\gamma_1 + \gamma_2) & -\frac{1}{2}(\gamma_1 + \gamma_3) & -\frac{1}{2}(\gamma_2 - \gamma_3) \\ -\frac{1}{2}(\gamma_1 + \gamma_2) & 0 & \frac{1}{2}(\gamma_2 + \gamma_3) & -\frac{1}{2}(\gamma_3 - \gamma_1) \\ \frac{1}{2}(\gamma_3 + \gamma_1) & -\frac{1}{2}(\gamma_2 + \gamma_3) & 0 & -\frac{1}{2}(\gamma_1 - \gamma_2) \\ \frac{1}{2}(\gamma_2 - \gamma_3) & \frac{1}{2}(\gamma_3 - \gamma_1) & \frac{1}{2}(\gamma_1 - \gamma_2) & 0 \end{pmatrix} \quad (3.6.14)$$

whereas for scalars

$$M_{\text{scalars}} \equiv C = \begin{pmatrix} 0 & \gamma_3 & -\gamma_2 \\ -\gamma_3 & 0 & \gamma_1 \\ \gamma_2 & -\gamma_1 & 0 \end{pmatrix} \quad (3.6.15)$$

the deformed  $\mathcal{L}_{\mathcal{N}=4}$  takes the form

$$\begin{aligned} \mathcal{L}_{\mathcal{N}=4} &= \text{Tr} \left( -\frac{1}{2} f^{\alpha\beta} f_{\alpha\beta} + i\lambda [\nabla, \bar{\lambda}] + \bar{a}_i \square a^i + i\psi^i [\nabla, \bar{\psi}_i] \right) \\ &+ g^2 \text{Tr} \left( -\frac{1}{4} [a^i, \bar{a}_i] [a^j, \bar{a}_j] + \frac{1}{2} [a^i, a^j]_{C_{ij}} [\bar{a}_i, \bar{a}_j]_{C_{ij}} \right) \\ &+ \left\{ ig \text{Tr} \left( [\bar{\psi}_i, \bar{\lambda}]_{B_{i4}} a^i + \frac{1}{2} \epsilon_{ijk} [\psi^i, \psi^j]_{B_{ij}} a^k \right) + h.c. \right\} \end{aligned} \quad (3.6.16)$$

while the bosonic sector reads

$$\begin{aligned} \mathcal{L}_b &= \text{tr} \left( \bar{q} (\square - m^2) q + \tilde{q} (\square - m^2) \tilde{q} \right) - \frac{g^2}{4} \text{tr} \left( \bar{q} q \bar{q} q + \tilde{q} \tilde{q} \tilde{q} \tilde{q} - 2\bar{q} \tilde{q} \tilde{q} q + 4\tilde{q} \tilde{q} \bar{q} q \right) \\ &+ \frac{g^2}{2} \text{tr} \left( \tilde{q} [a^i, \bar{a}_i] \tilde{q} - \bar{q} [a^i, \bar{a}_i] q + \bar{q} \bar{a}_1 a^1 q + \tilde{q} a^1 \bar{a}_1 \tilde{q} \right) \\ &+ \left\{ g^2 \text{tr} \left( \tilde{q} [\bar{a}_2, \bar{a}_3]_{C_{23}} q \right) - gm \text{tr} \left( e^{-i\pi(\gamma_2 - \gamma_3)} \bar{q} a^1 q + e^{i\pi(\gamma_2 - \gamma_3)} \tilde{q} a^1 \tilde{q} \right) + h.c. \right\} \end{aligned} \quad (3.6.17)$$

and the fermionic one

$$\mathcal{L}_f = i \text{tr} \left( \bar{\chi} \overleftrightarrow{\nabla} \chi - \tilde{\chi} \overleftrightarrow{\nabla} \tilde{\chi} \right) + \left\{ im \text{tr} \left( \tilde{\chi} \chi \right) + h.c. \right\} \quad (3.6.18)$$

Finally the boson–fermion interaction terms become

$$\begin{aligned} \mathcal{L}_{int} &= ig \text{tr} \left( e^{i\frac{\pi}{4}(\gamma_2 - \gamma_3)} \bar{\chi} \bar{\lambda} q - e^{-i\frac{\pi}{4}(\gamma_2 - \gamma_3)} \tilde{q} \bar{\lambda} \tilde{\chi} \right. \\ &\quad \left. + e^{i\frac{\pi}{4}(\gamma_2 - \gamma_3)} \tilde{q} \psi^1 \chi + e^{-i\frac{\pi}{4}(\gamma_2 - \gamma_3)} \tilde{\chi} \psi^1 q + \tilde{\chi} a^1 \chi \right) + h.c. \end{aligned} \quad (3.6.19)$$

We observe that the fundamental fields  $q$  and  $\tilde{q}$  experiment the  $\gamma_1$ -deformation only through the modified commutator  $[\bar{a}_2, \bar{a}_3]_{C_{23}}$  in  $\mathcal{L}_b$ . Moreover,  $\gamma_2$  and  $\gamma_3$  are always present in the combination  $(\gamma_2 - \gamma_3)$  so that the corresponding phases disappear when  $\gamma_2 = \gamma_3$ , in particular for supersymmetric deformations.

### 3.7 Conclusions

In this first part of the thesis we have studied the embedding of D7-branes in LM-Frolov backgrounds with the aim of finding the mesonic spectrum of the dual Yang-Mills theory with flavors, according to the gauge/gravity correspondence. Since these theories have  $\mathcal{N} = 1$  or no supersymmetry depending on the choice of the deformation parameters  $\hat{\gamma}_i$ , they provide an interesting playground in the study of generalizations of the AdS/CFT correspondence to more realistic models with less supersymmetry.

These geometries are smoothly related to the standard  $\text{AdS}_5 \times \text{S}^5$  from which they can be obtained by operating with  $TsT$  transformations. Therefore, if we consider D7-brane embeddings which closely mimic the ones of the undeformed case [30] we expect the flavor probes to share some properties with the probes of the undeformed case. Driven by this observation we have considered a spacetime filling D7-brane wrapped on a deformed three-sphere in the internal coordinates. We have found that for both the supersymmetric and the non-supersymmetric deformations a static configuration exists which is completely independent of the specific values of the deformation parameters  $\hat{\gamma}_i$ . As a consequence the D7-brane still lies at fixed values of its transverse directions and exhibits no quark condensate [30]. We remark that this shape is exact and stable in the supersymmetric as well as in the non-supersymmetric cases.

Although the shape of the brane does not feel the effects of the deformation, its fluctuations do. In fact, studying the scalar and vector fluctuations we have found that a non-trivial dependence on the  $\hat{\gamma}_{2,3}$  parameters appears both in terms which correct the free dynamics of the modes and in terms which couple the  $U(1)$  worldvolume gauge field to one of the scalars in the mutual orthogonal directions to the D3-D7 system. All the deformation-dependent contributions arise from the Dirac-Born-Infeld term in the D7-brane action, whereas the Wess-Zumino term does not feel the deformation. The  $\hat{\gamma}_1$  parameter, associated to a  $TsT$  transformation along the torus inside the D7 worldvolume, never enters the equations of motion.

A smooth limit to the undeformed equations of motion exists for  $\hat{\gamma}_i \rightarrow 0$ . In this limit all the modes decouple and we are back to the undeformed solutions of [36]. The effect of the deformations becomes negligible also in the UV limit ( $\rho \rightarrow \infty$ ). This is an expected result since the deformations involve tori in the internal space and in the UV limit the metric of the background reduces to flat four dimensional Minkowski spacetime.

On the other hand, the situation changes once we consider the general deformed equations. In fact, solving analytically these equations for elementary excitations of scalars and vectors we have found that the mass spectrum is still discrete and with a mass gap and the corresponding eigenstates match the one of the undeformed case. However, the mass eigenvalues acquire a non-trivial dependence on  $\hat{\gamma}_{2,3}$ . These new terms, being proportional to the  $U(1) \times U(1)$  quantum numbers  $(m_2, m_3)$ , induce a level spitting according to a Zeeman-like effect.

We have performed a detailed analysis of the level splitting and of the corresponding degeneracy. The situation turns out to be very different according to  $\hat{\gamma}_2$  and  $\hat{\gamma}_3$  being equal or not. In fact, for  $\hat{\gamma}_2 \neq \hat{\gamma}_3$  the degeneracy is almost completely broken since only a residual degeneracy associated to the invariance of the mass under  $(m_2, m_3) \rightarrow (-m_2, -m_3)$  survives. In particular, the breaking of  $SO(4)$  is manifest. Instead, for  $\hat{\gamma}_2 = \hat{\gamma}_3$  the mass levels split but for each value of the mass an accidental degeneracy survives which is remnant of the  $\mathcal{N} = 2$  case. While in the supersymmetric case ( $\hat{\gamma}_1 = \hat{\gamma}_2 = \hat{\gamma}_3$ ) this allows to arrange mesons in massive  $\mathcal{N} = 1$  multiplets according to the fact that our embedding preserves supersymmetry, this higher degree of degeneracy in the bosonic sector of the theory does not have a clear explanation at the moment. In order to make definite statements about the supersymmetry properties of the mesonic spectrum and supersymmetry breaking one should study the fermionic sector. A useful strategy could be the bottom–up approach described in [47]. We leave this interesting open problem for the future.

Our analysis shares some similarities with other cases considered in the literature.

First of all, we have found that a stable embedding of the probe brane can be realized which is static and independent of the deformation parameters. This feature has been already encountered for other brane configurations in deformed backgrounds. An example is given by particular dynamical probe D3–branes (giant gravitons) which have been first well understood in [55]. In fact, there it has been shown that giant gravitons exist and are stable even in the absence of supersymmetry and their dynamics turns out to be completely independent of the deformation parameters, being then equal to the one of the undeformed theory. Moreover, since the giants wrap the same cycle inside the internal deformed space as our D7–brane does, their bosonic fluctuations encode the same dependence on the deformation parameters observed in the mesonic spectrum coming from the D7.

A second similarity emerges with the case of flavors in non–commutative theories investigated in [41]. In fact, the non–trivial coupling between scalar and gauge modes that in our case is induced by the deformation resembles the one which appears in the case of D7–branes embedded in  $AdS_5 \times S^5$  with a  $B$  field turned on along spacetime directions. This is not surprising since both theories can be obtained performing a  $TsT$  transformation of  $AdS_5 \times S^5$ : If the  $TsT$  is performed in AdS one obtains the dual of a non–commutative theory while the LM–Frolov picture is recovered if this transformation deforms the internal  $S^5$ .

The field theory dual to the (super)gravity picture we have considered can be obtained by deforming the standard action for  $\mathcal{N} = 4$  super Yang–Mills coupled to massive  $\mathcal{N} = 2$  hypermultiplets by the  $\ast$ –product prescription [19]. In principle, in the supergravity dual description this should correspond to performing a  $TsT$  deformation *after* the embedding of the probe brane. However, as we have discussed, adding the flavor brane in the deformed background or deforming the Karch–Katz D3–D7 configuration are commuting operations.

Therefore, the prescription we propose on the field theory side is consistent with what we have done on the string theory side. It is important to stress that the choice of the embedding we have made is crucial for the above reasoning.

What we obtain is a deformed gauge field theory with massive fundamental matter parametrized by four real parameters  $\gamma_i$  and  $m$ . We can play with them in order to break global  $U(1)$  symmetries, conformality and/or supersymmetry in a very controlled way. In fact, in the quenching approximation a non-vanishing mass parameter related to the location of the probe in the dual geometry breaks conformal invariance and one of the  $U(1)$  global symmetries of the massless theory. On the other hand, the values of the deformation parameters  $\gamma_i$  determine the degree of supersymmetry of the theory, as already discussed. It is interesting to note that as we found on the gravity side, the three deformation parameters play different roles in the fundamental sector of the theory. In fact,  $\gamma_{2,3}$  always appear in the combination  $(\gamma_2 - \gamma_3)$ , so that if  $\gamma_2 = \gamma_3$  this sector gets deformed only by  $\gamma_1$ -dependent phases induced by the interaction with the adjoint matter. In the supersymmetric case this particular behavior is manifest when using superspace formalism since a non-trivial deformation appears only in the adjoint sector, whereas the flavor superpotential remains undeformed.

Let us conclude mentioning some directions in which this work could be extended. We have considered only the non-interacting mesonic sector. Expanding the D7-brane action beyond the second order in  $\alpha'$  one can get informations on the interactions among the mesons and understand how the deformation enters the couplings. Moreover, one could extend our analysis to mesons with large spin in Minkowski, similarly to what has been done in the ordinary, undeformed case [36].

Finally it could be very interesting to study in detail the other embeddings proposed in [57] and in particular the one which seems to exhibit chiral symmetry breaking. Moreover, going beyond the quenching approximation has been representing an interesting subject since the recent efforts to study back-reacted models [46].





## Part II

# Scattering amplitudes in $\mathcal{N} = 4$ SYM theory



# Chapter 4

## General introduction to scattering amplitudes

On-shell scattering amplitudes are one of the most basic quantities that can be computed in any theory. Their connections to physical observables of primary importance, like the cross sections and the time of decay of particles, make of them crucial objects in order to understand the behavior of a theory.

We are mainly interested in scattering processes in non-abelian gauge theories: For definiteness, we concentrate on the  $SU(N)$  gauge theory. The scattered particles are massless particles described by on-shell momenta  $p_i$  ( $p_i^2 = 0$ ) and helicity  $\lambda_i$ . Any particle carries also an adjoint gauge index  $a_i = 1, \dots, N^2 - 1$ .

In quantum field theories, the LSZ theorem [70] relates scattering amplitudes to Green's functions. At weak coupling, Green's functions can be computed from the lagrangian of the theory through the technology of Feynman diagrams. The symmetries of the action turn out to be manifest not at the level of single Feynman diagrams but when they are resummed into physical quantities. This usually complicates a lot the computation: Expected simplicity in the results is hidden inside very cumbersome intermediate expressions, in particular when loop corrections are taken into account. This fact motivated throughout the years a lot of activity with the aim to find shortcuts in the computational processes.

There are mainly two non-exclusive strategies in order to make the perturbative calculation of an amplitude more accessible

### 1) **Simplify the object**

By using the informations about the quantum numbers of the particles involved in the scattering process it is possible to move from the full amplitude to the simpler concept of *color and helicity ordered partial amplitudes*.

## 2) Improve the computational methods

When a naive Feynman diagram approach is used, proliferation in the number of terms with the number of loops and of scattered particles follows from the fact that neither global symmetries of the theory nor gauge symmetries are respected. *Symmetry respecting* approaches, by including these kinds of symmetries, reduce drastically the number of the contributions at any stage of the computation.

We can distinguish between **indirect** and **direct** symmetry respecting approaches. The firsts make use of analytic properties of the amplitudes, the seconds are more sophisticated versions of the common techniques based on Feynman diagrams. Both incorporates the simplifying properties of global and local invariance of the theory.

Indirect techniques have been extensively developed and used during the years, both at tree level [72, 73, 74] and at loops [78]. Most of the known results about the amplitudes at weak coupling are based on these techniques. However, the applicability of indirect methods is limited at loop level by a set of assumptions whose validity is not guaranteed at any loop order and for any SYM theory. Direct techniques have the advantage of not requiring any sort of assumptions. They are more sophisticated versions of the usual Feynman diagrammatic approach. As a consequence, their validity and applicability have the same full generality of the traditional techniques.

These new ideas have been very prolific in their applications to supersymmetric as well as non supersymmetric quantum field theories, QCD included [118]. Moreover, they led to new hypothesis about the UV behavior of supergravity theories [119]. However, the most remarkable results were found for the  $\mathcal{N} = 4$  SYM theory (see for example [97] for a review).

In this Chapter we introduce the concept of partial amplitudes and we describe the main indirect technique used for loop computations, namely the *unitarity cuts technique*. Moreover we discuss the main results found through these methods for amplitudes in  $\mathcal{N} = 4$  SYM theory and we show why these results actually ask for new inspections based on a direct approach.

## 4.1 Quantum number analysis

Quantum numbers of scattered particles can be used to separate the full scattering amplitude into simpler independent objects called *color ordered partial amplitudes*.

In a  $SU(N)$  gauge theory, a scattering amplitude involving  $n$  gluons is a function of their quantum numbers  $\{p_i, \lambda_i, a_i\}$ , i.e. their momenta, helicities  $\lambda_i = \pm$  and color numbers. At tree level, these informations, in particular the informations about the color, allow to decompose the full amplitude in basic building blocks proportional to different

color trace structures

$$\mathcal{A}_n(\{p_i, \lambda_i, a_i\}) = g^{n-2} \sum_{\sigma \in S_n/Z_n} \text{Tr}(T^{a_{\sigma_1}} \dots T^{a_{\sigma_n}}) A_n(\sigma(1^{\lambda_1}), \dots, \sigma(n^{\lambda_n})) \quad (4.1.1)$$

The sum runs over all possible non-cyclic permutations of the external particles in such a way that the traces appearing in this combination are all the possible traces of  $n$  distinct color matrices. The coefficients  $A_n$  are the color ordered partial amplitudes. In this sense, it is convenient to think of the traces in (4.1.1) as the elements of a basis over which expanding the full amplitude  $\mathcal{A}_n$  and the color ordered amplitudes  $A_n$  as its expansion coefficients.

At higher loops, formula (4.1.1) is still valid provided that the planar (large  $N$ ) limit is considered. This means that in these hypothesis the physical content of the full scattering amplitude  $\mathcal{A}_n$  is entirely contained in the simpler color ordered amplitudes  $A_n$ .

Note that at each amplitude with a fixed configuration of helicities  $\lambda_i$  corresponds a set of color ordered amplitudes  $A_n$ . Thus, when all possible configurations of helicities are considered, in principle the number of color ordered amplitudes becomes very large. However, discrete symmetries reduce the number of independent color ordered amplitudes  $A_n$ . In particular, a lot of connections between different color ordered amplitudes are produced by the P-parity that reverses all the helicities in an amplitudes, the C-parity that exchanges a particle with an anti-particle, and the cyclic permutation symmetry in the elements of  $A_n$  that follows from the cyclic symmetry of the color trace  $\text{Tr}(T^{a_{\sigma_1}} \dots T^{a_{\sigma_n}})$  associated to each  $A_n$ .

For example, by using these symmetries it is possible to show that in a four point amplitude there are just four independent partial amplitudes, namely

$$A_4(1^+, 2^+, 3^+, 4^+), \quad A_4(1^+, 2^+, 3^+, 4^-), \quad A_4(1^+, 2^+, 3^-, 4^-), \quad A_4(1^+, 2^-, 3^+, 4^-) \quad (4.1.2)$$

The same happens at five points. By going up with the number of scattered particles it is in general convenient to organize color ordered amplitudes by looking at the number of negative helicity gluons involved in the scattering process.

It is quite easy to show that scattering amplitudes of all particles or all but one particles with the same helicity vanishes in any YM theory at tree level. In SYM theories, this follows from imposing the Super-Ward identities [71]. Since the validity of SWI goes beyond the perturbative computations, this result is true at any loop order in perturbation theory for SYM theories

$$A_n^{(L)}(1^\pm, 2^\pm, \dots, n^\pm) = A_n^{(L)}(1^\mp, 2^\pm, \dots, n^\pm) = 0 \quad (4.1.3)$$

Thus, the first non-trivial amplitude in any SYM theory has all but two plus (or all but two minus) helicity gluons. These amplitudes are called *Maximally Helicity Violating*

(*MHV*) amplitudes. *MHV* planar amplitudes in  $\mathcal{N} = 4$  SYM theory are the main objects of our investigation in the second part of this thesis. Amplitudes with  $3, \dots, k+2$  negative helicity gluons are usually referred to as *NMHV*,  $\dots$ ,  $N^k$  *MHV* amplitudes.

When supersymmetric theories are considered, using supersymmetry transformations we can express any amplitude in terms of gluonic amplitudes. The following identity holds for the *MHV* case

$$A_n^{(L)}(1^-, 2_p^-, 3_p^+, 4^+, \dots, n^+) = \left( \frac{\langle 12 \rangle}{\langle 13 \rangle} \right)^{2|h_p|} A_n^{(L)}(1^-, 2_\phi^-, 3_\phi^+, 4^+, \dots, n^+) \quad (4.1.4)$$

where no subscript refers to gluons, the subscript  $\phi$  refers to scalar fields (the  $\pm$  apex indicates if they are particles or antiparticles) and  $p$  refers to any particle (scalar, fermion or gluon).

One of the main features of the *MHV* amplitudes is that loop corrections can be factorized into a universal scalar function  $M_n^{MHV}$ . Calling  $j$  and  $k$  the positions of the two negative helicity particles, we can write

$$\begin{aligned} A_n^{MHV}(1^+, \dots, j^-, \dots, k^-, \dots, n^+) &= A_{n,tree}^{MHV} + g^2 A_{n,1-loop}^{MHV} + \mathcal{O}(g^4) \\ &= A_{n,tree}^{MHV} M_n^{MHV}(\{s_{ij}\}, g^2) \end{aligned} \quad (4.1.5)$$

The function  $M_n^{MHV}$  is a function of the Mandelstam kinematic invariants  $s_{ij}$  and of the coupling constant  $g$ . On the other hand, the tree level amplitude takes a very easy form [75, 72]

$$A_{n,tree}^{MHV} = \frac{\langle jk \rangle^4}{\langle 12 \rangle \langle 23 \rangle \dots \langle n1 \rangle} \quad (4.1.6)$$

This formula, known as the Parke–Taylor formula, makes use of the spinor helicity formalism, where momenta  $p_\mu$  are replaced by the product of two-component commuting Weyl spinors  $\lambda_\alpha$  and  $\tilde{\lambda}_{\dot{\alpha}}$  of helicity  $\pm 1/2$  ( $p^{\alpha\dot{\alpha}} = \sigma_\mu^{\alpha\dot{\alpha}} p^\mu = \lambda_\alpha \tilde{\lambda}_{\dot{\alpha}}$ ) and  $\langle jk \rangle = \epsilon^{\alpha\beta} \lambda_\alpha \lambda_\beta$ .

## 4.2 Unitarity techniques and recursive relations

The factorization properties (4.1.5) of the *MHV* amplitudes reduce the problem of computing an amplitude to the problem of determining the scalar function  $M_n^{MHV}$ . Being a scalar function, it can be written as a combination of scalar loop integrals and rational functions

$$M_n^{MHV} = \sum_{j \in B} c_j \mathcal{I}_j + R \quad (4.2.1)$$

---

\*Acronym for *Next to MHV*

The set  $B$  of integrals and the rational functions  $R$  depend on the process that is considered, the loop order at which the process is computed and, of course, the theory in which the scattering process takes place.

Unitarity based techniques provide indirect methods to select the set of integrals  $B$  and to evaluate the coefficients  $c_j$  in the expansion (4.2.1). The simplifying properties of local and global invariance are incorporated into a recursive procedure that allows the analytic construction of on-shell loop amplitudes in terms of on-shell tree level (gauge and globally invariant) amplitudes.

These techniques are based on the unitarity property of the  $S$  matrix  $SS^\dagger = 1$ . Separating in the  $S$  matrix the interaction part  $T$

$$S = 1 + iT \quad (4.2.2)$$

it follows that

$$i(T^\dagger - T) = 2\Im(T) = T^\dagger T \quad (4.2.3)$$

The left hand side of this equation corresponds to a discontinuity of the scattering amplitude, i.e. to a branch cut in complex momenta space and this is related to the imaginary part of an amplitude. On the other hand the right hand side is given by the product of lower loop on-shell amplitudes and it can be interpreted as a higher loop amplitude with some propagator replaced by on-shell cut propagators

$$\frac{1}{\ell^2 + i\epsilon} \equiv \text{pp} \left( \frac{1}{\ell^2} \right) - 2\pi i \theta(\ell^0) \delta^+(\ell^2) \rightarrow -2\pi i \theta(\ell^0) \delta^+(\ell^2) \quad (4.2.4)$$

At the diagrammatic level, this replacement is universally known as *Cutkosky rules* [117]. For example, the discontinuity at a double cut in the  $s$ -channel for a four point amplitude at one loop can be written

$$\begin{aligned} -i \text{Disc} A_{4,1}|_{s\text{-cut}} &= (2\pi)^2 \sum_{\text{helicity}} \int \frac{d^D \ell}{(2\pi)^D} \delta^{(+)}(\ell^2) A_{n-j+2}^{\text{tree}}(K - \ell \dots, \ell) \times \\ &\quad \times \delta^{(+)}((\ell - K)^2) A_{j+2}^{\text{tree}}(-\ell \dots, \ell - K) \end{aligned} \quad (4.2.5)$$

The sum in this formula is taken over all possible helicities of the internal legs that have been cutted. The amplitudes are on-shell amplitudes. So eq. (4.2.5) tells us that by "sewing" together lower loop on-shell amplitudes it is possible to reconstruct the discontinuity at the cut, i.e. the imaginary part at the cut, of higher loop amplitudes.

The unitarity methods go beyond this by assuming that even the real part of the amplitude at the cut can be obtained by the sewing procedure simply replacing in (4.2.5) the  $\delta$  functions with the full propagators (basically using relation (4.2.4) in the opposite

sense). For example, at one loop both the real and the imaginary parts of the amplitude derive from the formula

$$A_{4,1}|_{s\text{-cut}} = \sum_{\text{helicity}} \int \frac{d^D \ell}{(2\pi)^D} \frac{i}{\ell^2} A_{n-j+2}^{\text{tree}}(K - \ell \dots, \ell) \frac{i}{(\ell - K)^2} A_{j+2}^{\text{tree}}(-\ell \dots, \ell - K) \quad (4.2.6)$$

The amplitudes entering in this formula continue to be on-shell amplitudes. Formula (4.2.6) is valid just for those terms with an  $s$ -channel branch cut. Terms with other branch cuts can be reconstructed by considering different sets of cuts. The full amplitude, up to rational terms, can be reconstructed by considering cuts in all possible channels. Rational terms can be computed at least at one loop by performing cuts in  $D = 4 - 2\epsilon$  dimensions [76, 77].

The procedure here outlined can be understood in this way. Suppose that a description of the amplitude in terms of the sum of Feynman diagrams (i.e. of sets of propagators and vertices) exists. When a cut on a particular channel is considered, basically one is selecting only those Feynman diagrams that exhibit the cut propagators. So, at each piece of the full amplitude, identified through a set of cuts and computed by gluing in a particular way lower loop amplitudes, it corresponds a set of propagators. By analyzing all possible sets of cuts one probes all possible combinations of propagators and thus all possible Feynman diagrams that contribute to the scattering process.

When a basis of integrals is known a priori, the reconstruction of the amplitude through unitarity gets heavily simplified since all possible sets of propagators are known from the very beginning. This is the case of any one loop process in any pure SYM theory [78, 101]. It is an old known result, in fact, that a good basis of integrals is composed by box, triangle and bubble scalar integrals with massless or massive legs (see Fig 4.2). For the  $\mathcal{N} = 4$

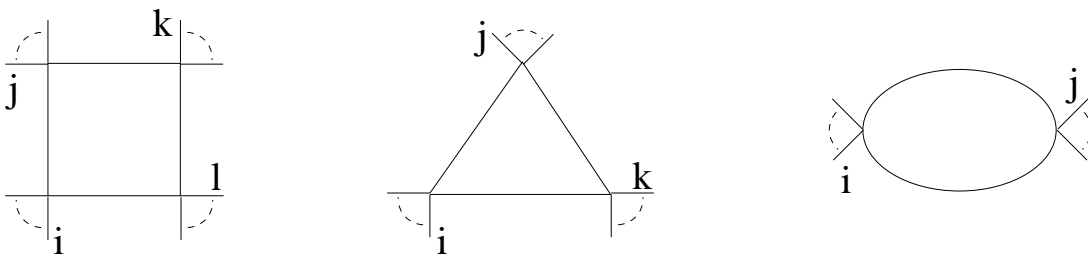


Figure 4.1: Massive and massless box, triangle and bubble one loop scalar integrals.

SYM theory the situation at one loop is more and more easier since it has been explicitly demonstrated [78] that at this perturbative order the contributions from triangles and bubbles cancel.

Higher loops are affected by complications even in  $\mathcal{N} = 4$  SYM theory. In particular, in contrast with the one loop case, a general basis of independent scalar integrals is not



known. This follows from the fact that the integrals in the proposed basis are actually related one to the other by a set of identities that occur between Feynman integrals. The most important of them are integration by parts identities [79] and the Lorentz invariance identities [81]. A set of master integrals can be identified only in particularly lucky cases such as the two loop four point scattering process with none [82] or one massive external leg [83]. However this is far from being the full story at two loops.

Despite that, parts of the full amplitude at higher loops containing specific sets of propagators can be isolated as well through the cutting techniques [84]. Nevertheless, the possibility to reconstruct the full amplitude at higher loops is more an assertion than a theorem, even for the easiest  $\mathcal{N} = 4$  SYM theory case.

In [85, 84] a general procedure, the *rung rule*, has been proposed to build up a basis of integrals contributing at higher loop once that a lower loop basis is known. Although it has been shown that the rung rule fails to reproduce all the integrals in the basis for the  $\mathcal{N} = 4$  MHV amplitudes since four loops on [109], nevertheless it has been use to point out some general features of the integral basis.

In general higher loop integrals can be formed by inserting extra lines inside a lower loop integral. For example, starting from a one-loop box integral and inserting an extra line, one produces doublebox, pentabox and bubblebox two loop integrals (see Fig 4.2).

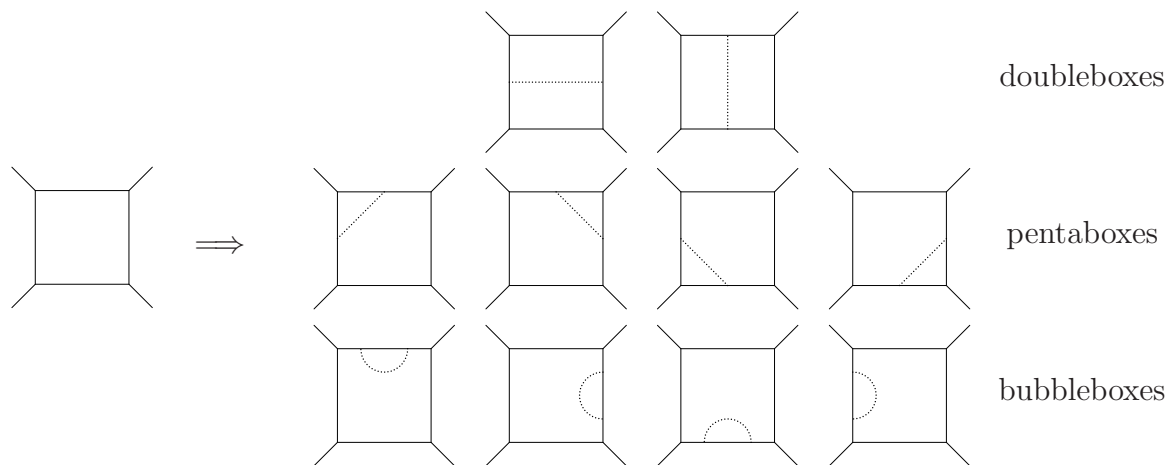


Figure 4.2: The addition of an extra internal (dashed) line allow to move from one loop to two loop integrals.

The rung rule is a more precise formalization of this observation. Basically, the rung rule asserts that once that all the integrals contributing to an amplitude at  $L - 1$  loop are known, then the integrals contributing at  $L$  loop are recovered by inserting inside the  $L - 1$  loop integrals an extra internal line (a "rung") in all possible ways (see Fig 4.3). Each inserted line must be multiplied by the imaginary unit  $i$  times the invariant constructed

by the momenta flowing in the lines connected by the extra rung. Note that when the

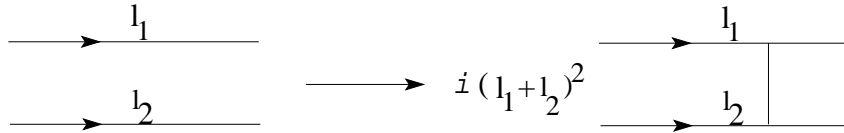


Figure 4.3: The rung rule.

external lines are massless, extra lines forming a bubble or a triangle has associated a null multiplicative factor. This means that, in these hypothesis, no bubbles or triangles can be formed at higher loops. This is the case, for example, of the four point amplitude in the  $\mathcal{N} = 4$  SYM theory. Since at one loop, the amplitude is proportional to the massless box integral, it is expected that at higher loops no extra bubbles and triangles can be formed.

For  $n > 4$  scattering processes, the one loop amplitude, even in the  $\mathcal{N} = 4$  SYM theory, is proportional to box integrals with massive legs and this argument cannot be used to exclude the presence of triangles at higher loops. Nevertheless, it is assumed that any MHV scattering process in the  $\mathcal{N} = 4$  SYM theory is triangle and bubble free at any loop order. This assumption is known as the *no-bubble no-triangle* prescription.

This prescription can be partially related to the ultraviolet behavior of the  $\mathcal{N} = 4$  SYM theory. A well known relation [1] valid for SYM theories and involving the number of supersymmetries  $\mathcal{N}$ , the number of loops  $L$  and the dimensionality  $D$

$$D < 2L(\mathcal{N} - 1) + 2 \quad (4.2.7)$$

implies that the  $\mathcal{N} = 4$  SYM theory at two loop is UV finite even in  $D = 6$ . Bubbles and triangles diverge in  $D = 6$  and their disappearance could be in principle suggested by the relation (4.2.7). However, this argument is far from being a demonstration of the no-triangle assumption. In fact, the UV behavior of triangles and bubbles does not prevent the possibility that they enter in the final expressions in linear combinations such that their UV divergent part in  $D = 6$  cancel. Moreover, the argument cannot be extended for  $L > 2$ . Last but not least, in four dimensional spacetime, where usually one works, just the bubbles diverge but this is completely unrelated to their disappearance even at one loop.

In spite of the lack of a general proof, the rung rule and the no-bubble no-triangle assumptions helped a lot in the computation of a higher loops  $\mathcal{N} = 4$  SYM MHV amplitudes.

The first higher loop computation was the four gluon amplitude  $(1^+, 2^+, 3^-, 4^-)$  at two

loops [85]. The result found for this object is

$$M_4^{2\text{loop}} = -\frac{1}{4}st \left\{ s \left( \text{Diagram 1} \right) + t \left( \text{Diagram 2} \right) \right\} \quad (4.2.8)$$

Actually this result was found without using the no-bubble no-triangle hypothesis. However, by using this hypothesis the computation of the amplitude becomes immediate. In fact, among all possible integrals that could appear at two loop (see Fig 4.2) just the two doubleboxes do not have sub-triangles or sub-bubbles. Thus, the computation of the amplitude gets reduced by the no-bubble no-triangle assumption to compute only the two coefficients of these integrals.

The no-bubble no-triangle assumption has been applied in more involved computations too: At higher loops (the four point amplitude at five loops has been computed in [86]) and with a larger number of scattered particles (up to five [87] and six [88, 89] gluons at two loops). The results found have opened the way to a lot of new relations and properties of MHV color ordered planar amplitudes in  $\mathcal{N} = 4$  SYM theory. However, the confidence that we have on these properties is linked to the validity of the assumptions of the unitarity computational techniques. As far as a general proof of these properties is not found (even for higher loops), there is always the possibility that the beautiful characteristics of  $\mathcal{N} = 4$  scattering amplitudes are just *a midsummer night dream*.

A partial example of this is given by the BDS ansatz, initially supposed valid for MHV amplitudes with any number of particles at any loop but falsified by a computation at two loop involving six particles scattered. A better established property of MHV amplitudes is the dual conformal invariance. A description of these two properties and of the state of the art in their validation follows in the next two Sections.

### 4.2.1 The BDS ansatz

The rung rule suggests that the integrals entering in the expression for an amplitude at higher loop are related to the lower loop contributing integrals. In particular, it relates the arguments of (some of) the loop integrals at different perturbative orders. Supposing to be able to compute all the integrals that contribute to an MHV amplitude at  $L - 1$  and at  $L$  loops in the dimensional regularization scheme, it seems reasonable to expect that the two results show some regularity.

The comparison of the four point two loop amplitude (4.2.8) with the same one loop

amplitude [1, 90] exhibits the first hints that a regularity actually exists. By fixing  $D = 4 - 2\epsilon$ , it was found

$$M_4^{2loop}(\epsilon) = \frac{1}{2} \left( M_2^{1loop}(\epsilon) \right)^2 + f^{(2)}(\epsilon) M_2^{1loop}(2\epsilon) + C^{(2)} + \mathcal{O}(\epsilon) \quad (4.2.9)$$

This relation between amplitudes is not completely new, since a similar structure for infrared  $\epsilon$  poles has been known since a long time [91, 92]. However, the extension to the finite parts makes equation (4.2.9) more and more precious, in particular if it is true for amplitudes at higher points too. A similar relation valid for the splitting functions [90], by linking higher to lower point amplitudes at fixed perturbative order seems to suggest that this is the case. Moreover, the rung rule and the no-bubble no-triangle hypothesis suggest that a similar behavior could be extended to higher loops too.

All these pieces of evidence have been collected in [92] in an iterative formula, known as *BDS ansatz*, valid for MHV planar amplitudes in  $\mathcal{N} = 4$  SYM theory. This formula connects MHV amplitudes at any perturbative order to the one loop amplitudes for any number of external particles. The BDS ansatz reads

$$M_n = \exp \left\{ \sum_{l=1}^{\infty} a^l \left( f^{(l)}(\epsilon) M_n^{(1)}(l\epsilon) + C^{(l)} + \mathcal{O}(\epsilon) \right) \right\} \quad (4.2.10)$$

where the factor

$$a \equiv \frac{N\alpha_s}{2\pi} (4\pi e^{-\gamma})^\epsilon \quad (4.2.11)$$

keeps track of the loop order. The coefficients  $f^l(\epsilon) = f_0^l + \epsilon f_1^l + \epsilon^2 f_2^l$  are independent of the number of external legs and  $f_0^l$  are the Taylor coefficients of the cusp anomalous dimension

$$f(a) = 4 \sum_{l=0}^{\infty} a^l f_0^{(l)} \quad (4.2.12)$$

By construction the presence of the cusp anomalous dimension includes in (4.2.10) the correct infrared behavior under collinear and soft limits [92]. Therefore possible deviations from the behavior imposed by the BDS ansatz can be found just in the IR regular terms and must vanish as soon as two particles become collinear in any possible channel.

A lot of work has been done in order to check the BDS ansatz. Principally perturbative computations have been performed using unitarity and assuming the no-bubble no-triangle hypothesis. Indirect checks due to the supposed equivalence between MHV planar amplitudes and Wilson loops have been done too [102, 103, 105]. The results show an agreement between unitarity calculations and the BDS ansatz for four and five point amplitudes. However, at six points and two loops [106, 88, 89] deviations have been observed. Their origin has been interpreted as due to the presence of three particle collinear limits for such amplitudes, while the BDS ansatz includes just the two particle collinear limits.

## 4.2.2 Dual conformal symmetry

A direct inspection of the form of the four point MHV amplitudes of the  $\mathcal{N} = 4$  SYM theory up to three loop puts in evidence the possibility that they satisfy a new symmetry, called *dual conformal symmetry* [108, 102].

The integrals that appear in those results, in fact, if regularized by keeping the external legs off-shell, exhibit a conformal  $SO(2, 4)$  symmetry unrelated to the conformal group of the  $\mathcal{N} = 4$  SYM theory. In order to distinguish it from the manifest  $SO(2, 4)$  invariance of the  $\mathcal{N} = 4$  lagrangian, this symmetry is referred to as *dual conformal symmetry*.

Consider, for example, the box integral that enters in the expression for the four point amplitude at one loop

$$I = \int d^D k \frac{1}{k^2 (k - p_1)^2 (k - p_1 - p_2)^2 (k + p_4)^2} \quad (4.2.13)$$

If the external legs are put off-shell  $p_i^2 \neq 0$ , in the integral we can safely keep  $D = 4$ . The dual conformal properties of this integral become manifest by using a set of dual coordinates  $x_i$ , related to the external and loop momenta. In this specific case

$$p_1 = x_1 - x_2 \equiv x_{12}, \quad p_2 = x_{23}, \quad p_3 = x_{34}, \quad p_4 = x_{41}, \quad k = x_{15} \quad (4.2.14)$$

Graphically, the  $x_i$  are the vertices of the dual diagram of the loop integral. The propa-

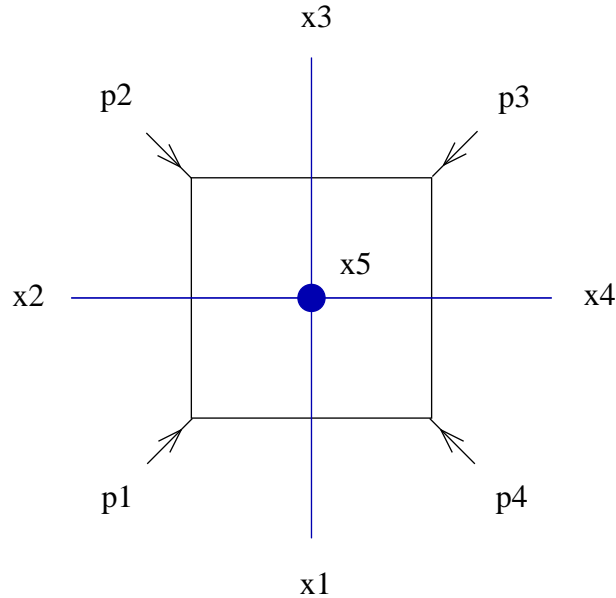


Figure 4.4: Dual diagram for the one loop box integral

gators of the integral are written in the  $x$  space as the square of differences of two of the

$x$ , namely  $x_{ij}^2$ . Indices  $i$  and  $j$  refer to the  $x$ 's at the extrema of the segments that form the dual diagram. Integral (4.2.13) can be rewritten as

$$I = \int d^D x_5 \frac{1}{x_{15}^2 x_{25}^2 x_{35}^2 x_{45}^2} \quad (4.2.15)$$

In this form, the integral is manifestly invariant with respect to translations and rotations of the  $x_i$  and, if  $D = 4$ , it transforms covariantly with respect to conformal inversions

$$\tilde{x}^\mu = \frac{x^\mu}{x^2} \quad (4.2.16)$$

This same analysis can be extended to all the four point integrals that have been found to contribute to the scattering amplitude up to three loops [108]. Note that these integrals are the ones recursively constructed from the one loop box by using the rung rule and the no-bubble no-triangle hypothesis. However, the relevance of the dual conformal symmetry goes beyond that of the rung rule.

First of all, supposing true the dual conformal symmetry for a general MHV amplitude, then the rung rule and the no-bubble no-triangle hypothesis follow as straightforward consequences. Triangle and bubble integrals, in fact, are not conformally covariant in the  $x$  space.

Moreover, the dual conformal symmetry constraints also eventual rational terms in the final expressions for the amplitudes. In fact, if the dual conformal symmetry is valid, the finite parts must be functions of conformal invariant ratios. These ratios in the  $x$  space have the general form

$$u_{ijkl} = \frac{x_{ij}^2 x_{kl}^2}{x_{ik}^2 x_{jl}^2}, \quad x_{ij} = x_i - x_j \quad (4.2.17)$$

Thus, on shell condition  $p_i^2 = 0$  and the definitions (4.2.14) imply that no such invariants can be built for four and five scattered particles. As a consequence, no rational functions exist for the four and five amplitudes and the  $\epsilon$ -finite part in their final expressions is given by the finite parts of the loop integrals that contribute to those amplitudes.

Last but not least, it is in principle possible to use dual conformal symmetry as an a priori criterion to see if a Feynman integral can contribute or not to an amplitude. Not all the integrals that can be constructed with the rung rule and the no-bubble no-triangle hypothesis enter in the final expressions for an amplitude at a fixed loop order. A direct inspection of the four point amplitude since three loops on [109, 110, 102] showed in fact that there are integrals that do not contribute to the amplitude, although they have been constructed following the rung rule. These integrals actually diverge even when the external legs are put off-shell and, as a consequence, are not conformal invariant objects. If we assume that planar MHV amplitudes respect the dual conformal symmetry, the null contribution from these integrals finds an immediate explanation.

Thus, if valid in general, dual conformal symmetry would be a great step toward the definition of a basis of independent contributing integrals at least for MHV amplitudes. However, in the lack of a general proof of its validity, this symmetry is just an assumption that can find support primarily from computations. In this sense, it assumes great importance the observation that at two loops both the five point and the six point amplitudes were found to be functions of conformal integrals only [87, 88].

*AdS/CFT* correspondence provides other more fundamental arguments in favor of the general validity of the dual conformal symmetry.

Scattering amplitudes at strong coupling are given by the area of the minimal surface that ends on a closed line formed by light-like segments on the boundary of *AdS* space [93]. Formally, this prescription for scattering amplitudes is exactly the same as the one for computing the expectation values of Wilson loops in *AdS/CFT* [96]. Dual conformal invariance of MHV scattering amplitudes at strong coupling follows from the ordinary conformal invariance of these Wilson loops.

It has been conjectured that even in the perturbative regime the expectation value of Wilson loops with a contour given by light-like segments could reproduce the results for the MHV scattering amplitudes. This conjecture has been tested by comparing unitarity results for MHV amplitudes and new computations for Wilson loops [102, 103, 105, 104] up to two loops. If proved at all perturbative orders, the equivalence between Wilson loops and scattering amplitudes would give a general proof of the dual conformal symmetry. Unfortunately, this general demonstration is still missing and the origins of the duality between MHV amplitudes and Wilson loops at weak coupling are still obscure.

### 4.3 Why a direct computation

In the previous Section we highlighted the main properties discovered about planar MHV amplitudes in  $\mathcal{N} = 4$  SYM theory. Although remarkable results have been acquired, still there are open problems and possible objections that can be expected.

First of all, the unitarity techniques, as we have seen, are based on a set of assumptions that consist in extending properties of MHV amplitudes directly observed at low loop and for low number of particles to any loop and any MHV process. In particular, there are three main assumptions that still wait for a general proof: 1) The possibility of reconstructing through the sewing procedure not just the imaginary part of an amplitude at a cut but the real part too; 2) The possibility of reconstructing correctly the rational parts of an amplitude by performing cuts in  $D = 4 - 2\epsilon$  dimension; 3) The no-bubble no-triangle hypothesis for the construction of higher loop integrals when a basis of lower loop integrals is known.

The failure of the BDS ansatz to predict the rational parts of six point MHV ampli-

tudes, although it finds a technical justification as the triple collinear limits are considered, on the other hand could be symptomatic of some problem in the general strategy adopted. The presence of the extra rational terms at six points can be understood on the basis of the dual conformal symmetry that allows for an arbitrary function of conformal cross ratios from six points on and excludes it at lower points. However, a general proof of the dual conformal invariance is confined at strong coupling. On the other hand, the perturbative computations performed in order to check it at weak coupling, being based on the no-bubble no-triangle hypothesis, partially assume some of the same consequences that the dual conformal symmetry would imply.

From this point of view, a computation of MHV scattering amplitudes through direct, assumption-free techniques, is definitively necessary. A direct approach, in fact, by overcoming the problematics of indirect approaches, can check the consistency of indirect computations and of their assumptions.

In order to accomplish this program it is required at least a computation of MHV amplitudes at two loop. All the known results at one loop, in fact, are completely well established and supported by evidences. The BDS ansatz correctly predicts at any loop order the IR behavior of the amplitudes. Thus possible deviations from the known results are expected only in the rational parts of the expression for the amplitudes. On the other hand, rational parts at four and five points are excluded by the dual conformal symmetry. Thus, the first non trivial check is for the four point MHV amplitude at two loop.

In the following Chapters we develop a direct computational technique that allows, in principle, to compute any two loop MHV process in  $\mathcal{N} = 4$  SYM theory. Moreover, we move from our expressions, valid for a generic number of scattered particles towards the four point amplitude.



# Chapter 5

## Superspace approach to scattering amplitudes in SYM theories

Superspace [1] is the most natural arena in which supersymmetric theories play. In particular, the supergraph technology turns out to be a powerful tool for a Feynman diagrammatic approach to the perturbative evaluation of physical quantities in SYM theories.

In this Chapter we describe the generalities of the superspace approach to scattering amplitudes in SYM theories. This provides a direct and symmetry respecting proposal for the computation of amplitudes in  $SU(N)$  supersymmetric gauge theories.

An amplitude in superspace formalism is a local expression in the spinorial coordinates. It is given by a string of superfields times a kinematic factor expressed as a combination of loop integrals. The informations about the quantum numbers of the interacting particles (which particles they are, their helicity, color, momentum) are carried by the string of superfields. In particular, all the ordinary fields in the same superfield carry the same helicity. Thus the notion of helicity decomposed amplitudes can be easily enhanced to the notion of helicity decomposed superamplitudes. To reach this goal an extension of the twistor formalism in superspace turns out to be very useful.

Our direct computational strategy is based on a combined use of ordinary superspace technologies and background field method. Moreover, we take advantage from the color ordering and from a proper employment of the helicity informations relative to the scattered particles.

The perturbative evaluation of a scattering amplitude can be reduced to the computation of the effective action. The amplitude, in fact, is computed as a combination of trees of vertices and propagators given by the Green functions.

In general, the evaluation of the complete effective action becomes more and more involved as soon as the number of loops and of interacting particles increases. Nevertheless

our superspace technology allows to overcome the problem of increasing complexity related to the increasing of the number of external particles.

The computation in the background field method follows from the identification of a relatively small set of vacuum diagrams that contain in an extremely compact form the full effective action. Thus, from the same set of vacuum diagrams it is in principle possible to derive any scattering amplitude at fixed perturbative order. This allows to treat all the amplitudes at a fixed order once for all and to find results valid for any number of interacting particles.

The basis of our computational techniques is constituted by a set of algebraic relations involving various spinorial structures in superspace (mainly superspace and spacetime covariant derivatives and field strength). These identities are the core of our technique: Although they are only a small set and are quite simple relations, they enter in the definition of the vertices of the theory and of the Feynman rules, they provide constraints on the form of the field propagators and of their expansion coefficients and they constitute the basic computational tools that are heavily used while managing the vacuum diagrams and extracting from them the effective action. Last but not least, their properties and their simplicity open the way for an automation of the (most part of the) computational steps with the help of the computer. We accomplished this project by writing completely new programs that deal with the spinorial structures through symbolic calculus languages (in particular `FORM` and `Mathematica`). The set up of these softwares, although time-consuming, gives us now a very fast tool to perform direct perturbative computations in superspace.

The most natural test-area for our techniques is represented by the MHV amplitudes in  $\mathcal{N} = 4$  SYM theory. As we have described in Chapter 4 the important features characterizing these objects give an immediate relevance to a direct computation that focuses on them. However, a remarkable feature of our technologies is that they can be extended without modifications to any SYM theory in four dimensions and to any helicity configuration of the particles involved in a scattering process.

This Chapter starts with a description of the twistor formalism in superspace and of the general features of a superamplitude. Then, we review the supersymmetric background field method and we give the Feynman rules suitable for any SYM theory. In the last two Sections we sketch the computational procedure that carry from the vacuum diagrams to the complete expression of the effective action and from there to the scattering amplitudes with an arbitrary number of interacting particles.

Although it was a common opinion that a direct Feynman diagram-based approach to the problem of the amplitudes was out of our present possibilities, in this and the following Chapters we show that a smart use of non-trivial superspace technologies makes this available at least for SYM theories.

## 5.1 The superamplitude

In this Section we describe the general superspace approach to the definition of superamplitudes in SYM theories. The discussion is suitable both for  $\mathcal{N} = 1$  and extended supersymmetric gauge theories.

### 5.1.1 The twistor formalism in superspace

In  $\mathcal{N} = 1$  superspace language the field content of a supersymmetric gauge theory is given in terms of covariant superspace derivatives and superfield strengths. All objects are functions of a real prepotential  $V$ , according to the following definitions (we work in chiral representation and use conventions of [1] summarized in the Appendix A)

$$\begin{aligned} \nabla_\alpha &= e^{-V} D_\alpha e^V \equiv D_\alpha - i\Gamma_\alpha \quad , \quad \bar{\nabla}_{\dot{\alpha}} = \bar{D}_{\dot{\alpha}} \equiv \bar{D}_{\dot{\alpha}} - i\bar{\Gamma}_{\dot{\alpha}} \\ \nabla_{\alpha\dot{\alpha}} &= -i\{\nabla_\alpha, \bar{\nabla}_{\dot{\alpha}}\} \equiv \partial_{\alpha\dot{\alpha}} - i\Gamma_{\alpha\dot{\alpha}} \end{aligned} \quad (5.1.1)$$

where  $\Gamma_\alpha, \bar{\Gamma}_{\dot{\alpha}}$  and  $\Gamma_{\alpha\dot{\alpha}}$  are the spinorial and spacetime connections respectively, while

$$W_\alpha = -\frac{1}{2} [\bar{\nabla}^{\dot{\alpha}}, \nabla_{\alpha\dot{\alpha}}] \quad , \quad \bar{W}_{\dot{\alpha}} = -\frac{1}{2} [\nabla^\alpha, \nabla_{\alpha\dot{\alpha}}] \quad (5.1.2)$$

are the (anti)chiral superfield strengths. Connections and field strengths are in the adjoint representation of the gauge group. While the bosonic connection  $\Gamma_{\alpha\dot{\alpha}}$  is subject to gauge-fixing, the field strengths transform covariantly.

The field content of the theory is made manifest in the WZ gauge,  $V| = D_\alpha V| = D^2 V| = 0$ . In this gauge, the bosonic connection  $\Gamma_{\alpha\dot{\alpha}}$  contains the ordinary gauge field as its  $\theta\bar{\theta}$  component

$$A_{\alpha\dot{\alpha}} = \Gamma_{\alpha\dot{\alpha}}| = \frac{1}{2} [\bar{D}_{\dot{\alpha}}, D_\alpha] V| \quad (5.1.3)$$

The field content of the covariant superfield strengths is instead

$$W_\alpha = \tilde{\lambda}_\alpha + \theta^\beta f_{\alpha\beta} + \theta^2 D' \quad , \quad \bar{W}_{\dot{\alpha}} = \tilde{\bar{\lambda}}_{\dot{\alpha}} + \bar{\theta}^{\dot{\beta}} \bar{f}_{\dot{\alpha}\dot{\beta}} + \bar{\theta}^2 \bar{D}' \quad (5.1.4)$$

We recognize  $(\tilde{\lambda}_\alpha, \tilde{\bar{\lambda}}_{\dot{\alpha}})$  as being the gaugino field,  $f_{\alpha\beta}, \bar{f}_{\dot{\alpha}\dot{\beta}}$  the (anti)self-dual components of the ordinary field strength and  $D'$  a complex scalar field.

In order to describe physical (on-shell) asymptotic states in terms of gauge superfields, we find convenient to fix the gauge of superspace,  $D^2 V = \bar{D}^2 V = 0$ , rather than the WZ gauge. In fact, this gauge does not break supersymmetry and it is therefore suitable for the kind of calculations we have in mind.

We implement the twistor formalism to superfields. Introducing commuting spinors  $(\lambda_\alpha, \bar{\lambda}_{\dot{\alpha}})$  as described before, we identify the positive (negative) helicity gluino  $\tilde{\lambda}_\alpha$  ( $\tilde{\bar{\lambda}}_{\dot{\alpha}}$ ) in

(5.1.3) with  $c\lambda_\alpha$  ( $c\bar{\lambda}_{\dot{\alpha}}$ ), where  $c$  is a ‘‘cocycle’’ which transforms the commuting spinor  $\lambda_\alpha$  into an anticommuting one. The cocycle satisfies

$$\begin{aligned} c^\dagger &= -c \quad , \quad c^2 = 1 \\ \theta^\alpha c\lambda_\alpha &= -c\lambda_\alpha\theta^\alpha \end{aligned} \quad (5.1.5)$$

In terms of these objects and introducing reference spinors  $(\mu_\alpha, \bar{\mu}_{\dot{\alpha}})$ , a suitable expansion for the real prepotential  $V$  in the gauge of superspace is

$$V = \theta^\alpha \frac{c\mu_\alpha}{\langle \lambda\mu \rangle} + \bar{\theta}^{\dot{\alpha}} \frac{c\bar{\mu}_{\dot{\alpha}}}{[\bar{\lambda}\bar{\mu}]} + \theta^\alpha \bar{\theta}^{\dot{\alpha}} \left( \frac{\mu_\alpha \bar{\lambda}_{\dot{\alpha}}}{\langle \lambda\mu \rangle} - \frac{\lambda_\alpha \bar{\mu}_{\dot{\alpha}}}{[\bar{\lambda}\bar{\mu}]} \right) - \frac{1}{2} \theta^\alpha \bar{\theta}^2 c\lambda_\alpha + \frac{1}{2} \bar{\theta}^{\dot{\alpha}} \theta^2 c\bar{\lambda}_{\dot{\alpha}} \quad (5.1.6)$$

where we have set the auxiliary field  $D'$  on-shell ( $D' = 0$ ). Moreover, we have chosen  $V| = 0$  by exploiting the residual gauge invariance

$$V \rightarrow V + G \quad \text{with} \quad D^2 G = \bar{D}^2 G = 0 \quad (5.1.7)$$

which survives after imposing the gauge of superspace  $*$ .

We can rewrite the expansion (5.1.6) as  $V = V^+ + V^-$ , where

$$\begin{aligned} V^+ &= c \frac{\bar{\mu}_{\dot{\beta}}}{[\bar{\lambda}\bar{\mu}]} \left[ -\bar{\theta}^{\dot{\beta}} + \bar{\theta}^{\dot{\beta}} \theta^\alpha c\lambda_\alpha + \frac{1}{2} \theta^\alpha \bar{\theta}^2 \bar{\lambda}^{\dot{\beta}} \lambda_\alpha \right] \equiv c \frac{\bar{\mu}_{\dot{\beta}}}{[\bar{\lambda}\bar{\mu}]} \bar{\chi}^{\dot{\beta}} \\ V^- &= c \frac{\mu_\beta}{\langle \lambda\mu \rangle} \left[ -\theta^\beta + \theta^\beta \bar{\theta}^{\dot{\alpha}} c\bar{\lambda}_{\dot{\alpha}} - \frac{1}{2} \bar{\theta}^{\dot{\alpha}} \theta^2 \lambda^\beta \bar{\lambda}_{\dot{\alpha}} \right] \equiv c \frac{\mu_\beta}{\langle \lambda\mu \rangle} \chi^\beta \end{aligned} \quad (5.1.8)$$

are given in terms of  $\chi, \bar{\chi}$  fields which do not depend on the reference polarization spinors.

Consequently, we can define  $\Gamma_{\alpha\dot{\alpha}} \equiv \Gamma_{\alpha\dot{\alpha}}^+ + \Gamma_{\alpha\dot{\alpha}}^-$ , where at linearized level  $\Gamma_{\alpha\dot{\alpha}}^\pm \equiv \frac{1}{2} [D_{\dot{\alpha}}, D_\alpha] V^\pm$ . The lowest components

$$\Gamma_{\alpha\dot{\alpha}}^+| = \frac{\lambda_\alpha \bar{\mu}_{\dot{\alpha}}}{[\bar{\lambda}\bar{\mu}]} \quad , \quad \Gamma_{\alpha\dot{\alpha}}^-| = \frac{\mu_\alpha \bar{\lambda}_{\dot{\alpha}}}{\langle \lambda\mu \rangle} \quad (5.1.9)$$

are the two possible polarization states of the gauge field  $A_{\alpha\dot{\alpha}}$ .

From the expansion of the prepotential  $V$  we find

$$\begin{aligned} W_\alpha &= i \left[ c\lambda_\alpha + \theta^\beta \lambda_\alpha \lambda_\beta - \frac{1}{2} \theta^\beta \bar{\theta}^{\dot{\alpha}} \lambda_\alpha \bar{\lambda}_{\dot{\alpha}} \lambda_\beta c \right] \\ \bar{W}_{\dot{\alpha}} &= i \left[ c\bar{\lambda}_{\dot{\alpha}} + \bar{\theta}^{\dot{\beta}} \bar{\lambda}_{\dot{\alpha}} \bar{\lambda}_{\dot{\beta}} - \frac{1}{2} \theta^\beta \bar{\theta}^{\dot{\beta}} \lambda_\beta \bar{\lambda}_{\dot{\beta}} \bar{\lambda}_{\dot{\alpha}} c \right] \end{aligned} \quad (5.1.10)$$

---

\*We note that since the physical components of  $G$  are  $G|$ ,  $D_\alpha G|$  and  $[D_\alpha, \bar{D}_{\dot{\alpha}}]G|$ , the residual gauge invariance acts only on the  $V$  components which depend on non-physical arbitrary quantities, that is  $V|$  and the reference spinors.

Defining spinorial derivatives in momentum space as

$$D_\alpha = \partial_\alpha + \frac{1}{2}\bar{\theta}^{\dot{\alpha}}\lambda_\alpha\bar{\lambda}_{\dot{\alpha}} \quad , \quad \bar{D}_{\dot{\alpha}} = \bar{\partial}_{\dot{\alpha}} + \frac{1}{2}\theta^\alpha\lambda_\alpha\bar{\lambda}_{\dot{\alpha}} \quad (5.1.11)$$

it is easy to check that, as a consequence of the twistors property  $\lambda^\alpha\lambda_\alpha = \bar{\lambda}^{\dot{\alpha}}\bar{\lambda}_{\dot{\alpha}} = 0$ , the previous expressions satisfy

$$\begin{aligned} \text{chirality conditions} & \quad \bar{D}_{\dot{\alpha}}W_\alpha = 0 \quad , \quad D_\alpha\bar{W}_{\dot{\alpha}} = 0 \\ \text{on-shell conditions} & \quad D^\alpha W_\alpha = 0 \quad , \quad \bar{D}^{\dot{\alpha}}\bar{W}_{\dot{\alpha}} = 0 \end{aligned} \quad (5.1.12)$$

Therefore, in the expansion (5.1.10) we recognize the on-shell gluini as first components and the on-shell positive and negative helicity components of the gauge field strength as  $\theta$  and  $\bar{\theta}$  components, respectively.

The addition of matter in a given representation of the gauge group is realized by the inclusion of a certain number of chiral and antichiral superfields  $\Phi_i, \bar{\Phi}_i$ , where  $i$  is a flavor index. On-shell (anti)chirals describe the propagation of scalar (anti)particles and positive (negative) helicity spinors.

### 5.1.2 Color-ordered superamplitudes

Having identified the helicity content of the gauge superfields, it is now easy to write the most general superspace expression for a color-ordered superamplitude.

As we have just described, fermionic helicity states are contained in  $W_\alpha$  (positive) and  $\bar{W}_{\dot{\alpha}}$  (negative), while gluons with definite helicity can be represented either by the field strengths and by the  $\Gamma_{\alpha\dot{\alpha}}^+$  and  $\Gamma_{\alpha\dot{\alpha}}^-$  parts of the bosonic connection.

We Fourier transform the superfields respect to the bosonic coordinates, while keeping the original dependence on the spinorial coordinates. Therefore, when we write an external superfield as  $A(1)$  ( $A$  stands for gauge connections or field strengths) we mean  $A(p_1, \theta, \bar{\theta})$  where  $p_1$  is the on-shell momentum of particle 1.

A color-ordered superamplitude is then given by a string of superfields, local in the spinorial coordinates, integrated on the superspace coordinates. For a given configuration of external helicities, with  $j$  positive helicity states and  $(n - j)$  negative helicity states, its expression is roughly of the form

$$\begin{aligned} \mathcal{A}(1^+, 2^+, \dots, j^+, (j+1)^-, \dots, n^-) = & \quad (5.1.13) \\ \int d^4\theta \text{Tr} (W(1)\Gamma^+(2) \cdots \bar{W}(j+1) \cdots \Gamma^-(n-1)\bar{W}(n)) & \quad G(p_1, \dots, p_n) \end{aligned}$$

with spinorial indices suitably contracted among them or with external momenta which may appear for dimensional reasons. Here  $G(p_1, \dots, p_n)$  is the kinematic coefficient which

can be computed perturbatively, and the trace is over gauge indices. The group structure can be stripped out as in the bosonic case (see equation (4.1.1)).

Performing the  $\theta$ -integration in (5.1.13) we reduce the integrand in components. Each component corresponds to an ordinary amplitude with a given number of fermionic and bosonic ordered helicity states.

As an example, we consider the four particle superamplitude  $\mathcal{A}(1^+, 2^+, 3^-, 4^-)$ . At one loop, its expression is well known [1] and given by

$$\mathcal{A}(1^+, 2^+, 3^-, 4^-) = \int d^4\theta \operatorname{Tr} \left( W^\alpha(1) W_\alpha(2) \bar{W}^{\dot{\alpha}}(3) \bar{W}_{\dot{\alpha}}(4) \right) G^{(1)}(p_1, p_2, p_3, p_4) \quad (5.1.14)$$

where  $G^{(1)}$  is the one-loop kinematic factor associated to the box diagram

$$G^{(1)}(p_1, p_2, p_3, p_4) = \int \frac{d^4k}{(2\pi)^4} \frac{1}{k^2(k-p_1)^2(k-p_1-p_2)^2(k+p_4)^2} \quad (5.1.15)$$

Higher order corrections are expected to have the same configuration of external superfields. The kinematic coefficient is the only part sensible to the loop order. This is the superspace translation of the factorization property (4.1.5) of MHV amplitudes.

In what follows we develop a superspace technique for computing  $G^{(2)}(p_1, \dots, p_n)$  for any number  $n$  of external particles.

## 5.2 The supergraph approach

The general strategy we are going to describe is valid for any  $\mathcal{N} = 1$  SYM theory, independently of the chiral matter content.

Superamplitudes can be constructed perturbatively from trees of vertices and propagators given by 1P-irreducible Green functions. To obtain a contribution to the S-matrix it is then sufficient to cut the external propagators and set the external lines on-shell with physical polarizations.

The generating function of 1PI diagrams is the effective action. Therefore, the problem of computing scattering amplitudes at a given loop order is reduced to determining the effective action up to that order.

We focus on the construction of the *gauge* effective action. In a generic  $\mathcal{N} = 1$  theory this is useful for evaluating gluons and gluino scattering amplitudes. In maximally supersymmetric theories, the ones we have in mind for applications, this is exhaustive since matter and gauge amplitudes are related by supersymmetry.

The important observation which simplifies dramatically the calculation is that we need evaluate the effective action only *on-shell*. In fact, on one hand 1PI diagrams with

external lines proportional to the equations of motion do not contribute to the 1PI sector of the amplitude: They are automatically zero once the external propagators are amputated and the corresponding lines are set on-shell. On the other hand, they do not either contribute to the construction of reducible diagrams, as can be directly proved. This is nothing but the general statement that Green functions proportional to the equations of motion are always vanishing (known as Zimmermann's theorem).

The most convenient approach for computing the effective action in Yang–Mills theories is background field method [98, 99]. In fact, by splitting the gauge fields into an external and a quantum part, it allows to gauge-fix the quantum component while keeping manifest covariance in the external fields. This leads to an expression for the effective action in terms of the external fields which is manifestly gauge invariant.

We use the supersymmetric generalization of the background field method [7, 1, 100] which can be applied for perturbative calculations in a generic  $\mathcal{N} = 1$  SYM theory.

### 5.2.1 Feynman rules in background field method

We quickly review the supersymmetric background field method by stressing the main ingredients useful for our calculation.

In superspace language, the quantum–background splitting is performed on the covariant derivatives (5.1.1) according to the prescription  $\nabla_\alpha = e^{-V} \nabla_\alpha e^V$ ,  $\bar{\nabla}_{\dot{\alpha}} = \bar{\nabla}_{\dot{\alpha}} = \bar{D}_{\dot{\alpha}}$  and  $\nabla_{\alpha\dot{\alpha}} = -i\{e^{-V} \nabla_\alpha e^V, \bar{D}_{\dot{\alpha}}\}$ , where plain and boldface letters indicate quantum and external quantities, respectively. As a consequence, the field strengths can be expanded in powers of the quantum  $V$  field

$$\begin{aligned} W_\alpha &= \frac{i}{2} \{ \bar{D}^{\dot{\alpha}}, \{ \bar{D}_{\dot{\alpha}}, e^{-V} \nabla_\alpha e^V \} \} = \mathbf{W}_\alpha + i \bar{D}^2 \nabla_\alpha V + \frac{i}{2} \bar{D}^2 [\nabla_\alpha V, V] + \dots \quad (5.2.1) \\ \bar{W}_{\dot{\alpha}} &= \frac{i}{2} \{ e^{-V} \nabla_\alpha e^V, \{ e^{-V} \nabla_\alpha e^V, \bar{D}_{\dot{\alpha}} \} \} = \bar{\mathbf{W}}_{\dot{\alpha}} - i \nabla^2 \bar{D}_{\dot{\alpha}} V + \frac{i}{2} \nabla^2 [\bar{D}_{\dot{\alpha}} V, V] + \dots \end{aligned}$$

For chiral superfields in the adjoint representation of the gauge group the splitting is  $\Phi = e^V \mathbf{\Phi} e^{-V}$  and  $\bar{\Phi} = \bar{\mathbf{\Phi}}$  where boldface objects are covariantly (anti)chiral superfields.

We gauge-fix the quantum  $V$  field by choosing the gauge  $\nabla^2 V = \bar{\nabla}^2 V = 0$ . Therefore, for a generic  $\mathcal{N} = 1$  SYM theory with interacting matter, the full action is

$$\mathcal{S}_{tot} = \mathcal{S}_{gauge} + \mathcal{S}_{matter} + \mathcal{S}_{gf} + \mathcal{S}_{FP} + \mathcal{S}_{NK} \quad (5.2.2)$$

where

$$\begin{aligned} \mathcal{S}_{gauge} &= \frac{1}{2g^2} \int d^6 z \operatorname{Tr}(W^\alpha W_\alpha) \\ \mathcal{S}_{matter} &= \int d^8 z \operatorname{Tr}(e^{-gV} \bar{\Phi}_i e^{gV} \Phi_i) + \int d^6 z \mathcal{V}(\Phi^i) + \int d^6 \bar{z} \bar{\mathcal{V}}(\bar{\Phi}^i) \end{aligned}$$

$$\begin{aligned}
\mathcal{S}_{gf} &= -\frac{1}{2g^2} \text{Tr} \int d^8z V \left( \nabla^2 \bar{\nabla}^2 + \bar{\nabla}^2 \nabla^2 \right) V \\
\mathcal{S}_{FP} &= \text{Tr} \int d^8z (c' + \bar{c}') L_{\frac{1}{2}V} \left( (c + \bar{c}) + \text{coth} \left( L_{\frac{1}{2}V} (c - \bar{c}) \right) \right) \\
\mathcal{S}_{NK} &= \text{Tr} \int d^8z \bar{b} b
\end{aligned} \tag{5.2.3}$$

Here  $c, c'$  ( $\bar{b}, \bar{c}, \bar{c}'$ ) are the Faddeev–Popov ghosts and  $b$  ( $\bar{b}$ ) are the Nielsen–Kallosh ghosts. They are full covariantly (anti)chiral superfields. NK ghosts give contributions only at one loop.

Once we have specified the superpotential  $\mathcal{V}$ , from the action (5.2.2) we can read the vertices suitable for loop calculations at a given order, while from the quadratic part we obtain the following propagators

$$\begin{aligned}
\langle VV \rangle &= \frac{1}{\hat{\square}} \\
\langle \bar{\Phi}\Phi \rangle &= -\frac{1}{\square_+} & \langle \Phi\bar{\Phi} \rangle &= -\frac{1}{\square_-} \\
\langle \bar{c}'c \rangle &= -\frac{1}{\square_+} & \langle c'\bar{c} \rangle &= \frac{1}{\square_-}
\end{aligned} \tag{5.2.4}$$

where  $\square_{\pm}$  and  $\hat{\square}$  have been defined in (B.0.4) as functions of the external superfields. Moreover, every time we contract a chiral superfield we get an extra  $\bar{\nabla}^2$ , while antichirals give an extra  $\nabla^2$  (in the rest of the thesis we avoid using boldface symbols for background fields since it should be clear from the context which is quantum and which is external).

As already discussed, we are interested in computing the on-shell gauge effective action. In background field method this means that the external gauge fields satisfy  $\nabla^\alpha W_\alpha = 0$ ,  $\bar{\nabla}^{\dot{\alpha}} \bar{W}_{\dot{\alpha}} = 0$  and, consequently,  $\nabla^2 W_\alpha = \bar{\nabla}^2 \bar{W}_{\dot{\alpha}} = 0$ ,  $\nabla^{\alpha\dot{\alpha}} W_\alpha = \nabla^{\alpha\dot{\alpha}} \bar{W}_{\dot{\alpha}} = 0$ .

In this case, the propagators take the simplified form (B.0.9). It is convenient to expand them in powers of spinorial derivatives as

$$\begin{aligned}
\frac{1}{\square_+} &= \frac{1}{\square - iW^\alpha \nabla_\alpha} = A + B^\alpha \nabla_\alpha + C \nabla^2 \\
\frac{1}{\square_-} &= \frac{1}{\square - i\bar{W}^{\dot{\alpha}} \bar{\nabla}_{\dot{\alpha}}} = \bar{A} + \bar{B}^{\dot{\alpha}} \bar{\nabla}_{\dot{\alpha}} + \bar{C} \bar{\nabla}^2
\end{aligned} \tag{5.2.5}$$

and

$$\begin{aligned}
\frac{1}{\hat{\square}} &= \frac{1}{\square_+ - i\bar{W}^{\dot{\alpha}} \bar{\nabla}_{\dot{\alpha}}} \\
&= A + B^\alpha \nabla_\alpha + C \nabla^2 + \bar{D}^{\dot{\alpha}} \bar{\nabla}_{\dot{\alpha}} + E^{\alpha\dot{\alpha}} \nabla_\alpha \bar{\nabla}_{\dot{\alpha}} + \bar{F}^{\dot{\alpha}} \nabla^2 \bar{\nabla}_{\dot{\alpha}} + \bar{G} \bar{\nabla}^2 + H^\alpha \nabla_\alpha \bar{\nabla}^2 + L \nabla^2 \bar{\nabla}^2
\end{aligned} \tag{5.2.6}$$



or, equivalently

$$\begin{aligned} \frac{1}{\hat{\square}} &= \frac{1}{\square - iW^\alpha \nabla_\alpha} \\ &= \bar{A} + \bar{B}^\alpha \bar{\nabla}_\alpha + \bar{C} \bar{\nabla}^2 + D^\alpha \nabla_\alpha + \bar{E}^{\alpha\dot{\alpha}} \bar{\nabla}_{\dot{\alpha}} \nabla_\alpha + F^\alpha \bar{\nabla}^2 \nabla_\alpha + G \nabla^2 + \bar{H}^\alpha \bar{\nabla}_\alpha \nabla^2 + \bar{L} \bar{\nabla}^2 \nabla^2 \end{aligned} \quad (5.2.7)$$

The coefficients are given as power series in the background fields, as discussed in Appendices C and D. In the same Appendices we derive a lot of identities that the coefficients satisfy. These relations follow from basic algebraic relations involving the covariant derivatives and the covariant propagators.

As an example of the power expansion of the coefficients, in Fig 5.1 we draw the expansion of the coefficients of the chiral propagator up to three fields (see Appendices C and D for the corresponding algebraic expression). The straight lines on the right hand sides correspond to  $1/\square$  covariant propagators. Similar expansions for the coefficients of the antichiral propagator are easily obtained by taking the bar of these expressions.

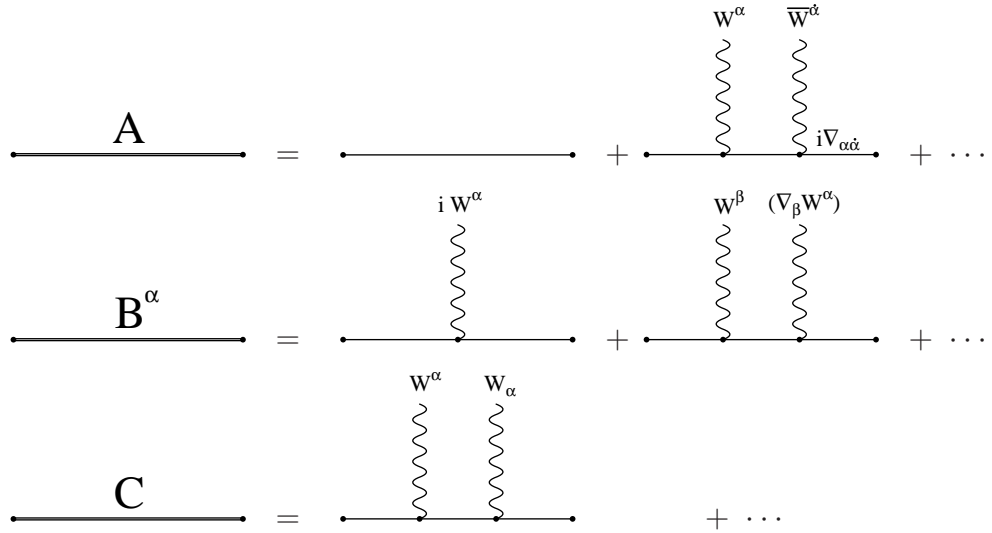


Figure 5.1: Expansion of the  $A, B, C$  coefficients up to two external fields.

### 5.3 From the effective action...

The general prescription for computing the effective action  $\Gamma = \int e^S$  at a given loop order is to draw all possible vacuum diagrams at that order by using the covariant Feynman rules given above. We then expand the covariant propagators in powers of spinorial derivatives as in eqs. (5.2.5)–(5.2.7) and perform covariant  $\nabla$ -algebra [1, 100] in order

to reduce the supergraph to a sum of ordinary Feynman momentum integrals. This is achieved by integrating by parts the spinorial derivatives and playing with their algebra (see Appendix B) until we obtain a  $\nabla^2\bar{\nabla}^2$  for each loop. The result is a linear combination of expressions local in the spinorial variables, integrated over  $d^4\theta$ .

The contribution to the effective action is eventually given by a sum of ordinary Feynman diagrams with the internal propagators carrying coefficients  $A, B, \dots, L$ . From this expression, a 1PI Green function with  $n$  external lines is obtained by expanding these coefficients at order  $n$  in the external fields. This amounts to take the explicit expression of the coefficients as power series in  $W$  and  $\bar{W}$  and further expand the  $1/\square$  covariant propagators inside them in powers of the bosonic connection  $\Gamma_{\alpha\dot{\alpha}}$  (see eq. (C.0.37)). It follows that 1PI Green functions are generically of the form  $\langle W_\alpha, \dots \bar{W}_{\dot{\alpha}}, \dots \Gamma_{\beta\dot{\beta}} \rangle$  with, possibly, covariant derivatives acting on the fields in order to have all the indices contracted.

As a simple example, we review in this language the well known calculation of the one-loop effective action in  $\mathcal{N} = 4$  theory [1].

The contribution from (matter and ghosts) chiral superfields is given by a vacuum one-loop diagram where the internal line is  $1/\square_+$ . Since we are contracting a chiral with an antichiral superfield we have a factor  $\nabla^2\bar{\nabla}^2$  in the loop. This factor is already sufficient to perform  $\nabla$ -algebra, so no extra derivatives need come out from the expansion (5.2.5) of the propagator. Therefore, the only non-trivial contribution arises from  $\frac{1}{\square_+} \rightarrow A$ . Inserting the explicit expression (C.0.4) for  $A$ , we find that at one-loop a chiral loop contributes to a  $\langle W\bar{W} \rangle$  two-point function, a  $\langle W(\nabla W)\bar{W} \rangle$  three-point function etc... However, at one loop the contributions from the chiral matter fields and the chiral ghosts fields cancel exactly.

The contributions we are left with come from a vector loop when we consider a vacuum one-loop diagram with propagator  $1/\hat{\square}$ . In this case the correct number of spinorial derivatives required by  $\nabla$ -algebra have to be extracted from the expansion of the propagator. From eq. (5.2.6) we see that this happens when  $\frac{1}{\hat{\square}} \rightarrow L\nabla^2\bar{\nabla}^2$ . Expanding the  $L$  coefficient as in (D.0.15) we find that the first non-trivial Green function is a  $\langle WW\bar{W}\bar{W} \rangle$  four-point function [1].

A second example is given in Fig 5.2 where a pure chiral two-loop contribution to the gauge effective action is drawn. This result is easily obtained by moving towards the left vertex the antichiral derivatives from the expansion of the  $\frac{1}{\square_-}$  on the middle line. Since  $\bar{\nabla}^3 = 0$ , all the terms that present a  $\bar{\nabla}$  on the far left of the middle line are zero. So, the middle line propagator can be replaced by

$$\bar{A} - \{\bar{\nabla}^{\dot{\alpha}}, \bar{B}_{\dot{\alpha}}\} + \frac{1}{2}\{\bar{\nabla}^{\dot{\alpha}}, [\bar{\nabla}_{\dot{\alpha}}, \bar{C}]\} \quad (5.3.1)$$

By using identity (C.0.24) we can reduce the middle line to the simple  $A$  coefficient. No extra spinorial derivatives can be originated by the middle line. On both the upper and

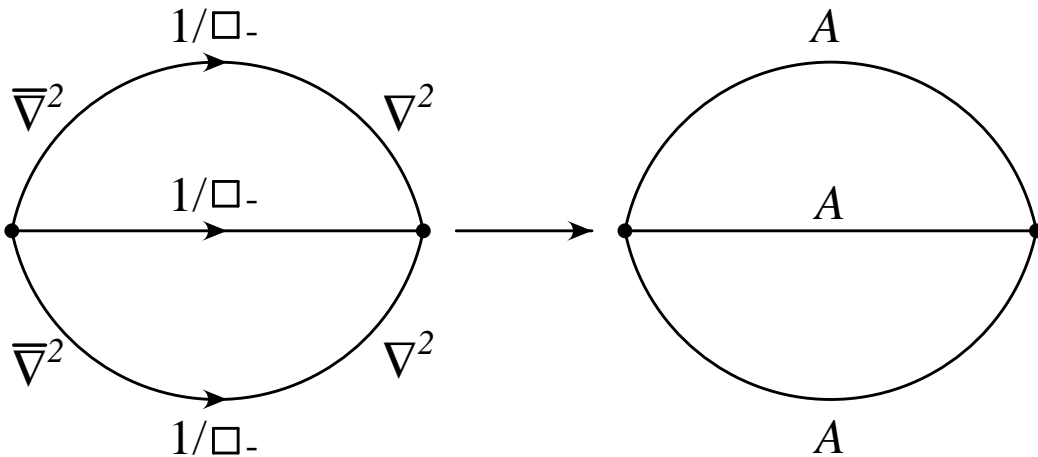


Figure 5.2: Pure chiral two loop contribution to the gauge effective action

the lower loop we are left with the same structure, namely

$$\bar{\nabla}^2 \frac{1}{\square_-} \nabla^2 = \frac{1}{\square_+} \bar{\nabla}^2 \nabla^2 \quad (5.3.2)$$

A simple algebra shows that a  $\bar{\nabla}^2 \nabla^2$  factor can be produced from the  $A$  coefficient inside  $\frac{1}{\square_+}$  only. As a consequence, the result on the right side of Fig 5.2 is produced.

## 5.4 ...to MHV scattering amplitudes

We are mainly interested in the evaluation of scattering amplitudes at two-loops. Extensions of the procedures that we are going to describe here follow immediately by using the two loop case as an example.

At two loop, amplitudes are given by irreducible two-loop diagrams with external lines set on-shell, by two-loop diagrams with trees attached to some of the external lines and, finally, by one-loop (ir)reducible diagrams attached to each other.

Following the procedure described in the previous Section, we compute the effective action up to two loops as a function of the  $A, B, \dots, L$  coefficients. Expanding the coefficients up to a suitable order in the external fields we give rise to  $n$  points scattering amplitudes for  $n$  arbitrary. The great advantage of our procedure is that the evaluation of *all* the amplitudes is reduced to the evaluation of a single object, the on-shell effective action, which can then be considered as the *master equation* of the theory.

In order to be definite, we focus on MHV amplitudes of the form  $(- - + \dots +)$ . However, there is nothing special in the evaluation of these amplitudes. Our procedure

can be easily adapted to any other external configuration.

We list the various steps for going from the effective action to the scattering amplitudes.

Step 1:

Fix the number  $n$  of external particles involved in the scattering process. Then expand the  $A, B, \dots, L$  coefficients up to power  $n$  in the external fields. Since we are interested in MHV amplitudes of the form  $(- - + \dots +)$ , taking into account that  $\overline{W}_\alpha$  carries helicity  $-1$  we can restrict the expansions to terms with at most *two*  $\overline{W}$ 's close to each other. In fact, as long as irreducible contributions are concerned this is all we need. When we attach trees to a two-loop diagram in order to generate a reducible contribution, two  $\overline{W}$ 's might be not sufficient if attaching a tree to a  $\overline{W}$  line we can produce  $W$  terms. However, it is not difficult to convince that from a  $\overline{W}$  line at least one line of the same helicity always comes out. This is an obvious consequence of helicity conservation and can be explicitly checked in superspace language. Therefore, in the effective action we can neglect contributions proportional to more than two  $\overline{W}$ 's and contributions where the two  $\overline{W}$ 's are not close to each other. As explained in Appendices C and D, these rules allow to take advantage of non-trivial identities which greatly simplify the process of expanding the propagators. There, we list the expansions of the coefficients suitable for MHV amplitudes up to six particles.

Step 2:

Substitute in the effective action the explicit expressions of the coefficients and keep only terms with a number of external fields less or equal to  $n$ . Since different coefficients carry a different number of external fields, we can easily classify the various contributions according to the topology of the associated diagram. For example, contributions which arise from a diagram with a  $A$  coefficient on one line will give rise to bubbles when taking the  $1/\square_0$  part of  $A$  (see eqs. (C.0.4), (C.0.37) and Fig 5.1). Similarly, contributions with a  $B$  coefficient on one line will give rise to triangles when we take the first order term in the  $B$  expansion (see eq. (C.0.5)). For the terms with a number of external fields  $k < n$  further expand covariant propagators and derivatives (see equations (A.0.15) and (C.0.37)) and keep terms up to  $l - k$  connections  $\Gamma$ 's.

Step 3:

Fourier transform external fields and propagators to momentum space following the conventions in Appendix G. Working out the associated group factor, the various contributions end up to be the product of a given trace structure of a string of external fields times a loop momentum integral.

Step 4:

In general, the momentum integrals have vector-like or tensor-like numerators. It is therefore necessary to apply Passarino-Veltman reduction in order to rewrite them as a linear combination of scalar integrals.

Step 5:

Once we have the effective action in terms of scalar integrals, we generate all possible contributions to the  $n$ -point  $(- - + \cdots +)$  scattering amplitude by constructing trees of 1PI diagrams. 1PI contributions are obtained from terms in the effective action with exactly  $n$  external lines, once we identify the external lines with background on-shell fields and sum over all possible cyclic permutations of their quantum numbers (momenta, helicity and gauge index). Reducible contributions are obtained by attaching trees to 1PI contributions with a smaller number of external lines or by attaching lower loop order diagrams and, again, summing over all cyclic permutations of the external particles. Since at one loop the first non-trivial Green function is  $(W\overline{W}\overline{W})$ , when we attach two one-loop diagrams in order to get a two-loop contribution to  $(- - + \cdots +)$  we are forced to connect two  $\overline{W}$ 's lines. Note that the first case where these contributions appear is the six-point amplitude.

As long as we are not interested in the final result for the amplitude but only in the structure of scalar momentum integrals involved, this is it. The main observation is Steps 1-5 can be implemented by computer's programs once we have determined the effective action. On the other hand, the same  $\nabla$ -algebra procedure, which is the key step for the determination of the effective action, can be performed by following a mechanical procedure that can be programmed. Even if rigid procedures are not the smartest way to perform the  $\nabla$ -algebra and this, in principle, could produce more than the minimal set of contributing diagrams, however the computational power of a computer is extremely useful to make exceptionally quick and comfortable the extraction of these contributions. Moreover, it is always possible (even if not tightly necessary) to use the large number of identities between the coefficients worked out in the Appendices C and D and reduce the output of the computer to a minimal set of diagrams. A description of the system of programs we developed and extensively used along the computation is given in Appendix J.



# Chapter 6

## Two loop effective action in $\mathcal{N} = 4$ SYM theory

The  $\mathcal{N} = 4$  SYM theory, although it has been widely studied in the last decades, is still nowadays one of the main subject of modern theoretical research and reserves again a lot of surprises. As discussed in Chapter 4, although the cutting techniques discovered a lot of remarkable properties of planar MHV amplitudes, the general validity of the method and of the regularities that it seems to reveal are questionable. It is so natural that the first application of our direct computational technologies points in the direction to give new insights in the contest of this theory or to confirm the old issues.

The aim of this Chapter is to write a general *master formula* for the  $n$  point 1PI MHV effective action at two loops in  $\mathcal{N} = 4$  SYM theory. From there, by following the general procedure outlined in Section 5.4, it is in principle possible to extract the two loop MHV scattering amplitude for any number of scattered particles.

We divide the computational procedure into three conceptually different steps:

- 1) From the gauge fixed  $\mathcal{N} = 4$  lagrangian, we extrapolate the interaction vertices. In principle, there is an infinite series of quantum vertices. However, as soon as we are interested in a two loop computation we need to keep only the cubic and the quartic quantum vertices. These vertices are used to form the vacuum diagrams. By looking at the covariant propagators forming the diagrams, we can divide them into nine different classes. Diagrams inside the same class are distinguishable for a different distribution of spinorial derivatives at the vertices. We have a total of 43 distinct vacuum diagrams in which all the scattering amplitudes of the  $\mathcal{N} = 4$  SYM theory at two loop are summarized in an extremely compact form.
- 2) We follow the  $\nabla$ -algebra procedure in order to extrapolate from each vacuum diagram the contributions to the planar MHV amplitude. In some case the  $\nabla$ -algebra is quite trivial, as in the example of Fig. 5.2. In the most of the cases, in particular

when the vector propagator  $\frac{1}{\square}$  is involved, the computations are very long. Confidence in our results follows from the perfect agreement between hand made and computer made results for each of the vacuum diagrams.

- 3) In principle, at the end of the previous step we have already an expression for the all- $n$  MHV effective action. However, some of the terms in the expressions presents UV divergences in  $D = 4$ . Since the  $\mathcal{N} = 4$  SYM theory is UV finite, it must be that all the divergent terms sum into finite contributions: This is the case. This fact is a very complex test for our results and for all the computational strategy we followed. In order to get this point a key role is played by the identities between the propagator coefficients listed in Appendices C and D.

In the following three Sections each of these three steps are analyzed in details. The final expression that we get is a UV finite *master equation* for the MHV planar effective action at two loop. This is the main result of the second part of the thesis.

After UV divergences are canceled, the master equation is given by a linear combination of Feynman diagrams dependent on the expansion coefficients of the covariant propagators. Each term in the combination is UV finite. As a consequence, no diagrams with bubbles are present. However, this is not a demonstration of the validity of the no-bubble hypothesis at two loop for any number of interacting particles. In fact, other bubbles are produced when we Fourier transform to momentum space the effective action and perform the Passarino-Veltman reduction on vector and tensor loop integrals. Of course, the extra bubbles enter the final expression in combinations such that their UV divergent part cancel.

Less and less can be said at this level about the no-triangle hypothesis. In fact, in the master equation there are a lot of terms that include triangles and their supposed cancellation at this level has still the appearance of a miracle.

We start the computation of the master equation by analyzing the gauge fixed  $\mathcal{N} = 4$  lagrangian and by extracting from there the interaction vertices.

## 6.1 $\mathcal{N} = 4$ Lagrangian, vertices and vacuum diagrams

The physical content of the  $\mathcal{N} = 4$  vector multiplet is given by a spin-1 vector, 4 spin- $\frac{1}{2}$  Majorana spinors and 6 scalars, all transforming in the adjoint representation of the gauge group  $SU(N)$ .

The field content can be organized in  $\mathcal{N} = 1$  superfields as a vector superfield  $V$  and 3 chiral superfields  $\Phi_i$ . The full action of the theory is recovered from the the general expression (5.2.2) for SYM theories by fixing the superpotential  $\mathcal{V}(\Phi^i)$  to be

$$\mathcal{V}(\Phi^i) = +\frac{ig}{3!} \text{Tr} (\epsilon_{ijk} \Phi^i [\Phi^j, \Phi^k]) \quad (6.1.1)$$



### 6.1.1 $\mathcal{N} = 4$ SYM quantum vertices

By performing the quantum–background splitting as prescribed by the background field method (see Section 5.2.1) and by expanding the  $\mathcal{N} = 4$  SYM action in powers of the quantum fields, we can work out the quantum vertices of the theory needed for two loop calculations. In what follows we list and divide them in five different classes according to their field content.

#### 1) Pure (anti)chiral 3pt vertex

$$\begin{aligned}
& + \frac{ig}{3!} \text{Tr} \int d^6 z \epsilon_{ijk} \Phi^i [\Phi^j, \Phi^k] + \frac{ig}{3!} \text{Tr} \int d^6 \bar{z} \epsilon_{ijk} \bar{\Phi}^i [\bar{\Phi}^j, \bar{\Phi}^k] \longrightarrow \\
& V_1 = ig(if^{abc}) \Phi_1^a \Phi_2^b \Phi_3^c \quad \bar{V}_1 = ig(if^{abc}) \bar{\Phi}_1^a \bar{\Phi}_2^b \bar{\Phi}_3^c \quad (6.1.2)
\end{aligned}$$

#### 2) 3pt and 4pt chiral–vector vertices

$$\begin{aligned}
& \int d^8 z \text{Tr} (e^{-gV} \bar{\Phi}_i e^{gV} \Phi_i) \longrightarrow \\
& V_2 = g(if^{abc}) \bar{\Phi}_i^a V^b \Phi_i^c \quad V_3 = -\frac{g^2}{2} (f^{abe} f^{cde}) \bar{\Phi}_i^a V^b V^c \Phi_i^d \quad (6.1.3)
\end{aligned}$$

#### 3) 3pt pure vector vertex

From the expansion of the gauge action we read

$$\begin{aligned}
& \frac{1}{2g^2} \int d^6 z \text{Tr} W^\alpha W_\alpha \longrightarrow \\
& \frac{g}{2} \int d^8 z \text{Tr} \left( V \{ \nabla^\alpha V, \bar{\nabla}^2 \nabla_\alpha V \} + \frac{1}{3} [ [\nabla^\alpha V, V], V ] i W_\alpha \right) \\
& = -\frac{g}{2} if^{abc} \int d^8 z \text{Tr} \left( (\nabla^\alpha V^a) V^b \bar{\nabla}^2 \nabla_\alpha V^c + \frac{1}{3} (\nabla^\alpha V^a) V^b [i W_\alpha, V]^c \right) \quad (6.1.4)
\end{aligned}$$

For these expressions see also [100].

In view of building the pure vector vacuum diagrams, we consider the six permutations of the three quantum lines (three cyclic permutations plus three anticyclic ones). Then, we integrate by parts in order to free one line, let's say the upper one. In so doing we find

$$\begin{aligned}
& \frac{g}{2} \int d^8 z \text{Tr} (V \{ \nabla^\alpha V, \bar{\nabla}^2 \nabla_\alpha V \}) \rightarrow \\
& \frac{g}{2} if^{abc} V^a \left( -2 \bar{\nabla}^2 V^b \nabla^2 V^c + 2 \nabla^\alpha V^b \nabla_\alpha \bar{\nabla}^2 V^c - 2 \bar{\nabla}^{\dot{\alpha}} V^b \bar{\nabla}_{\dot{\alpha}} \nabla^2 V^c + \nabla^\alpha V^b i \nabla_{\alpha \dot{\alpha}} \bar{\nabla}^{\dot{\alpha}} V^c \right. \\
& \quad \left. - \bar{\nabla}^{\dot{\alpha}} V^b i \nabla_{\alpha \dot{\alpha}} \nabla^\alpha V^c - i \nabla^{\alpha \dot{\alpha}} V^b \bar{\nabla}_{\dot{\alpha}} \nabla_\alpha V^c - \nabla^\alpha V^b [i W_\alpha, V]^c \right. \\
& \quad \left. + \text{exchange of lines } b \text{ and } c \right) \quad (6.1.5)
\end{aligned}$$

and

$$\begin{aligned} & \frac{g}{2} \int d^8 z \operatorname{Tr} \left( \frac{1}{3} [[\nabla^\alpha V, V], V] i W_\alpha \right) \rightarrow \\ & \frac{g}{2} i f^{abc} V^a \left( \nabla^\alpha V^b [i W_\alpha, V]^c + \text{exchange of lines } b \text{ and } c \right) \end{aligned} \quad (6.1.6)$$

where ‘‘exchange of lines  $b$  and  $c$ ’’ means writing terms with the two entries interchanged taking into account a sign from  $f^{acb} \rightarrow -f^{abc}$  and possible signs from the exchange of fermions\*.

Summing the two contributions, the terms containing  $W_\alpha$  cancel! This simplification of the vertex implies that a smaller number of vacuum diagrams can be constructed. Thus, this cancellation can be interpreted as an automatic resummation of a lot of terms in the effective action.

In conclusion, the analogous of the permuted vertex we need use is

$$\begin{aligned} V_4 &= \frac{g}{2} i f^{abc} V^a \left( -2 \bar{\nabla}^2 V^b \nabla^2 V^c + 2 \nabla^\alpha V^b \nabla_\alpha \bar{\nabla}^2 V^c - 2 \bar{\nabla}^{\dot{\alpha}} V^b \bar{\nabla}_{\dot{\alpha}} \nabla^2 V^c \right. \\ & \quad \left. + \nabla^\alpha V^b i \nabla_{\alpha \dot{\alpha}} \bar{\nabla}^{\dot{\alpha}} V^c - \bar{\nabla}^{\dot{\alpha}} V^b i \nabla_{\alpha \dot{\alpha}} \nabla^\alpha V^c - i \nabla^{\alpha \dot{\alpha}} V^b \bar{\nabla}_{\dot{\alpha}} \nabla_\alpha V^c \right. \\ & \quad \left. + \text{exchange of lines } b \text{ and } c \right) \\ &= -\frac{g}{2} i f^{abc} \left( -2 \bar{\nabla}^2 V^a V^b \nabla^2 V^c + \dots \right) \end{aligned} \quad (6.1.7)$$

#### 4) 4pt pure vector vertex

From the gauge action we read

$$\begin{aligned} & \frac{1}{2g^2} \int d^6 z \operatorname{Tr} W^\alpha W_\alpha \rightarrow \quad (6.1.8) \\ & \frac{g^2}{2} \int d^8 z \operatorname{Tr} \left( -\frac{1}{3} (\bar{\nabla}^2 \nabla^\alpha V) [V, [V, \nabla_\alpha V]] - \frac{1}{4} [V, \nabla^\alpha V] \bar{\nabla}^2 [V, \nabla_\alpha V] \right. \\ & \quad \left. + \frac{i}{12} [[[\nabla^\alpha V, V], V], V] W_\alpha \right) \rightarrow \\ V_5 &= (f^{abe} f^{cde}) \left( \frac{g^2}{8} V^a (\nabla^\alpha V^b) \bar{\nabla}^2 (V^c (\nabla_\alpha V^d)) + \frac{g^2}{6} (\bar{\nabla}^2 \nabla^\alpha V^a) V^b V^c (\nabla_\alpha V^d) \right) \\ &= \frac{g^2}{8} (f^{abe} f^{cde}) \left( V^a \nabla^\alpha V^b \bar{\nabla}^2 V^c \nabla_\alpha V^d - \frac{1}{3} V^a \nabla^\alpha V^b V^c \bar{\nabla}^2 \nabla_\alpha V^d \right. \\ & \quad \left. + V^a \nabla^\alpha V^b \bar{\nabla}^{\dot{\alpha}} V^c \bar{\nabla}_{\dot{\alpha}} \nabla_\alpha V^d \right) \\ V_6 &= \frac{g^2}{24} (f^{abf} f^{fcg} f^{gde}) (\nabla^\alpha V)^a V^b V^c V^d W^e \end{aligned}$$

---

\*See Appendix I for a detailed discussion

## 5) 3pt and 4pt ghost–vector vertices

Interactions between ghosts and vector fields are described by the following vertices

$$\begin{aligned}
& \text{Tr} \int d^8 z \ (c' + \bar{c}') L_{\frac{1}{2}gV} \left[ (c + \bar{c}) + \coth \left( L_{\frac{1}{2}gV} \right) (c - \bar{c}) \right] \longrightarrow \quad (6.1.9) \\
& \text{Tr} \int d^8 z \ \left\{ \frac{g}{2} (c' + \bar{c}') [V, c + \bar{c}] + \frac{g^2}{12} (c' + \bar{c}') [V, [V, c - \bar{c}]] \right\} \longrightarrow \\
V_7 &= \frac{g}{2} (i f^{abc}) c'^a V^b c^c & \bar{V}_7 &= \frac{g}{2} (i f^{abc}) \bar{c}'^a V^b \bar{c}^c \\
V_8 &= \frac{g}{2} (i f^{abc}) c'^a V^b \bar{c}^c & \bar{V}_8 &= \frac{g}{2} (i f^{abc}) \bar{c}'^a V^b c^c \\
V_9 &= \frac{g^2}{12} (f_{abe} f_{ecd}) c^a V^b V^c c'^d & \bar{V}_9 &= -\frac{g^2}{12} (f_{abe} f_{ecd}) \bar{c}^a V^b V^c \bar{c}'^d \\
V_{10} &= \frac{g^2}{12} (f_{abe} f_{ecd}) c^a V^b V^c \bar{c}'^d & \bar{V}_{10} &= -\frac{g^2}{12} (f_{abe} f_{ecd}) \bar{c}^a V^b V^c c'^d
\end{aligned}$$

Note that the Nielsen–Kallosh ghosts are not present because they contribute at one loop only.

### 6.1.2 Vacuum graphs and combinatorics

Using the vertices listed in the previous Section, we can build up the the two–loop vacuum diagrams in which the effective action is built in<sup>†</sup>. We can distinguish between two classes of diagrams: 1) The *cubic vertex vacuum diagrams* and 2) the *tadpole–like vacuum diagrams*. More in detail we have

- 1) Diagrams coming from the contractions  $\langle V_1 \bar{V}_1 \rangle$ ,  $\langle V_2 V_2 \rangle$ ,  $\langle V_4 V_4 \rangle$ ,  $\langle V_7 \bar{V}_7 \rangle$  and  $\langle V_8 \bar{V}_8 \rangle$  (see Fig 6.1) The name of these diagrams is a consequence of the fact that the quantum vertices forming them are cubic vertices.
- 2) Diagrams from the higher point vertices  $V_3$ ,  $V_5$ ,  $V_{10}$ ,  $\bar{V}_{10}$  and  $V_6$  (see Fig 6.2) These diagrams are formed by the four point quantum interactions. The fact that their loops are formed by two covariant propagators, one on each loop, allow to think at them as to squares of one loop diagrams in view of computing the  $\nabla$ –algebra.

Note that in this list of diagrams we have never used vertices  $V_9$  and  $\bar{V}_9$ . Although they are four point vertices, they cannot form two loop vacuum diagrams. Thus they do not contribute at this perturbative order.

A quick inspection shows that graph (i) in Fig 6.2 cannot contribute to the MHV effective action since it would give strings with at least four  $\bar{W}$ 's. Therefore, we will discard it in the rest of the discussion.

---

<sup>†</sup>For the vertices we follow the same labeling  $V_i$  of the previous Section

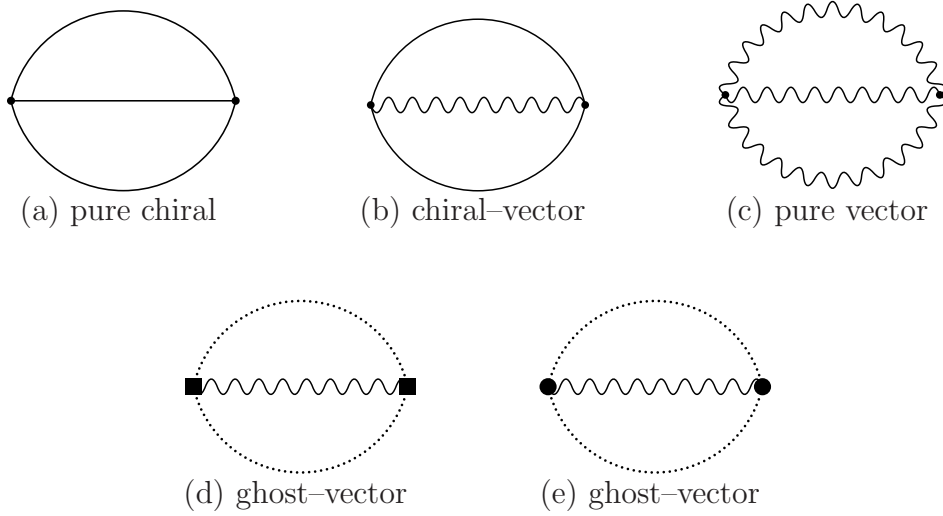


Figure 6.1: Cubic vertex vacuum diagrams

In diagrams (d) and (e) of Fig 6.1 where ghosts are involved we distinguish between graphs built up with pure (anti)chiral vertices of type 7 (graphs (d) with square vertices) and mixed chiral-anti chiral vertices of type 8 (graphs (e) with blob vertices). This distinction is useful since the  $\nabla$ -algebra and the combinatorial factors are different in the two cases.

The combinatorial factors including signs and coefficients from the second order expansion of  $e^S$ , from the vertices and from the propagators times the actual combinatorics are summarized in Table 6.1. In diagrams (a-e)  $f^{abc}$  is the color factor from the left

Graph	Combinatoric	Graph	Combinatoric
(a)	$-\frac{1}{2}g^2(f^{abc}f^{def})$	(e)	$-\frac{1}{4}g^2(f^{abc}f^{def})$
(b)	$\frac{3}{2}g^2(f^{abc}f^{def})$	(f)	$\frac{3}{2}g^2(f^{abe}f^{ecd})$
(c)	$-\frac{1}{8}g^2(f^{abc}f^{def})$	(g)	$\frac{1}{8}g^2(f^{abe}f^{ecd})$
(d)	$\frac{1}{8}g^2(f^{abc}f^{def})$	(h)	$\frac{1}{12}g^2(f^{abe}f^{ecd})$

Table 6.1: Combinatoric for vacuum diagrams

vertex,  $f^{def}$  the one from the right vertex both with the indices ordered from the upper to the bottom line. For diagrams (f-h) the way the color indices are distributed on the lines will be explicitly indicated in the pictures containing the results of the  $\nabla$ -algebra

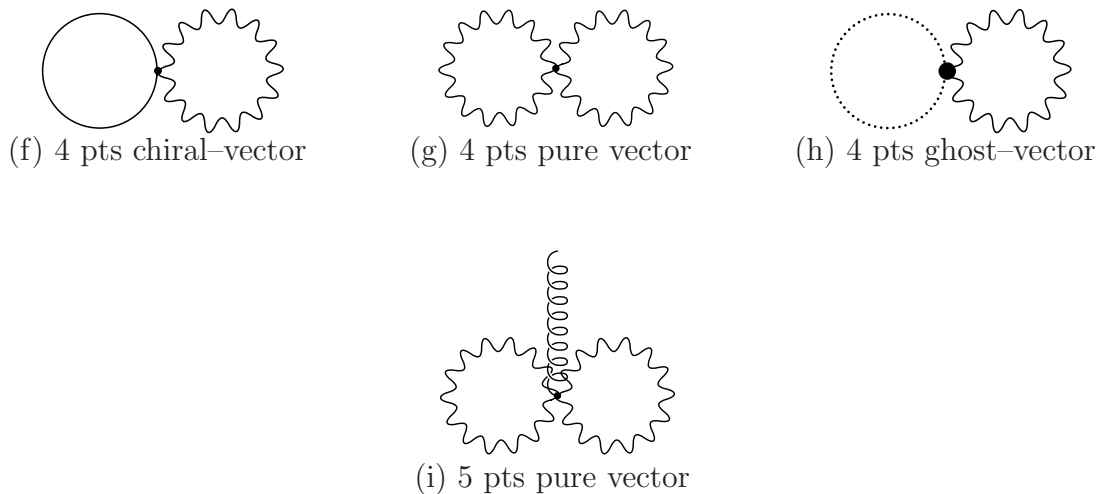


Figure 6.2: Tadpole-like vacuum diagrams

(see Section 6.2.2).

We stress that each picture (a)–(i) refers actually to a class of one or more vacuum diagrams that come out from the same vertices contractions but differs for the distribution of spinorial derivatives on the left and the right vertices.

A further remarkable observation is that the results that we attribute here to the  $\mathcal{N} = 4$  SYM theory, actually can be partially used for other SYM theories too. Since the differences between two SYM theories are given by the matter content of the theories and are contained in the superpotential  $\mathcal{V}(\Phi^i)$ , at the level of vacuum diagrams they manifest themselves only in the graphs involving chiral lines (i.e. in diagrams (a), (b) of Fig 6.1 and (f) of Fig 6.2) and in their combinatorial factors. All the diagrams involving vectors and ghosts are shared by all the SYM theories. For example, the pure  $\mathcal{N} = 1$  SYM theory can be obtained from the same analysis here performed by simply discarding all the parts involving the chiral matter fields.

## 6.2 $\nabla$ -algebra for the two-loop contributions

In the previous Section, using the interaction vertices of the  $\mathcal{N} = 4$  action we built all two-loop vacuum diagrams. In this Section we analyze them case by case and we perform the covariant derivative algebra ( $\nabla$ -algebra) in the planar limit and by keeping terms that contain up to two  $\overline{W}$ . Thus our results are suitable for the computation of MHV amplitudes.

As we have previously mentioned,  $\mathcal{N} = 4$  SYM theory is UV finite. In spite of

this, power counting analysis of the  $\nabla$ -algebra results shows that there are UV divergent diagrams. We postpone the problem of the cancellation of the divergences after the description of the  $\nabla$ -algebra results. However, in the following we distinguish between UV finite graphs (we close them in boxes) and UV divergent ones. We will take care of the latter in Section 6.3.

Before entering the calculation, we remind the expansion of the propagators as given in the appendices C and D. The chiral propagators are given by

$$\begin{aligned}\frac{1}{\square_+} &= A + B^\alpha \nabla_\alpha + C \nabla^2 \\ \frac{1}{\square_-} &= \bar{A} + \bar{B}^{\dot{\alpha}} \bar{\nabla}_{\dot{\alpha}} + \bar{C} \bar{\nabla}^2\end{aligned}\tag{6.2.1}$$

For the vector propagator we write

$$\begin{aligned}\frac{1}{\hat{\square}} &= A + B^\alpha \nabla_\alpha + C \nabla^2 + \bar{D}^{\dot{\alpha}} \bar{\nabla}_{\dot{\alpha}} + E^{\alpha\dot{\alpha}} \nabla_\alpha \bar{\nabla}_{\dot{\alpha}} + \bar{F}^{\dot{\alpha}} \nabla^2 \bar{\nabla}_{\dot{\alpha}} + \bar{G} \bar{\nabla}^2 + H^\alpha \nabla_\alpha \bar{\nabla}^2 + L \nabla^2 \bar{\nabla}^2 \\ &= \bar{A} + \bar{B}^{\dot{\alpha}} \bar{\nabla}_{\dot{\alpha}} + \bar{C} \bar{\nabla}^2 + D^\alpha \nabla_\alpha + \bar{E}^{\alpha\dot{\alpha}} \bar{\nabla}_{\dot{\alpha}} \nabla_\alpha + F^\alpha \bar{\nabla}^2 \nabla_\alpha + G \nabla^2 + \bar{H}^{\dot{\alpha}} \bar{\nabla}_{\dot{\alpha}} \nabla^2 + \bar{L} \bar{\nabla}^2 \nabla^2\end{aligned}\tag{6.2.2}$$

Moreover

$$\begin{aligned}\nabla_\alpha \frac{1}{\square_+} &= \mathcal{A}_\alpha + \mathcal{B}_\alpha^\beta \nabla_\beta + \mathcal{C}_\alpha \nabla^2 \\ \bar{\nabla}_{\dot{\alpha}} \frac{1}{\square_-} &= \bar{\mathcal{A}}_{\dot{\alpha}} + \bar{\mathcal{B}}_{\dot{\alpha}}^{\dot{\beta}} \bar{\nabla}_{\dot{\beta}} + \bar{\mathcal{C}}_{\dot{\alpha}} \bar{\nabla}^2 \\ \nabla_\alpha \frac{1}{\hat{\square}} &= \mathcal{D}_\alpha^\beta \nabla_\beta + \bar{\mathcal{E}}_\alpha^{\beta\dot{\beta}} \bar{\nabla}_{\dot{\beta}} \nabla_\beta + \mathcal{F}_\alpha^\beta \bar{\nabla}^2 \nabla_\beta + \mathcal{G}_\alpha \nabla^2 + \bar{\mathcal{H}}_\alpha^{\dot{\beta}} \bar{\nabla}_{\dot{\beta}} \nabla^2 + \bar{\mathcal{L}}_\alpha \bar{\nabla}^2 \nabla^2 \\ \bar{\nabla}_{\dot{\alpha}} \frac{1}{\hat{\square}} &= \bar{\mathcal{D}}_{\dot{\alpha}}^{\dot{\beta}} \bar{\nabla}_{\dot{\beta}} + \mathcal{E}_{\dot{\alpha}}^{\beta\dot{\beta}} \nabla_\beta \bar{\nabla}_{\dot{\beta}} + \bar{\mathcal{F}}_{\dot{\alpha}}^{\dot{\beta}} \nabla^2 \bar{\nabla}_{\dot{\beta}} + \bar{\mathcal{G}}_{\dot{\alpha}} \bar{\nabla}^2 + \mathcal{H}_{\dot{\alpha}}^\beta \nabla_\beta \bar{\nabla}^2 + \mathcal{L}_{\dot{\alpha}} \nabla^2 \bar{\nabla}^2 \\ \bar{\nabla}_{\dot{\alpha}} \nabla_\alpha \frac{1}{\hat{\square}} &= d_{\alpha\dot{\alpha}}^\beta \nabla_\beta + \bar{e}_{\alpha\dot{\alpha}}^{\beta\dot{\beta}} \bar{\nabla}_{\dot{\beta}} \nabla_\beta + f_{\alpha\dot{\alpha}}^\beta \bar{\nabla}^2 \nabla_\beta + g_{\alpha\dot{\alpha}} \nabla^2 + \bar{h}_{\alpha\dot{\alpha}}^{\dot{\beta}} \bar{\nabla}_{\dot{\beta}} \nabla^2 + \bar{l}_{\alpha\dot{\alpha}} \bar{\nabla}^2 \nabla^2\end{aligned}\tag{6.2.3}$$

The results of the  $\nabla$ -algebra are expressed in term of these expansion coefficients. It is important to point out that these results are fully general in the number of interacting particles and they potentially include all possible external helicity configurations. The selection of a particular scattering process (for example a MHV process with a fixed number of particles) enters after the  $\nabla$ -algebra procedure and is based on the knowledge of the explicit form of the power expansion of the coefficients.

### 6.2.1 Diagrams with cubic vertices

We analyze first of all the cubic vertex diagrams of Fig. 6.1. For this class of diagrams, in the planar limit the  $\nabla$ -algebra gets simplified. In fact, the planarity of the diagrams requires that at the final stage one of the lines must be free from any background insertion. This result can be reached in three steps: Firstly choose a line and free it up from the derivatives coming from the vertices. Then replace the propagator on that line with its expansion previously described and integrate away the new covariant derivatives that the expansion coefficients carry. As last step, we need insert the expansions for the covariant propagators present on the other two lines and select on each line only the terms that produces a  $\nabla^2\bar{\nabla}^2$  or  $\bar{\nabla}^2\nabla^2$ . Here enters the planar limit: Looking at the explicit expressions for the coefficients, only diagrams with at least a coefficient that includes a single  $\frac{1}{\square}^\ddagger$  have to be considered.

The computational procedure here described is general enough to be applied to all vacuum diagrams in this class. Moreover it is extremely mechanic. These two features made possible to transpose the computation of the  $\nabla$ -algebra for these diagrams in useful and time conserving computer programs. We describe them in Appendix J.

#### Pure chiral graph

The pure chiral diagram in Fig. 6.1 (a) is built by contracting the  $V_1$  and  $\bar{V}_1$  vertices (6.1.2) coming from the superpotential part of the action

$$ig(if^{abc})\Phi_1^a\Phi_2^b\Phi_3^c + ig(if^{abc})\bar{\Phi}_1^a\bar{\Phi}_2^b\bar{\Phi}_3^c \quad (6.2.4)$$

When contracting, we find convenient to treat the two diagrams, the one with the chiral vertex on the left and the one with the chiral vertex on the right, separately. We can summarize the results in the following table (we put arrows on chiral propagators with the convention that they go from a chiral to an anti-chiral leg)

$$V_1 \begin{array}{c} \xrightarrow{1/\square} \\ \nabla^2 \curvearrowright \\ \xrightarrow{1/\square} \\ \nabla^2 \curvearrowleft \\ \xrightarrow{1/\square} \end{array} \bar{V}_1 \longrightarrow \begin{array}{c} A \\ \circ \\ A \\ \circ \\ A \end{array} \quad (6.2.5)$$

---

<sup>‡</sup>They are  $A, \bar{A}, \mathcal{B}_\alpha^\beta, \bar{\mathcal{B}}_\alpha^{\dot{\beta}}$  and  $\bar{e}_{\alpha\dot{\alpha}}^{\beta\dot{\beta}}$

$\bar{V}_1 \begin{array}{c} \xrightarrow{1/\square_+} \\ \nabla^2 \quad \bar{\nabla}^2 \\ \xleftarrow{1/\square_+} \\ \nabla^2 \quad \bar{\nabla}^2 \\ \xrightarrow{1/\square_+} \\ \end{array} V_1 \longrightarrow \begin{array}{c} \bar{A} \\ \bar{A} \\ \bar{A} \end{array}$ 
(6.2.6)

It is important to remark that we have not yet impose the planar limit on each of these contributions. We postpone this problem after finishing with the  $\nabla$ -algebra of the other sectors of the theory: We will take care of it in Section 6.3 where the cancellation of UV divergences is considered.

Before concluding this section, we remember that the combinatorial factor is

$$-\frac{1}{2}g^2(f^{abc}f^{def}) \tag{6.2.7}$$

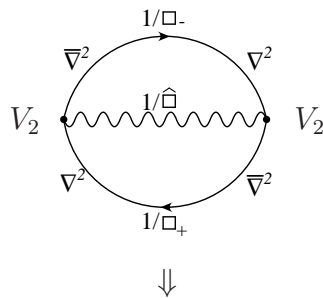
The  $\nabla$ -algebra relative to this sector has been described in details after Fig. 5.2.

### Chiral–vector graphs

The second type of graphs we consider are the ones obtained from the cubic chiral–vector vertex  $V_2$  (6.1.3) (see Fig. 6.1 (b)). The vertex has this form

$$g(if^{abc})\bar{\Phi}_i^a V^b \Phi_i^c \quad i = 1, 2, 3 \tag{6.2.8}$$

Note that in this case the exchange of the right and left vertices does not give rise to a different situation as in the pure chiral case. Studying the only graph that can be written, we get





$$\begin{aligned}
& \begin{array}{c} A \\ \text{---} \\ \bar{A} \\ \text{---} \\ A \end{array} + \begin{array}{c} B^\alpha \\ \text{---} \\ \bar{A} \\ \text{---} \\ \bar{B}^{\dot{\alpha}} i \nabla_{\alpha \dot{\alpha}} - \bar{C} i W_\alpha \end{array} + \begin{array}{c} \bar{D}^{\dot{\alpha}} \\ \text{---} \\ \bar{A} \\ \text{---} \\ B^\alpha i \nabla_{\alpha \dot{\alpha}} - C i \bar{W}_{\dot{\alpha}} \end{array} \\
& + \begin{array}{c} A i \nabla^{\alpha \dot{\alpha}} \\ \text{---} \\ \bar{A} \\ \text{---} \\ E_{\alpha \dot{\alpha}} \end{array} + \begin{array}{c} A i \bar{W}^{\dot{\alpha}} \\ \text{---} \\ \bar{A} \\ \text{---} \\ \bar{F}_{\dot{\alpha}} \end{array} + \begin{array}{c} \bar{F}^{\dot{\alpha}} \\ \text{---} \\ A i \nabla^{\alpha}_{\dot{\alpha}} \\ \text{---} \\ \bar{B}^{\dot{\beta}} i \nabla_{\alpha \dot{\beta}} - \bar{C} i W_\alpha \end{array} + \begin{array}{c} \bar{A} \\ \text{---} \\ \delta_{be} \\ \text{---} \\ L \end{array}
\end{aligned} \tag{6.2.9}$$

Even here, we did not impose the planar limit on these results. Notice that there are cases in which this operation is straightforward: One of these cases is the last tadpole-like diagram, where we were forced to add a  $\delta_{be}$  on the color indices.

After some integration by parts and by using relations (C.0.12)–(C.0.17) and (D.0.3)–(D.0.8) given in Appendices C and D, it is possible to re-write (6.2.9) in a form that is manifestly self conjugated. Keeping only the terms that are relevant for an MHV amplitude (in particular, let us remember that the addenda in  $L$  have always two  $\bar{W}$  external fields (see expression (D.0.15))), the amplitude takes the following form

$$\begin{aligned}
& \begin{array}{c} 1/\square_- \\ \nabla^2 \quad \nabla^2 \\ V_2 \text{---} \text{---} \text{---} V_2 \\ \nabla^2 \quad \nabla^2 \\ 1/\square_+ \end{array} \\
& \Downarrow \\
& \frac{1}{2} \begin{array}{c} A \\ \text{---} \\ \bar{A} \\ \text{---} \\ A \end{array} + \frac{1}{2} \begin{array}{c} \bar{A} \\ \text{---} \\ A \\ \text{---} \\ \bar{A} \end{array} - \frac{1}{2} \begin{array}{c} A i \nabla^{\alpha \dot{\alpha}} \\ \text{---} \\ \bar{A} \\ \text{---} \\ E_{\alpha \dot{\alpha}} \end{array} - \frac{1}{2} \begin{array}{c} \bar{A} i \nabla^{\alpha \dot{\alpha}} \\ \text{---} \\ A \\ \text{---} \\ \bar{E}_{\alpha \dot{\alpha}} \end{array}
\end{aligned}$$

$$\begin{aligned}
& -\frac{1}{2} \left( \begin{array}{c} A \\ \text{---} \overline{A} \text{---} \\ \text{---} \overline{F}^{\dot{\alpha}i} \overline{W}_{\dot{\alpha}} + H^{\alpha i} W_{\alpha} \end{array} \right) + \left( \begin{array}{c} D^{\alpha} \\ \text{---} A \text{---} \\ \text{---} \overline{B}^{\dot{\alpha}i} \nabla_{\alpha\dot{\alpha}} - \overline{C}iW_{\alpha} \end{array} \right) + \left( \begin{array}{c} \overline{D}^{\dot{\alpha}} \\ \text{---} \overline{A} \text{---} \\ \text{---} B^{\alpha i} \nabla_{\alpha\dot{\alpha}} - Ci\overline{W}_{\dot{\alpha}} \end{array} \right) + \left( \begin{array}{c} \frac{1}{\square} \\ \text{---} \text{---} \\ L \end{array} \right) \delta_{be}
\end{aligned}
\tag{6.2.10}$$

The combinatorial factor of these graphs is

$$\frac{3}{2} g^2 (f^{abc} f^{def})
\tag{6.2.11}$$

The factor 3 comes from the 3 different chiral fields that enter the vertex (6.1.3).

### Vector-ghosts graphs

Using vertices  $V_7$ ,  $\overline{V}_7$ ,  $V_8$  and  $\overline{V}_8$  (6.1.9) we can draw four different diagrams

$$\begin{array}{cc}
\begin{array}{c} \text{---} \overline{V}_7 \text{---} \\ \text{---} \text{---} \\ \text{---} V_7 \text{---} \end{array} & \begin{array}{c} \text{---} V_7 \text{---} \\ \text{---} \text{---} \\ \text{---} \overline{V}_7 \text{---} \end{array} \\
\begin{array}{c} \text{---} V_8 \text{---} \\ \text{---} \text{---} \\ \text{---} \overline{V}_8 \text{---} \end{array} & \begin{array}{c} \text{---} \overline{V}_8 \text{---} \\ \text{---} \text{---} \\ \text{---} V_8 \text{---} \end{array}
\end{array}
\tag{6.2.12}$$

The first two are of type (d), whereas the last two of type (e) of Fig. 6.1. We consider them separately.

- Type (d) graphs 

We consider the first two graphs in (6.2.12). The  $\nabla$ -algebra of these graphs can be reduced to the one of the pure-chiral diagram by first moving one of the  $\nabla^2$  (or  $\overline{\nabla}^2$ ) on the vector line, using  $\frac{1}{\square} \nabla^2 = \frac{1}{\square} \nabla^2$  (and analogous) and bring  $\nabla^2$  (or  $\overline{\nabla}^2$ ) back on the original line. The results are then straightforwardly read from formulas (6.2.5) and (6.2.6)

$$\begin{array}{c}
\begin{array}{c}
\text{1/}\square\text{-} \\
\overline{\nabla}^2 \quad \nabla^2 \\
V_7 \quad \text{1/}\widehat{\square} \quad \overline{V}_7 \\
\overline{\nabla}^2 \quad \nabla^2 \\
\text{1/}\square\text{-}
\end{array}
\longrightarrow
\begin{array}{c}
A \\
\text{---} \\
A \\
A
\end{array}
\end{array}
\quad (6.2.13)$$

$$\begin{array}{c}
\begin{array}{c}
\text{1/}\square\text{-} \\
\nabla^2 \quad \overline{\nabla}^2 \\
\overline{V}_7 \quad \text{1/}\widehat{\square} \quad V_7 \\
\nabla^2 \quad \overline{\nabla}^2 \\
\text{1/}\square\text{-}
\end{array}
\longrightarrow
\begin{array}{c}
\overline{A} \\
\text{---} \\
\overline{A} \\
\overline{A}
\end{array}
\end{array}
\quad (6.2.14)$$

The combinatorial factor multiplying this result is

$$\frac{1}{8} g^2 (f^{abc} f^{def}) \quad (6.2.15)$$

- Type (e) graphs 

We consider the graphs constructed using twice  $V_8$  or twice  $\overline{V}_8$  (second line of (6.2.12)). Consider first the  $\langle V_8 V_8 \rangle$  case. The  $\nabla$ -algebra is the same as the one for the chiral-vector diagram. Therefore, from (6.2.10) we read the result for this sector

$$\begin{array}{c}
\begin{array}{c}
\text{1/}\square\text{-} \\
\overline{\nabla}^2 \quad \nabla^2 \\
V_8 \quad \text{1/}\widehat{\square} \quad V_8 \\
\nabla^2 \quad \overline{\nabla}^2 \\
\text{1/}\square\text{+}
\end{array} \\
\Downarrow \\
\frac{1}{2} \begin{array}{c} A \\ \text{---} \\ \overline{A} \\ A \end{array} + \frac{1}{2} \begin{array}{c} \overline{A} \\ \text{---} \\ A \\ \overline{A} \end{array} - \frac{1}{2} \begin{array}{c} A i \nabla^{\alpha\dot{\alpha}} \\ \text{---} \\ \overline{A} \\ E_{\alpha\dot{\alpha}} \end{array} - \frac{1}{2} \begin{array}{c} \overline{A} i \nabla^{\alpha\dot{\alpha}} \\ \text{---} \\ A \\ \overline{E}_{\alpha\dot{\alpha}} \end{array}
\end{array}$$

$$\begin{aligned}
& -\frac{1}{2} \left( \begin{array}{c} A \\ \text{---} \text{---} \text{---} \\ \bar{A} \\ \text{---} \text{---} \text{---} \\ \bar{F}^{\dot{\alpha}i} \bar{W}_{\dot{\alpha}} + H^{\alpha i} W_{\alpha} \end{array} \right) + \left( \begin{array}{c} D^{\alpha} \\ \text{---} \text{---} \text{---} \\ A \\ \text{---} \text{---} \text{---} \\ \bar{B}^{\dot{\alpha}i} \nabla_{\alpha\dot{\alpha}} - \bar{C}iW_{\alpha} \end{array} \right) + \left( \begin{array}{c} \bar{D}^{\dot{\alpha}} \\ \text{---} \text{---} \text{---} \\ \bar{A} \\ \text{---} \text{---} \text{---} \\ B^{\alpha i} \nabla_{\alpha\dot{\alpha}} - Ci\bar{W}_{\dot{\alpha}} \end{array} \right) + \left( \begin{array}{c} \frac{1}{\square} \\ \text{---} \text{---} \text{---} \\ \delta_{be} \\ \text{---} \text{---} \text{---} \\ L \end{array} \right) \\
& \hspace{20em} (6.2.16)
\end{aligned}$$

The  $\langle \bar{V}_8 \bar{V}_8 \rangle$  gives these same  $\nabla$ -algebra results.

The combinatorial factor turns out to be

$$-\frac{1}{8} g^2 (f^{abc} f^{def}) \times 2 \quad (6.2.17)$$

where the extra factor 2 comes from summing  $\langle V_8 V_8 \rangle$  and  $\langle \bar{V}_8 \bar{V}_8 \rangle$ .

### Summing chirals, mixed and ghost diagrams

It is useful to sum the previous contributions from chiral (6.2.5), (6.2.6), mixed (6.2.10) and ghost (6.2.13), (6.2.14), (6.2.16) diagrams since some simplification occurs. The result, including combinatorial factors (6.1), is (Finite diagrams in boxes)

$$\begin{aligned}
& -\frac{3}{8} \left( \begin{array}{c} A \\ \text{---} \text{---} \text{---} \\ A \\ \text{---} \text{---} \text{---} \\ A \end{array} \right) - \frac{3}{8} \left( \begin{array}{c} \bar{A} \\ \text{---} \text{---} \text{---} \\ \bar{A} \\ \text{---} \text{---} \text{---} \\ \bar{A} \end{array} \right) + \frac{5}{8} \left( \begin{array}{c} A \\ \text{---} \text{---} \text{---} \\ \bar{A} \\ \text{---} \text{---} \text{---} \\ A \end{array} \right) + \frac{5}{8} \left( \begin{array}{c} \bar{A} \\ \text{---} \text{---} \text{---} \\ A \\ \text{---} \text{---} \text{---} \\ \bar{A} \end{array} \right) \\
& -\frac{5}{8} \left( \begin{array}{c} Ai\nabla^{\alpha\dot{\alpha}} \\ \text{---} \text{---} \text{---} \\ \bar{A} \\ \text{---} \text{---} \text{---} \\ E_{\alpha\dot{\alpha}} \end{array} \right) - \frac{5}{8} \left( \begin{array}{c} \bar{A}i\nabla^{\alpha\dot{\alpha}} \\ \text{---} \text{---} \text{---} \\ A \\ \text{---} \text{---} \text{---} \\ \bar{E}_{\alpha\dot{\alpha}} \end{array} \right) - \frac{5}{8} \left( \begin{array}{c} \bar{A} \\ \text{---} \text{---} \text{---} \\ A \\ \text{---} \text{---} \text{---} \\ \bar{F}^{\dot{\alpha}i} \bar{W}_{\dot{\alpha}} + H^{\alpha i} W_{\alpha} \end{array} \right) + \frac{5}{4} \left( \begin{array}{c} \frac{1}{\square} \\ \text{---} \text{---} \text{---} \\ \delta_{be} \\ \text{---} \text{---} \text{---} \\ L \end{array} \right)
\end{aligned}$$

$$(6.2.18)$$

Taking into account the planar limit on the graphs of the third line, further simplifications occur. We will be back to the planar limit when we have computed everything.

### Pure vector graphs

We construct diagrams (c) of Fig. 5.1 by contracting the cubic gauge vertex (6.1.4)

$$-\frac{g}{2} (i f^{abc}) \left( (\nabla^\alpha V)^a V^b (\bar{\nabla}^2 \nabla_\alpha V)^c + \frac{1}{3} (\nabla^\alpha V)^a V^b [i W_\alpha, V]^c \right) \quad (6.2.19)$$

with itself. In order to keep track of all possible contractions of vectors lines we write the left vertex as the sum of the six permutations of factors. After some integrations by parts done for freeing one line from derivatives, it can be written as (6.1.7)

$$\begin{aligned} V_4 &= \frac{g}{2} i f^{abc} V^a \left( -2(\bar{\nabla}^2 V)^b (\nabla^2 V)^c + 2(\nabla^\alpha V)^b (\nabla_\alpha \bar{\nabla}^2 V)^c - 2(\bar{\nabla}^{\dot{\alpha}} V)^b (\bar{\nabla}_{\dot{\alpha}} \nabla^2 V)^c \right. \\ &\quad \left. + (\nabla^\alpha V)^b i(\nabla_{\alpha \dot{\alpha}} \bar{\nabla}^{\dot{\alpha}} V)^c - (\bar{\nabla}^{\dot{\alpha}} V)^b i(\nabla_{\alpha \dot{\alpha}} \nabla^\alpha V)^c - i(\nabla^{\alpha \dot{\alpha}} V)^b (\bar{\nabla}_{\dot{\alpha}} \nabla_\alpha V)^c \right. \\ &\quad \left. + \text{exchange of lines } b \text{ and } c \right) \\ &= -\frac{g}{2} i f^{abc} \left( -2(\bar{\nabla}^2 V)^a V^b (\nabla^2 V)^c + \dots \right) \end{aligned} \quad (6.2.20)$$

As right vertex, instead, we keep the two vertices (6.2.19). The contraction of (6.2.20) with (6.2.19) produces 24 graphs on which we have to perform  $\nabla$ -algebra. However, it is immediate to see that 6 of them are zero.

It is important to stress few points concerning the right vertex:

1) if  $z_1$  and  $z_2$  are the superspace coordinates of the left and the right vertices respectively, on each line we have to deal with strings of the form

$$(\dots \nabla \dots) \frac{1}{\square} \delta(z_1 - z_2) (\dots \nabla \dots) \quad (6.2.21)$$

where the derivatives on the left act on the variable  $z_1$ , whereas the ones on the right act on  $z_2$ . It is convenient to trade the  $z_2$ -derivatives with  $z_1$ -derivatives using well-known

relations (see [1]). In so doing, the first term in (6.2.19) picks up two minus signs, whereas the second term picks up one minus. However, ...

2) ... the second term, when thought of as right vertex, needs  $W_\alpha$  as second entry of the commutator in order to fix the correct order of color indices. Therefore, we pick up an extra minus sign from the commutator which, together with the sign from sliding  $\nabla_\alpha$ , does not give any sign.

Therefore, as right vertex we use the following expression

$$-\frac{g}{2}(if^{abc}) \left( (\nabla^\alpha V)^a V^b (\overline{\nabla}^2 \nabla_\alpha V)^c + \frac{1}{3} (\nabla^\alpha V)^a V^b [V, iW_\alpha]^c \right) \quad (6.2.22)$$

where derivatives are acting on  $z_1$ .

Below we give in a graph by graph analysis the results of the  $\nabla$ -algebra. The results keep trace of planarity and MHV condition. Note also that again we take advantage of simplifications which allow to write, in the middle of some expression,  $\overline{\nabla}^2 1/\hat{\square} = 1/\hat{\square}_+ \overline{\nabla}^2$ , etc. Moreover, in order to simplify a little bit the result, we performed some easy resummation between the diagrams of different sectors.

**We put UV finite diagrams inside boxes.**

All the contributions of this section must be multiplied by combinatorial factor

$$-\frac{1}{8}g^2 (f^{abc} f^{def}) \quad (6.2.23)$$

More details on the construction of these vacuum diagrams, in particular on the signs that they carry, can be found in Appendix I.

**First contributions: Sector A**

These contributions come from contracting each term of (6.2.20) with the first term in (6.2.19). We take into account signs coming from sliding derivatives from  $z_2$  to  $z_1$  and signs coming from exchange of fermions in the contraction.

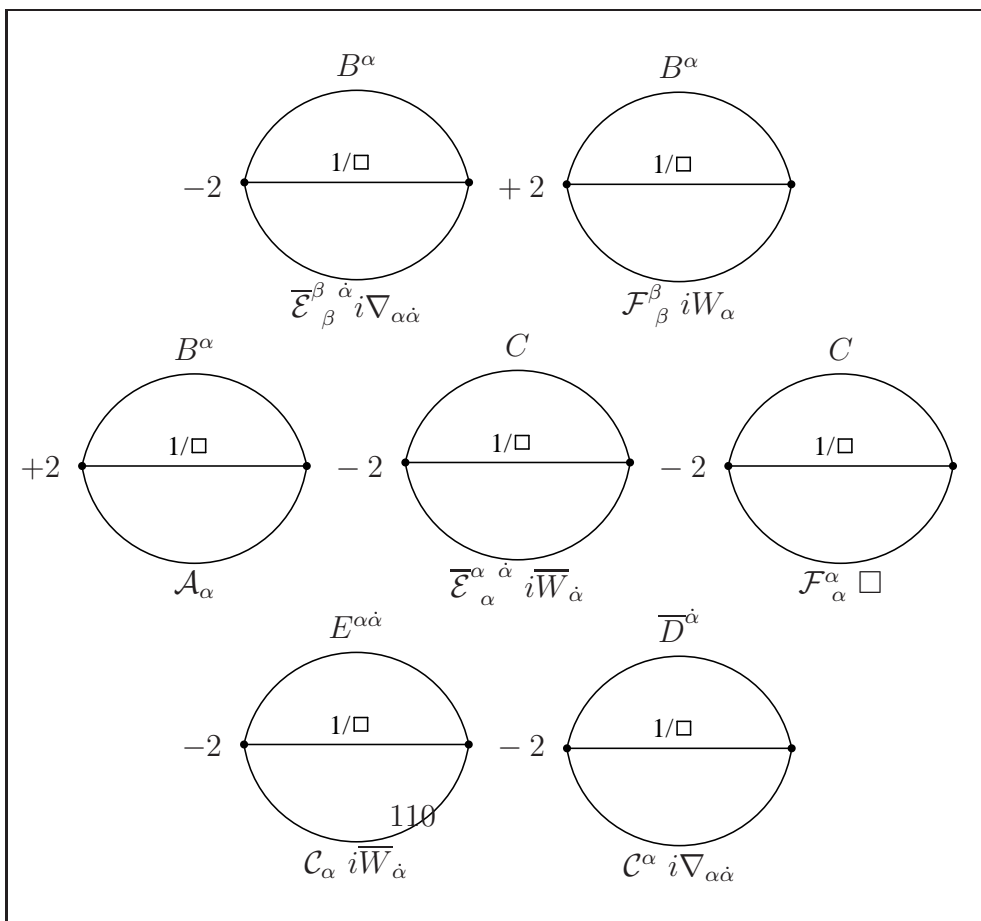
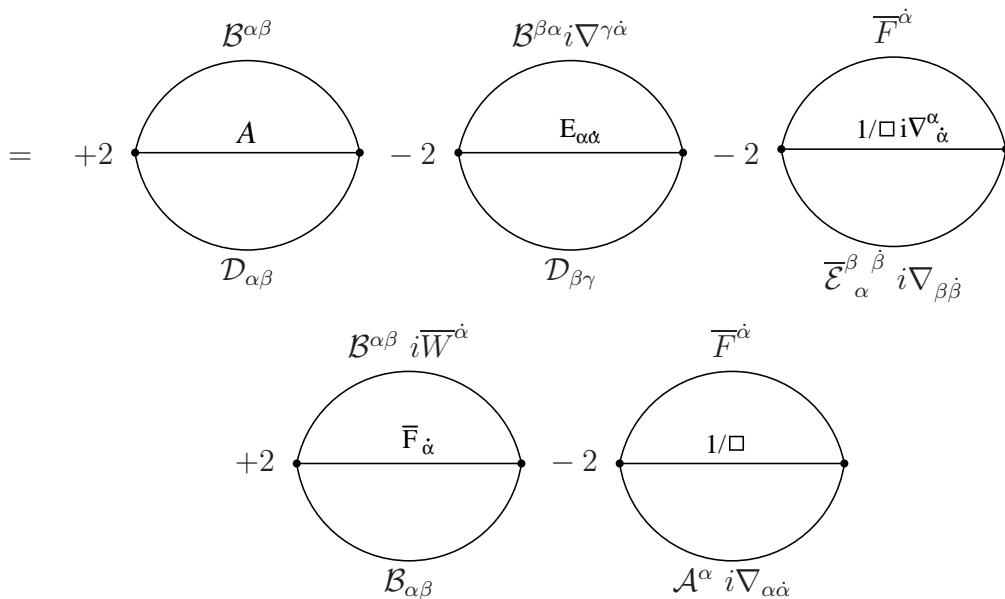
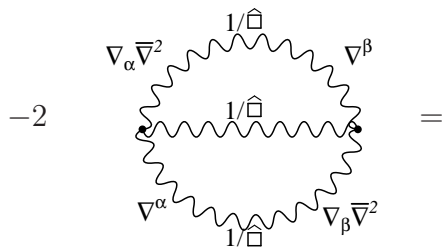
2A

$$-2 \left( \text{Diagram with four wavy lines and } 1/\square \text{ labels} \right) = -2 \left( \text{Diagram with arcs } \mathcal{F}^{\alpha\beta} \text{ and } \mathcal{C}_\alpha iW_\beta \text{ and a central } 1/\square \text{ line} \right) \quad (6.2.24)$$

4A

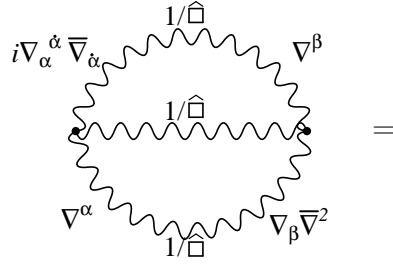
$$4A \left( \text{Diagram with four wavy lines and } 1/\square \text{ labels} \right) = \left( \text{Diagram with arcs } \bar{F}^{\dot{\beta}} \text{ and } \bar{\mathcal{E}}_{\alpha\beta\dot{\beta}} \text{ and a central } i\nabla^{\alpha\dot{\alpha}} 1/\square i\nabla_{\dot{\alpha}}^\beta \text{ line} \right) = \left( \text{Diagram with arcs } i\nabla^{\alpha\dot{\alpha}} C i\nabla_{\dot{\alpha}}^\beta \text{ and } \mathcal{F}_{\alpha\beta} \text{ and a central } 1/\square \text{ line} \right) - \left( \text{Diagram with arcs } C \text{ and } \mathcal{F}_{\alpha\beta} \text{ and a central } i\nabla^{\alpha\dot{\alpha}} 1/\square i\nabla_{\dot{\alpha}}^\beta \text{ line} \right) \quad (6.2.26)$$

2Ax





4Ax



$$= - \begin{array}{c} \mathcal{D}^{\alpha\beta} \\ \text{---} \text{---} \text{---} \text{---} \\ \text{---} \text{---} \text{---} \text{---} \\ \text{---} \text{---} \text{---} \text{---} \\ \text{---} \text{---} \text{---} \text{---} \\ \mathcal{A} \\ \text{---} \text{---} \text{---} \text{---} \\ i\nabla_\alpha^{\dot{\alpha}} \mathcal{H}_{\dot{\alpha}\beta} \end{array} + \begin{array}{c} i\nabla^{\beta\dot{\beta}} \bar{\mathcal{D}}_{\dot{\beta}}^{\dot{\alpha}} \\ \text{---} \text{---} \text{---} \text{---} \\ \text{---} \text{---} \text{---} \text{---} \\ \text{---} \text{---} \text{---} \text{---} \\ \mathcal{E}_{\dot{\alpha}}^{\alpha} \\ \text{---} \text{---} \text{---} \text{---} \\ \mathcal{D}_{\beta\alpha} \end{array}$$

$$+ \begin{array}{c} \bar{\mathcal{F}}^{\dot{\alpha}} \\ \text{---} \text{---} \text{---} \text{---} \\ \text{---} \text{---} \text{---} \text{---} \\ \text{---} \text{---} \text{---} \text{---} \\ i\nabla_\alpha^{\dot{\alpha}} 1/\square \\ \text{---} \text{---} \text{---} \text{---} \\ \bar{\mathcal{E}}_\alpha^{\beta\dot{\beta}} i\nabla_{\beta\dot{\beta}} \end{array} - \begin{array}{c} \bar{\mathcal{F}}^{\dot{\alpha}} \\ \text{---} \text{---} \text{---} \text{---} \\ \text{---} \text{---} \text{---} \text{---} \\ \text{---} \text{---} \text{---} \text{---} \\ 1/\square \\ \text{---} \text{---} \text{---} \text{---} \\ i\nabla^{\beta\dot{\beta}} \bar{\mathcal{B}}_{\dot{\beta}} i\nabla_{\beta\dot{\alpha}} \end{array}$$

$- \begin{array}{c} B^\alpha \\ \text{---} \text{---} \text{---} \text{---} \\ \text{---} \text{---} \text{---} \text{---} \\ \text{---} \text{---} \text{---} \text{---} \\ 1/\square \\ \text{---} \text{---} \text{---} \text{---} \\ i\nabla_\alpha^{\dot{\alpha}} \bar{\mathcal{C}}_{\dot{\alpha}} \\ \bar{\mathcal{D}}^{\dot{\alpha}} \end{array}$	$- \begin{array}{c} E^{\alpha\dot{\alpha}} \\ \text{---} \text{---} \text{---} \text{---} \\ \text{---} \text{---} \text{---} \text{---} \\ \text{---} \text{---} \text{---} \text{---} \\ 1/\square \\ \text{---} \text{---} \text{---} \text{---} \\ i\nabla^{\beta\dot{\beta}} \mathcal{H}_{\beta\alpha} i\nabla_{\beta\dot{\alpha}} \\ \bar{\mathcal{D}}^{\dot{\alpha}} \end{array}$
$- \begin{array}{c} \text{---} \text{---} \text{---} \text{---} \\ \text{---} \text{---} \text{---} \text{---} \\ \text{---} \text{---} \text{---} \text{---} \\ 1/\square \\ \text{---} \text{---} \text{---} \text{---} \\ i\nabla^{\alpha\dot{\beta}} \mathcal{E}_{\beta\alpha\dot{\alpha}} \end{array}$	$- \begin{array}{c} \text{---} \text{---} \text{---} \text{---} \\ \text{---} \text{---} \text{---} \text{---} \\ \text{---} \text{---} \text{---} \text{---} \\ 1/\square \\ \text{---} \text{---} \text{---} \text{---} \\ i\nabla^{\alpha\dot{\beta}} \bar{\mathcal{F}}_{\dot{\beta}} i\nabla_{\alpha\dot{\alpha}} \end{array}$

(6.2.27)

5A

$$\begin{aligned}
& - \text{Diagram} = \\
& = - \text{Diagram}_1 - \text{Diagram}_2 \\
& \quad - \text{Diagram}_3 + \text{Diagram}_4 \\
& \quad + \text{Diagram}_5 + \text{Diagram}_6 + \text{Diagram}_7 + \text{Diagram}_8
\end{aligned}$$

The diagrams are:

- Diagram 1:** A circle with a horizontal line through its center. Above the line is  $A$ , below is  $\mathcal{H}_{\dot{\alpha}\beta}$ . Above the circle is  $i\nabla^{\alpha\dot{\alpha}}\mathcal{D}_{\dot{\alpha}}^{\beta}$ , below is  $\bar{F}^{\dot{\alpha}}$ .
- Diagram 2:** A circle with a horizontal line through its center. Above the line is  $E_{\dot{\alpha}}^{\alpha}$ , below is  $\bar{\mathcal{D}}_{\dot{\beta}\dot{\alpha}}$ . Above the circle is  $i\nabla^{\beta\dot{\beta}}\mathcal{D}_{\dot{\beta}}^{\alpha}$ , below is  $\bar{F}^{\dot{\beta}}$ .
- Diagram 3:** A circle with a horizontal line through its center. Above the line is  $1/\square$ , below is  $i\nabla_{\dot{\alpha}}^{\alpha}\bar{\mathcal{E}}_{\alpha}^{\beta\dot{\beta}}i\nabla_{\beta\dot{\beta}}$ .
- Diagram 4:** A circle with a horizontal line through its center. Above the line is  $i\nabla^{\alpha\dot{\alpha}}1/\square$ , below is  $\bar{B}_{\dot{\alpha}}i\nabla_{\alpha\dot{\beta}}$ .
- Diagram 5:** A circle with a horizontal line through its center. Above the line is  $B^{\alpha}$ , below is  $\bar{\mathcal{C}}_{\dot{\alpha}}$ . Above the circle is  $i\nabla_{\alpha}^{\dot{\alpha}}1/\square$ , below is  $\bar{\mathcal{D}}^{\dot{\beta}}$ .
- Diagram 6:** A circle with a horizontal line through its center. Above the line is  $E^{\beta\dot{\beta}}$ , below is  $\mathcal{H}_{\dot{\alpha}\beta}i\nabla_{\alpha\dot{\beta}}$ . Above the circle is  $i\nabla^{\alpha\dot{\alpha}}1/\square$ , below is  $\bar{\mathcal{D}}^{\dot{\beta}}$ .
- Diagram 7:** A circle with a horizontal line through its center. Above the line is  $i\nabla^{\alpha\dot{\alpha}}1/\square$ , below is  $\mathcal{E}_{\dot{\alpha}\alpha\dot{\beta}}$ .
- Diagram 8:** A circle with a horizontal line through its center. Above the line is  $i\nabla^{\alpha\dot{\alpha}}1/\square$ , below is  $\bar{F}_{\dot{\alpha}}i\nabla_{\alpha\dot{\beta}}$ .

(6.2.28)

$$5Ax \quad - \quad \begin{array}{c} \text{1/\square} \\ \text{wavy line} \\ \text{1/\square} \\ \text{wavy line} \\ \text{1/\square} \end{array} \quad =$$

$$= \quad - \quad \begin{array}{c} \overline{F}^{\dot{\beta}} \\ \text{circle} \\ \text{1/\square i}\nabla^{\alpha\dot{\alpha}} \\ \text{circle} \\ i\nabla^{\beta}_{\dot{\alpha}} \overline{\mathcal{E}}_{\beta\alpha\dot{\beta}} \end{array}$$

$$- \quad \begin{array}{c} i\nabla^{\alpha\dot{\alpha}} \mathcal{F}_{\alpha}^{\beta} \\ \text{circle} \\ \text{1/\square} \\ \text{circle} \\ C i\nabla_{\beta\dot{\alpha}} \end{array} \quad - \quad \begin{array}{c} C \\ \text{circle} \\ \text{1/\square i}\nabla^{\alpha\dot{\alpha}} \\ \text{circle} \\ i\nabla^{\beta}_{\dot{\alpha}} \mathcal{F}_{\beta\alpha} \end{array}$$

(6.2.29)

6A

$$- \text{[Diagram: A circle with four wavy lines. Top: } i\nabla^{\alpha\dot{\alpha}} \text{ and } 1/\hat{\square}. \text{ Right: } \nabla^{\beta}. \text{ Bottom: } \nabla_{\beta}\bar{\nabla}^2 \text{ and } 1/\hat{\square}. \text{ Left: } \bar{\nabla}_{\dot{\alpha}}\nabla_{\alpha} \text{ and } 1/\hat{\square}. \text{]} =$$

$$= + \text{[Diagram: A circle with a horizontal line through the center. Top: } 1/\square i\nabla^{\alpha\dot{\alpha}} \text{ and } \bar{F}^{\dot{\beta}}. \text{ Bottom: } i\nabla_{\alpha\dot{\alpha}} \bar{B}_{\dot{\beta}} \text{]} =$$

$i\nabla^{\alpha\dot{\alpha}} H^{\beta}$  $d_{\alpha\dot{\alpha}\beta}$ $C$	$B^{\alpha}$  $1/\square i\nabla_{\alpha}^{\dot{\alpha}}$ $i\nabla_{\dot{\alpha}}^{\beta} H_{\beta}$ $E^{\alpha\dot{\beta}}$
$+$ $1/\square i\nabla^{\alpha\dot{\alpha}}$ $i\nabla_{\alpha\dot{\alpha}} \bar{C}$	$+$ $1/\square i\nabla_{\alpha}^{\dot{\alpha}}$ $i\nabla_{\dot{\alpha}}^{\beta} E_{\beta\dot{\beta}}$

(6.2.30)

6Ax

$$\begin{aligned}
 & \begin{array}{c} \nabla_{\dot{\alpha}} \nabla_{\alpha} \\ \nabla^{\beta} \\ \nabla_{\beta} \nabla^2 \\ i \nabla^{\alpha \dot{\alpha}} \\ 1/\square \end{array} = \\
 & = - \begin{array}{c} E^{\beta \dot{\beta}} \\ i \nabla^{\alpha \dot{\alpha}} A \\ \bar{e}_{\alpha \dot{\alpha} \beta \dot{\beta}} \end{array} - \begin{array}{c} \bar{F}^{\dot{\beta}} \\ i \nabla^{\alpha \dot{\alpha}} 1/\square \\ \bar{\mathcal{E}}_{\alpha \dot{\alpha}}^{\beta} i \nabla_{\beta \dot{\beta}} \end{array} + \begin{array}{c} \bar{F}^{\dot{\alpha}} \\ 1/\square \\ i \nabla_{\alpha}^{\dot{\alpha}} \bar{B}^{\dot{\beta}} i \nabla_{\alpha \dot{\beta}} \end{array} \\
 & \boxed{ \begin{array}{cc} + \begin{array}{c} i \nabla^{\alpha \dot{\alpha}} D^{\beta} \\ 1/\square \\ f_{\alpha \dot{\alpha} \beta} \\ E^{\alpha \dot{\alpha}} \end{array} - \begin{array}{c} B^{\beta} \\ i \nabla^{\alpha \dot{\alpha}} 1/\square \\ f_{\alpha \dot{\alpha} \beta} \\ \bar{D}^{\dot{\alpha}} \end{array} \\ - \begin{array}{c} 1/\square \\ i \nabla_{\dot{\alpha}}^{\beta} E_{\alpha}^{\dot{\beta}} i \nabla_{\beta \dot{\beta}} \end{array} - \begin{array}{c} 1/\square \\ i \nabla_{\dot{\alpha}}^{\alpha} D_{\alpha} \end{array} \end{array}
 \end{aligned}$$

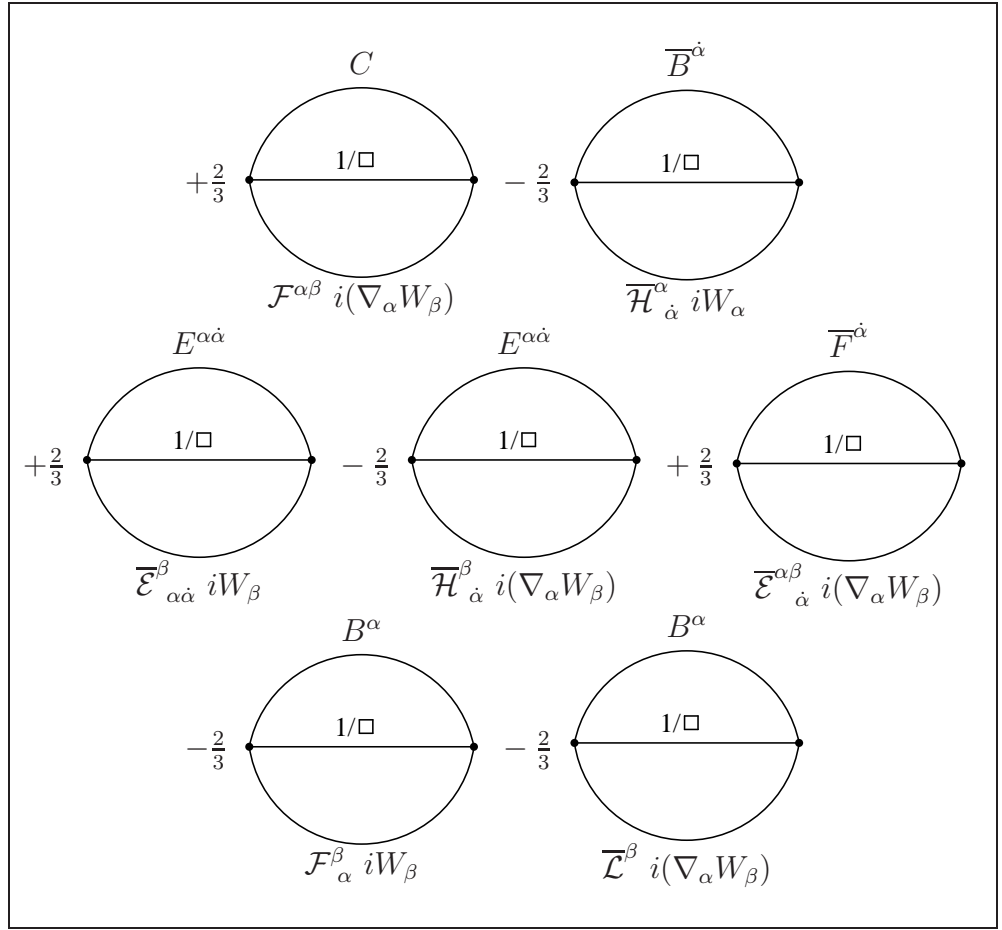
(6.2.31)

**Second contributions: B sector**

These contributions come from contracting each term of (6.2.20) with the second vertex (6.2.19). The results are:

$$2B \quad -\frac{2}{3} \quad \begin{array}{c} \nabla^\alpha \quad 1/\hat{\square} \quad \nabla^\beta \\ \nabla^\alpha \quad 1/\hat{\square} \\ \nabla_\alpha \bar{\nabla}^2 \quad 1/\hat{\square} \quad iW_\beta \end{array} \quad = \quad = \quad +\frac{2}{3} \quad \begin{array}{c} \mathcal{F}^{\alpha\beta} \\ 1/\square \\ \mathcal{C}_\alpha \quad iW_\beta \end{array} \quad (6.2.32)$$

$$2Bx \quad -\frac{2}{3} \quad \begin{array}{c} \nabla_\alpha \bar{\nabla}^2 \quad 1/\hat{\square} \quad \nabla^\beta \\ \nabla^\alpha \quad 1/\hat{\square} \\ \nabla^\alpha \quad 1/\hat{\square} \quad iW_\beta \end{array} \quad = \quad = \quad -\frac{2}{3} \quad \begin{array}{c} \mathcal{B}^{\alpha\beta} \\ 1/\square \\ \bar{\mathcal{L}}_\alpha \quad iW_\beta \end{array}$$



(6.2.33)

$$1B+3B \quad -\frac{2}{3} \quad +\frac{2}{3} \quad =$$

$$\begin{aligned}
&= \quad +\frac{2}{3} \quad \begin{array}{c} F^\alpha \\ \text{---} \circ \text{---} \\ | \\ \frac{1}{\square} iW_\alpha \end{array} \quad \boxed{\begin{array}{c} E^{\alpha\dot{\alpha}} \\ \text{---} \circ \text{---} \\ | \\ \overline{B}_\alpha iW_\alpha \end{array}} \quad -\frac{2}{3}
\end{aligned} \tag{6.2.34}$$

We stress that the results of the last two subsections contains only terms up to two  $\overline{W}$ 's. Moreover we did not report terms that come up from different graphs but canceled exactly between each other. That is why, for example, we found convenient to report the sum of graphs 1B and 3B.

## 6.2.2 Diagrams with quartic vertices

### Chiral–Vector 4 pts graphs

In order to construct graph (f) of Fig. 5.1 we start from the vertex  $V_3$  of eq. (6.1.4)

$$V_3 = -\frac{g^2}{2} (f^{abe} f^{cde}) \bar{\Phi}_i^a V^b V^c \Phi_i^d \tag{6.2.35}$$

and perform self–contractions. The result of the  $\nabla$ –algebra is straightforward

$$\frac{1}{\square} \begin{array}{c} \text{---} \circ \text{---} \\ | \\ \text{---} \text{---} \end{array} L \tag{6.2.36}$$

We add to this graph color labels, since in quartic vertices it will become important to distinguish between different color contractions (see Appendix E).

The combinatorial factor associated to this graph is

$$\frac{3}{2} g^2 (f^{abe} f^{ecd}) \tag{6.2.37}$$

Note that in the picture of equation (6.2.36) we included also small arrows inside loops. They signal which is the sense one must follow to read color labels associated to



coefficients inside each loop. So, for example, equations (6.2.36) is proportional to the following color structure

$$f_{abe}f_{ecd} \left( \frac{1}{\square} \right)_{ad} (L)_{bc} \quad (6.2.38)$$

Color labels associated to  $\frac{1}{\square}$  and  $L$  are in the order specified by the extra arrows inside the loops.

### Pure Vector 4 pts graphs

Consider the vertex  $V_5$  of eq. (6.1.8)

$$V_5 = \frac{g^2}{8} (f^{abe} f^{cde}) \left( V^a \nabla^\alpha V^b \bar{\nabla}^2 V^c \nabla_\alpha V^d - \frac{1}{3} V^a \nabla^\alpha V^b V^c \bar{\nabla}^2 \nabla_\alpha V^d + V^a \nabla^\alpha V^b \bar{\nabla}^{\dot{\alpha}} V^c \bar{\nabla}_{\dot{\alpha}} \nabla_\alpha V^d \right) \quad (6.2.39)$$

and take all possible contractions. Each term in  $V_5$  gives rise to three different graphs depending on how the legs are contracted. Different contractions differ both for the color structure (we keep track of this in the pictures) and for  $\nabla$ -algebra. Regarding the last issue we need pay attention since in this case we have to deal with closed loops. We regard them as limit cases of open lines when the extremal points are joined together. In this way, it is possible to identify which are the derivatives operating on the right of the propagators and apply the same procedure we described for the right cubic gauge vertex in order to slide derivatives from the right to the left.

In listing the result of the  $\nabla$ -algebra we keep only contributions that are relevant for an MHV amplitude (so we discard terms that have more than two  $\bar{W}$ 's)

$$\begin{aligned}
& -\frac{4}{3} H^\alpha \left( \begin{array}{c} \text{b} \quad \text{c} \\ \text{a} \quad \text{d} \end{array} \right) B_\alpha \\
+ & \boxed{ C \left( \begin{array}{c} \text{c} \quad \text{b} \\ \text{a} \quad \text{d} \end{array} \right) \mathcal{F}_\alpha } - \frac{1}{3} L \left( \begin{array}{c} \text{c} \quad \text{b} \\ \text{a} \quad \text{d} \end{array} \right) \mathcal{B}_\alpha + \bar{F}^{\dot{\alpha}} \left( \begin{array}{c} \text{c} \quad \text{b} \\ \text{a} \quad \text{d} \end{array} \right) \bar{\mathcal{E}}_{\alpha\dot{\alpha}} \\
+ & H^\alpha \left( \begin{array}{c} \text{d} \quad \text{b} \\ \text{a} \quad \text{c} \end{array} \right) \mathcal{C}_\alpha - \frac{1}{3} B^\alpha \left( \begin{array}{c} \text{d} \quad \text{b} \\ \text{a} \quad \text{c} \end{array} \right) \bar{\mathcal{L}}_\alpha + \boxed{ E^{\alpha\dot{\alpha}} \left( \begin{array}{c} \text{d} \quad \text{b} \\ \text{a} \quad \text{c} \end{array} \right) \bar{\mathcal{H}}_{\alpha\dot{\alpha}} }
\end{aligned}$$

(6.2.40)

In the last graph we have made use of  $\bar{E}^{\alpha\dot{\alpha}} = -E^{\alpha\dot{\alpha}} + Li\nabla^{\alpha\dot{\alpha}}$ , selecting only MHV contributing terms.

The combinatorial factor is

$$\frac{1}{8}g^2(f^{abe}f^{ecd}) \quad (6.2.41)$$

### Ghosts–Vector 4 pts graphs

We now consider the last diagram (h) of Fig. 5.1. It is constructed by using the following vertices (see eq. 6.1.9)

$$V_{10} = \frac{g^2}{12}(f_{abe}f_{ecd})c^aV^bV^c\bar{c}^d \quad \bar{V}_{10} = -\frac{g^2}{12}(f_{abe}f_{ecd})\bar{c}^aV^bV^c c^d \quad (6.2.42)$$

As in the case of the chiral–vector four point diagrams there is only one possibility of contracting legs and the result is

$$2 \frac{1}{\square} \quad \begin{array}{c} \text{d} \\ \text{b} \\ \text{a} \quad \bullet \quad \text{c} \end{array} \quad L \quad (6.2.43)$$

The first contribution comes from vertex  $V_{10}$ , while the second one from  $\bar{V}_{10}$ . In any case, the combinatorial factor is

$$\frac{1}{12}g^2(f^{abe}f^{ecd}) \quad (6.2.44)$$

It is important to note that for an MHV amplitude  $A$  and  $\bar{A}$  can be substituted by  $1/\square$  ( $L$  contains already two  $\bar{W}$ 's) and the two contributions are indeed the same.

## 6.3 Cancellation of UV divergences

It is an old issue that the  $\mathcal{N} = 4$  theory is UV finite at any perturbative order in  $D = 4$  [12]. On the other hand, as we have seen after  $\nabla$ -algebra there are a lot of diagrams that are singularly divergences. So, it must happens that the sum of all these divergent is a finite expression. A detailed analysis of the divergent terms shows that actually this is the case!

There are two order of consequences: 1) Cancellation of divergences is a non trivial check that the procedure we followed for the derivation of the results (the vertices, the combinatorial factors and the procedure to build up vacuum diagrams) is indeed correct; 2)

Since the resummation of divergences occur before we expand the coefficients  $A, B, \dots, L$  in the external fields, we can prove the cancellation for the complete two loop effective action. The final expression we get is a formula valid for all  $n$ . This is what we called the *master equation* for the MHV effective action at two loops in  $\mathcal{N} = 4$  theory.

### 6.3.1 Divergent terms revisited

From power counting the only two possible sources of divergences are

- 1) If there are two propagators  $\frac{1}{\square_0}$  on one loop (self-energy diagrams)
- 2) If there are three propagators  $\frac{1}{\square_0}$  and two spacetime derivatives in the same loop (triangle with two spacetime derivatives).

It is worth noting that since we are using a covariant formalism, we do not have explicit  $\frac{1}{\square_0}$  but always covariant  $\frac{1}{\square}$ . Fortunately, power counting works with the same criteria 1) and 2) also for covariant propagators.

$\nabla$ -algebra results are written in terms of the coefficients of the expansion of covariant propagators. In order to extract possible divergent structures, we write for any coefficient that has  $\frac{1}{\square}$  as lowest order component

$$X = \hat{X} + \frac{1}{\square} \tag{6.3.1}$$

and for any coefficient whose lowest order component is  $\frac{1}{\square}W\frac{1}{\square}$  §

$$X = \tilde{X} + \frac{1}{\square}W\frac{1}{\square} \tag{6.3.2}$$

Replacements (6.3.1) and (6.3.2) allow to isolate divergent terms from finite ones in  $\nabla$ -algebra results. After applying (6.3.1), (6.3.2), each graph that includes a divergence produces finite terms that include  $\hat{X}$  or  $\tilde{X}$  and divergent ones that satisfy 1) or 2). The divergent contributions can be further manipulated and their sum can be shown to be written in terms of finite expressions. Collecting the results, we then have finite terms with two distinct origins: Finite terms with  $\hat{X}$  and  $\tilde{X}$  that derive from (6.3.1), (6.3.2) and finite terms from the manipulation of divergent graphs. At the end of this procedure, all UV divergences are canceled.

In what follows we divide the  $\nabla$ -algebra results that include divergences in three categories:

---

§With  $\frac{1}{\square}W\frac{1}{\square}$  we mean any structure with two propagators and a background field. This symbol includes also possible extra spacetime derivatives that can appear at the right of the second propagator.

- a. Cubic vertex graphs that satisfy power counting criteria 1) and 2) on both loops. We call these *Double Divergent graphs*.
- b. Cubic vertex graphs that satisfy power counting criteria 1) or 2) only on one of the two loops. We call these *Single Divergent graphs*.
- c. Divergent contributions from tadpoles. We call these simply *Tadpole divergent graphs*.

Inside these categories we make a further classification, dividing Pure-Vector sector from all the other contributions<sup>¶</sup>. As done before, in what follows we close the resulting finite contributions in boxes.

For each diagram we include the numerical combinatorial factor (sign included) following Tab. 6.1. We do not include the factor  $g^2 f^{abc} f^{def}$ .

The computations behind the results in this Section are quite heavy. We tried to give as much references as possible to the formulas we used.

### 6.3.2 Double Divergent Graphs

Consider cubic vertex graphs that satisfy power counting on both loops. These are graphs which have on each line a coefficient whose lowest order term is  $\frac{1}{\square}$ . We list the contributions separately according to their origin.

- Consider first contributions coming from the sum of all but the pure-vector sectors (see eq. (6.2.18)): All the graphs in the first line are double divergent. They are

$$\begin{aligned}
 & -\frac{3}{8} \begin{array}{c} A \\ \circlearrowleft \\ A \\ \circlearrowright \\ A \end{array} \quad -\frac{3}{8} \begin{array}{c} \bar{A} \\ \circlearrowleft \\ \bar{A} \\ \circlearrowright \\ \bar{A} \end{array} \quad +\frac{5}{8} \begin{array}{c} A \\ \circlearrowleft \\ \bar{A} \\ \circlearrowright \\ A \end{array} \quad +\frac{5}{8} \begin{array}{c} \bar{A} \\ \circlearrowleft \\ A \\ \circlearrowright \\ \bar{A} \end{array} \\
 & \hspace{20em} (6.3.3)
 \end{aligned}$$

Imposing the planar limit and separating the divergent terms from the finite ones

---

<sup>¶</sup>The same classification has been used in Section 6.2.

with the help of (6.3.1), (6.3.2), we get

$$\begin{aligned}
& \frac{1}{2} \begin{array}{c} \frac{1}{\square} \\ \circlearrowleft \\ \frac{1}{\square} \end{array} + \frac{3}{4} \begin{array}{c} \hat{A} \\ \circlearrowleft \\ \frac{1}{\square} \end{array} + \frac{3}{4} \begin{array}{c} \hat{\bar{A}} \\ \circlearrowleft \\ \frac{1}{\square} \end{array} \\
& - \frac{1}{2} \begin{array}{c} \hat{A} \\ \circlearrowleft \\ \hat{A} \end{array} - \frac{1}{2} \begin{array}{c} \hat{\bar{A}} \\ \circlearrowleft \\ \hat{\bar{A}} \end{array} + \frac{5}{2} \begin{array}{c} \hat{A} \\ \circlearrowleft \\ \hat{\bar{A}} \end{array} \quad (6.3.4)
\end{aligned}$$

The first line includes the divergent terms while in the second line there are the finite ones.

- Consider the Pure-Vector sector: There is only one contribution to this category, namely the first graph of the sector  $2Ax$  (see eq. (6.2.25))

$$\begin{array}{c} \mathcal{B}^{\alpha\beta} \\ -\frac{1}{4} \begin{array}{c} \circlearrowleft \\ A \\ \circlearrowright \\ \mathcal{D}_{\alpha\beta} \end{array} \end{array} \quad (6.3.5)$$

We can rewrite (6.3.5) by setting (see eq. (C.0.30) and (D.0.19))

$$\mathcal{B}^{\alpha\beta} = \mathcal{P}^{\alpha\beta} + \left( \hat{A} + \frac{1}{\square} \right) c^{\alpha\beta} \quad \mathcal{D}^{\alpha\beta} = \mathcal{Q}^{\alpha\beta} + \left( \hat{A} + \frac{1}{\square} \right) c^{\alpha\beta} \quad (6.3.6)$$

where

$$\begin{aligned}
\mathcal{P}^{\alpha\beta} &= \{ \nabla^\alpha, B^\beta \} \\
\mathcal{Q}^{\alpha\beta} &= \{ \nabla^\alpha, B^\beta \} - \{ \nabla^\alpha, \bar{F}^{\dot{\alpha}} \} i \nabla_{\dot{\alpha}}^\beta - E^{\alpha\dot{\alpha}} i \nabla_{\dot{\alpha}}^\beta + [ \nabla^\alpha, L ] i W^\beta - F^\alpha i W^\beta
\end{aligned} \quad (6.3.7)$$

The result is

$$- \frac{1}{2} \begin{array}{c} \frac{1}{\square} \\ \circlearrowleft \\ \frac{1}{\square} \end{array} - \frac{3}{2} \begin{array}{c} \hat{A} \\ \circlearrowleft \\ \frac{1}{\square} \end{array} + \frac{1}{4} \begin{array}{c} (\mathcal{P}_\alpha^\alpha + \mathcal{Q}_\alpha^\alpha) \\ \circlearrowleft \\ \frac{1}{\square} \end{array}$$

$$\begin{aligned}
& -\frac{3}{2} \text{ (circle with } \hat{A} \text{ on top and } \hat{A} \text{ on bottom, } 1/\square_0 \text{ on horizontal line)} + \frac{1}{2} \text{ (circle with } \hat{A} \text{ on top, } (\mathcal{P}_\alpha^\alpha + \mathcal{Q}_\alpha^\alpha) \text{ on bottom, } 1/\square_0 \text{ on horizontal line)} \\
& - \frac{1}{4} \text{ (circle with } \mathcal{P}^{\alpha\beta} \text{ on top, } \mathcal{Q}_{\alpha\beta} \text{ on bottom, } 1/\square_0 \text{ on horizontal line)} \quad (6.3.8)
\end{aligned}$$

where in the first line we collected the divergent terms and in the second the finite ones.

Note that the first and worst divergent term in (6.3.8) cancels exactly with the first term in eq. (6.3.4). The other terms of (6.3.8) take the following form

$$\begin{aligned}
& -\frac{3}{2} \text{ (circle with } \hat{A} \text{ on top, } \frac{1}{\square} \text{ on bottom, } 1/\square \text{ on horizontal line)} + \frac{1}{2} \text{ (circle with } H^\alpha \text{ on top, } \frac{1}{\square} i W_\alpha \text{ on bottom, } 1/\square \text{ on horizontal line)} \\
& -\frac{1}{2} \text{ (circle with } \mathcal{A}^\alpha \text{ on top, } B_\alpha \text{ on bottom, } 1/\square_0 \text{ on horizontal line)} - \frac{1}{2} \text{ (circle with } \mathcal{A}^\alpha \text{ on top, } D_\alpha \text{ on bottom, } 1/\square_0 \text{ on horizontal line)} \\
& - \frac{1}{4} \text{ (circle with } \mathcal{P}^{\alpha\beta} \text{ on top, } \mathcal{Q}_{\alpha\beta} \text{ on bottom, } 1/\square_0 \text{ on horizontal line)} \\
& -\frac{1}{2} \text{ (circle with } \hat{A} \text{ on top, } F^\alpha i W_\alpha \text{ on bottom, } 1/\square_0 \text{ on horizontal line)} - \frac{3}{2} \text{ (circle with } \hat{A} \text{ on top, } \hat{A} \text{ on bottom, } 1/\square_0 \text{ on horizontal line)} \\
& - \frac{1}{4} \text{ (circle with } B^\alpha i \nabla_\alpha^{\dot{\alpha}} - C i \bar{W}^{\dot{\alpha}} \text{ on top, } \bar{\mathcal{C}}_{\dot{\alpha}} - \bar{B}_{\dot{\alpha}} \text{ on bottom, } 1/\square_0 \text{ on horizontal line)} \quad (6.3.9)
\end{aligned}$$

To get this expression, we have used equations (6.3.7) and (C.0.12).

Consider now the sum of expressions (6.3.4) and (6.3.9): The divergent terms (see the first lines) sum up to give

$$\begin{aligned}
& +\frac{1}{2} \text{ (circle with } H^\alpha \text{ on top, } \frac{1}{\square} i W_\alpha \text{ on bottom, } 1/\square \text{ on horizontal line)} + \frac{3}{4} \text{ (circle with } (\bar{A} - A) \text{ on top, } \frac{1}{\square} \text{ on bottom, } 1/\square \text{ on horizontal line)} \\
& = +\frac{1}{2} \text{ (circle with } H^\alpha \text{ on top, } \frac{1}{\square} i W_\alpha \text{ on bottom, } 1/\square \text{ on horizontal line)}
\end{aligned}$$

$$\begin{aligned}
& +\frac{3}{4} \text{circle}(\overline{c}^{\dot{\alpha}}, 1/\square_0, [\nabla_{\dot{\alpha}}, \frac{1}{\square}]) - \frac{3}{4} \text{circle}(\overline{B}^{\dot{\alpha}}, 1/\square_0, [\nabla_{\dot{\alpha}}, \frac{1}{\square}]) \\
& \hspace{15em} (6.3.10)
\end{aligned}$$

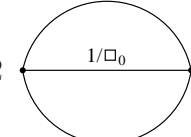
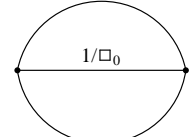
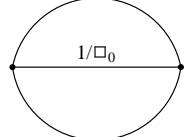
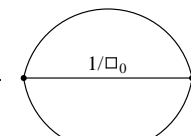
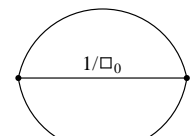
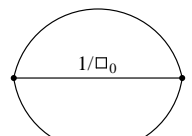
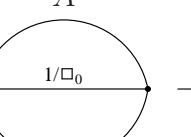
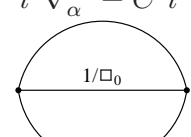
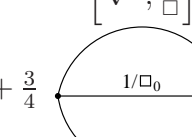
where we have used the identity (C.0.21).

$$\overline{A} - A = \frac{1}{2} \{ \overline{\nabla}^{\dot{\alpha}}, \overline{B}_{\dot{\alpha}} \} - \frac{1}{2} \{ \overline{\nabla}^{\dot{\alpha}}, \overline{C}_{\dot{\alpha}} \} \tag{6.3.11}$$

Therefore, Double Divergent diagrams sums to give a divergent term

$$\begin{aligned}
& +\frac{1}{2} \text{circle}(H^{\alpha}, 1/\square, \frac{1}{\square} i W_{\alpha}) \\
& \hspace{15em} (6.3.12)
\end{aligned}$$

and the following finite ones

$-2$	$\hat{A}$  $\hat{A}$	$-\frac{1}{2}$	$\hat{\overline{A}}$  $\hat{\overline{A}}$	$+\frac{5}{2}$	$\hat{A}$  $\hat{\overline{A}}$
	$\mathcal{A}^{\alpha}$		$\mathcal{A}^{\alpha}$		$\mathcal{P}^{\alpha\beta}$
$-\frac{1}{2}$	 $B_{\alpha}$	$-\frac{1}{2}$	 $D_{\alpha}$	$-\frac{1}{4}$	 $\mathcal{Q}_{\alpha\beta}$
	$\hat{A}$		$B^{\alpha} i \nabla_{\alpha}^{\dot{\alpha}} - C i \overline{W}^{\dot{\alpha}}$		$[\nabla_{\dot{\alpha}}, \frac{1}{\square}]$
$-\frac{1}{2}$	 $F^{\alpha} i W_{\alpha}$	$-\frac{1}{4}$	 $\overline{C}_{\dot{\alpha}} - \overline{B}_{\dot{\alpha}}$	$+\frac{3}{4}$	 $\overline{C}_{\dot{\alpha}} - \overline{B}_{\dot{\alpha}}$

$$\hspace{15em} (6.3.13)$$

### 6.3.3 Single Divergent Graphs

It is more difficult to deal with these type of divergences since many more graphs are involved. However, a bit of care in the computation allows to get the following results.

#### All but the Pure-Vector Single Divergent Graphs

We start by studying the divergent graphs coming from the pure-chiral, vector-chiral and vector-ghosts sectors. From equation (6.2.18) and by using the replacements (6.3.1), (6.3.2), we find the following divergent terms

$$\begin{aligned}
 & -\frac{5}{8} \begin{array}{c} \frac{1}{\square} i \nabla^{\alpha\dot{\alpha}} \\ \text{---} \text{---} \text{---} \\ \text{---} \text{---} \text{---} \\ (E_{\alpha\dot{\alpha}} + \bar{E}_{\alpha\dot{\alpha}}) \end{array} - \frac{5}{8} \begin{array}{c} \frac{1}{\square} \\ \text{---} \text{---} \text{---} \\ \text{---} \text{---} \text{---} \\ \bar{F}^{\dot{\alpha}} i \bar{W}_{\dot{\alpha}} + H^{\alpha} i W_{\alpha} \end{array} + \frac{5}{4} \begin{array}{c} \frac{1}{\square} \\ \text{---} \text{---} \text{---} \\ \text{---} \text{---} \text{---} \\ L \end{array} \delta_{be} \quad (6.3.14)
 \end{aligned}$$

whereas the finite contributions, using  $\bar{E}^{\alpha\dot{\alpha}} = -E^{\alpha\dot{\alpha}} + iL\nabla^{\alpha\dot{\alpha}}$  and up to terms with more than 2  $\bar{W}$ 's, are

$$\begin{aligned}
 & +\frac{5}{8} \begin{array}{c} (A - \bar{A}) \\ \text{---} \text{---} \text{---} \\ \frac{1}{\square_0} i \nabla^{\alpha\dot{\alpha}} \\ \text{---} \text{---} \text{---} \\ E_{\alpha\dot{\alpha}} \end{array} - \frac{5}{8} \begin{array}{c} (A - \bar{A}) i \nabla^{\alpha\dot{\alpha}} \\ \text{---} \text{---} \text{---} \\ \frac{1}{\square_0} \\ \text{---} \text{---} \text{---} \\ E_{\alpha\dot{\alpha}} \end{array} \\
 & -\frac{5}{8} \begin{array}{c} \hat{A} \\ \text{---} \text{---} \text{---} \\ \frac{1}{\square_0} \\ \text{---} \text{---} \text{---} \\ \bar{F}^{\dot{\alpha}} i \bar{W}_{\dot{\alpha}} + H^{\alpha} i W_{\alpha} \end{array} - \frac{5}{8} \begin{array}{c} \hat{\bar{A}} \\ \text{---} \text{---} \text{---} \\ \frac{1}{\square_0} \\ \text{---} \text{---} \text{---} \\ \bar{F}^{\dot{\alpha}} i \bar{W}_{\dot{\alpha}} + H^{\alpha} i W_{\alpha} \end{array} \quad (6.3.15)
 \end{aligned}$$

The divergent contributions in (6.3.14) can be further manipulated and become

$$\begin{aligned}
 & \frac{5}{8} \begin{array}{c} \frac{1}{\square} \nabla^{\alpha\dot{\alpha}} \\ \text{---} \text{---} \text{---} \\ \frac{1}{\square} \\ \text{---} \text{---} \text{---} \\ L \nabla_{\alpha\dot{\alpha}} \end{array} - \frac{5}{8} \begin{array}{c} \frac{1}{\square} \\ \text{---} \text{---} \text{---} \\ \frac{1}{\square} \\ \text{---} \text{---} \text{---} \\ \bar{F}^{\dot{\alpha}} i \bar{W}_{\dot{\alpha}} + H^{\alpha} i W_{\alpha} \end{array} + \frac{5}{4} \begin{array}{c} \frac{1}{\square} \\ \text{---} \text{---} \text{---} \\ \text{---} \text{---} \text{---} \\ L \end{array} \delta_{be} \quad (6.3.16)
 \end{aligned}$$



By using the identities

$$\begin{array}{c} \frac{1}{\square} \nabla^{\alpha\dot{\alpha}} \\ \circlearrowleft \\ \frac{1}{\square} \\ \hline \\ \circlearrowright \\ L \nabla_{\alpha\dot{\alpha}} \end{array} = - \begin{array}{c} \frac{1}{\square} \\ \circlearrowleft \\ \frac{1}{\square} \\ \hline \\ \circlearrowright \\ L \square \end{array} \quad (6.3.17)$$

and

$$L \square = -\bar{F}^{\dot{\alpha}} i \bar{W}_{\dot{\alpha}} - H^{\alpha} i W_{\alpha} \quad (6.3.18)$$

the divergent diagrams with cubic vertices in (6.3.16) cancel and we are left with

$$+\frac{5}{4} \begin{array}{c} \frac{1}{\square} \\ \circlearrowleft \\ \delta_{be} \\ \circlearrowright \\ L \end{array} = +\frac{5}{4} \begin{array}{c} (\frac{1}{\square} - \frac{1}{\square_0}) \\ \circlearrowleft \\ \delta_{be} \\ \circlearrowright \\ L \end{array} \quad (6.3.19)$$

In the last line we expanded  $\frac{1}{\square} = \frac{1}{\square_0} + \dots$ . The  $\frac{1}{\square_0}$  contribution cancels since it is a tadpole. The term proportional to  $(\frac{1}{\square} - \frac{1}{\square_0})$  is indeed finite (see the discussion after (6.3.37) in Section 6.3.4).

So all divergent contributions from these sectors of the theory sum up to zero. Summarizing, the convergent terms from this sector are (see equations (6.3.15) and (6.3.19))

$$\begin{array}{c} \begin{array}{ccc} \begin{array}{c} (A - \bar{A}) \\ \circlearrowleft \\ \frac{1}{\square_0} i \nabla^{\alpha\dot{\alpha}} \\ \hline \\ \circlearrowright \\ E_{\alpha\dot{\alpha}} \end{array} & \begin{array}{c} (A - \bar{A}) i \nabla^{\alpha\dot{\alpha}} \\ \circlearrowleft \\ \frac{1}{\square_0} \\ \hline \\ \circlearrowright \\ E_{\alpha\dot{\alpha}} \end{array} \\ +\frac{5}{8} & -\frac{5}{8} \\ \begin{array}{c} \hat{A} \\ \circlearrowleft \\ \frac{1}{\square_0} \\ \hline \\ \circlearrowright \\ \bar{F}^{\dot{\alpha}} i \bar{W}_{\dot{\alpha}} + H^{\alpha} i W_{\alpha} \end{array} & \begin{array}{c} \hat{A} \\ \circlearrowleft \\ \frac{1}{\square_0} \\ \hline \\ \circlearrowright \\ \bar{F}^{\dot{\alpha}} i \bar{W}_{\dot{\alpha}} + H^{\alpha} i W_{\alpha} \end{array} & \begin{array}{c} (\frac{1}{\square} - \frac{1}{\square_0}) \\ \circlearrowleft \\ \delta_{be} \\ \circlearrowright \\ L \end{array} \\ -\frac{5}{8} & -\frac{5}{8} & +\frac{5}{4} \end{array} \end{array} \quad (6.3.20)$$

## Pure–Vector Single Divergent Graphs

Since the number of divergent graphs in this sector is very high, it is useful to group the graphs with respect to the coefficient that appears on the non-divergent loop. In this way it is possible to divide the analysis in five divergent subsectors. We remind that in each sector there are finite contributions associated with hat and tilde coefficients (see replacements (6.3.1) and (6.3.2)) and finite contributions associated with manipulations of divergent terms.

- **Divergences with  $E_{\alpha\dot{\alpha}}$**

From graphs (2Ax,2), (4Ax,2), (5A,2) and (6Ax,1)<sup>||</sup> we have two divergent contributions

$$\frac{1}{4} \begin{array}{c} E^{\alpha\dot{\alpha}} \\ \text{---} \\ \text{---} \\ \text{---} \\ \frac{1}{\square} \\ \text{---} \\ \frac{1}{\square} i\nabla_{\alpha\dot{\alpha}} \end{array} + \frac{1}{8} \begin{array}{c} E^{\alpha\dot{\alpha}} \\ \text{---} \\ \text{---} \\ \text{---} \\ \frac{1}{\square} \\ \text{---} \\ i\nabla_{\alpha\dot{\alpha}} \frac{1}{\square} \end{array} \quad (6.3.21)$$

and the following finite ones

$$\begin{array}{cccc} -\frac{1}{4} \begin{array}{c} E^{\alpha\dot{\alpha}} \\ \text{---} \\ \text{---} \\ \text{---} \\ \frac{1}{\square_0} \\ \text{---} \\ \hat{\mathcal{B}}_{\alpha}^{\beta} i\nabla_{\beta\dot{\alpha}} \\ E^{\alpha\dot{\alpha}} \end{array} & -\frac{1}{4} \begin{array}{c} E^{\beta\dot{\alpha}} \\ \text{---} \\ \text{---} \\ \text{---} \\ \frac{1}{\square_0} i\nabla_{\dot{\alpha}}^{\alpha} \\ \hat{\mathcal{D}}_{\beta\alpha} \\ E^{\beta\dot{\alpha}} \end{array} & +\frac{1}{8} \begin{array}{c} E^{\alpha\dot{\alpha}} \\ \text{---} \\ \text{---} \\ \text{---} \\ \frac{1}{\square_0} \\ \text{---} \\ i\nabla_{\alpha\dot{\alpha}} \hat{A} \\ E^{\alpha\dot{\alpha}} \end{array} & +\frac{1}{8} \begin{array}{c} E^{\beta\dot{\beta}} \\ \text{---} \\ \text{---} \\ \text{---} \\ \frac{1}{\square_0} i\nabla^{\alpha\dot{\alpha}} \\ \hat{\mathcal{C}}_{\beta\dot{\beta}\alpha\dot{\alpha}} \\ E^{\alpha\dot{\beta}} \end{array} \\ +\frac{1}{8} \begin{array}{c} \text{---} \\ \text{---} \\ \text{---} \\ \frac{1}{\square_0} \\ \text{---} \\ i\nabla_{\alpha}^{\dot{\beta}} \hat{\mathcal{D}}_{\dot{\beta}\alpha} \end{array} & +\frac{1}{8} \begin{array}{c} \text{---} \\ \text{---} \\ \text{---} \\ \frac{1}{\square_0} i\nabla_{\dot{\alpha}}^{\alpha} \\ \hat{\mathcal{D}}_{\alpha\beta} \end{array} & -\frac{1}{8} \begin{array}{c} \text{---} \\ \text{---} \\ \text{---} \\ \frac{1}{\square_0} \\ \text{---} \\ i\nabla_{\dot{\alpha}}^{\beta} \hat{\mathcal{D}}_{\beta\alpha} \end{array} & -\frac{1}{8} \begin{array}{c} \text{---} \\ \text{---} \\ \text{---} \\ \frac{1}{\square_0} i\nabla_{\alpha}^{\dot{\alpha}} \\ \hat{\mathcal{D}}_{\dot{\alpha}\beta} \end{array} \end{array} \quad (6.3.22)$$

<sup>||</sup>I use the notation (A,n), where A means the sector 2A, 2B, ... and n position of the graph in the list.

The divergent contributions (6.3.21) can be rewritten in this way:

$$\begin{array}{c}
 \begin{array}{c}
 E^{\alpha\dot{\alpha}} \\
 \frac{3}{8} \text{---} \text{---} \text{---} \text{---} \\
 \text{---} \text{---} \text{---} \text{---} \\
 \frac{1}{\square} i \nabla_{\alpha\dot{\alpha}}
 \end{array}
 \quad
 \boxed{
 \begin{array}{c}
 E^{\alpha\dot{\alpha}} \\
 + \frac{1}{8} \text{---} \text{---} \text{---} \text{---} \\
 \text{---} \text{---} \text{---} \text{---} \\
 [i \nabla_{\alpha\dot{\alpha}}, \frac{1}{\square}]
 \end{array}
 }
 \end{array}
 \tag{6.3.23}$$

The first of these contribution is divergent, while the second is not.

- **Divergences with  $H_\alpha$**

From graph (3B,1) we have the simple divergent contribution

$$-\frac{1}{12} \begin{array}{c} H^\alpha \\ \text{---} \text{---} \text{---} \text{---} \\ \text{---} \text{---} \text{---} \text{---} \\ \frac{1}{\square} i W_\alpha \end{array}
 \tag{6.3.24}$$

and no convergent ones.

- **Divergences with  $\overline{F}_\dot{\alpha}$**

The contributing graphs in this sector are the following: (2Ax,3), (2Ax,4), (2Ax,5), (4A,1), (4Ax,3) and (4Ax,4), (5A,3), (5A,4), (5Ax,1), (6A,1), (6Ax,2) and (6Ax,3). After replacements (6.3.1), (6.3.2) they give divergent contributions

$$\begin{array}{ccc}
 -\frac{1}{4} \begin{array}{c} \overline{F}^{\dot{\alpha}} \\ \text{---} \text{---} \text{---} \text{---} \\ \text{---} \text{---} \text{---} \text{---} \\ \frac{1}{\square} i \overline{W}^{\dot{\beta}} \frac{1}{\square} i \nabla_{\alpha\dot{\beta}} \end{array} &
 -\frac{1}{2} \begin{array}{c} \overline{F}^{\dot{\alpha}} \\ \text{---} \text{---} \text{---} \text{---} \\ \text{---} \text{---} \text{---} \text{---} \\ \frac{1}{\square} i \overline{W}_{\dot{\alpha}} \end{array} &
 +\frac{1}{4} \begin{array}{c} \overline{F}^{\dot{\alpha}} \\ \text{---} \text{---} \text{---} \text{---} \\ \text{---} \text{---} \text{---} \text{---} \\ \frac{1}{\square} i \overline{W}^{\dot{\beta}} i \nabla_{\beta\dot{\alpha}} \frac{1}{\square} i \nabla_{\alpha\dot{\alpha}} \end{array} \\
 -\frac{1}{8} \begin{array}{c} \overline{F}^{\dot{\beta}} \\ \text{---} \text{---} \text{---} \text{---} \\ \text{---} \text{---} \text{---} \text{---} \\ \frac{1}{\square} i \overline{W}_{\dot{\beta}} \frac{1}{\square} \end{array} &
 -\frac{1}{8} \begin{array}{c} \overline{F}^{\dot{\alpha}} \\ \text{---} \text{---} \text{---} \text{---} \\ \text{---} \text{---} \text{---} \text{---} \\ \frac{1}{\square} i \overline{W}^{\dot{\beta}} \frac{1}{\square} i \nabla_{\alpha\dot{\beta}} \end{array} &
 +\frac{1}{8} \begin{array}{c} \overline{F}^{\dot{\alpha}} \\ \text{---} \text{---} \text{---} \text{---} \\ \text{---} \text{---} \text{---} \text{---} \\ i \nabla^{\beta\dot{\beta}} \frac{1}{\square} i \overline{W}_{\dot{\beta}} \frac{1}{\square} i \nabla_{\beta\dot{\alpha}} \end{array}
 \end{array}
 \tag{6.3.25}$$

where we have used (6.3.2). Moreover, we get the following finite terms

$$\begin{aligned}
& +\frac{1}{4} \begin{array}{c} \overline{F}^{\dot{\alpha}} \\ \circlearrowleft \\ \frac{1/\square_0 i\nabla_{\dot{\alpha}}^{\alpha}}{\tilde{\mathcal{E}}_{\alpha}^{\beta\dot{\beta}} i\nabla_{\beta\dot{\beta}}^{\alpha}} \\ \overline{F}^{\dot{\beta}} \end{array} + \frac{1}{4} \begin{array}{c} \overline{F}^{\dot{\alpha}} \\ \circlearrowleft \\ \frac{1/\square_0}{\tilde{\mathcal{A}}^{\alpha} i\nabla_{\alpha\dot{\alpha}}} \\ \overline{F}^{\dot{\alpha}} \end{array} + \frac{1}{4} \begin{array}{c} \hat{\mathcal{B}}_{\alpha}^{\dot{\alpha}} i\overline{W}^{\dot{\alpha}} \\ \circlearrowleft \\ \frac{1/\square_0}{\overline{F}_{\dot{\alpha}}} \\ \overline{F}^{\dot{\alpha}} \end{array} \\
& +\frac{1}{8} \begin{array}{c} i\nabla^{\alpha\dot{\alpha}} 1/\square_0 i\nabla_{\dot{\alpha}}^{\beta} \\ \circlearrowleft \\ \frac{\tilde{\mathcal{E}}_{\alpha\beta\dot{\beta}}}{\overline{F}^{\dot{\alpha}}} \end{array} - \frac{1}{8} \begin{array}{c} i\nabla_{\dot{\alpha}}^{\alpha} 1/\square_0 \\ \circlearrowleft \\ \frac{\tilde{\mathcal{E}}_{\alpha}^{\beta\dot{\beta}}}{\overline{F}^{\dot{\beta}}} i\nabla_{\beta\dot{\beta}}^{\alpha} \end{array} + \frac{1}{8} \begin{array}{c} 1/\square_0 \\ \circlearrowleft \\ \frac{i\nabla^{\beta\dot{\beta}} \tilde{\mathcal{B}}_{\dot{\beta}}}{\overline{F}^{\dot{\beta}}} i\nabla_{\beta\dot{\alpha}}^{\alpha} \end{array} \\
& +\frac{1}{8} \begin{array}{c} 1/\square_0 \\ \circlearrowleft \\ \frac{i\nabla_{\dot{\alpha}}^{\alpha} \tilde{\mathcal{E}}_{\alpha}^{\beta\dot{\beta}}}{\overline{F}^{\dot{\beta}}} i\nabla_{\beta\dot{\beta}}^{\alpha} \end{array} - \frac{1}{8} \begin{array}{c} i\nabla^{\alpha\dot{\alpha}} 1/\square_0 \\ \circlearrowleft \\ \frac{\tilde{\mathcal{B}}_{\dot{\alpha}}}{\overline{F}^{\dot{\beta}}} i\nabla_{\alpha\dot{\beta}}^{\alpha} \end{array} + \frac{1}{8} \begin{array}{c} 1/\square_0 i\nabla^{\alpha\dot{\alpha}} \\ \circlearrowleft \\ \frac{i\nabla_{\dot{\alpha}}^{\beta} \tilde{\mathcal{E}}_{\beta\alpha\dot{\beta}}}{\overline{F}^{\dot{\alpha}}} \end{array} \\
& -\frac{1}{8} \begin{array}{c} 1/\square_0 i\nabla^{\alpha\dot{\alpha}} \\ \circlearrowleft \\ \frac{i\nabla_{\alpha\dot{\alpha}}}{\tilde{\mathcal{B}}_{\dot{\beta}}} \end{array} + \frac{1}{8} \begin{array}{c} i\nabla^{\alpha\dot{\alpha}} 1/\square_0 \\ \circlearrowleft \\ \frac{\tilde{\mathcal{E}}_{\alpha}^{\beta\dot{\beta}}}{\tilde{\mathcal{E}}_{\alpha}^{\dot{\beta}}} i\nabla_{\beta\dot{\beta}}^{\alpha} \end{array} - \frac{1}{8} \begin{array}{c} 1/\square_0 \\ \circlearrowleft \\ \frac{i\nabla_{\dot{\alpha}}^{\alpha} \tilde{\mathcal{B}}_{\dot{\beta}}}{\tilde{\mathcal{B}}_{\dot{\beta}}} i\nabla_{\alpha\dot{\beta}}^{\alpha} \end{array}
\end{aligned}$$

(6.3.26)

After integrating by parts spacetime derivatives, it is possible to write eq. (6.3.25) in this form (up to non-planar terms)

$$-\frac{1}{2} \begin{array}{c} \overline{F}^{\dot{\alpha}} \\ \circlearrowleft \\ \frac{1/\square}{\frac{1}{\square} i\overline{W}_{\dot{\alpha}}} \end{array}$$

$$(6.3.27)$$

In the first line we collected the only UV divergent term while in the second line the finite ones.

- **Divergences with  $\overline{\mathcal{L}}_{\alpha}$**

There is only one contributing graph with this coefficient: So from (2Bx,1) we get the divergent term

$$(6.3.28)$$

and the finite one

$$(6.3.29)$$

After some integration by parts and using the relation

$$\overline{\mathcal{L}}^{\alpha} = [\nabla^{\alpha}, L] - H^{\alpha} \quad (6.3.30)$$

it is possible to write (6.3.28) (up to terms with more than 2  $\overline{W}$ 's) as

$$-\frac{1}{6} \begin{array}{c} H^\alpha \\ \text{---} \\ \text{---} \\ \text{---} \\ \text{---} \\ \frac{1}{\square} iW_\alpha \end{array} \quad (6.3.31)$$

• **Divergences with  $\mathcal{H}_{\dot{\alpha}\alpha}$**

Consider graphs (4Ax,1) and (5A,1). After replacements (6.3.1), (6.3.2), their divergent parts give

$$+\frac{3}{8} \begin{array}{c} \frac{1}{\square} i\nabla^{\alpha\dot{\alpha}} \\ \text{---} \\ \text{---} \\ \text{---} \\ \mathcal{H}_{\dot{\alpha}\alpha} \end{array} + \frac{3}{8} \begin{array}{c} [i\nabla^{\alpha\dot{\alpha}}, \frac{1}{\square}] \\ \text{---} \\ \text{---} \\ \text{---} \\ \mathcal{H}_{\dot{\alpha}\alpha} \end{array} \quad (6.3.32)$$

while the finite terms are

$$\boxed{+\frac{1}{8} \begin{array}{c} i\nabla^{\alpha\dot{\alpha}} \mathcal{H}_{\dot{\alpha}}^\beta \\ \text{---} \\ \text{---} \\ \text{---} \\ \hat{\mathcal{D}}_{\alpha\beta} \end{array} - \frac{1}{8} \begin{array}{c} \hat{A} \\ \text{---} \\ \text{---} \\ \text{---} \\ i\nabla^{\alpha\dot{\alpha}} \mathcal{H}_{\dot{\alpha}\alpha} \end{array} + \frac{1}{8} \begin{array}{c} \mathcal{H}^{\dot{\alpha}\beta} \\ \text{---} \\ \text{---} \\ \text{---} \\ i\nabla_{\dot{\alpha}}^\alpha \hat{\mathcal{D}}_{\alpha\beta} \end{array} + \frac{1}{8} \begin{array}{c} \hat{A} \\ \text{---} \\ \text{---} \\ \text{---} \\ i\nabla^{\alpha\dot{\alpha}} 1/\square_0 \end{array} \mathcal{H}_{\dot{\alpha}\alpha}} \quad (6.3.33)$$

By using  $\mathcal{H}_{\dot{\alpha}\alpha} = \{\overline{\nabla}_{\dot{\alpha}}, H_\alpha\} - E_{\alpha\dot{\alpha}} + iL\nabla_{\alpha\dot{\alpha}}$  it is possible to manipulate (6.3.32) and get

$$\begin{aligned} & \frac{3}{8} \begin{array}{c} [i\nabla^{\alpha\dot{\alpha}}, \frac{1}{\square}] \\ \text{---} \\ \text{---} \\ \text{---} \\ \mathcal{H}_{\dot{\alpha}\alpha} \end{array} - \frac{3}{8} \begin{array}{c} \frac{1}{\square} i\nabla^{\alpha\dot{\alpha}} \\ \text{---} \\ \text{---} \\ \text{---} \\ E_{\alpha\dot{\alpha}} \end{array} - \frac{3}{8} \begin{array}{c} \frac{1}{\square} \nabla^{\alpha\dot{\alpha}} \\ \text{---} \\ \text{---} \\ \text{---} \\ L\nabla_{\alpha\dot{\alpha}} \end{array} + \frac{3}{8} \begin{array}{c} \frac{1}{\square} i\nabla^{\alpha\dot{\alpha}} \\ \text{---} \\ \text{---} \\ \text{---} \\ \{\overline{\nabla}_{\dot{\alpha}}, H_\alpha\} \end{array} \\ & = -\frac{3}{8} \begin{array}{c} \frac{1}{\square} i\nabla^{\alpha\dot{\alpha}} \\ \text{---} \\ \text{---} \\ \text{---} \\ E_{\alpha\dot{\alpha}} \end{array} + \frac{3}{8} \begin{array}{c} L\square \\ \text{---} \\ \text{---} \\ \text{---} \\ \frac{1}{\square} \end{array} - \frac{3}{4} \begin{array}{c} H^\alpha \\ \text{---} \\ \text{---} \\ \text{---} \\ \frac{1}{\square} iW_\alpha \end{array} \end{aligned}$$

$$\boxed{
\begin{array}{c}
\begin{array}{cc}
\begin{array}{c}
\text{[}i\nabla^{\alpha\dot{\alpha}}, \frac{1}{\square}\text{]} \\
\text{---} \\
\text{1/}\square_0 \\
\text{---} \\
\mathcal{H}_{\dot{\alpha}\alpha}
\end{array}
&
\begin{array}{c}
H^\alpha i\nabla_{\dot{\alpha}} \\
\text{---} \\
\text{1/}\square_0 \\
\text{---} \\
\text{[}\nabla_{\dot{\alpha}}, \frac{1}{\square}\text{]}
\end{array}
\end{array}
\end{array}
}
\quad (6.3.34)$$

As usual, we write on different lines the divergent and the finite terms.

Consider now the sum of all the divergent terms we found in this section, that is the first line of equations (6.3.23), (6.3.27), (6.3.34) plus (6.3.24) and (6.3.31). They sum up to the following simple expression

$$\begin{array}{c}
\begin{array}{ccc}
\begin{array}{c}
L\square \\
\text{---} \\
\text{1/}\square \\
\text{---} \\
\frac{1}{\square}
\end{array}
&
- &
\begin{array}{c}
H^\alpha \\
\text{---} \\
\text{1/}\square \\
\text{---} \\
\frac{1}{\square} iW_\alpha
\end{array}
&
- &
\frac{1}{2} &
\begin{array}{c}
\overline{F}^{\dot{\alpha}} \\
\text{---} \\
\text{1/}\square \\
\text{---} \\
\frac{1}{\square} i\overline{W}_{\dot{\alpha}}
\end{array}
\end{array} \\
= &
- &
\frac{1}{4} &
\begin{array}{c}
\frac{1}{\square} iW^\alpha \\
\text{---} \\
\text{1/}\square \\
\text{---} \\
H_\alpha
\end{array}
&
+ &
\frac{1}{4} &
\begin{array}{c}
\frac{1}{\square} i\overline{W}^{\dot{\alpha}} \\
\text{---} \\
\text{1/}\square \\
\text{---} \\
\overline{F}_{\dot{\alpha}}
\end{array}
\end{array}
\quad (6.3.35)$$

where in the last equation we used (6.3.18).

Adding to this expression the divergence we found at the end of section (6.3.2) (see equation (6.3.12)), we find that the divergent part of all cubic-vertex diagrams is

$$\begin{array}{c}
\begin{array}{cc}
\begin{array}{c}
\frac{1}{\square} iW^\alpha \\
\text{---} \\
\text{1/}\square \\
\text{---} \\
H_\alpha
\end{array}
&
+ &
\frac{1}{4} &
\begin{array}{c}
\frac{1}{\square} i\overline{W}^{\dot{\alpha}} \\
\text{---} \\
\text{1/}\square \\
\text{---} \\
\overline{F}_{\dot{\alpha}}
\end{array}
\end{array}
\end{array}
\quad (6.3.36)$$

In the next section we will show that an opposite divergent contribution comes from the tadpoles. So we end up with an UV free formula for the effective action.

### 6.3.4 Tadpole divergent graphs

Consider now the divergences associated with tadpole diagrams. In particular, we refer to equations (6.2.36), (6.2.40) and (6.2.43).

In this sector we can distinguish two different types of divergences: When on one loop there is a single  $\frac{1}{\square}$  and when there is only one external  $W$  or  $\overline{W}$  field inserted in.

In the first type, we include contributions from eq. (6.2.36), (6.2.43) and from part of the third graph of equation (6.2.40)\*\*. It is immediate to see that the divergent terms sum up to

$$\begin{aligned}
 & \frac{5}{3} \begin{array}{c} \frac{1}{\square_0} \\ \text{a} \quad \text{d} \\ \text{c} \quad \text{b} \\ L \end{array} + \frac{1}{12} \begin{array}{c} \frac{1}{\square_0} \\ \text{a} \quad \text{c} \\ \text{d} \quad \text{b} \\ L \end{array} \\
 & \boxed{ + \frac{5}{3} \begin{array}{c} (\frac{1}{\square} - \frac{1}{\square_0}) \\ \text{a} \quad \text{d} \\ \text{c} \quad \text{b} \\ L \end{array} + \frac{1}{12} \begin{array}{c} (\frac{1}{\square} - \frac{1}{\square_0}) \\ \text{a} \quad \text{c} \\ \text{d} \quad \text{b} \\ L \end{array} }
 \end{aligned} \tag{6.3.37}$$

The first line vanishes since the diagrams are genuine tadpoles. We then concentrate on the second line. We have already encountered these type of graphs (see eq.(6.3.19)). We show now how the cancellation of the divergences occurs. Consider the following loop

$$\begin{array}{c} (\frac{1}{\square} - \frac{1}{\square_0}) \\ \text{---} \circ \text{---} \\ \text{---} \end{array} \tag{6.3.38}$$

and in the expansion of the covariant propagator  $\frac{1}{\square}$  take only terms that contribute to

---

\*\*See equation (C.0.30).



the divergence of (6.3.38)

$$\begin{aligned} \frac{1}{\square} - \frac{1}{\square_0} &= \frac{1}{\square_0} \Gamma^{\alpha\dot{\alpha}} i\partial_{\alpha\dot{\alpha}} \frac{1}{\square_0} + \frac{1}{2} \frac{1}{\square_0} (i\partial^{\alpha\dot{\alpha}} \Gamma_{\alpha\dot{\alpha}}) \frac{1}{\square_0} \\ &\quad + \frac{1}{2} \frac{1}{\square_0} \Gamma^{\alpha\dot{\alpha}} \Gamma_{\alpha\dot{\alpha}} \frac{1}{\square_0} + \frac{1}{\square_0} \Gamma^{\alpha\dot{\alpha}} i\partial_{\alpha\dot{\alpha}} \frac{1}{\square_0} \Gamma^{\beta\dot{\beta}} i\partial_{\beta\dot{\beta}} \frac{1}{\square_0} \end{aligned} \quad (6.3.39)$$

Replacing (6.3.39) in (6.3.38) and writing the corresponding loop integrals (we denote with  $\ell$  loop momentum and with  $p_i$  external momenta) we get

$$\begin{aligned} \left( \frac{1}{\square} - \frac{1}{\square_0} \right) \text{ (circle diagram)} &= I_1 + I_2 + I_3 + I_4 \\ I_1 &= \Gamma^{\alpha\dot{\alpha}}(p_1) \int d^d \ell \frac{-(\ell + p_1)_{\alpha\dot{\alpha}}}{\ell^2 (\ell + p_1)^2} \\ I_2 &= \frac{1}{2} (p_1)^{\alpha\dot{\alpha}} \Gamma_{\alpha\dot{\alpha}}(p_1) \int d^d \ell \frac{1}{\ell^2 (\ell + p_1)^2} \\ I_3 &= \frac{1}{2} \Gamma^{\alpha\dot{\alpha}}(p_1) \Gamma_{\alpha\dot{\alpha}}(p_2) \int d^d \ell \frac{1}{\ell^2 (\ell + p_1 + p_2)^2} \\ I_4 &= -\Gamma^{\alpha\dot{\alpha}}(p_1) \Gamma^{\beta\dot{\beta}}(p_2) \int d^d \ell \frac{(\ell + p_1)_{\alpha\dot{\alpha}} (\ell + p_1 + p_2)_{\beta\dot{\beta}}}{\ell^2 (\ell + p_1)^2 (\ell + p_1 + p_2)^2} \end{aligned} \quad (6.3.40)$$

In (6.3.40) we use the convention that outgoing momenta are positive. Moreover we remind that  $\frac{1}{\square_0} = -\frac{1}{p^2}$  and this provides an extra minus sign in  $I_4$  compared to the rest. By using standard formulas<sup>††</sup> it is straightforward to see that  $I_1$  cancels exactly against  $I_2$  and  $I_3$  cancels the divergent part of  $I_4$  (when we take  $\ell_{\alpha\dot{\alpha}} \ell_{\beta\dot{\beta}}$  in the numerator of  $I_4$ ). So, what we are left with are only UV finite terms coming from the other terms in  $I_4$  and from the higher order expansion of  $\frac{1}{\square}$  in (6.3.39).

The second type of divergences comes from the pure-vector graphs of eq. (6.2.40) of  $\nabla$ -algebra. In particular, we can distinguish two subclasses of divergent diagrams.

In the first one we include the part of the third diagram in (6.2.40) proportional to  $\{\nabla^\alpha, B_\alpha\}$  and the part of the sixth proportional to the commutator  $[\nabla^\alpha, L]$  (remember

---

<sup>††</sup>See for instance Appendix A of [116]

that  $\bar{\mathcal{L}}^\alpha = [\nabla^\alpha, L] - H^\alpha$ )

$$\begin{aligned}
 & -\frac{1}{24} \begin{array}{c} L \\ \text{a} \quad \text{c} \\ \bullet \\ \text{d} \quad \text{b} \\ \{\nabla^\alpha, B_\alpha\} \end{array} \quad -\frac{1}{24} \begin{array}{c} [\nabla^\alpha, L] \\ \text{a} \quad \text{d} \\ \bullet \\ \text{c} \quad \text{b} \\ B_\alpha \end{array} \quad (6.3.41)
 \end{aligned}$$

Integrating by parts the  $\nabla^\alpha$  appearing in the second graph, we get

$$\begin{aligned}
 & -\frac{1}{24} \begin{array}{c} L \\ \text{a} \quad \text{c} \\ \bullet \\ \text{d} \quad \text{b} \\ \mathcal{P}_\alpha^\alpha \end{array} \quad + \frac{1}{24} \begin{array}{c} L \\ \text{a} \quad \text{d} \\ \bullet \\ \text{c} \quad \text{b} \\ \mathcal{P}_\alpha^\alpha \end{array} \quad (6.3.42)
 \end{aligned}$$

Both the contributions of (6.3.42) are not divergent on-shell. In fact the only linear term in  $\mathcal{P}_\alpha^\alpha$  is proportional to  $(\nabla^\alpha W_\alpha)$ , which is zero on-shell.

The second subclass of divergent tadpoles are due to the linear terms in the coefficients  $B_\alpha$ ,  $C_\alpha$ ,  $\mathcal{E}_{\dot{\alpha}\alpha\dot{\beta}}$  and  $\bar{\mathcal{E}}_{\alpha\dot{\alpha}\dot{\beta}}$ . The graphs contributing are the first, the fourth, the fifth one of (6.2.40) and the part of the sixth proportional to  $H_\alpha$ . We can extrapolate from these terms the divergences by using the substitution (6.3.2). We get the divergent contributions:

$$\begin{aligned}
 & -\frac{1}{6} \begin{array}{c} H^\alpha \\ \text{a} \quad \text{b} \\ \bullet \\ \text{d} \quad \text{c} \\ i\frac{1}{\square}W_\alpha\frac{1}{\square} \end{array} \quad -\frac{1}{12} \begin{array}{c} H^\alpha \\ \text{a} \quad \text{d} \\ \bullet \\ \text{c} \quad \text{b} \\ i\frac{1}{\square}W_\alpha\frac{1}{\square} \end{array} \quad -\frac{1}{4} \begin{array}{c} \bar{F}^{\dot{\alpha}} \\ \text{a} \quad \text{c} \\ \bullet \\ \text{d} \quad \text{b} \\ i\frac{1}{\square}\bar{W}_{\dot{\alpha}}\frac{1}{\square} \end{array} \quad (6.3.43)
 \end{aligned}$$

and the finite ones:

(6.3.44)

This graphs are multiplied by the combinatorial color factor

$$g^2(f^{abe} f^{ecd}) \quad (6.3.45)$$

By considering carefully the color structure of diagrams in (6.3.43) and using Jacobi identity (E.1.5), it is possible to rewrite them in the following way

(6.3.46)

We then find convenient to rewrite the tadpoles in (6.3.46) by multiplying for  $1 = (\frac{1}{\square} \square)$  the 4 points vertex. This produces a loop integral structure that is exactly the one of the cubic vertex diagrams (6.3.36). Then, by integrating by parts the  $\square$  on the right vertex, we find

$$\begin{array}{cc}
\begin{array}{c} H^\alpha \square \\ -\frac{1}{4} \left( \text{circle with } 1/\square_0 \text{ and } i \frac{1}{\square} W_\alpha \frac{1}{\square} \right) \end{array} & 
\begin{array}{c} H^\alpha \nabla^{\beta\dot{\beta}} \\ -\frac{1}{4} \left( \text{circle with } 1/\square_0 \text{ and } i \frac{1}{\square} W_\alpha \frac{1}{\square} \nabla_{\beta\dot{\beta}} \right) \end{array} \\
\begin{array}{c} \bar{F}^{\dot{\alpha}} \square \\ -\frac{1}{4} \left( \text{circle with } 1/\square_0 \text{ and } i \frac{1}{\square} \bar{W}_{\dot{\alpha}} \frac{1}{\square} \right) \end{array} & 
\begin{array}{c} \bar{F}^{\dot{\alpha}} \nabla^{\beta\dot{\beta}} \\ -\frac{1}{4} \left( \text{circle with } 1/\square_0 \text{ and } i \frac{1}{\square} \bar{W}_{\dot{\alpha}} \frac{1}{\square} \nabla_{\beta\dot{\beta}} \right) \end{array}
\end{array}
\tag{6.3.47}$$

The first terms in (6.3.47) cancels exactly against (6.3.36). No other divergent terms are left! The second line gives the last finite terms we have to keep.

Summarizing, all the divergent graphs present in the  $\nabla$ -algebra results of Section 6.2 sum into squared expressions of equations (6.3.20), (6.3.22), (6.3.23), (6.3.26), (6.3.27), (6.3.29), (6.3.33), (6.3.34), (6.3.37), (6.3.42), (6.3.44) and (6.3.47).

These contributions need be combined with finite contributions from Section 6.2, namely equations (6.2.18), (6.2.24), (6.2.25), (6.2.26), (6.2.27), (6.2.28), (6.2.29), (6.2.30), (6.2.31), (6.2.32), (6.2.33), (6.2.34), (6.2.40).

The total sum provides the *master equation* for the 2-loop  $n$ -point MHV effective action of the  $\mathcal{N} = 4$  SYM theory in the planar limit.

Note that from the absence of UV divergences it follows that no bubble diagrams are present at this level. However, this is not a proof of the no-bubble part of the no-bubble no-triangle hypothesis. In fact, bubbles can be produced in further passages of the computation of an amplitude. In particular, the contributing diagrams of the master equation should be interpreted in configuration space. As we Fourier transform to momentum space and we perform the Passarino-Veltman reduction on vector and tensor loop integrals (see Step 5 in Section 5.4) a lot of bubble-like scalar integrals are produced. Of course, they are produced in combinations such that their UV divergent part cancel but this do not allow to conclude that the full integral cancel.

For what concerns the triangles, the master equation contains a lot of triangle-like diagrams: Triangles, in fact, are produced by coefficients whose expansion starts at first order in the external fields  $W, \overline{W}$  (for example  $B_\alpha, \mathcal{C}_\alpha, \dots$ ) and there are a lot of these coefficients. Thus the cancellation of the triangles is, at this stage of the computation, a miraculous accident.



# Chapter 7

## Towards the four point MHV amplitude

The previous Chapter ends with a master equation that encodes in our formalism the all- $n$  two loop MHV planar effective action of the  $\mathcal{N} = 4$  SYM theory. In this Chapter we want to extrapolate from there the four point MHV effective action, i.e. the first non trivial effective action. In particular, we look for that part of the full effective action that contributes to the  $A(1^+, 2^+, 3^-, 4^-)$  color ordered amplitude. The scattering amplitude can then be obtained from the effective action by summing over the permutations of the quantum numbers (momenta, helicity and color numbers) of the interacting particles.

In Section 5.4 the complete procedure to move from the master equation for the effective action to the  $n$  particle MHV scattering amplitude is presented in five steps. In this Chapter we follow that scheme but we optimize it for the four point particle case.

In particular, we show that the four point effective action gets contributions just from 1PI effective action diagrams dressed with two  $W$ 's and two  $\overline{W}$ 's. Thus we do not need to include trees of 1PI diagrams nor diagrams including connections  $\Gamma$ . While showing this, we automatically demonstrate that at two and three points the effective action vanishes on shell as it should. These results follow from general features about covariant supergraphs, in particular their behavior under exchange of lines (Up-Down symmetry) and of vertices (Left-Right symmetry) and their Lorentz structure.

Since the cancellation of UV divergences implies that there are no bubbles at the level of the effective action, at four points all the contributions can be reduced to have one of the four loop structures of Fig 7.1. More precisely, all the contributions to the four point effective actions in configuration space are given by the product of a tensorial structure described by two  $W$ 's and two  $\overline{W}$ 's times a kinematic structure given by one of the loop structures 7.1 and two spacetime derivatives that allow to preserve the Lorentz invariance of each contributing term.

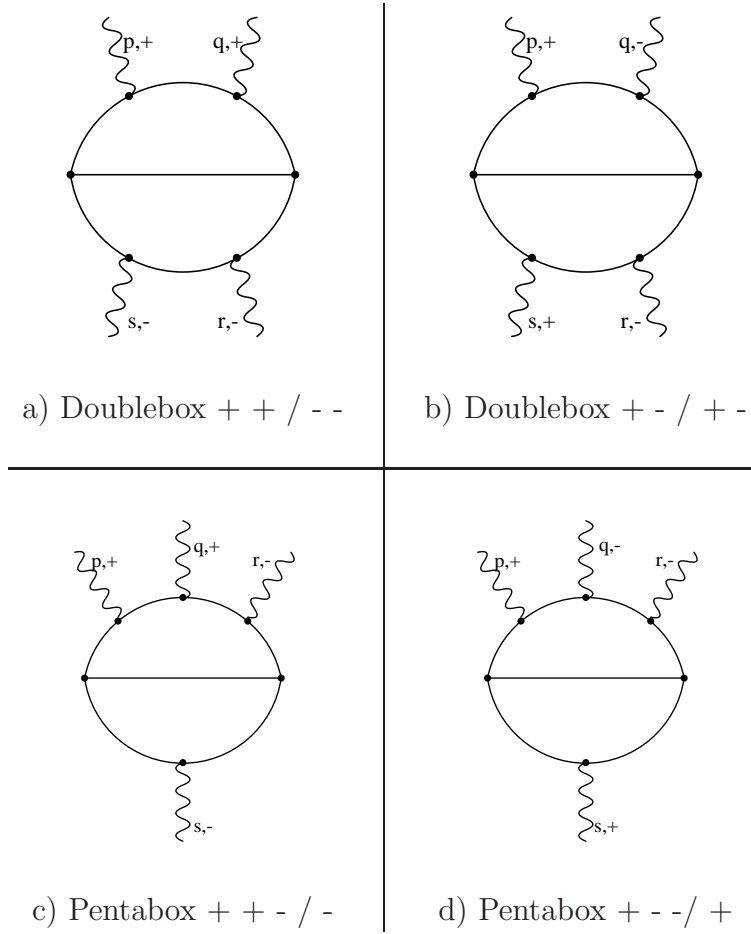


Figure 7.1: Four point topologies for the  $\mathcal{N} = 4$  SYM theory

The factorization properties of helicity structures for MHV amplitudes (4.1.5) implies that the  $W$ 's and the  $\overline{W}$ 's appear with indices contracted between themselves. In momentum space this means that a structure like

$$W^\alpha(p_1) W_\alpha(p_2) \overline{W}^{\dot{\alpha}}(p_3) \overline{W}_{\dot{\alpha}}(p_4) \quad (7.0.1)$$

should be present in front of each contribution\*. In our computation, this index structure turns out to be a consequence of Passarino–Veltman reduction of vector and tensor integrals and of the on-shell conditions (B.0.8).

After PV reduction the effective action is given by a complicated combination of doublebox and pentabox-like scalar integrals with various numerators too. However, by working out this expression with the aid of various identities occurring between the integrals,

---

\*See eq. (5.1.14) for the four point helicity structure at one loop



it is possible to cancel all the pentabox-like contributions. This fact is a consequence of an incredible combination of the coefficients of each contribution.

The final result for the four point effective action is quite asymmetric in the two doublebox structures, since in one sector it presents only one term while the other sectors is given by a linear combination of various scalar integrals. It is possible to recognize inside our expression the contributions that reproduce the results for the color ordered four point amplitude computed through the indirect techniques. However we have many other terms. Various checks of the validity of our result are still in progress.

The first Section of this Chapter is devoted to describe the computation of the four point effective action and to sketch its characteristics in the configuration space. Although a good part of the arguments here exposed are valid for  $n > 4$  too, our attention is mostly attended to the four point case. In the second Section we give our final expression for the effective action in momentum space. In order to follow the computations scattered along the Chapter, Appendices E, F, G and H play a fundamental role.

## 7.1 Up to four points

While we look for the  $n$ -point effective action, the first operation to do is to replace all the coefficients that appear in the formula for the all- $n$  effective action with their power expansions in the external fields. After this operation, we are left with a large number of covariant graphs that are functions of covariant propagators  $\frac{1}{\square}$ , covariant derivatives  $\nabla_{\alpha\dot{\alpha}}$  and a number of background fields  $W_\alpha, \overline{W}_{\dot{\alpha}}$  smaller or equal to  $n$ . MHV condition further constraints the number of  $W$ 's and  $\overline{W}$ 's to be smaller than  $n - 2$  and than 2 respectively.

At this point a second expansion must be performed. In fact covariant propagators and derivatives must be expanded up to the required number of connections  $\Gamma$ . This operation allows to distinguish between two classes of covariant contributing diagrams:

- 1) Diagrams with  $n$   $W$ 's and  $\overline{W}$ 's:

They do not need any further expansion and covariant propagators and derivatives are simply replaced by their  $\Gamma$  independent terms

$$\frac{1}{\square} \longrightarrow \frac{1}{\square_0} \qquad \nabla_{\alpha\dot{\alpha}} \longrightarrow \partial_{\alpha\dot{\alpha}} \qquad (7.1.1)$$

No connections enter in the final expression for the amplitude from these contributions.

- 2) Diagrams with  $m < n$   $W$ 's and  $\overline{W}$ 's:

All covariant objects must be expanded and replaced inside covariant diagrams up to  $(n - m)$  order in the connections. At the end, the resulting diagrams present  $m$   $W$ 's and  $\overline{W}$ 's and  $(n - m)$   $\Gamma$ 's.

This second class of diagrams obliges to start the analysis of the  $n$ -point effective action from the lowest  $W$  covariant terms that come out from the master equation. Since the master equation for the  $\mathcal{N} = 4$  SYM theory is free of bubbles, we have to start our analysis from the two  $W$  covariant contribution.

Note that, in principle, the two classes of diagrams 1) and 2) must be kept distinct since their superfield content is different. Possible cancellations between the two sectors would eventually be manifest just at the component level, not at the superfield one. However, the on-shell superfield formalism allows us to rewrite two and three point covariant contributions as four point covariant contributions before expanding  $\frac{1}{\square}$  and  $\nabla$ . This, as outlined in the introduction to this Chapter, has two implications:

- a) When we are interested in the four point effective action we do not have to worry about connections. Connections start to become relevant since five points on;
- b) This is a direct proof of the well known fact [9, 68] that the two and the three point amplitudes vanish on-shell.

The proof of the vanishing of the effective action up to four points makes use of general properties of the covariant diagrams that we call *geometric symmetries*. Geometric symmetries follow from the fact that, given a vacuum diagram (for example a cubic vertex vacuum diagram of Fig 6.1), it is always possible to interchange two quantum lines or two quantum vertices. In the first case we talk about Up-Down symmetry while in the second of Left-Right symmetry of the vacuum diagrams. After that  $\nabla$ -algebra is performed and coefficients  $A, B, \dots, L$  are replaced by their explicit expressions, the covariant effective action diagrams that come out still is remnant of these geometric symmetries and many untrivial relations between various terms can be worked out by using UD and LR. We show in the next sections which of these relations are fundamental to prove the vanishing of the two and the three point amplitudes. A detailed description of UD and LR symmetries is given in Appendix F.

### 7.1.1 Two point covariant contributions

By power expanding in the external fields the coefficients that appear in the effective action and by using Up-Down and Left-Right symmetry, we find the following covariant contributions up to two  $W$ 's:

$$\begin{aligned}
 \text{Two point function} &= +\frac{3}{2}i \int \frac{1}{\square} W^\alpha \nabla_{\dot{\alpha}} \frac{1}{\square} \\
 &\quad -\frac{3}{2}i \int \frac{1}{\square} W^\alpha \frac{1}{\square} \nabla_{\dot{\alpha}} \\
 &\quad +\frac{5}{4}i \int \frac{1}{\square} W^\alpha \frac{1}{\square} \\
 &\quad \frac{1}{\square} \overline{W}_{\dot{\alpha}} \frac{1}{\square} \quad \frac{1}{\square} \overline{W}_{\dot{\alpha}} \frac{1}{\square} \quad \frac{1}{\square} \overline{W}^{\dot{\alpha}} \nabla_{\alpha\dot{\alpha}} \frac{1}{\square}
 \end{aligned}$$



Note that these relations involve covariant diagrams, not ordinary ones. As soon as the covariant propagators  $\frac{1}{\square}$  are expanded in the connections  $\Gamma$ , they turn out to be very complicated relations involving a lot of ordinary diagrams. Thus, these relations are actually highly non-trivial relations.

Using (7.1.3), (7.1.4) and (7.1.5), the two point function (7.1.2) can be rewritten in a very compact form

$$\text{Two point function} = -\frac{9}{4}i \begin{array}{c} \frac{1}{\square} W^\alpha \frac{1}{\square} \\ \circlearrowleft \\ \frac{1}{\square} \overline{W}^{\dot{\alpha}} \left[ \frac{1}{\square}, \nabla_{\alpha\dot{\alpha}} \right] \end{array} + \frac{1}{4} \begin{array}{c} \frac{1}{\square} (\nabla W)^{\alpha\beta} \frac{1}{\square} \\ \circlearrowleft \\ \frac{1}{\square} (\nabla W)_{\alpha\beta} \frac{1}{\square} \end{array} \quad (7.1.6)$$

We consider now the two diagrams in (7.1.6) and we manipulate them separately

- 1) Consider the first diagram in (7.1.6). By using the Jacobi identities it is possible to write the commutator  $[\nabla_{\alpha\dot{\alpha}}, \frac{1}{\square}]$  as

$$\begin{aligned} \left[ \nabla_{\alpha\dot{\alpha}}, \frac{1}{\square} \right] &= -i \left[ \{ \nabla_\alpha, \overline{\nabla}_{\dot{\alpha}} \}, \frac{1}{\square} \right] = \\ &= -i \left( \left\{ \nabla_\alpha, \left[ \overline{\nabla}_{\dot{\alpha}}, \frac{1}{\square} \right] \right\} + \left\{ \overline{\nabla}_{\dot{\alpha}}, \left[ \nabla_\alpha, \frac{1}{\square} \right] \right\} \right) = \\ &= i \left( \left\{ \nabla_\alpha, \frac{1}{\square} W^\beta \nabla_{\beta\dot{\alpha}} \frac{1}{\square} \right\} + \left\{ \overline{\nabla}_{\dot{\alpha}}, \frac{1}{\square} \overline{W}^{\dot{\beta}} \nabla_{\alpha\dot{\beta}} \frac{1}{\square} \right\} \right) \end{aligned} \quad (7.1.7)$$

Substituting expression (7.1.7) in the first diagram in (7.1.6) and integrating by parts the spinorial derivatives<sup>†</sup>, we get

$$\begin{aligned} -\frac{9}{4}i \begin{array}{c} \frac{1}{\square} W^\alpha \frac{1}{\square} \\ \circlearrowleft \\ \frac{1}{\square} \overline{W}^{\dot{\alpha}} \left[ \frac{1}{\square}, \nabla_{\alpha\dot{\alpha}} \right] \end{array} &= -\frac{9}{4} \begin{array}{c} \frac{1}{\square} W^\alpha \frac{1}{\square} W^\beta \nabla_{\beta\dot{\alpha}} \frac{1}{\square} \\ \circlearrowleft \\ \frac{1}{\square} \overline{W}_{\dot{\alpha}} \frac{1}{\square} \overline{W}^{\dot{\beta}} \nabla_{\alpha\dot{\beta}} \frac{1}{\square} \end{array} + \frac{9}{4} \begin{array}{c} \frac{1}{\square} W^\alpha \frac{1}{\square} W^\beta \nabla_{\beta\dot{\alpha}} \frac{1}{\square} \\ \circlearrowleft \\ \frac{1}{\square} \overline{W}^{\dot{\beta}} \nabla_{\alpha\dot{\beta}} \frac{1}{\square} \overline{W}_{\dot{\alpha}} \frac{1}{\square} \end{array} \\ &+ \frac{9}{4} \begin{array}{c} \frac{1}{\square} W^\alpha \frac{1}{\square} \overline{W}^{\dot{\beta}} \nabla_{\alpha\dot{\beta}} \frac{1}{\square} \\ \circlearrowleft \\ \frac{1}{\square} W^\beta \nabla_{\beta\dot{\alpha}} \frac{1}{\square} \overline{W}_{\dot{\alpha}} \frac{1}{\square} \end{array} \end{aligned} \quad (7.1.8)$$

---

<sup>†</sup>See the comments in the next Section for an exhaustive description of the procedure

2) Consider the second diagram in (7.1.6) and suppose to integrate by parts the spinorial derivative that appears in the first line. After using LR symmetry, we get

$$\begin{aligned}
\frac{1}{4} \begin{array}{c} \frac{1}{\square}(\nabla W)^{\alpha\beta}\frac{1}{\square} \\ \circlearrowleft \\ \frac{1}{\square}(\nabla W)_{\alpha\beta}\frac{1}{\square} \end{array} &= -\frac{1}{2} \begin{array}{c} \frac{1}{\square}W^{\alpha}\frac{1}{\square}\overline{W}^{\dot{\alpha}}\nabla_{\dot{\alpha}}^{\beta}\frac{1}{\square} \\ \circlearrowleft \\ \frac{1}{\square}(\nabla W)_{\alpha\beta}\frac{1}{\square} \end{array} + \frac{1}{2} \begin{array}{c} \frac{1}{\square}(\nabla W)^{\alpha\beta}\frac{1}{\square}\overline{W}^{\dot{\alpha}}\nabla_{\beta\dot{\alpha}}\frac{1}{\square} \\ \circlearrowleft \\ \frac{1}{\square}W_{\alpha}\frac{1}{\square} \end{array} \quad (7.1.9)
\end{aligned}$$

Integrating by parts the last spinorial derivative we get the final result

$$\begin{aligned}
\frac{1}{4} \begin{array}{c} \frac{1}{\square}(\nabla W)^{\alpha\beta}\frac{1}{\square} \\ \circlearrowleft \\ \frac{1}{\square}(\nabla W)_{\alpha\beta}\frac{1}{\square} \end{array} &= +\frac{1}{2} \begin{array}{c} \frac{1}{\square}W^{\alpha}\frac{1}{\square}\overline{W}^{\dot{\alpha}}\nabla_{\dot{\alpha}}^{\beta}\frac{1}{\square} \\ \circlearrowleft \\ \frac{1}{\square}W_{\alpha}\frac{1}{\square}\overline{W}^{\dot{\beta}}\nabla_{\beta\dot{\beta}}\frac{1}{\square} \end{array} \quad (7.1.10)
\end{aligned}$$

Summarizing the results, the contributions (7.1.2) can be rewritten as the sum of the right hand sides of equations (7.1.8) and (7.1.10)

$$\begin{aligned}
\text{Two point contribution to} &= -\frac{9}{4} \begin{array}{c} \frac{1}{\square}W^{\alpha}\frac{1}{\square}W^{\beta}\nabla_{\beta}^{\dot{\alpha}}\frac{1}{\square} \\ \circlearrowleft \\ \frac{1}{\square}\overline{W}_{\dot{\alpha}}\frac{1}{\square}\overline{W}^{\dot{\beta}}\nabla_{\alpha\dot{\beta}}\frac{1}{\square} \end{array} + \frac{9}{4} \begin{array}{c} \frac{1}{\square}W^{\alpha}\frac{1}{\square}W^{\beta}\nabla_{\beta}^{\dot{\alpha}}\frac{1}{\square} \\ \circlearrowleft \\ \frac{1}{\square}\overline{W}^{\dot{\beta}}\nabla_{\alpha\dot{\beta}}\frac{1}{\square}\overline{W}_{\dot{\alpha}}\frac{1}{\square} \end{array} \\
\text{the 4 point effective action} &+ \frac{9}{4} \begin{array}{c} \frac{1}{\square}W^{\alpha}\frac{1}{\square}\overline{W}^{\dot{\beta}}\nabla_{\alpha\dot{\beta}}\frac{1}{\square} \\ \circlearrowleft \\ \frac{1}{\square}W^{\beta}\nabla_{\beta}^{\dot{\alpha}}\frac{1}{\square}\overline{W}_{\dot{\alpha}}\frac{1}{\square} \end{array} + \frac{1}{2} \begin{array}{c} \frac{1}{\square}W^{\alpha}\frac{1}{\square}\overline{W}^{\dot{\alpha}}\nabla^{\beta}\frac{1}{\square} \\ \circlearrowleft \\ \frac{1}{\square}W_{\alpha}\frac{1}{\square}\overline{W}^{\dot{\beta}}\nabla_{\beta\dot{\beta}}\frac{1}{\square} \end{array} \quad (7.1.11)
\end{aligned}$$

So, the original expression (7.1.2) for the two point function has been rewritten as the sum of four point covariant terms. No connection  $\Gamma$  is present. In particular the two point function gives contributions to both the doublebox  $++ / --$  and the doublebox  $+ - / - +$  sectors (see Fig 7.1). Since we are left with no two  $W$ 's diagrams, the two point function is zero [9].

### 7.1.2 Three point covariant contributions

The three point diagrams that contribute to the 4 point MHV effective action must contain two  $W$ 's and one  $\overline{W}$  or two  $\overline{W}$ 's and one  $W$ . In fact, configurations with three external fields with the same helicity are excluded by the MHV condition.

This observation allows us to predict the form of all covariant diagrams that appear at three points. Consider the two  $W$ 's one  $\overline{W}$  case as an example. By Lorentz and supersymmetry invariance of the diagrams, we know that all the indices that enter in a Feynman graph must be saturated. This is possible only by introducing in the graph a spacetime derivative  $\nabla_{\alpha\dot{\alpha}}$  and by requiring that one of the  $W$ 's has a spinorial derivative acting on it. Dimensional arguments forbid to introduce extra derivatives<sup>‡</sup>. So, each three point graph is built up with these elements:

$$W_\alpha, \quad (\nabla W)_{\alpha\beta}, \quad \overline{W}_{\dot{\alpha}}, \quad \nabla_{\alpha\dot{\alpha}} \quad (7.1.12)$$

More precisely, since by on-shellness  $(\nabla^\alpha W_\alpha) = 0$ , indices between elements (7.1.12) must be contracted in the following way

$$W^\alpha, \quad (\nabla W)_\alpha{}^\beta, \quad \overline{W}^{\dot{\alpha}}, \quad \nabla_{\beta\dot{\alpha}} \quad (7.1.13)$$

These elements can enter in various reciprocal locations with respect to themselves and to the propagators  $\frac{1}{\square}$ . However, their index structure is constrained to be the one shown in (7.1.13). Examples of three points diagrams that come out when the coefficients inside the master equation are replaced with their power expansion are represented in (7.1.14)

$$\begin{array}{ccc}
 \frac{1}{\square} W^\alpha \frac{1}{\square} \overline{W}^{\dot{\alpha}} \nabla_{\dot{\alpha}}^\beta \frac{1}{\square} & \frac{1}{\square} (\nabla W)^{\beta\alpha} \frac{1}{\square} W_\beta \frac{1}{\square} & \frac{1}{\square} (\nabla^{\alpha\dot{\alpha}} W^\beta) \frac{1}{\square} \overline{W}_{\dot{\alpha}} \frac{1}{\square} \\
 A) \quad \begin{array}{c} \text{---} \\ \circ \\ \text{---} \\ \frac{1}{\square} (\nabla W)_{\alpha\beta} \frac{1}{\square} \end{array} , & B) \quad \begin{array}{c} \frac{1}{\square} (\nabla W)^{\beta\alpha} \frac{1}{\square} W_\beta \frac{1}{\square} \\ \circ \\ \frac{1}{\square} \overline{W}^{\dot{\alpha}} \frac{1}{\square} \nabla_{\alpha\dot{\alpha}} \end{array} , & C) \quad \begin{array}{c} \frac{1}{\square} (\nabla^{\alpha\dot{\alpha}} W^\beta) \frac{1}{\square} \overline{W}_{\dot{\alpha}} \frac{1}{\square} \\ \circ \\ \frac{1}{\square} (\nabla W)_{\alpha\beta} \frac{1}{\square} \end{array}
 \end{array} \quad (7.1.14)$$

Suppose now to integrate by parts the spinorial derivative that appears in  $(\nabla W)_{\alpha\beta}$ . From a technical point of view, this operation can be managed in this way:

- 1) By observing that  $(\nabla W)_{\alpha\beta} = \nabla_\alpha W_\beta + W_\beta \nabla_\alpha$ , replace this expression for  $(\nabla W)_{\alpha\beta}$  inside the diagrams (7.1.14). On-shell condition  $(\nabla W)_{\alpha\beta} = (\nabla W)_{\beta\alpha}$  give us the possibility to choose the index carried by the spinorial derivative. We fix this ambiguity by imposing that  $\nabla$  carries the same index carried by the other chiral  $W$  field present in the diagram. In what follows, let's suppose that this index is  $\alpha$ ;

<sup>‡</sup>Lorentz and supersymmetry invariance let open the possibility to include extra spacetime derivatives with indexes contracted between them. However this would change the dimensionality of the diagram.

- 2) Move towards the left (right) vertex the  $\nabla_\alpha$  that appears to the left (right) of  $W_\beta$ ;
- 3) Once the spinorial derivative is arrived at the vertices, integrate it by parts on the other lines;
- 4) Move the spinorial derivative close to the left vertex towards the right. It is immediate to see that no terms with  $\nabla$ 's operating on the right vertex survive. All we are left with are commutators of  $\nabla$ 's with propagators  $\frac{1}{\square}$  and spacetime derivatives  $\nabla_{\alpha\dot{\alpha}}$ .

Since these commutators are proportional to  $\overline{W}$ 's, this procedure assures us that all three point diagrams are transformed in combinations of four point diagrams. Note that the choice of spinor index carried by the spinorial derivative plays a crucial role. Our prescription at step 1) avoids by on-shell conditions to produce back other  $(\nabla W)_{\alpha\beta}$  terms when spinorial derivatives are moved along the lines of the diagram.

Note that the operations 1)–4) require just three main ingredients: Commutation relations between covariant objects (see Appendix B), integration by parts of spinorial derivatives and on-shell conditions (5.1.12)<sup>§</sup>.

As examples, we report the results of the integration of spinorial derivatives on the diagrams (7.1.14).

$$\begin{aligned}
A) \quad & \frac{1}{\square} W^\alpha \frac{1}{\square} \overline{W}^{\dot{\alpha}} \nabla_{\dot{\alpha}}^\beta \frac{1}{\square} \\
& \begin{array}{c} \text{---} \\ \bigcirc \\ \text{---} \\ \frac{1}{\square} (\nabla W)_{\alpha\beta} \frac{1}{\square} \end{array} = - \begin{array}{c} \frac{1}{\square} W^\alpha \frac{1}{\square} \overline{W}^{\dot{\alpha}} \nabla_{\dot{\alpha}}^\beta \frac{1}{\square} \\ \text{---} \\ \bigcirc \\ \text{---} \\ \frac{1}{\square} W_\beta \frac{1}{\square} \overline{W}^{\dot{\beta}} \nabla_{\dot{\alpha}\dot{\beta}} \frac{1}{\square} \end{array} + \begin{array}{c} \frac{1}{\square} W^\alpha \frac{1}{\square} \overline{W}^{\dot{\alpha}} \nabla_{\dot{\alpha}}^\beta \frac{1}{\square} \\ \text{---} \\ \bigcirc \\ \text{---} \\ \frac{1}{\square} \overline{W}^{\dot{\beta}} \nabla_{\alpha\dot{\beta}} \frac{1}{\square} W_\beta \frac{1}{\square} \end{array} \\
& \hspace{20em} (7.1.15)
\end{aligned}$$

$$\begin{aligned}
B) \quad & \frac{1}{\square} (\nabla W)^{\beta\alpha} \frac{1}{\square} W_\beta \frac{1}{\square} \\
& \begin{array}{c} \text{---} \\ \bigcirc \\ \text{---} \\ \frac{1}{\square} \overline{W}^{\dot{\alpha}} \frac{1}{\square} \nabla_{\alpha\dot{\alpha}} \end{array} = - \begin{array}{c} \frac{1}{\square} W^\alpha \frac{1}{\square} W_\alpha \frac{1}{\square} \\ \text{---} \\ \bigcirc \\ \text{---} \\ \frac{1}{\square} \overline{W}^{\dot{\alpha}} \frac{1}{\square} \overline{W}_{\dot{\alpha}} \end{array} - \begin{array}{c} \frac{1}{\square} W^\alpha \frac{1}{\square} W_\beta \frac{1}{\square} \overline{W}^{\dot{\beta}} \nabla_{\beta\dot{\beta}} \frac{1}{\square} \\ \text{---} \\ \bigcirc \\ \text{---} \\ \frac{1}{\square} \overline{W}^{\dot{\alpha}} \frac{1}{\square} \nabla_{\alpha\dot{\alpha}} \end{array}
\end{aligned}$$

---

<sup>§</sup>We followed the same procedure described in points 1)–4) to integrate by parts the spinorial derivative in (7.1.8) and (7.1.9).

$$\begin{aligned}
& + \begin{array}{c} \frac{1}{\square} W^\alpha \frac{1}{\square} W^\beta \frac{1}{\square} \\ \text{---} \text{---} \text{---} \\ \frac{1}{\square} \overline{W}^{\dot{\alpha}} \frac{1}{\square} \overline{W}^{\dot{\beta}} \nabla_{\beta\dot{\beta}} \frac{1}{\square} \nabla_{\alpha\dot{\alpha}} \\ \frac{1}{\square} \overline{W}^{\dot{\beta}} \nabla_{\beta\dot{\beta}} \frac{1}{\square} W^\alpha \frac{1}{\square} W_\beta \frac{1}{\square} \\ \text{---} \text{---} \text{---} \\ \frac{1}{\square} \overline{W}^{\dot{\alpha}} \frac{1}{\square} \nabla_{\alpha\dot{\alpha}} \end{array} - \begin{array}{c} \frac{1}{\square} W^\alpha \frac{1}{\square} W^\beta \frac{1}{\square} \\ \text{---} \text{---} \text{---} \\ \frac{1}{\square} \overline{W}^{\dot{\beta}} \nabla_{\beta\dot{\beta}} \frac{1}{\square} \overline{W}^{\dot{\alpha}} \frac{1}{\square} \nabla_{\alpha\dot{\alpha}} \\ \text{---} \text{---} \text{---} \\ \frac{1}{\square} \overline{W}^{\dot{\alpha}} \frac{1}{\square} \nabla_{\alpha\dot{\alpha}} \end{array} \\
& + \begin{array}{c} \frac{1}{\square} \overline{W}^{\dot{\alpha}} \frac{1}{\square} \nabla_{\alpha\dot{\alpha}} \\ \text{---} \text{---} \text{---} \\ \frac{1}{\square} \overline{W}^{\dot{\alpha}} \frac{1}{\square} \nabla_{\alpha\dot{\alpha}} \end{array}
\end{aligned} \tag{7.1.16}$$

$$\begin{aligned}
C) \quad & \begin{array}{c} \frac{1}{\square} (\nabla W)^{\alpha\dot{\alpha}\beta} \frac{1}{\square} \overline{W}_{\dot{\alpha}} \frac{1}{\square} \\ \text{---} \text{---} \text{---} \\ \frac{1}{\square} (\nabla W)_{\alpha\beta} \frac{1}{\square} \end{array} = - \begin{array}{c} \frac{1}{\square} W^\alpha \overline{W}^{\dot{\alpha}} \frac{1}{\square} \overline{W}_{\dot{\alpha}} \frac{1}{\square} \\ \text{---} \text{---} \text{---} \\ \frac{1}{\square} W_\alpha \frac{1}{\square} \end{array} + \begin{array}{c} \frac{1}{\square} (\nabla W)^{\alpha\dot{\alpha}\beta} \frac{1}{\square} \overline{W}_{\dot{\alpha}} \frac{1}{\square} \overline{W}^{\dot{\beta}} \nabla_{\beta\dot{\beta}} \frac{1}{\square} \\ \text{---} \text{---} \text{---} \\ \frac{1}{\square} W_\alpha \frac{1}{\square} \end{array} \\
& - \begin{array}{c} \frac{1}{\square} (\nabla W)^{\alpha\dot{\alpha}\beta} \frac{1}{\square} \overline{W}_{\dot{\alpha}} \frac{1}{\square} \\ \text{---} \text{---} \text{---} \\ \frac{1}{\square} W_\beta \frac{1}{\square} \overline{W}^{\dot{\beta}} \nabla_{\alpha\dot{\beta}} \frac{1}{\square} \end{array} - \begin{array}{c} \frac{1}{\square} (\nabla W)^{\alpha\dot{\alpha}\beta} \frac{1}{\square} \overline{W}^{\dot{\beta}} \nabla_{\beta\dot{\beta}} \frac{1}{\square} \overline{W}_{\dot{\alpha}} \frac{1}{\square} \\ \text{---} \text{---} \text{---} \\ \frac{1}{\square} W_\alpha \frac{1}{\square} \end{array}
\end{aligned} \tag{7.1.17}$$

In the results we kept just diagrams that contribute to the  $A(1^+, 2^+, 3^-, 4^-)$  color ordered planar amplitude<sup>¶</sup>.

Thus, all three point covariant terms can be rewritten as combination of four point covariant terms. This result implies that the three point amplitude vanish on-shell<sup>||</sup>. Moreover, together with the result we found for the two point covariant contribution (7.1.11), this analysis of the three point function assures us that connections  $\Gamma$  from the expansion of covariant propagators  $\frac{1}{\square}$  and covariant derivatives  $\nabla_{\alpha\dot{\alpha}}$  play a role just from five points on.

<sup>¶</sup>This means that the two  $\overline{W}$ 's must be consecutive by reading clockwise the diagram

<sup>||</sup>On-shellness is a fundamental ingredient of procedure 1)-4)



### 7.1.3 Four point covariant contributions

Each four point graph is a function of  $W$ 's,  $\overline{W}$ 's, covariant propagators  $\frac{1}{\square}$  and spacetime derivatives  $\nabla_{\alpha\dot{\alpha}}$ . If we are interested in a process that involves at most four particles, the covariant propagators and derivatives can be replaced by ordinary propagators  $\frac{1}{\square_0}$  and derivatives  $\partial_{\alpha\dot{\alpha}}$ .

MHV condition imposes to have two  $W$ 's and two  $\overline{W}$ 's. Supersymmetry invariance and dimensional analysis require the presence of two spacetime derivatives to saturate open spinorial indices. All possible index contractions and relative positions between background fields and spacetime derivatives are acceptable.

In principle, situations with just one spacetime derivative, a chiral  $\nabla_{\alpha}$  and an anti-chiral  $\overline{\nabla}_{\dot{\alpha}}$  covariant derivative applied to a chiral  $W$  and an anti-chiral  $\overline{W}$  field satisfy constraints due to the request of symmetry invariance and mass dimensions. However, any such diagram, by integrating by parts one of the spinorial derivatives, can be transformed into a graph with two spacetime derivatives and no spinorial ones. In eq. (7.1.18) we give an example of this mechanism.

$$\begin{aligned}
 & \nabla^{\alpha\dot{\alpha}} \frac{1}{\square} W^{\beta} \frac{1}{\square} (\nabla_{\alpha} W_{\beta}) \frac{1}{\square} \\
 i & \quad \begin{array}{c} \text{---} \bullet \text{---} \\ \text{---} \text{---} \text{---} \\ \text{---} \bullet \text{---} \end{array} \\
 & \frac{1}{\square} (\overline{\nabla}_{\dot{\alpha}} \overline{W}^{\dot{\beta}}) \frac{1}{\square} \overline{W}_{\dot{\beta}} \frac{1}{\square} \\
 & = - \begin{array}{c} \nabla^{\beta\dot{\alpha}} \frac{1}{\square} W^{\alpha} \frac{1}{\square} W_{\beta} \frac{1}{\square} \\ \text{---} \bullet \text{---} \\ \text{---} \text{---} \text{---} \\ \text{---} \bullet \text{---} \end{array} + \mathcal{O}(W^3 \overline{W}^2) \quad (7.1.18) \\
 & \frac{1}{\square} (\nabla_{\alpha\dot{\alpha}} \overline{W}^{\dot{\beta}}) \frac{1}{\square} \overline{W}_{\dot{\beta}} \frac{1}{\square}
 \end{aligned}$$

Thus, we can assert that any four point diagram contributing to the MHV effective action is function of two  $W$ 's, two  $\overline{W}$ 's and two spacetime derivatives  $\nabla_{\alpha\dot{\alpha}}$ .

Consider now the case of a cubic vertex diagram: Due to the absence of UV divergences, the external fields rearrange along the quantum lines in such a way to reproduce a doublebox or a pentabox topology (see Fig 7.1).

There is just one exception to this rule, i.e. when the two spacetime derivatives can be substituted with a  $\square$  and this cancels a propagator  $\frac{1}{\square}$ . We can distinguish between two cases: 1) When the canceled propagator is the one on the middle line, the cubic vertex diagram is turned into a tadpole-like diagram. Some subtlety due to color factors must be carefully considered (see appendix E); 2) When the canceled propagator is in any other position, the diagram is turned into a trianglebox like diagram. Color structure is not problematic in this case.

In order to reduce the number of sectors in which the four point effective action is partitioned, it is convenient to rewrite tadpoles and triangleboxes as pentabox and doublebox-like diagrams. The key trick consist in inserting  $1 = \frac{1}{\square} \square = \frac{1}{2} \frac{1}{\square} \nabla^{\alpha\dot{\alpha}} \nabla_{\alpha\dot{\alpha}}$  where a propagator is missing (see Fig 7.2).

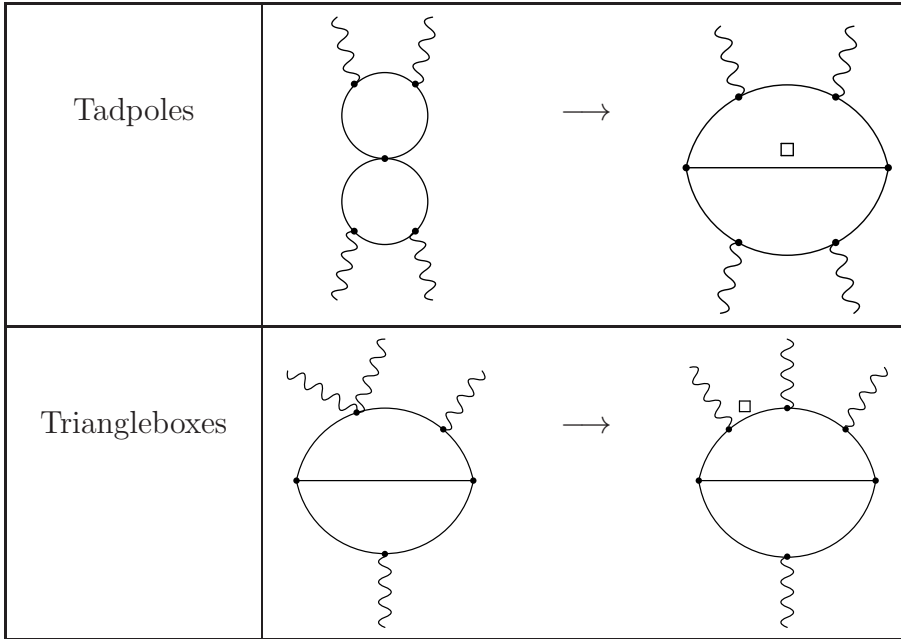


Figure 7.2: Tadpoles and triangleboxes can be written as doubleboxes and pentaboxes

Summarizing, the structure of the terms that contribute at four points includes two  $W$ 's, two  $\bar{W}$ 's and two spacetime derivatives. The topology of each diagram can be traced back to one of the four topologies of Fig 7.1.

The diagrams are produced from three different sources:

- 1) From the two point contribution enhanced to four point (see eq. (7.1.11));
- 2) From the three point contribution enhanced to four point through the integration by parts of spinorial derivatives;
- 3) From the contributions that come out with four  $W$ 's directly from the master equation.

The total number of terms from sectors 1), 2) and 3) includes a few hundreds different diagrams. Their sum constitutes the full expression for the four point effective action.

In Fig 7.3 we give some example of four point effective action diagrams, one for each sector.

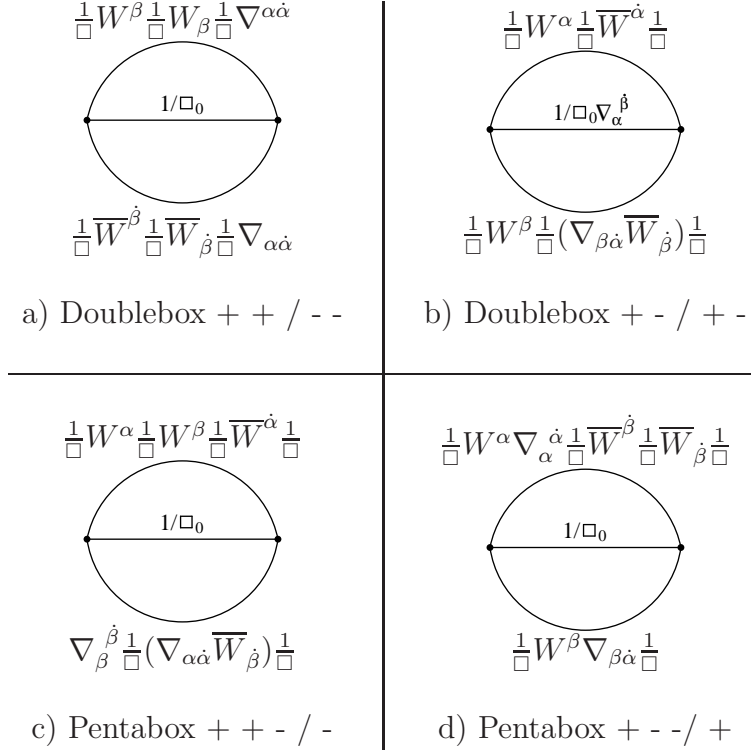


Figure 7.3: Examples of contributions to the four point effective action

## 7.2 The results

After having reshuffled the two, three and four point functions as described in the previous Section, in order to get the final expression for the four point effective action it is worth to move all the diagrams to momentum space. The conventions that we followed while Fourier transforming are given in Appendix G.

A general effective action contribution in momentum space reads

$$\int d^4\theta \frac{d^4 p_1 \cdots d^4 p_4}{(2\pi)^{16}} \delta(\sum (p_i)) (tr(t^a t^b t^c t^d) + tr(t^d t^c t^b t^a))$$

$$\times (W^\alpha(p_1))^a (W^\beta(p_2))^b (\overline{W}^{\dot{\alpha}}(p_3))^c (\overline{W}^{\dot{\beta}}(p_4))^d \times G_{\alpha\beta\dot{\alpha}\dot{\beta}}(p_1, p_2, p_3, p_4) \quad (7.2.1)$$

where the function  $G_{\alpha\beta\dot{\alpha}\dot{\beta}}$  represents the loop integral structure and can be written

$$G_{\alpha\beta\dot{\alpha}\dot{\beta}} \propto \int d^d k d^d \ell \frac{v_{\alpha\dot{\alpha}} w_{\beta\dot{\beta}}}{\text{denominator}} \quad (v, w) = \{p_1, p_2, p_3, p_4, k, \ell\} \quad (7.2.2)$$

The denominator is given by the propagator structure relative to one of the four sectors

of Fig 7.1 in which the effective action is divided. The conventions we follow for the denominators are summarized in Fig G.3. At numerator,  $v$  and  $w$  are the Fourier transform of the two spacetime derivatives present in all the contributions of the four point effective action. They can be loop or external momenta. When one (two) of them is a loop momentum, the loop integral has a vector (tensor) Lorentz structure.

PV reduction (see Appendix H) allows to express vector and tensor integrals as combinations of scalar integrals. In particular PV reduction and on-shell conditions transform the expression (7.2.1) in this way

$$\begin{aligned}
& \int d^4\theta \frac{d^4p_1 \cdots d^4p_4}{(2\pi)^{16}} \delta(\sum(p_i)) (tr(t^a t^b t^c t^d) + tr(t^d t^c t^b t^a)) \\
& \times \left( W^\alpha(p_1) \right)^a \left( W_\alpha(p_2) \right)^b \left( \overline{W}^{\dot{\alpha}}(p_3) \right)^c \left( \overline{W}_{\dot{\alpha}}(p_4) \right)^d \\
& \times \left( a_s G_s(p_1, p_2, p_3, p_4) + \sum_v a_v G_v(p_1, p_2, p_3, p_4) + \sum_t a_t G_t(p_1, p_2, p_3, p_4) \right)
\end{aligned} \tag{7.2.3}$$

Note that this general structure assures that our expressions for the effective action (and consequently for the scattering amplitudes) are real.

The integrals  $G_s$ ,  $G_v$  and  $G_t$  in (7.2.3) have the same denominator structure but differ at numerator. The  $G_s$  integrals have a trivial numerator while the  $G_v$  and  $G_t$  ones exhibit respectively one and two squared loop structure like, for example,  $k^2$  or  $\ell^2(k + p_1)^2$ .

The different mass dimension in these three classes of loop integrals is compensated by the coefficients  $a_s$ ,  $a_v$  and  $a_t$ . This coefficients are rational functions of the Mandelstam variables  $s = (p_1 + p_2)^2$ ,  $t = (p_1 + p_4)^2$  and  $u = (p_1 + p_3)^2$ . Note that  $G_t$  integrals are produced only by contributions with a tensor Lorentz structure,  $G_v$  by vector and tensor structures and  $G_s$  by vector and scalar structures. Moreover we stress that it is only after the PV reduction that the expected helicity structure (7.0.1) emerges.

We are now ready to exhibit the results that we get after Fourier transforming and having done the PV reduction. We divide the results in the two doublebox and the two pentabox sectors. We do not report the explicit denominator structure of these diagrams but only the numerators of the various contributions. The conventions we used for the denominators can be read in Fig G.3. The numerators are expressed as scalar products or, equivalently, as squared of loop and external momenta. We have used a mixed notation in order to try to keep more compact the expressions\*\*.

---

\*\*We remind that in our superspace conventions the relation between the two structures is  $v^{\beta\dot{\beta}} w_{\beta\dot{\beta}} = (v + w)^2 - v^2 - w^2$ .

**Doublebox** ++ / --

$$\text{Doublebox } ++ / -- = - \left( \frac{1}{2}s + \frac{1}{8}(\ell + p_1)^2 + \frac{1}{8}(\ell - p_2)^2 \right) \quad (7.2.4)$$

**Doublebox** +- / +-

$$\begin{aligned} \text{Doublebox } +- / +- &= -\frac{1}{8}t + \frac{1}{8} \left( (k + \ell)^{\beta\dot{\beta}} (p_{14})_{\beta\dot{\beta}} + \frac{t}{s} (k - \ell)^{\beta\dot{\beta}} (p_{12})_{\beta\dot{\beta}} \right) \\ &\quad - \frac{t}{16s} \left( (k)^{\beta\dot{\beta}} (k)_{\beta\dot{\beta}} + (\ell)^{\beta\dot{\beta}} (\ell)_{\beta\dot{\beta}} \right) \\ &\quad + \frac{1}{16s} \left( (k)^{\beta\dot{\beta}} (k)^{\gamma\dot{\gamma}} + (\ell)^{\beta\dot{\beta}} (\ell)^{\gamma\dot{\gamma}} \right) \times \\ &\quad \times \left( (p_1)_{\beta\dot{\beta}} (p_2)_{\gamma\dot{\gamma}} - (p_1)_{\beta\dot{\beta}} (p_3)_{\gamma\dot{\gamma}} + (p_2)_{\beta\dot{\beta}} (p_2)_{\gamma\dot{\gamma}} + (p_2)_{\beta\dot{\beta}} (p_3)_{\gamma\dot{\gamma}} \right) \\ &\quad + \frac{t}{16s^2} \left( (k)^{\beta\dot{\beta}} (k)^{\gamma\dot{\gamma}} + (\ell)^{\beta\dot{\beta}} (\ell)^{\gamma\dot{\gamma}} \right) (p_{12})_{\beta\dot{\beta}} (p_{12})_{\gamma\dot{\gamma}} \\ &\quad + \frac{1}{8} \left( 2 + \frac{t}{s} \right) (k)^{\beta\dot{\beta}} (\ell)_{\beta\dot{\beta}} - \frac{t}{8s^2} (k)^{\beta\dot{\beta}} (p_{12})_{\beta\dot{\beta}} (\ell)^{\gamma\dot{\gamma}} (p_{12})_{\gamma\dot{\gamma}} \\ &\quad + \frac{1}{8s} (k)^{\beta\dot{\beta}} (\ell)^{\gamma\dot{\gamma}} \left( - (p_1)_{\beta\dot{\beta}} (p_2)_{\gamma\dot{\gamma}} - (p_1)_{\beta\dot{\beta}} (p_3)_{\gamma\dot{\gamma}} \right. \\ &\quad \quad \left. - (p_2)_{\beta\dot{\beta}} (p_2)_{\gamma\dot{\gamma}} - 2 (p_2)_{\beta\dot{\beta}} (p_3)_{\gamma\dot{\gamma}} \right. \\ &\quad \quad \left. + 2 (p_3)_{\beta\dot{\beta}} (p_1)_{\gamma\dot{\gamma}} + (p_3)_{\beta\dot{\beta}} (p_2)_{\gamma\dot{\gamma}} \right) \\ &\quad - \frac{1}{4} \left( \ell^2 + (k + p_{14})^2 \right) \end{aligned} \quad (7.2.5)$$

**Pentabox** ++ - / -

$$\begin{aligned} \text{Pentabox } ++ - / - &= -\frac{1}{4} \left( (k)^{\beta\dot{\beta}} (p_1)_{\beta\dot{\beta}} + \frac{t}{s} (k)^{\beta\dot{\beta}} (p_{12})_{\beta\dot{\beta}} \right) \\ &\quad + \frac{1}{4} \left( (\ell)^{\beta\dot{\beta}} (p_1)_{\beta\dot{\beta}} + \frac{t}{s} (\ell)^{\beta\dot{\beta}} (p_{12})_{\beta\dot{\beta}} \right) \\ &\quad + \frac{1}{4} (\ell)^{\beta\dot{\beta}} (\ell)_{\beta\dot{\beta}} - \frac{1}{4} (k)^{\beta\dot{\beta}} (\ell)_{\beta\dot{\beta}} \end{aligned}$$

$$+\frac{1}{4s}(k)^{\beta\dot{\beta}}(\ell)^{\gamma\dot{\gamma}}\left((p_{12})_{\beta\dot{\beta}}(p_3)_{\gamma\dot{\gamma}}-(p_3)_{\beta\dot{\beta}}(p_{12})_{\gamma\dot{\gamma}}\right) \quad (7.2.6)$$

**Pentabox** + - - / +

$$\begin{aligned} \text{Pentabox } + - - / + &= +\frac{1}{4}(k)^{\beta\dot{\beta}}(p_1)_{\beta\dot{\beta}} - \frac{1}{4}(\ell)^{\beta\dot{\beta}}(p_{12})_{\beta\dot{\beta}} \\ &\quad - \frac{1}{4}(\ell)^{\beta\dot{\beta}}(\ell)_{\beta\dot{\beta}} + \frac{1}{4}(k)^{\beta\dot{\beta}}(\ell)_{\beta\dot{\beta}} \\ &\quad + \frac{1}{4s}(k)^{\beta\dot{\beta}}(\ell)^{\gamma\dot{\gamma}}\left((p_1)_{\beta\dot{\beta}}(p_2)_{\gamma\dot{\gamma}} - (p_2)_{\beta\dot{\beta}}(p_1)_{\gamma\dot{\gamma}}\right) \\ &\quad - \frac{1}{4}(\ell - p_2)^2 \end{aligned} \quad (7.2.7)$$

We remember that these expressions are multiplied by

$$\begin{aligned} &\pm \int d^4\theta \frac{d^4p_1 \cdots d^4p_4}{(2\pi)^{16}} \delta(\sum(p_i)) \left( \text{tr}(t^a t^b t^c t^d) + \text{tr}(t^d t^c t^b t^a) \right) \\ &\times \left( W^\alpha(p_1) \right)^a \left( W_\alpha(p_2) \right)^b \left( \overline{W}^{\dot{\alpha}}(p_3) \right)^c \left( \overline{W}_{\dot{\alpha}}(p_4) \right)^d \end{aligned} \quad (7.2.8)$$

where we get the plus sign for the doublebox structures and the minus sign for the pentabox ones. This difference of sign is due to color factors (see Tab E.1).

Although these expressions are a bit scary, it is possible to reduce them. All the integrals involved in the results, in fact, are scalar integrals and they can be thought as functions  $f(s, t)$  of the independent Mandelstam variables. As a consequence, transformations on the external momenta (in particular exchanges of external momenta) that leave the Mandelstam variables unchanged can be used to discover useful identities between the integrals. The relations between the scalar integrals are developed in Appendix H.1.

The identities among scalar integrals make possible to discover a lot of cancellations in the previous results. Dramatic simplifications between the contributions in different sectors occur. In particular the two pentabox sectors (7.2.6) and (7.2.7) can be resummed and produce only one term proportional to the first pentabox. More precisely, the sum of the two pentabox sectors reads

$$-\frac{1}{4}(\ell + p_{14})^2 \times \text{pentabox } ++-/- \quad (7.2.9)$$

where “pentabox ++-/-” represents the denominator structure give by picture C) in Fig G.3.

Amazingly, the contribution (7.2.9) cancels exactly the two squared terms proportional to the first doublebox (see eq. (7.2.4)) once that the relative minus sign (7.2.8) between doubleboxes and pentaboxes is taken into account.

Thus, we are left with an expression for the four point amplitude that is proportional to the two doubleboxes only. Moreover, the part proportional to the first of the two doubleboxes is extremely simple, since it is made by one term only. More precisely, we have

**Doublebox** ++ / --

$$2b \text{ ++ / --} = -\frac{1}{2}s \quad (7.2.10)$$

**Doublebox** +- / +-

$$\begin{aligned} 2b \text{ +- / +-} &= -\frac{1}{2}t \\ &\quad -\frac{1}{4}(k-\ell)^2 \\ &\quad +\frac{t}{8s} \left[ (k-p_2)^2 - (k+p_1)^2 - (k-\ell)^2 \right] \\ &\quad +\frac{1}{4s} \left[ -2(\ell+p_1)^2(k+p_{14})^2 + \ell^2(k+p_{14})^2 + (k-p_2)^2(\ell+p_1)^2 \right. \\ &\quad \quad \left. +k^2(k+p_1)^2 + \ell^2(\ell+p_1)^2 - (k-p_2)^2(k+p_1)^2 - k^2(k+p_{14})^2 \right] \\ &\quad +\frac{t}{8s^2} \left[ ((k+p_1)^2)^2 + ((k-p_2)^2)^2 - 2(k+p_1)^2(k-p_2)^2 \right. \\ &\quad \quad \left. + (k+p_1)^2(\ell-p_2)^2 + (k-p_2)^2(\ell+p_1)^2 - 2(k+p_1)^2(\ell+p_1)^2 \right] \end{aligned} \quad (7.2.11)$$

Written in another way, the sum of expressions (7.2.10) and (7.2.11) gives the following formula for the effective action

The diagram shows a doublebox structure with four external wavy lines representing momenta  $p_1, p_2, p_3, p_4$ . The top-left and top-right lines are labeled  $p_1$  and  $p_2$  respectively, with arrows pointing right. The bottom-left and bottom-right lines are labeled  $p_4$  and  $p_3$  respectively, with arrows pointing left. The internal lines are labeled  $1$  (top) and  $1-k$  (middle), with arrows pointing right. The diagram is multiplied by a factor of  $\left(-\frac{s}{2}\right)$ .

$$\begin{aligned}
& + \begin{array}{c} \text{Diagram 1: A square loop with external momenta } p_1, p_2, p_3, p_4 \text{ and internal momenta } k, l. \end{array} \times \left( -\frac{t}{2} + \frac{t}{8s} (k-p_2)^2 + \frac{1}{4s} (k-p_2)^2 (\ell+p_1)^2 \right. \\
& \qquad \qquad \qquad \left. + \frac{t}{8s^2} ((k-p_2)^2)^2 + \frac{t}{8s^2} (k-p_2)^2 (\ell+p_1)^2 \right) \\
& + \begin{array}{c} \text{Diagram 2: A triangle loop with external momenta } p_1, p_2, p_3 \text{ and internal momenta } k, l. \end{array} \times \left( -\frac{t}{8s} - \frac{1}{4s} (k-p_2)^2 + \frac{t}{8s^2} (k+p_1)^2 - \frac{t}{4s^2} ((k-p_2)^2 + (\ell+p_1)^2) \right) \\
& + \begin{array}{c} \text{Diagram 3: A triangle loop with external momenta } p_1, p_2, p_3 \text{ and internal momenta } k, l. \end{array} \times \left( -\frac{1}{2s} (\ell+p_1)^2 + \frac{1}{4s} (k-p_2)^2 \right) \\
& + \begin{array}{c} \text{Diagram 4: A box loop with external momenta } p_1, p_2, p_3, p_4 \text{ and internal momenta } k, l. \end{array} \times \left( -\frac{1}{4} - \frac{t}{8s} \right) \\
& + \begin{array}{c} \text{Diagram 5: A triangle loop with external momenta } p_1, p_2, p_3 \text{ and internal momenta } k, l. \end{array} \times \left( \frac{1}{4s} \right) \\
& + \begin{array}{c} \text{Diagram 6: A triangle loop with external momenta } p_1, p_2, p_3 \text{ and internal momenta } k, l. \end{array} \times \left( \frac{t}{8s^2} \right) \\
& + \begin{array}{c} \text{Diagram 7: A box loop with external momenta } p_1, p_2, p_3, p_4 \text{ and internal momenta } k, l. \end{array} \times \left( \frac{1}{4s} \right) \\
& + \begin{array}{c} \text{Diagram 8: A box loop with external momenta } p_1, p_2, p_3, p_4 \text{ and internal momenta } k, l. \end{array} \times \left( -\frac{1}{4s} \right) \tag{7.2.12}
\end{aligned}$$

This expression gets multiplied by (7.2.8). To obtain from there the color ordered amplitude  $A(1^+, 2^+, 3^-, 4^-)$  we have to drop the  $p_i$  integrals, sum over the permutations of the momenta  $p_i$  (this involves also to interchange the internal symmetry indices) and keep terms proportional to the color trace structure  $tr(t^a t^b t^c t^d)$  only. This turns out to be equivalent to sum the results (7.2.12) over the cyclic permutations of the external momenta, i.e. to add to these two equations the same expressions with  $s \leftrightarrow t$ .

A few comments about this expression for the four point effective action are necessary.

- When we extract from (7.2.12) the formula for the four point scattering amplitude we cannot reproduce in a straightforward way the results derived with the cutting techniques (see eq. (4.2.8) and [85]). In particular, when we compare the two results we see that equation (7.2.10) plus the first line of eq. (7.2.11) give exactly the result (4.2.8) computed with the indirect techniques.



Nevertheless we have a lot of extra contributions in (7.2.11). All these contributions share the general feature to have a non-trivial numerator. It is not to exclude the possibility that these integrals actually cancel. In general, it is true that each two loop four point scalar integral can be reduced to a linear combination of a set of scalar master integrals. Thus it could be the case that the extra pieces in (7.2.11) cancel once that they are rewritten in terms of the master integrals.

- Is our result wrong? We could transform this question in two different questions:
  - 1) Is it possible that we have done a mistake somewhere in the calculation?
  - 2) Which kind of properties should a result exhibit in order to be trustable?

The answer to the first question is that, of course, the length of the computation makes a computational mistake possible. However, this mistake should have very special features.

In fact, if it affects the  $\nabla$ -algebra procedure it should not touch the cancellation of the UV divergent terms. If it affects the power expansion of the coefficients of the propagators it should do it in such a way that all the general relations among the coefficients are respected. It could be a problem of the PC programs we wrote but we made a lot of checks on each single part of them. Moreover we managed to perform the calculation by following different procedures with respect to the best way sketched in Fig J.1 of Appendix J but always we got the same answer here above described.

More in general, this mistake should be a big mistake, since the number of extra terms in our results is large, but, on the other hand it cannot be so big, otherwise the nice cancellations that occur between the two pentabox sectors and the nice result (7.2.10) proportional to the first doublebox would be inexplicable.

Moreover, it should affect mainly the second doublebox sector. Under this point of view, it is worth to mention that the derivation of the master equation for the effective action is blind with respect to the various sectors that contribute at four points. In general, in fact, a diagram of the master equation produces contributions to more than one sector of the four point function. The same can be said for the elaboration of the two point and three point covariant contributions described in the Section 7.1. Thus it is very unlikely that the mistake is in these parts of the computations, although they are the most tricky ones.

About the second question, there are two features that make a result trustable: The infrared divergences and the analysis of the cuts in the  $s$  and the  $t$  channels. In particular, the combination of the extra contributions of eq. (7.2.11) should be IR free and its cut in the  $s$  and the  $t$  channels should be zero.

The analysis of the IR divergences requires or the knowledge of the analytic form of each of the extra integrals of (7.2.11) or, alternatively, a numerical evaluation of them<sup>††</sup>. This second road is preferred since it allows quicker checks. Unfortunately

---

<sup>††</sup>Public programs like FIESTA [124] are very useful in order to get this goal

the analysis is complicated by the fact that the extra integrals in (7.2.11) present both IR and UV divergences and it is not guaranteed that a numerical evaluation can distinguish between them.

Thus we expect that easier checks would come from the analysis of the cuts in the  $s$  and the  $t$  channel. This is work in progress.

- Are the cutting techniques wrong? If the extra integrals do not cancel, no mistakes are present in our calculation and we are able to show that our results has the correct behaviours at the IR poles and at the cuts, this should be the logical answer that we would be left with.

From this point of view, it is important to note that the extra terms in our results present integrals with triangles and bubbles. These are produced when the numerators in (7.2.11) cancel one or two of the propagators in the same loop at denominator. Moreover, there are other integral structures with numerators that do not cancel any of the propagators. This structures are assumed to be absent or are even not considered by the cutting techniques. They are these ansatzs of the indirect techniques that should be eventually reconsidered more carefully.

Summarizing, although our results in (7.2.12) for the two loop four point MHV effective action look strange, they are the end of a procedure that presents strong internal checks at various stages of the computation. However, these internal checks cannot be completely exhaustive about the validity of our results and more general checks are required. The results of these extra checks could open various scenarios about what we know (or we suppose to know up to know) about MHV amplitudes in  $\mathcal{N} = 4$  SYM theory.

# Chapter 8

## Conclusions

In the second part of this thesis we have studied the problem of scattering amplitudes in YM theories. The great interest in these objects is due both to phenomenological reasons and to remarkable properties of MHV color ordered amplitudes that recently emerged in the context of  $\mathcal{N} = 4$  SYM theory through the *AdS/CFT* correspondence.

At weak coupling, what we know about the quantum corrections to the amplitudes are the results of computations performed using indirect computational methods, primarily the cutting techniques. The validity of these techniques is based on assumptions that arbitrarily extend to any perturbative order and to any number of interacting particles regularities in the MHV amplitudes observed at the first loops and for only a few scattered particles.

In order to give more insights into the validity of indirect techniques and to the properties that they display, in the second part of the thesis we have developed a direct, assumption-free computational method based on a Feynman diagrammatic approach in superspace.

Our method makes available the complete effective action at a fixed loop order in any SYM theory. From there, the scattering amplitudes follow by composing trees of vertexes and propagators given by the 1PI Green functions.

The strategy we have described along the thesis makes use of background field method in superspace. The computation of the effective action follows from the identification of a set of vacuum diagrams in superspace. The propagators of these diagrams are background covariant propagators and represent the propagation of quantum fields and their interactions with the external background fields. Thus, the effective action is implicitly built in the vacuum propagators in an extremely compact way.

The  $\nabla$ -algebra procedure and a suitable expansion of the propagators in power of spinorial derivatives allow to extract from the vacuum diagrams the complete effective

action. This expression turns out to be a linear combination of Feynman diagrams depending on the expansion coefficients of the covariant propagators.

The coefficients are functions of the external fields and can be expanded in power series with respect to them. However, as long as it is possible to deal with the coefficients before they are expanded, our expressions for the effective action are completely independent of the number of interacting particles. The explicit expression for a specific  $n$ -point effective action is extracted from the all- $n$  formulas by expanding the coefficients only in a second time.

Along the computation a special role is played by a lot of relations satisfied by the coefficients. Their origin can be traced back to the basic algebraic identities satisfied by the covariant superspace derivatives. Thus, they enjoy the same generality of the basic superspace relations. The relations between the coefficients help in simplifying the all- $n$  expressions and furnish non trivial consistency checks in various steps of the computation.

We have firstly applied the computational strategy here summarized to compute the two loop all- $n$  MHV effective action in  $\mathcal{N} = 4$  SYM theory. With respect to the general strategy, computations in  $\mathcal{N} = 4$  SYM theory requires an extra constraint that must be satisfied. This theory, in fact, is UV finite. Thus, the cancellation of the UV divergences in the results becomes a key check of the consistency all our computational apparatus.

Indeed, a careful analysis of the divergent contributions show that they can be re-summed into finite terms. The relations between the propagator coefficients display all their usefulness while getting this result.

Thus, the main result of the second part of the thesis is the following: We have given a formula for the two-loop MHV effective action of the  $\mathcal{N} = 4$  SYM theory that is manifestly UV finite and valid for any number of interacting particles. From this formula it is in principle possible to extract any two loop MHV scattering amplitude.

As an immediate application of our techniques we extrapolated the four point effective action. It turns out that only 1PI diagrams contribute at four points. Moreover all the contribution has a well defined structure involving the field strengths and of the spacetime derivatives whose origins can be traced back to supersymmetry, Lorentz invariance and on-shell conditions.

After moving to momentum space and performing the Passarino-Veltman reduction, all the contributions to the effective action present the same helicity structure that can be factorized out. What we are left with is a linear combination of scalar integrals. Four different topological sectors can be recognized. Two of them are doubleboxes and two are pentaboxes.

Non-trivial cancellations can be worked out between the two pentabox sectors and one of the doublebox sectors. At the end of these cancellations the result we get is a half of what is necessary to reproduce the formula for the color ordered amplitude

computed through the indirect techniques. The other half we need can be found in the other doublebox sector. However, other extra contributions occur in this sector. The interpretation of the extra terms is still an open problem and requires extra checks that are in progress.



## Chapter 9

# Acknowledgments

Chi è arrivato a leggere dall'introduzione fino a qui si ricordi che . . .

*"Io conosco un pianeta su cui c'è un signor Chermisi.*

*Non ha mai respirato un fiore. Non ha mai guardato una stella.*

*Non ha mai voluto bene a nessuno. Non fa altro che addizioni.*

*E tutto il giorno ripete come te: "Io sono un uomo serio! Io sono un uomo serio!"  
e si gonfia di orgoglio. Ma non è un uomo, è un fungo!"*

Non tutti, però, sono funghi . . .

My first thought is due to my supervisor S. Penati and my collaborators M. T. Grisaru and M. Pirrone. My hope is that they could appreciate my acquaintance as much as I appreciated theirs.

A great thank goes to my Ph.D. mates – and former student–mates – A. Amariti, S. Alioli and E. Re for a friendship that started in the physics but that soon went beyond it.

Last but not least, ehi . . . mamma, papà, Franci e zio (e zia Rosalimpia . . .), I know that if it was for you I could even not mention you here, but you see . . . somewhere sometime something . . . and I think that this is the place, the time and the kind of things that gives you that joy that you like.

*"Gli uomini non hanno più tempo per conoscere nulla.  
Comprano dai mercanti le cose già fatte.  
Ma siccome non esistono mercanti di amici,  
gli uomini non hanno più amici.  
Se tu vuoi un amico, addomesticami!"*

Addomesticare un Ratto? Ebbene, succedono anche di queste cose . . .

Nell'antica mitologia greca il destino di un'uomo era deciso dal filare, tessere e recidere il filo della vita da parte delle tre Moire. Si dice che queste donne avessero un occhio solo che si palleggiavano l'un l'altra di volta in volta per vedere il presente ed il futuro.

Nella mia vita di studente che in queste pagine si conclude posso anche io rintracciare tre donne che, palleggiandomi fra loro come l'occhio delle Moire nel mito, hanno contribuito in modo determinante a ciò che ora sono. La mia maestra Nuccia ha filato ciò che poi Elena si è trovata a svolgere e dipanare. Infine, Silvia, ora tocca a te decidere di tagliare il filo.

C'è però un'altra persona che devo e dovrò sempre tener presente nelle mie attività future. Non è però cosa difficile ricordare un uomo che in sé raccoglie tutto quello che un giovane dovrebbe sapere di ciò che lo ha preceduto e che ha creato il mondo in cui oggi ci troviamo. Sono estremamente felice di averti conosciuto, Marc, e non credo che una semplice frase nei ringraziamenti di una tesi (nè una torta di compleanno spedita agli antipodi) possa esprimere tutta la mia riconoscenza nei tuoi confronti.

Passiamo agli amici e qualcuno lo dimenticherò di sicuro. Non vogliatmene: scrivo di fretta e con la mente stanca la pagina numero xxx di troppo di questo malloppone. E poi, non mi piaceva leggere i cataloghi delle navi, figuriamoci se mi piace scriverli! Quindi, se qualcuno non trova di sé qui mentre legge, prego il suo cuore di scovare ciò che i suoi occhi cercano e non vedono. Perché mai nulla è come appare ma bisogna sempre porsi in ascolto e cercare. E solo il cuore sa sentire e ascoltare per davvero. A buon intenditor . . .

Un pensiero a chi ha condiviso con me l'incontenibile senso di fratellanza che nasce sulla cima di un 4000. Simo, Vir e soprattutto tu Ema. Vero è che abbiamo condiviso negli anni molto più che la sola montagna ma la libertà ho trovato insieme a voi in quei luoghi è un sentimento indescrivibile, che *intender non può chi no lo prova*.

Stando in ambito universitario: Anto! Marco! "terroni" amici di un purosangue brianzolo come me! Incredibile ma vero! Lo stesso si può dire dei bergamaschi Andrea, Giacomo e Paolo, della brianzola di passaporto Elisa, della buona Ceci e del quasi milanese Fede, del vero milanese Marco, della comasca Silvia e dello yankee Sean. Per non parlare poi degli amici stranieri Elisa (accento sulla a, prego!), Stephane e Sophie: spero tanto per loro che non vengano mai più attaccati sul far del tramonto da un branco di capre piemontesi! Ma possibile che non ci siano altri purosangue brianzoli? Beh, puri puri forse no, di certo però Giordano, Luca e Pietro hanno respirato aria buona a lungo. Ed anche Tommaso ora è in una provincia dal buon nome.



I brianzoli, però non mi sono di certo mancati, perchè nelle lunghe serate di sfogo tirando una palla in un cesto, era con gente della mia terra che il più delle volte ci si confrontava. Questo sin dai tempi delle giovanili di Arosio con Marco Pozzi e Rosso; poi su fino ai campionati senior mai vinti con la Verano di Teo, Gerry, Vale, Michi, Galbia, Diego "Raul" e Mambro (ehi, ragazzo: grazie per venerdì!); per finire, la Nibionno di tanti bravi ragazzi, un grande allenatore, ed ottimi amici vecchi (vero Buch?) e meno vecchi (BumBum Kappe, tu meno vecchio? Ebbene sì!) il cui sguardo corre, bellissimo, a cercare la propria bambina sugli spalti appena la palla si insacca da dietro l'arco. Che dire . . . abbiamo condiviso più di un bel gioco e chissà che la cosa non continui un giorno.

Ecco . . . ho fatto anche io il mio catalogo, mannaggia a me!

Pensieri particolari ora per chi ha più o meno consapevolmente contribuito ad un buon epilogo della storia qui sopra raccontata. Caty e Madda (e Albino!) avete avuto tanto tanto buon cuore verso di me e mi avete sempre dato tante iniezioni di fiducia. Fil . . . , a te sono toccati i miei momenti più duri . . . non so perchè ma per mia fortuna sono capitati quando c'eri anche tu. Diana . . . in genepy veritas . . . soprattutto se bevuto sul far del giorno. Ci siamo capiti e di altro non c'è bisogno. Caro Guarna, ricordati sempre che non conta chi scrive tesi di dottorato ma in che modo uno affronta le proprie sfide ed io non ne conosco che le affrontano con la tua energia. Chiudo il cerchio dei pensieri tornando molto vicino al punto di partenza: Marta, tu sei una persona che definire speciale è toglierle qualcosa. Spero che quando sarà il tuo turno di scrivere la pagina dei ringraziamenti della tesi di dottorato, vorrai ricordarti di me anche se non so, a oggi, dirti se mi sarà possibile essere presente come tu sei stata.

È tempo di terminare.

*Gli uomini coltivano 5000 rose nello stesso giardino . . .  
e non trovano quello che cercano . . .  
e tuttavia quello che cercano potrebbe essere trovato in una sola rosa,  
rossa, nera o di qualsiasi colore.  
Ma gli occhi sono ciechi: bisogna cercare col cuore.  
Così finisce il tempo del mio dottorato in fisica.*



# Appendix A

## Basic conventions for Superspace

In this appendix we report the most basilar conventions for superspace we used.

- 1) Spinorial derivatives of Grassmann variables

$$\begin{aligned} \partial_\alpha \theta^\beta &= \delta_\alpha^\beta & \partial^\alpha \theta_\beta &= -\delta_\alpha^\beta \\ \partial_\alpha \theta_\beta &= +c_{\alpha\beta} & \partial^\alpha \theta^\beta &= +c^{\alpha\beta} \end{aligned} \quad (\text{A.0.1})$$

- 2) Ricci tensor contractions

$$\begin{aligned} c_{\alpha\beta} c^{\gamma\delta} &= \delta_\alpha^\gamma \delta_\beta^\delta - \delta_\beta^\gamma \delta_\alpha^\delta \\ c^{\alpha\beta} c_{\alpha\beta} &= 2 & c^{\alpha\beta} c_{\beta\alpha} &= -2 \end{aligned} \quad (\text{A.0.2})$$

Written in matrix form

$$\begin{pmatrix} 0 & -i \\ i & 0 \end{pmatrix} \quad (\text{A.0.3})$$

- 3) Hermitian conjugation

$$(\psi^\alpha)^\dagger = \bar{\psi}^{\dot{\alpha}} \quad (\psi_\alpha)^\dagger = -\bar{\psi}_{\dot{\alpha}} \quad (\text{A.0.4})$$

Notice that on derivatives this means

$$\left( \overrightarrow{\partial}_\alpha \right)^\dagger = -\overleftarrow{\partial}_{\dot{\alpha}} = +\overrightarrow{\partial}_{\dot{\alpha}} \quad (\text{A.0.5})$$

For the Ricci tensor it holds

$$(c_{\alpha\beta})^\dagger = c_{\dot{\alpha}\dot{\beta}} \quad (\text{A.0.6})$$

From equations (A.0.1), (A.0.5), (A.0.6) we get

$$\begin{aligned} \bar{\partial}_{\dot{\alpha}} \bar{\theta}^{\dot{\beta}} &= \delta_{\dot{\alpha}}^{\dot{\beta}} & \bar{\partial}^{\dot{\alpha}} \bar{\theta}_{\dot{\beta}} &= -\delta_{\dot{\alpha}}^{\dot{\beta}} \\ \bar{\partial}_{\dot{\alpha}} \bar{\theta}_{\dot{\beta}} &= +c_{\dot{\alpha}\dot{\beta}} & \bar{\partial}^{\dot{\alpha}} \bar{\theta}^{\dot{\beta}} &= +c^{\dot{\alpha}\dot{\beta}} \end{aligned} \quad (\text{A.0.7})$$

4) Products of Grassmann variables

$$\begin{aligned}\theta^\alpha \theta^\beta &= \theta^2 c^{\beta\alpha} & \bar{\theta}^{\dot{\alpha}} \bar{\theta}^{\dot{\beta}} &= \bar{\theta}^2 c^{\dot{\beta}\dot{\alpha}} \\ \partial_\alpha \theta^2 &= \theta_\alpha & \bar{\partial}_{\dot{\alpha}} \bar{\theta}^2 &= \bar{\theta}_{\dot{\alpha}}\end{aligned}\tag{A.0.8}$$

5) Spacetime derivative

$$i\partial_{\alpha\dot{\alpha}} = p_{\alpha\dot{\alpha}} = \lambda_\alpha \bar{\lambda}_{\dot{\alpha}}\tag{A.0.9}$$

6) Superspace covariant derivatives

$$\begin{aligned}D_\alpha &= \partial_\alpha + \frac{i}{2} \bar{\theta}^{\dot{\alpha}} \partial_{\alpha\dot{\alpha}} \\ \bar{D}_{\dot{\alpha}} &= \bar{\partial}_{\dot{\alpha}} + \frac{i}{2} \theta^\alpha \partial_{\alpha\dot{\alpha}}\end{aligned}\tag{A.0.10}$$

It holds that

$$\{D_\alpha, \bar{D}_{\dot{\alpha}}\} = i\partial_{\alpha\dot{\alpha}}\tag{A.0.11}$$

7) Field strengths

$$\begin{aligned}W_\alpha &= i\bar{D}^2 (e^{-V} D_\alpha e^V) \\ \bar{W}_{\dot{\alpha}} &= iD^2 (e^V \bar{D}_{\dot{\alpha}} e^{-V})\end{aligned}\tag{A.0.12}$$

Linearizing

$$\begin{aligned}W_\alpha &= i\bar{D}^2 D_\alpha V \\ \bar{W}_{\dot{\alpha}} &= iD^2 \bar{D}_{\dot{\alpha}} V\end{aligned}\tag{A.0.13}$$

8) Covariant derivatives

In a non-abelian field theory and in real representation the covariant derivatives are defined as

$$\begin{aligned}\nabla_\alpha &= e^{-\frac{V}{2}} D_\alpha e^{\frac{V}{2}} & \bar{\nabla}_{\dot{\alpha}} &= e^{\frac{V}{2}} \bar{D}_{\dot{\alpha}} e^{-\frac{V}{2}} \\ \nabla_{\alpha\dot{\alpha}} &= -i \{ \nabla_\alpha, \bar{\nabla}_{\dot{\alpha}} \}\end{aligned}\tag{A.0.14}$$

If we write the covariant derivatives in terms of the connections  $\Gamma_\alpha$

$$\begin{aligned}\nabla_\alpha &= D_\alpha - i\Gamma_\alpha & \bar{\nabla}_{\dot{\alpha}} &= \bar{D}_{\dot{\alpha}} - i\bar{\Gamma}_{\dot{\alpha}} \\ \nabla_{\alpha\dot{\alpha}} &= \partial_{\alpha\dot{\alpha}} - i\Gamma_{\alpha\dot{\alpha}}\end{aligned}\tag{A.0.15}$$

we find that, in full generality,

$$\Gamma_{\alpha\dot{\alpha}} = -i (\bar{D}_{\dot{\alpha}} \Gamma_\alpha) - i (D_\alpha \bar{\Gamma}_{\dot{\alpha}}) - \{ \Gamma_\alpha, \bar{\Gamma}_{\dot{\alpha}} \}\tag{A.0.16}$$

At linear order in the vector field  $V$ , from the definitions (A.0.14), we write

$$\Gamma_\alpha = \frac{i}{2} (D_\alpha V) \quad \bar{\Gamma}_{\dot{\alpha}} = -\frac{i}{2} (\bar{D}_{\dot{\alpha}} V)\tag{A.0.17}$$

From (A.0.16) and (A.0.17), it follows

$$\Gamma_{\alpha\dot{\alpha}} = \frac{1}{2} ([\bar{D}_{\dot{\alpha}}, D_\alpha] V)\tag{A.0.18}$$

# Appendix B

## On-shell $\nabla$ -algebra

In this Appendix we give the (anti)commutation algebra for covariant derivatives and several on-shell identities which have been used in the course of two-loop  $\nabla$ -algebra.

The basic commutators for full and background covariant derivatives are

$$\begin{aligned}
\{\nabla_\alpha, \bar{\nabla}_{\dot{\alpha}}\} &= i\nabla_{\alpha\dot{\alpha}} \\
[\nabla_\alpha, \nabla_{\beta\dot{\beta}}] &= C_{\alpha\beta}\bar{W}_{\dot{\beta}} \quad , \quad [\bar{\nabla}_{\dot{\alpha}}, \nabla_{\beta\dot{\beta}}] = C_{\dot{\alpha}\dot{\beta}}W_\beta \\
[\nabla_\alpha, \bar{\nabla}^2] &= i\nabla_\alpha^{\dot{\alpha}}\bar{\nabla}_{\dot{\alpha}} + iW_\alpha \quad , \quad [\bar{\nabla}_{\dot{\alpha}}, \nabla^2] = i\nabla_{\dot{\alpha}}^\alpha\nabla_\alpha + i\bar{W}_{\dot{\alpha}} \\
[\nabla^2, \nabla_{\alpha\dot{\alpha}}] &= -\bar{W}_{\dot{\alpha}}\nabla_\alpha \quad , \quad [\bar{\nabla}^2, \nabla_{\alpha\dot{\alpha}}] = -W_\alpha\bar{\nabla}_{\dot{\alpha}}
\end{aligned} \tag{B.0.1}$$

$$\begin{aligned}
[\nabla_{\alpha\dot{\alpha}}, \nabla_{\beta\dot{\beta}}] &= -ic_{\alpha\beta}(\bar{\nabla}_{\dot{\alpha}}\bar{W}_{\dot{\beta}}) - ic_{\dot{\alpha}\dot{\beta}}(\nabla_\alpha W_\beta) \\
\nabla_\alpha^{\dot{\beta}}\nabla_{\beta\dot{\beta}} &= -\frac{i}{2}c_{\alpha\beta}(\bar{\nabla}^{\dot{\beta}}\bar{W}_{\dot{\beta}}) + i(\nabla_\alpha W_\beta) + c_{\beta\alpha}\square \\
\nabla_{\dot{\alpha}}^\beta\nabla_{\beta\dot{\beta}} &= -\frac{i}{2}c_{\dot{\alpha}\dot{\beta}}(\nabla^\beta W_\beta) + i(\bar{\nabla}_{\dot{\alpha}}\bar{W}_{\dot{\beta}}) + c_{\dot{\beta}\dot{\alpha}}\square \\
[\nabla_\alpha, \square] &= \bar{W}^{\dot{\alpha}}\nabla_{\alpha\dot{\alpha}} - \frac{1}{2}(\nabla_\alpha^{\dot{\alpha}}\bar{W}_{\dot{\alpha}})
\end{aligned} \tag{B.0.2}$$

$$\begin{aligned}
[\nabla^2, \bar{\nabla}^2] &= i\nabla^{\alpha\dot{\alpha}}\bar{\nabla}_{\dot{\alpha}}\nabla_\alpha + iW^\alpha\nabla_\alpha - i\bar{W}^{\dot{\alpha}}\bar{\nabla}_{\dot{\alpha}} + \square \\
&= -i\nabla^{\alpha\dot{\alpha}}\nabla_\alpha\bar{\nabla}_{\dot{\alpha}} + iW^\alpha\nabla_\alpha - i\bar{W}^{\dot{\alpha}}\bar{\nabla}_{\dot{\alpha}} - \square
\end{aligned} \tag{B.0.3}$$

Background covariant propagators are given by  $\frac{1}{\square_\pm}$  and  $\frac{1}{\hat{\square}}$  where

$$\begin{aligned}
\square_+ &= \square - iW^\alpha\nabla_\alpha - \frac{i}{2}(\nabla^\alpha W_\alpha) & \square &= \frac{1}{2}\nabla^{\alpha\dot{\alpha}}\nabla_{\alpha\dot{\alpha}} \\
\square_- &= \square - i\bar{W}^{\dot{\alpha}}\bar{\nabla}_{\dot{\alpha}} - \frac{i}{2}(\bar{\nabla}^{\dot{\alpha}}\bar{W}_{\dot{\alpha}}) \\
\hat{\square} &= \square - iW^\alpha\nabla_\alpha - i\bar{W}^{\dot{\alpha}}\bar{\nabla}_{\dot{\alpha}}
\end{aligned} \tag{B.0.4}$$

As a consequence of the previous (anti)commutation relations they satisfy

$$\bar{\nabla}^2 \nabla^2 \bar{\nabla}^2 = \square_+ \bar{\nabla}^2 \quad , \quad \nabla^2 \bar{\nabla}^2 \nabla^2 = \square_- \nabla^2 \quad (\text{B.0.5})$$

$$[\bar{\nabla}_{\dot{\alpha}}, \frac{1}{\square_+}] = 0 \quad , \quad [\nabla_{\alpha}, \frac{1}{\square_-}] = 0 \quad (\text{B.0.6})$$

$$\nabla^2 \bar{\nabla}^2 \frac{1}{\square_+} = \frac{1}{\square_-} \nabla^2 \bar{\nabla}^2 \quad , \quad \bar{\nabla}^2 \nabla^2 \frac{1}{\square_-} = \frac{1}{\square_+} \bar{\nabla}^2 \nabla^2 \quad (\text{B.0.7})$$

When computing scattering amplitudes we work with *on-shell* background fields, that is fields satisfying

$$\nabla^{\alpha} W_{\alpha} = 0 \quad \nabla^2 W_{\alpha} = 0 \quad \nabla^{\alpha\dot{\alpha}} W_{\alpha} = 0 \quad \nabla_{\alpha} W_{\beta} = \nabla_{\beta} W_{\alpha} \quad (\text{B.0.8})$$

plus the corresponding barred equations for  $\bar{W}_{\dot{\alpha}}$ . Under these assumptions the covariant propagators take the simplified form

$$\begin{aligned} \frac{1}{\square_+} &= \frac{1}{\square_- - iW^{\alpha}\nabla_{\alpha}} \quad , \quad \frac{1}{\square_-} = \frac{1}{\square_- - i\bar{W}^{\dot{\alpha}}\bar{\nabla}_{\dot{\alpha}}} \\ \frac{1}{\hat{\square}} &= \frac{1}{\square_+ - i\bar{W}^{\dot{\alpha}}\bar{\nabla}_{\dot{\alpha}}} = \frac{1}{\square_- - iW^{\alpha}\nabla_{\alpha}} \end{aligned} \quad (\text{B.0.9})$$

and satisfy the on-shell identity

$$\nabla^2 \frac{1}{\hat{\square}} = \frac{1}{\hat{\square}} \nabla^2 = \frac{1}{\square_-} \nabla^2 \quad , \quad \bar{\nabla}^2 \frac{1}{\hat{\square}} = \frac{1}{\hat{\square}} \bar{\nabla}^2 = \frac{1}{\square_+} \bar{\nabla}^2 \quad (\text{B.0.10})$$

Further on-shell identities involving the propagators are

$$\left[ \nabla_{\alpha}, \frac{1}{\square} \right] = -\frac{1}{\square} \bar{W}^{\dot{\alpha}} \nabla_{\alpha\dot{\alpha}} \frac{1}{\square} \quad (\text{B.0.11})$$

$$\left[ \bar{\nabla}_{\dot{\alpha}}, \frac{1}{\square} \right] = -\frac{1}{\square} W^{\alpha} \nabla_{\alpha\dot{\alpha}} \frac{1}{\square} \quad (\text{B.0.12})$$

$$\left[ \nabla_{\alpha\dot{\alpha}}, \frac{1}{\square} \right] = i\frac{1}{\square} \left( (\nabla_{\alpha} W^{\beta}) \nabla_{\beta\dot{\alpha}} + (\bar{\nabla}_{\dot{\alpha}} \bar{W}^{\beta}) \nabla_{\alpha\beta} + \{W_{\alpha}, \bar{W}_{\dot{\alpha}}\} \right) \frac{1}{\square} \quad (\text{B.0.13})$$

$$\left[ \nabla_{\alpha}, \frac{1}{\square_+} \right] = -\frac{1}{\square_+} \bar{W}^{\dot{\alpha}} \nabla_{\alpha\dot{\alpha}} \frac{1}{\square_+} + i\frac{1}{\square_+} (\nabla_{\alpha} W^{\beta}) \nabla_{\beta} \frac{1}{\square_+} \quad (\text{B.0.14})$$

$$\left[ \bar{\nabla}_{\dot{\alpha}}, \frac{1}{\square_-} \right] = -\frac{1}{\square_-} W^{\alpha} \nabla_{\alpha\dot{\alpha}} \frac{1}{\square_-} + i\frac{1}{\square_-} (\bar{\nabla}_{\dot{\alpha}} \bar{W}^{\beta}) \bar{\nabla}_{\beta} \frac{1}{\square_-} \quad (\text{B.0.15})$$

$$\left[ \nabla^2, \frac{1}{\square_+} \right] = \frac{1}{\square_+} \bar{W}^{\dot{\alpha}} \nabla_{\alpha\dot{\alpha}} \nabla^{\alpha} \frac{1}{\square_+} - \frac{1}{\square_+} \bar{W}^{\dot{\alpha}} \bar{W}_{\dot{\alpha}} \frac{1}{\square_+} \quad (\text{B.0.16})$$

$$\left[ \bar{\nabla}^2, \frac{1}{\square_-} \right] = \frac{1}{\square_-} W^{\alpha} \nabla_{\alpha\dot{\alpha}} \bar{\nabla}^{\dot{\alpha}} \frac{1}{\square_-} - \frac{1}{\square_-} W^{\alpha} W_{\alpha} \frac{1}{\square_-} \quad (\text{B.0.17})$$

$$\left[ \nabla_{\alpha}, \frac{1}{\hat{\square}} \right] = \frac{1}{\hat{\square}} (i\nabla_{\alpha} W^{\beta}) \nabla_{\beta} \frac{1}{\hat{\square}} \quad (\text{B.0.18})$$

$$\left[ \bar{\nabla}_{\dot{\alpha}}, \frac{1}{\hat{\square}} \right] = \frac{1}{\hat{\square}} (i\bar{\nabla}_{\dot{\alpha}} \bar{W}^{\beta}) \bar{\nabla}_{\beta} \frac{1}{\hat{\square}} \quad (\text{B.0.19})$$

# Appendix C

## Expansion of the covariant (anti)chiral propagators and their derivatives

We now compute the coefficients in the expansion of the on-shell (anti)chiral propagators  $1/\square_{\pm}$  as defined in eq. (B.0.9). We provide expressions suitable for computing MHV amplitudes up to six external particles.

As explained in the text, since we are interested in the evaluation of  $(- - + \dots +)$  amplitudes, when computing the coefficients we keep only terms with at most two  $\overline{W}$ 's. Moreover, if two  $\overline{W}$ 's are present we keep only terms where they are close to each other or, as it is clear from the cyclicity of the trace, where they appear at the two extremes of the string of fields. As an immediate consequence, we can take advantage of important identities which simplify dramatically the calculation. For instance, setting the external fields on-shell and up to terms with two  $\overline{W}$ 's separated by a string of  $W$ 's, the following identities hold

$$\begin{aligned}
 & (\text{any string with at least one } W) \times \left( \overline{W}^{\dot{\alpha}} \overline{W}_{\dot{\alpha}} - \overline{W}^{\dot{\alpha}} \nabla_{\dot{\alpha}}^{\alpha} \frac{1}{\square} \overline{W}^{\dot{\beta}} \nabla_{\alpha \dot{\beta}} \right) = 0 \\
 & (\text{any string with at least one } \overline{W}) \times \left( W^{\alpha} W_{\alpha} - W^{\alpha} \nabla_{\alpha}^{\dot{\alpha}} \frac{1}{\square} W^{\beta} \nabla_{\beta \dot{\alpha}} \right) = 0 \\
 & (\text{any string with at least one } W) \times \left\{ \nabla_{\alpha}, \frac{1}{\square} \overline{W}^{\dot{\beta}} \nabla_{\beta \dot{\beta}} \frac{1}{\square} \right\} = 0 \\
 & (\text{any string with at least one } \overline{W}) \times \left\{ \overline{\nabla}_{\dot{\alpha}}, \frac{1}{\square} W^{\beta} \nabla_{\beta \dot{\beta}} \frac{1}{\square} \right\} = 0 \tag{C.0.1}
 \end{aligned}$$

The expansion of the on-shell chiral propagator can be done recursively. Starting from the explicit expression for  $\square_{+}$  in eq. (B.0.9) we can write the following chain of identities

$$\frac{1}{\square_{+}} = \frac{1}{\square} + \frac{1}{\square} i W^{\alpha} \nabla_{\alpha} \frac{1}{\square_{+}}$$

$$= \frac{1}{\square} + \frac{1}{\square} i W^\alpha \nabla_\alpha \frac{1}{\square} + \frac{1}{\square} i W^\alpha \nabla_\alpha \frac{1}{\square} i W^\beta \nabla_\beta \frac{1}{\square} + \dots \quad (\text{C.0.2})$$

In each term we use the on-shell (anti)commutators listed in Appendix B for bringing all the spinorial derivatives at the very right. Defining

$$\frac{1}{\square_+} = A + B^\alpha \nabla_\alpha + C \nabla^2 \quad (\text{C.0.3})$$

we then find

$$\begin{aligned} A = & \left[ \frac{1}{\square} - i \frac{1}{\square} W^\alpha \frac{1}{\square} \overline{W}^{\dot{\alpha}} \nabla_{\alpha \dot{\alpha}} \frac{1}{\square} + \frac{1}{\square} W^\alpha \frac{1}{\square} (\nabla_\alpha W^\beta) \frac{1}{\square} \overline{W}^{\dot{\beta}} \nabla_{\beta \dot{\beta}} \frac{1}{\square} \right. \\ & + i \frac{1}{\square} W^\alpha \frac{1}{\square} (\nabla_\alpha W^\beta) \frac{1}{\square} (\nabla_\beta W^\gamma) \frac{1}{\square} \overline{W}^{\dot{\gamma}} \nabla_{\gamma \dot{\gamma}} \frac{1}{\square} \\ & \left. - \frac{1}{\square} W^\alpha \frac{1}{\square} (\nabla_\alpha W^\beta) \frac{1}{\square} (\nabla_\beta W^\gamma) \frac{1}{\square} (\nabla_\gamma W^\delta) \frac{1}{\square} \overline{W}^{\dot{\delta}} \nabla_{\delta \dot{\delta}} \frac{1}{\square} \right] \end{aligned} \quad (\text{C.0.4})$$

$$\begin{aligned} B^\alpha = & \left[ i \frac{1}{\square} W^\alpha \frac{1}{\square} - \frac{1}{\square} W^\beta \frac{1}{\square} (\nabla_\beta W^\alpha) \frac{1}{\square} - \frac{1}{\square} W^\beta \frac{1}{\square} W_\beta \frac{1}{\square} \overline{W}^{\dot{\alpha}} \nabla_{\dot{\alpha}} \frac{1}{\square} \right. \\ & - i \frac{1}{\square} W^\beta \frac{1}{\square} (\nabla_\beta W^\gamma) \frac{1}{\square} (\nabla_\gamma W^\alpha) \frac{1}{\square} - i \frac{1}{\square} W^\beta \frac{1}{\square} (\nabla_\beta W^\gamma) \frac{1}{\square} W_\gamma \frac{1}{\square} \overline{W}^{\dot{\alpha}} \nabla_{\dot{\alpha}} \frac{1}{\square} \\ & + \frac{1}{\square} W^\beta \frac{1}{\square} (\nabla_\beta W^\gamma) \frac{1}{\square} (\nabla_\gamma W^\delta) \frac{1}{\square} (\nabla_\delta W^\alpha) \frac{1}{\square} \\ & \left. + \frac{1}{\square} W^\beta \frac{1}{\square} (\nabla_\beta W^\gamma) \frac{1}{\square} (\nabla_\gamma W^\delta) \frac{1}{\square} W_\delta \frac{1}{\square} \overline{W}^{\dot{\alpha}} \nabla_{\dot{\alpha}} \frac{1}{\square} \right. \\ & + \frac{1}{\square} W^\beta \frac{1}{\square} \overline{W}^{\dot{\beta}} \nabla_{\beta \dot{\beta}} \frac{1}{\square} W^\alpha \frac{1}{\square} \\ & - i \frac{1}{\square} W^\beta \frac{1}{\square} W_\beta \frac{1}{\square} \overline{W}^{\dot{\gamma}} \nabla_{\dot{\gamma}} \frac{1}{\square} (\nabla_\gamma W^\alpha) \frac{1}{\square} + i \frac{1}{\square} W^\beta \frac{1}{\square} (\nabla_\beta W^\gamma) \frac{1}{\square} \overline{W}^{\dot{\gamma}} \nabla_{\dot{\gamma}} \frac{1}{\square} W^\alpha \frac{1}{\square} \\ & + i \frac{1}{\square} W^\beta \frac{1}{\square} \overline{W}^{\dot{\beta}} \nabla_{\beta \dot{\beta}} \frac{1}{\square} W^\gamma \frac{1}{\square} (\nabla_\gamma W^\alpha) \frac{1}{\square} \\ & + \frac{1}{\square} W^\beta \frac{1}{\square} W_\beta \frac{1}{\square} \overline{W}^{\dot{\gamma}} \nabla_{\dot{\gamma}} \frac{1}{\square} (\nabla_\gamma W^\delta) \frac{1}{\square} (\nabla_\delta W^\alpha) \frac{1}{\square} \\ & - \frac{1}{\square} W^\beta \frac{1}{\square} \overline{W}^{\dot{\beta}} \nabla_{\beta \dot{\beta}} \frac{1}{\square} W^\gamma \frac{1}{\square} (\nabla_\gamma W^\delta) \frac{1}{\square} (\nabla_\delta W^\alpha) \frac{1}{\square} \\ & + \frac{1}{\square} W^\beta \frac{1}{\square} (\nabla_\beta W^\gamma) \frac{1}{\square} W_\gamma \frac{1}{\square} \overline{W}^{\dot{\delta}} \nabla_{\dot{\delta}} \frac{1}{\square} (\nabla_\delta W^\alpha) \frac{1}{\square} \\ & - \frac{1}{\square} W^\beta \frac{1}{\square} (\nabla_\beta W^\gamma) \frac{1}{\square} \overline{W}^{\dot{\gamma}} \nabla_{\dot{\gamma}} \frac{1}{\square} W^\delta \frac{1}{\square} (\nabla_\delta W^\alpha) \frac{1}{\square} \\ & \left. - \frac{1}{\square} W^\beta \frac{1}{\square} (\nabla_\beta W^\gamma) \frac{1}{\square} (\nabla_\gamma W^\delta) \frac{1}{\square} \overline{W}^{\dot{\delta}} \nabla_{\delta \dot{\delta}} \frac{1}{\square} W^\alpha \frac{1}{\square} \right] \end{aligned} \quad (\text{C.0.5})$$



$$\begin{aligned}
C = & \left[ \frac{1}{\square} W^\alpha \frac{1}{\square} W_\alpha \frac{1}{\square} + i \frac{1}{\square} W^\alpha \frac{1}{\square} (\nabla_\alpha W^\beta) \frac{1}{\square} W_\beta \frac{1}{\square} \right. & (C.0.6) \\
& \left. - \frac{1}{\square} W^\alpha \frac{1}{\square} (\nabla_\alpha W^\beta) \frac{1}{\square} (\nabla_\beta W^\gamma) \frac{1}{\square} W_\gamma \frac{1}{\square} \right. \\
& + i \frac{1}{\square} W^\alpha \frac{1}{\square} W_\alpha \frac{1}{\square} \overline{W}^{\dot{\beta}} \nabla_{\dot{\beta}}^\beta \frac{1}{\square} W_\beta \frac{1}{\square} - i \frac{1}{\square} W^\alpha \frac{1}{\square} \overline{W}^{\dot{\alpha}} \nabla_{\alpha\dot{\alpha}} \frac{1}{\square} W^\beta \frac{1}{\square} W_\beta \frac{1}{\square} \\
& - \frac{1}{\square} W^\alpha \frac{1}{\square} W_\alpha \frac{1}{\square} \overline{W}^{\dot{\beta}} \nabla_{\dot{\beta}}^\beta \frac{1}{\square} (\nabla_\beta W^\gamma) \frac{1}{\square} W_\gamma \frac{1}{\square} \\
& + \frac{1}{\square} W^\alpha \frac{1}{\square} \overline{W}^{\dot{\alpha}} \nabla_{\alpha\dot{\alpha}} \frac{1}{\square} W^\beta \frac{1}{\square} (\nabla_\beta W^\gamma) \frac{1}{\square} W_\gamma \frac{1}{\square} \\
& + \frac{1}{\square} W^\alpha \frac{1}{\square} (\nabla_\alpha W^\beta) \frac{1}{\square} \overline{W}^{\dot{\beta}} \nabla_{\beta\dot{\beta}} \frac{1}{\square} W_\gamma \frac{1}{\square} W_\gamma \frac{1}{\square} \\
& \left. - \frac{1}{\square} W^\alpha \frac{1}{\square} (\nabla_\alpha W^\beta) \frac{1}{\square} W_\beta \frac{1}{\square} \overline{W}^{\dot{\gamma}} \nabla_{\dot{\gamma}}^\gamma \frac{1}{\square} W_\gamma \frac{1}{\square} \right]
\end{aligned}$$

We stopped the expansions at the 5th order in the external fields so that in principle we are able to compute amplitudes up to six points.

For the anti-chiral propagator  $1/\square_-$  we proceed in the same manner. We find

$$\frac{1}{\square_-} = \bar{A} + \bar{B}^{\dot{\alpha}} \bar{\nabla}_{\dot{\alpha}} + \bar{C} \bar{\nabla}^2 \quad (C.0.7)$$

where

$$\bar{A} = \left[ \frac{1}{\square} - i \frac{1}{\square} \overline{W}^{\dot{\alpha}} \frac{1}{\square} W^\alpha \nabla_{\alpha\dot{\alpha}} \frac{1}{\square} + \frac{1}{\square} \overline{W}^{\dot{\alpha}} \frac{1}{\square} (\nabla_{\dot{\alpha}} \overline{W}^{\dot{\beta}}) \frac{1}{\square} W^\beta \nabla_{\beta\dot{\beta}} \frac{1}{\square} \right] \quad (C.0.8)$$

$$\bar{B}^{\dot{\alpha}} = \left[ i \frac{1}{\square} \overline{W}^{\dot{\alpha}} \frac{1}{\square} - \frac{1}{\square} \overline{W}^{\dot{\beta}} \frac{1}{\square} (\nabla_{\dot{\beta}} \overline{W}^{\dot{\alpha}}) \frac{1}{\square} - \frac{1}{\square} \overline{W}^{\dot{\beta}} \frac{1}{\square} \overline{W}_{\dot{\beta}} \frac{1}{\square} W^\alpha \nabla_{\alpha\dot{\alpha}} \frac{1}{\square} \right. \quad (C.0.9)$$

$$\left. + \frac{1}{\square} \overline{W}^{\dot{\beta}} \frac{1}{\square} W^\beta \nabla_{\beta\dot{\beta}} \frac{1}{\square} \overline{W}^{\dot{\alpha}} \frac{1}{\square} \right]$$

$$\bar{C} = \frac{1}{\square} \overline{W}^{\dot{\alpha}} \frac{1}{\square} \overline{W}_{\dot{\alpha}} \frac{1}{\square} \quad (C.0.10)$$

The reduced number of terms in  $\bar{A}, \bar{B}, \bar{C}$  compared to  $A, B, C$  is due to the MHV selection rule which requires the presence of no more than two  $\overline{W}$ 's.

The coefficients that we have determined are not all independent, but satisfy general identities which arise from the algebra of covariant derivatives. We list such identities and their origin since they are crucial for canceling UV divergences in the  $\mathcal{N} = 4$  SYM case.

Starting from the the first identity in eq. (B.0.5) rewritten as

$$\frac{1}{\square_+} \nabla^2 \nabla^2 \bar{\nabla}^2 = \bar{\nabla}^2 \quad (\text{C.0.11})$$

and expanding  $\frac{1}{\square_+}$  in terms of its coefficients, we find

$$A\square + C\bar{W}^{\dot{\alpha}}\bar{W}_{\dot{\alpha}} - B^\alpha \nabla_\alpha^{\dot{\alpha}} \bar{W}_{\dot{\alpha}} = 1 \quad (\text{C.0.12})$$

$$B^\alpha iW_\alpha + C\square = 0 \quad (\text{C.0.13})$$

$$B_\alpha \square - iB^\beta (\nabla_\beta W_\alpha) - AiW_\alpha + C\bar{W}^{\dot{\alpha}} \nabla_{\alpha\dot{\alpha}} = 0 \quad (\text{C.0.14})$$

Analogously, using the second identity in (B.0.5) we obtain

$$\bar{A}\square + \bar{C}W^\alpha W_\alpha - \bar{B}^{\dot{\alpha}} \nabla_{\dot{\alpha}}^\alpha W_\alpha = 1 \quad (\text{C.0.15})$$

$$\bar{B}^{\dot{\alpha}} i\bar{W}_{\dot{\alpha}} + \bar{C}\square = 0 \quad (\text{C.0.16})$$

$$\bar{B}_{\dot{\alpha}} \square - i\bar{B}^{\dot{\beta}} (\bar{\nabla}_{\dot{\beta}} \bar{W}_{\dot{\alpha}}) - \bar{A}i\bar{W}_{\dot{\alpha}} + \bar{C}W^\alpha \nabla_{\alpha\dot{\alpha}} = 0 \quad (\text{C.0.17})$$

Further relations can be worked out from the identities in eq. (B.0.6). Inserting there the expansions for  $1/\square_\pm$  we obtain

$$[\bar{\nabla}_{\dot{\alpha}}, A] - B^\alpha i\nabla_{\alpha\dot{\alpha}} + Ci\bar{W}_{\dot{\alpha}} = 0 \quad (\text{C.0.18})$$

$$\{\bar{\nabla}_{\dot{\alpha}}, B^\alpha\} + Ci\nabla_{\dot{\alpha}}^\alpha = 0 \quad (\text{C.0.19})$$

$$[\bar{\nabla}_{\dot{\alpha}}, C] = 0 \quad (\text{C.0.20})$$

and

$$[\nabla_\alpha, \bar{A}] - \bar{B}^{\dot{\alpha}} i\nabla_{\alpha\dot{\alpha}} + \bar{C}iW_\alpha = 0 \quad (\text{C.0.21})$$

$$\{\nabla_\alpha, \bar{B}^{\dot{\alpha}}\} + \bar{C}i\nabla_{\dot{\alpha}}^\alpha = 0 \quad (\text{C.0.22})$$

$$[\nabla_\alpha, \bar{C}] = 0 \quad (\text{C.0.23})$$

Finally, inserting the expansions of  $\frac{1}{\square_\pm}$  in eq. (B.0.7) we find

$$A = \bar{A} - \{\bar{\nabla}_{\dot{\alpha}}, \bar{B}_{\dot{\alpha}}\} + \frac{1}{2}\{\bar{\nabla}_{\dot{\alpha}}, [\bar{\nabla}_{\dot{\alpha}}, \bar{C}]\} \quad (\text{C.0.24})$$

$$B^\alpha i\nabla_{\alpha\dot{\alpha}} - Ci\bar{W}_{\dot{\alpha}} = [\bar{\nabla}_{\dot{\alpha}}, \bar{A}] + \frac{1}{2}[\bar{\nabla}_{\dot{\alpha}}^{\dot{\beta}}, \{\bar{\nabla}_{\dot{\beta}}, \bar{B}_{\dot{\alpha}}\}] \quad (\text{C.0.25})$$

$$B^\alpha iW_\alpha + C\square = \frac{1}{2}\{\bar{\nabla}_{\dot{\alpha}}, [\bar{\nabla}_{\dot{\alpha}}, \bar{A}]\} \quad (\text{C.0.26})$$

From the previous identities we also find

$$\{\bar{\nabla}_{\dot{\alpha}}, [\bar{\nabla}_{\dot{\alpha}}, A]\} = \{\nabla_\alpha, [\nabla_\alpha, \bar{A}]\} = 0 \quad (\text{C.0.27})$$

In the process of doing  $\nabla$ -algebra we find convenient to write also the following expansions

$$\begin{aligned}\nabla_\alpha \frac{1}{\square_+} &= \mathcal{A}_\alpha + \mathcal{B}_\alpha^\beta \nabla_\beta + \mathcal{C}_\alpha \nabla^2 \\ \bar{\nabla}_{\dot{\alpha}} \frac{1}{\square_-} &= \bar{\mathcal{A}}_{\dot{\alpha}} + \bar{\mathcal{B}}_{\dot{\alpha}}^{\dot{\beta}} \bar{\nabla}_{\dot{\beta}} + \bar{\mathcal{C}}_{\dot{\alpha}} \bar{\nabla}^2\end{aligned}\tag{C.0.28}$$

where the new coefficients are given in terms of the original ones by

$$\mathcal{A}_\alpha = [\nabla_\alpha, A] \tag{C.0.29}$$

$$\mathcal{B}_\alpha^\beta = \{\nabla_\alpha, B^\beta\} + A \delta_\alpha^\beta \equiv \mathcal{P}_\alpha^\beta + A \delta_\alpha^\beta \tag{C.0.30}$$

$$\mathcal{C}_\alpha = [\nabla_\alpha, C] - B_\alpha \tag{C.0.31}$$

and

$$\bar{\mathcal{A}}_{\dot{\alpha}} = [\bar{\nabla}_{\dot{\alpha}}, \bar{A}] \tag{C.0.32}$$

$$\bar{\mathcal{B}}_{\dot{\alpha}}^{\dot{\beta}} = \{\bar{\nabla}_{\dot{\alpha}}, \bar{B}^{\dot{\beta}}\} + \bar{A} \delta_{\dot{\alpha}}^{\dot{\beta}} \equiv \bar{\mathcal{P}}_{\dot{\alpha}}^{\dot{\beta}} + \bar{A} \delta_{\dot{\alpha}}^{\dot{\beta}} \tag{C.0.33}$$

$$\bar{\mathcal{C}}_{\dot{\alpha}} = [\bar{\nabla}_{\dot{\alpha}}, \bar{C}] - \bar{B}_{\dot{\alpha}} \tag{C.0.34}$$

Using (C.0.34), the identity (C.0.24) can be rewritten as

$$A - \bar{A} = \frac{1}{2} \{\bar{\nabla}^{\dot{\alpha}}, \bar{\mathcal{C}}_{\dot{\alpha}} - \bar{B}_{\dot{\alpha}}\} \tag{C.0.35}$$

The expansion of the coefficients as given above is suitable for performing  $\nabla$ -algebra. However, they are given in terms of the covariant  $\frac{1}{\square}$  propagator which is a function of the background bosonic connection  $\Gamma_{\alpha\dot{\alpha}}$ .

In order to compute an  $n$  point correlator, that is the  $n$ -derivative of the effective action respect to the background fields, we need also extract the background dependence from  $\frac{1}{\square}$ . Recalling that

$$\square = \frac{1}{2} \nabla^{\alpha\dot{\alpha}} \nabla_{\alpha\dot{\alpha}} \tag{C.0.36}$$

and using equation (A.0.15) we find

$$\begin{aligned}\frac{1}{\square} &= \frac{1}{\square_0} + \frac{1}{\square_0} \Gamma^{\alpha\dot{\alpha}} i \partial_{\alpha\dot{\alpha}} \frac{1}{\square_0} + \frac{1}{2} \frac{1}{\square_0} (i \partial^{\alpha\dot{\alpha}} \Gamma_{\alpha\dot{\alpha}}) \frac{1}{\square_0} \\ &\quad + \frac{1}{2} \frac{1}{\square_0} \Gamma^{\alpha\dot{\alpha}} \Gamma_{\alpha\dot{\alpha}} \frac{1}{\square_0} + \frac{1}{\square_0} \Gamma^{\alpha\dot{\alpha}} i \partial_{\alpha\dot{\alpha}} \frac{1}{\square_0} \Gamma^{\beta\dot{\beta}} i \partial_{\beta\dot{\beta}} \frac{1}{\square_0} + \dots\end{aligned}\tag{C.0.37}$$

This expression was used in (6.3.39) where the cancellation of UV divergences of tadpoles is concerned.



# Appendix D

## Expansion of the covariant vector propagator and its derivatives

In order to expand the vector propagator, it is first of all convenient to write the on-shell  $\hat{\square}$  in terms of  $\square_+$  or  $\square_-$ , as in eq. (B.0.9). It follows that we can write two different expansions

$$\begin{aligned} \frac{1}{\hat{\square}} &= \frac{1}{\square_+ - i\bar{W}^{\dot{\alpha}}\bar{\nabla}_{\dot{\alpha}}} & (D.0.1) \\ &= A + B^{\alpha}\nabla_{\alpha} + C\nabla^2 + \bar{D}^{\dot{\alpha}}\bar{\nabla}_{\dot{\alpha}} + E^{\alpha\dot{\alpha}}\nabla_{\alpha}\bar{\nabla}_{\dot{\alpha}} + \bar{F}^{\dot{\alpha}}\nabla^2\bar{\nabla}_{\dot{\alpha}} + \bar{G}\bar{\nabla}^2 + H^{\alpha}\nabla_{\alpha}\bar{\nabla}^2 + L\nabla^2\bar{\nabla}^2 \end{aligned}$$

or

$$\begin{aligned} \frac{1}{\hat{\square}} &= \frac{1}{\square_- - iW^{\alpha}\nabla_{\alpha}} & (D.0.2) \\ &= \bar{A} + \bar{B}^{\dot{\alpha}}\bar{\nabla}_{\dot{\alpha}} + \bar{C}\bar{\nabla}^2 + D^{\alpha}\nabla_{\alpha} + \bar{E}^{\alpha\dot{\alpha}}\bar{\nabla}_{\dot{\alpha}}\nabla_{\alpha} + F^{\alpha}\bar{\nabla}^2\nabla_{\alpha} + G\nabla^2 + \bar{H}^{\dot{\alpha}}\bar{\nabla}_{\dot{\alpha}}\nabla^2 + \bar{L}\bar{\nabla}^2\nabla^2 \end{aligned}$$

where  $A, B, C$  and  $\bar{A}, \bar{B}, \bar{C}$  are the coefficients appearing in the expansion of the (anti)chiral propagators.

When doing  $\nabla$ -algebra we use indifferently (D.0.1) or (D.0.2) according to what is more convenient for the particular diagram under investigation.

Identifying the two expressions for  $\frac{1}{\hat{\square}}$  we find the following set of identities

$$C = G \qquad \bar{C} = \bar{G} \qquad (D.0.3)$$

$$H^{\alpha} = F^{\alpha} \qquad \bar{F}^{\dot{\alpha}} = \bar{H}^{\dot{\alpha}} \qquad (D.0.4)$$

$$L = \bar{L} \qquad (D.0.5)$$

$$A = \bar{A} + \bar{E}^{\alpha\dot{\alpha}} i\nabla_{\alpha\dot{\alpha}} - F^{\alpha} iW_{\alpha} + \bar{F}^{\dot{\alpha}} i\bar{W}_{\dot{\alpha}} + L \square \qquad (D.0.6)$$

$$B^\alpha = D^\alpha + \bar{F}^{\dot{\alpha}} i\nabla_{\dot{\alpha}}^\alpha - L iW^\alpha \quad ; \quad \bar{B}^{\dot{\alpha}} = \bar{D}^{\dot{\alpha}} + F^\alpha i\nabla_\alpha^{\dot{\alpha}} - L i\bar{W}^{\dot{\alpha}} \quad (\text{D.0.7})$$

$$E^{\alpha\dot{\alpha}} = -\bar{E}^{\alpha\dot{\alpha}} + L i\nabla^{\alpha\dot{\alpha}} \quad (\text{D.0.8})$$

$$L\Box + F^\alpha iW_\alpha + \bar{F}^{\dot{\alpha}} i\bar{W}_{\dot{\alpha}} = 0 \quad (\text{D.0.9})$$

which allow to express the coefficients in (D.0.2) in terms of the ones in (D.0.1). It is then sufficient to list the explicit expression for the coefficients in (D.0.1).

As in the (anti)chiral case, the expansion of the vector propagator can be done recursively according to

$$\begin{aligned} \frac{1}{\hat{\Box}} &= \frac{1}{\Box_+} + \frac{1}{\Box_+} i\bar{W}^{\dot{\alpha}} \nabla_{\dot{\alpha}} \frac{1}{\hat{\Box}} \\ &= \frac{1}{\Box_+} + \frac{1}{\Box_+} i\bar{W}^{\dot{\alpha}} \nabla_{\dot{\alpha}} \frac{1}{\Box_+} + \frac{1}{\Box_+} i\bar{W}^{\dot{\alpha}} \nabla_{\dot{\alpha}} \frac{1}{\Box_+} i\bar{W}^{\dot{\beta}} \nabla_{\dot{\beta}} \frac{1}{\Box_+} + \dots \end{aligned} \quad (\text{D.0.10})$$

Applying the MHV selection rule, setting the external fields on-shell and stopping the expansion at the correct order for computing amplitudes up to six external particles, we find

$$\begin{aligned} \bar{D}^{\dot{\alpha}} &= \left[ iA\bar{W}^{\dot{\alpha}} \frac{1}{\Box} - \frac{1}{\Box} \bar{W}^{\dot{\beta}} \frac{1}{\Box} (\nabla_{\dot{\beta}} \bar{W}^{\dot{\alpha}}) \frac{1}{\Box} + iB^{\alpha} \bar{W}^{\dot{\alpha}} \frac{1}{\Box} \bar{W}^{\dot{\beta}} \nabla_{\alpha\dot{\beta}} \frac{1}{\Box} \right. \\ &\quad \left. + iB^{\beta} \bar{W}^{\dot{\beta}} \frac{1}{\Box} (\nabla_{\beta\dot{\beta}} \bar{W}^{\dot{\alpha}}) \frac{1}{\Box} - i \frac{1}{\Box} \bar{W}^{\dot{\beta}} B^{\alpha} (\nabla_{\alpha\dot{\beta}} \bar{W}^{\dot{\alpha}}) \frac{1}{\Box} \right] \end{aligned} \quad (\text{D.0.11})$$

$$\begin{aligned} E^{\alpha\dot{\alpha}} &= \left[ iA\bar{W}^{\dot{\alpha}} B^{\alpha} - iB^{\alpha} \bar{W}^{\dot{\alpha}} \frac{1}{\Box} \right. \\ &\quad + B^{\beta} \bar{W}^{\dot{\alpha}} \frac{1}{\Box} (\nabla_{\beta} W^{\alpha}) \frac{1}{\Box} + B^{\alpha} \bar{W}^{\dot{\beta}} \frac{1}{\Box} (\nabla_{\dot{\beta}} \bar{W}^{\dot{\alpha}}) \frac{1}{\Box} \\ &\quad - \frac{1}{\Box} \bar{W}^{\dot{\beta}} B^{\alpha} (\nabla_{\dot{\beta}} \bar{W}^{\dot{\alpha}}) \frac{1}{\Box} - \frac{1}{\Box} \bar{W}^{\dot{\beta}} \frac{1}{\Box} (\nabla_{\dot{\beta}} \bar{W}^{\dot{\alpha}}) B^{\alpha} \\ &\quad + iB^{\beta} \bar{W}^{\dot{\alpha}} \frac{1}{\Box} (\nabla_{\beta} W^{\gamma}) \frac{1}{\Box} (\nabla_{\gamma} W^{\alpha}) \frac{1}{\Box} + iB^{\beta} \bar{W}^{\dot{\beta}} \frac{1}{\Box} (\nabla_{\dot{\beta}} \bar{W}^{\dot{\alpha}}) \frac{1}{\Box} (\nabla_{\beta} W^{\alpha}) \frac{1}{\Box} \\ &\quad + iB^{\beta} \bar{W}^{\dot{\alpha}} \frac{1}{\Box} \bar{W}^{\dot{\beta}} \nabla_{\beta\dot{\beta}} B^{\alpha} + iB^{\beta} \bar{W}^{\dot{\beta}} \frac{1}{\Box} (\nabla_{\beta\dot{\beta}} \bar{W}^{\dot{\alpha}}) B^{\alpha} - i \frac{1}{\Box} \bar{W}^{\dot{\beta}} C (\nabla_{\dot{\beta}}^{\alpha} \bar{W}^{\dot{\alpha}}) \frac{1}{\Box} \\ &\quad - iC \bar{W}^{\dot{\alpha}} \frac{1}{\Box} \bar{W}^{\dot{\beta}} \nabla_{\dot{\beta}}^{\alpha} \frac{1}{\Box} - iC \bar{W}^{\dot{\beta}} \frac{1}{\Box} (\nabla_{\dot{\beta}}^{\alpha} \bar{W}^{\dot{\alpha}}) \frac{1}{\Box} \\ &\quad - B^{\beta} W b^{\dot{\alpha}} \frac{1}{\Box} (\nabla_{\beta} W^{\gamma}) \frac{1}{\Box} (\nabla_{\gamma} W^{\delta}) \frac{1}{\Box} (\nabla_d W^{\alpha}) \frac{1}{\Box} \\ &\quad - B^{\beta} \bar{W}^{\dot{\beta}} \frac{1}{\Box} (\nabla_{\dot{\beta}} \bar{W}^{\dot{\alpha}}) \frac{1}{\Box} (\nabla_{\beta} W^{\gamma}) \frac{1}{\Box} (\nabla_g W^{\alpha}) \frac{1}{\Box} \\ &\quad \left. + C \bar{W}^{\dot{\alpha}} \frac{1}{\Box} \bar{W}^{\dot{\beta}} \nabla_{\dot{\beta}}^{\alpha} \frac{1}{\Box} (\nabla_{\beta} W^{\alpha}) \frac{1}{\Box} + C \bar{W}^{\dot{\beta}} \frac{1}{\Box} (\nabla_{\dot{\beta}}^{\alpha} W^{\dot{\alpha}}) \frac{1}{\Box} (\nabla_{\beta} W^{\alpha}) \frac{1}{\Box} \right] \end{aligned} \quad (\text{D.0.12})$$

$$\begin{aligned}
& - iB^\beta \bar{W}^{\dot{\beta}} \frac{1}{\square} (\bar{\nabla}_{\dot{\beta}} \bar{W}^{\dot{\alpha}}) \frac{1}{\square} (\nabla_\beta W^\gamma) \frac{1}{\square} (\nabla_\gamma W^\delta) \frac{1}{\square} (\nabla_\delta W^\alpha) \frac{1}{\square} \\
& + iC \bar{W}^{\dot{\beta}} \frac{1}{\square} (\nabla_\beta \bar{W}^{\dot{\alpha}}) \frac{1}{\square} (\nabla_\beta W^\gamma) \frac{1}{\square} (\nabla_\gamma W^\alpha) \frac{1}{\square} \\
& + iC \bar{W}^{\dot{\alpha}} \frac{1}{\square} \bar{W}^{\dot{\beta}} \nabla_{\dot{\beta}} \frac{1}{\square} (\nabla_\beta W^\gamma) \frac{1}{\square} (\nabla_\gamma W^\alpha) \frac{1}{\square} ]
\end{aligned}$$

$$\bar{F}^{\dot{\alpha}} = \left[ iB^\alpha \bar{W}^{\dot{\alpha}} B_\alpha + iC \bar{W}^{\dot{\alpha}} \frac{1}{\square} + iA \bar{W}^{\dot{\alpha}} C \right. \tag{D.0.13}$$

$$\begin{aligned}
& - B^\alpha \bar{W}^{\dot{\alpha}} \frac{1}{\square} (\nabla_\alpha W^\beta) B_\beta - B^\alpha \bar{W}^{\dot{\beta}} \frac{1}{\square} (\bar{\nabla}_{\dot{\beta}} \bar{W}^{\dot{\alpha}}) B_\alpha - B^\alpha \bar{W}^{\dot{\alpha}} B^\beta (\nabla_\alpha W_\beta) \frac{1}{\square} \\
& - C \bar{W}^{\dot{\beta}} \frac{1}{\square} (\bar{\nabla}_{\dot{\beta}} \bar{W}^{\dot{\alpha}}) \frac{1}{\square} - \frac{1}{\square} \bar{W}^{\dot{\beta}} C (\bar{\nabla}_{\dot{\beta}} \bar{W}^{\dot{\alpha}}) \frac{1}{\square} - \frac{1}{\square} \bar{W}^{\dot{\beta}} \frac{1}{\square} (\bar{\nabla}_{\dot{\beta}} \bar{W}^{\dot{\alpha}}) C \\
& - iB^\alpha \bar{W}^{\dot{\alpha}} \frac{1}{\square} (\nabla_\alpha W^\beta) \frac{1}{\square} (\nabla_\beta W^\gamma) B_\gamma + iB^\alpha \bar{W}^{\dot{\alpha}} \frac{1}{\square} (\nabla_\alpha W^\beta) B^\gamma (\nabla_\beta W_\gamma) \frac{1}{\square} \\
& - iB^\alpha \bar{W}^{\dot{\beta}} \frac{1}{\square} (\bar{\nabla}_{\dot{\beta}} \bar{W}^{\dot{\alpha}}) \frac{1}{\square} (\nabla_\alpha W^\beta) B_\beta + iB^\alpha \bar{W}^{\dot{\beta}} \frac{1}{\square} (\bar{\nabla}_{\dot{\beta}} \bar{W}^{\dot{\alpha}}) B^\beta (\nabla_\alpha W_\beta) \frac{1}{\square} \\
& + iB^\alpha \bar{W}^{\dot{\alpha}} \frac{1}{\square} \bar{W}^{\dot{\beta}} \nabla_{\alpha\dot{\beta}} C + iC \bar{W}^{\dot{\alpha}} \frac{1}{\square} \bar{W}^{\dot{\beta}} \nabla_{\dot{\beta}}^\beta B_\beta \\
& + iB^\alpha \bar{W}^{\dot{\beta}} \frac{1}{\square} (\nabla_{\alpha\dot{\beta}} \bar{W}^{\dot{\alpha}}) C + iC \bar{W}^{\dot{\beta}} \frac{1}{\square} (\nabla_{\dot{\beta}}^\alpha \bar{W}^{\dot{\alpha}}) B_\alpha \\
& + B^\alpha \bar{W}^{\dot{\beta}} \frac{1}{\square} (\bar{\nabla}_{\dot{\beta}} \bar{W}^{\dot{\alpha}}) \frac{1}{\square} (\nabla_\alpha W^\beta) \frac{1}{\square} (\nabla_\beta W^\gamma) B_\gamma \\
& - B^\alpha \bar{W}^{\dot{\beta}} \frac{1}{\square} (\bar{\nabla}_{\dot{\beta}} \bar{W}^{\dot{\alpha}}) \frac{1}{\square} (\nabla_\alpha W^\beta) B^\gamma (\nabla_\beta W_\gamma) \frac{1}{\square} \\
& - C \bar{W}^{\dot{\alpha}} \frac{1}{\square} \bar{W}^{\dot{\beta}} \nabla_{\dot{\beta}}^\beta \frac{1}{\square} (\nabla_\beta W^\alpha) B_\alpha - C \bar{W}^{\dot{\beta}} \frac{1}{\square} (\nabla_{\dot{\beta}}^\alpha \bar{W}^{\dot{\alpha}}) \frac{1}{\square} (\nabla_\alpha W^\beta) B_\beta \\
& + C \bar{W}^{\dot{\alpha}} \frac{1}{\square} \bar{W}^{\dot{\beta}} \nabla_{\dot{\beta}}^\beta B^\gamma (\nabla_\beta W_\gamma) \frac{1}{\square} + C \bar{W}^{\dot{\beta}} \frac{1}{\square} (\nabla_{\dot{\beta}}^\alpha \bar{W}^{\dot{\alpha}}) B^\beta (\nabla_\alpha W_\beta) ]
\end{aligned}$$

$$\bar{G} = + \frac{1}{\square} \bar{W}^{\dot{\alpha}} \frac{1}{\square} \bar{W}_{\dot{\alpha}} \frac{1}{\square} \tag{D.0.14}$$

$$\begin{aligned}
H^\alpha = & \left[ + \frac{1}{\square} \bar{W}^{\dot{\alpha}} \frac{1}{\square} \bar{W}_{\dot{\alpha}} B^\alpha + B^\alpha \bar{W}^{\dot{\alpha}} \frac{1}{\square} \bar{W}_{\dot{\alpha}} \frac{1}{\square} - \frac{1}{\square} \bar{W}^{\dot{\alpha}} B^\alpha \bar{W}_{\dot{\alpha}} \frac{1}{\square} \right. \\
& + iB^\beta \bar{W}^{\dot{\alpha}} \frac{1}{\square} \bar{W}_{\dot{\alpha}} \frac{1}{\square} (\nabla_\beta W^\alpha) \frac{1}{\square} - B^\beta \bar{W}^{\dot{\alpha}} \frac{1}{\square} \bar{W}_{\dot{\alpha}} \frac{1}{\square} (\nabla_\beta W^\gamma) \frac{1}{\square} (\nabla_\gamma W^\alpha) \frac{1}{\square} \\
& \left. - iB^\beta \bar{W}^{\dot{\alpha}} \frac{1}{\square} \bar{W}_{\dot{\alpha}} \frac{1}{\square} (\nabla_\beta W^\gamma) \frac{1}{\square} (\nabla_\gamma W^\delta) \frac{1}{\square} (\nabla_\delta W^\alpha) \frac{1}{\square} \right]
\end{aligned}$$

$$\begin{aligned}
L = & \left[ -B^\alpha \bar{W}^{\dot{\alpha}} \frac{1}{\square} \bar{W}_{\dot{\alpha}} B_\alpha + C \bar{W}^{\dot{\alpha}} \frac{1}{\square} \bar{W}_{\dot{\alpha}} \frac{1}{\square} + \frac{1}{\square} \bar{W}^{\dot{\alpha}} C \bar{W}_{\dot{\alpha}} \frac{1}{\square} + \frac{1}{\square} \bar{W}^{\dot{\alpha}} \frac{1}{\square} \bar{W}_{\dot{\alpha}} C \right. \\
& - i B^\alpha \bar{W}^{\dot{\alpha}} \frac{1}{\square} \bar{W}_{\dot{\alpha}} \frac{1}{\square} (\nabla_\alpha W^\beta) B_\beta + i B^\alpha \bar{W}^{\dot{\alpha}} \frac{1}{\square} \bar{W}_{\dot{\alpha}} B^\beta (\nabla_\alpha W_\beta) \frac{1}{\square} \\
& \left. + B^\alpha \bar{W}^{\dot{\alpha}} \frac{1}{\square} \bar{W}_{\dot{\alpha}} \frac{1}{\square} (\nabla_\alpha W^\beta) \frac{1}{\square} (\nabla_\beta W^\gamma) B_\gamma - B^\alpha \bar{W}^{\dot{\alpha}} \frac{1}{\square} \bar{W}_{\dot{\alpha}} (\nabla_\alpha W_\beta) B^\gamma (\nabla_\beta W_\gamma) \frac{1}{\square} \right] \quad (D.0.15)
\end{aligned}$$

To get expressions with an explicit dependence on background fields,  $A$ ,  $B$  and  $C$  must be replaced with their expansions (C.0.4), (C.0.5) and (C.0.6).

In order to facilitate the  $\nabla$ -algebra procedure, it is convenient to define also the following expansions

$$\nabla_\alpha \frac{1}{\square} = \mathcal{D}_\alpha^\beta \nabla_\beta + \bar{\mathcal{E}}_\alpha^{\beta\dot{\beta}} \bar{\nabla}_{\dot{\beta}} \nabla_\beta + \mathcal{F}_\alpha^\beta \bar{\nabla}^2 \nabla_\beta + \mathcal{G}_\alpha \nabla^2 + \bar{\mathcal{H}}_\alpha^{\dot{\beta}} \bar{\nabla}_{\dot{\beta}} \nabla^2 + \bar{\mathcal{L}}_\alpha \bar{\nabla}^2 \nabla^2 \quad (D.0.16)$$

$$\bar{\nabla}_{\dot{\alpha}} \frac{1}{\square} = \bar{\mathcal{D}}_{\dot{\alpha}}^{\dot{\beta}} \bar{\nabla}_{\dot{\beta}} + \mathcal{E}_{\dot{\alpha}}^{\beta\dot{\beta}} \nabla_\beta \bar{\nabla}_{\dot{\beta}} + \bar{\mathcal{F}}_{\dot{\alpha}}^{\dot{\beta}} \nabla^2 \bar{\nabla}_{\dot{\beta}} + \bar{\mathcal{G}}_{\dot{\alpha}} \bar{\nabla}^2 + \mathcal{H}_{\dot{\alpha}}^{\beta} \nabla_\beta \bar{\nabla}^2 + \mathcal{L}_{\dot{\alpha}} \nabla^2 \bar{\nabla}^2 \quad (D.0.17)$$

$$\bar{\nabla}_{\dot{\alpha}} \nabla_\alpha \frac{1}{\square} = d_{\alpha\dot{\alpha}}^\beta \nabla_\beta + \bar{e}_{\alpha\dot{\alpha}}^{\beta\dot{\beta}} \bar{\nabla}_{\dot{\beta}} \nabla_\beta + f_{\alpha\dot{\alpha}}^{\beta} \bar{\nabla}^2 \nabla_\beta + g_{\alpha\dot{\alpha}} \nabla^2 + \bar{h}_{\alpha\dot{\alpha}}^{\dot{\beta}} \bar{\nabla}_{\dot{\beta}} \nabla^2 + \bar{l}_{\alpha\dot{\alpha}} \bar{\nabla}^2 \nabla^2 \quad (D.0.18)$$

The new coefficients are given in terms of the ones in eqs. (C.0.3), (C.0.7), (C.0.29)–(C.0.34), (D.0.11) according to

$$\begin{aligned}
\mathcal{D}_\alpha^\beta &= \mathcal{B}_\alpha^\beta - i \bar{\mathcal{H}}_\alpha^{\dot{\alpha}} \nabla_{\dot{\alpha}}^\beta + i \bar{\mathcal{L}}_\alpha W^\beta \equiv \mathcal{Q}_\alpha^\beta + A \delta_\alpha^\beta \\
\bar{\mathcal{E}}_\alpha^{\beta\dot{\beta}} &= - \left[ \nabla_\alpha, E^{\beta\dot{\beta}} \right] + \bar{D}^{\dot{\beta}} \delta_\alpha^\beta + i \bar{\mathcal{L}}_\alpha \nabla^{\beta\dot{\beta}} \\
\mathcal{G}_\alpha &= [\nabla_\alpha, C] - B_\alpha = \mathcal{C}_\alpha \\
\mathcal{F}_\alpha^\beta &= \{ \nabla_\alpha, H^\beta \} + \bar{G} \delta_\alpha^\beta \\
\bar{\mathcal{H}}_\alpha^{\dot{\alpha}} &= \{ \nabla_\alpha, \bar{F}^{\dot{\alpha}} \} + E_\alpha^{\dot{\alpha}} \\
\bar{\mathcal{L}}_\alpha &= [\nabla_\alpha, L] - H_\alpha \quad (D.0.19)
\end{aligned}$$

$$\begin{aligned}
\bar{\mathcal{D}}_{\dot{\alpha}}^{\dot{\beta}} &= \bar{\mathcal{B}}_{\dot{\alpha}}^{\dot{\beta}} - i \mathcal{H}_{\dot{\alpha}}^{\beta} \nabla_\beta^{\dot{\beta}} + i \mathcal{L}_{\dot{\alpha}} \bar{W}^{\dot{\beta}} \\
\mathcal{E}_{\dot{\alpha}}^{\beta\dot{\beta}} &= \left[ \bar{\nabla}_{\dot{\alpha}}, E^{\beta\dot{\beta}} \right] + B^\beta \delta_{\dot{\alpha}}^{\dot{\beta}} - i \bar{F}^{\dot{\beta}} \nabla_{\dot{\alpha}}^\beta \\
\bar{\mathcal{F}}_{\dot{\alpha}}^{\dot{\beta}} &= \left\{ \bar{\nabla}_{\dot{\alpha}}, \bar{F}^{\dot{\beta}} \right\} + C \delta_{\dot{\alpha}}^{\dot{\beta}} \\
\mathcal{H}_{\dot{\alpha}}^{\beta} &= \left\{ \bar{\nabla}_{\dot{\alpha}}, H^\beta \right\} - E_{\dot{\alpha}}^\beta + i L \nabla_{\dot{\alpha}}^\beta \\
\mathcal{L}_{\dot{\alpha}} &= \left[ \bar{\nabla}_{\dot{\alpha}}, L \right] - \bar{F}_{\dot{\alpha}} \\
\bar{\mathcal{G}}_{\dot{\alpha}} &= \left[ \bar{\nabla}_{\dot{\alpha}}, \bar{C} \right] - \bar{B}_{\dot{\alpha}} = \bar{\mathcal{C}}_{\dot{\alpha}} \quad (D.0.20)
\end{aligned}$$



and

$$\begin{aligned}
\bar{e}_{\alpha\dot{\alpha}}^{\beta\dot{\beta}} &= \left\{ \bar{\nabla}_{\dot{\alpha}}, \bar{\mathcal{E}}_{\alpha}^{\beta\dot{\beta}} \right\} + \mathcal{D}_{\alpha}^{\beta} \delta_{\dot{\alpha}}^{\dot{\beta}} \\
f_{\alpha\dot{\alpha}}^{\beta} &= \left[ \bar{\nabla}_{\dot{\alpha}}, \mathcal{F}_{\alpha}^{\beta} \right] - \bar{\mathcal{E}}_{\alpha}^{\beta}{}_{\dot{\alpha}} \\
\bar{h}_{\alpha\dot{\alpha}}^{\beta\dot{\beta}} &= \left[ \bar{\nabla}_{\dot{\alpha}}, \bar{\mathcal{H}}_{\alpha}^{\beta\dot{\beta}} \right] - \mathcal{G}_{\alpha} \delta_{\dot{\alpha}}^{\dot{\beta}} \\
\bar{l}_{\alpha\dot{\alpha}} &= \left\{ \bar{\nabla}_{\dot{\alpha}}, \bar{\mathcal{L}}_{\alpha} \right\} + \bar{\mathcal{H}}_{\alpha\dot{\alpha}} \\
d_{\alpha\dot{\alpha}}^{\beta} &= \left[ \bar{\nabla}_{\dot{\alpha}}, \mathcal{D}_{\alpha}^{\beta} \right] \\
g_{\alpha\dot{\alpha}} &= \left\{ \bar{\nabla}_{\dot{\alpha}}, \mathcal{G}_{\alpha} \right\}
\end{aligned} \tag{D.0.21}$$

A crucial quantity which enters the cancellation of UV divergences in  $\mathcal{N} = 4$  SYM is  $\mathcal{Q}_{\alpha}^{\alpha}$  with  $\mathcal{Q}_{\alpha}^{\beta}$  defined in (D.0.19). Using the identities (C.0.35), (D.0.6)–(D.0.9) we find

$$\begin{aligned}
\mathcal{Q}_{\alpha}^{\alpha} &= \left\{ \nabla_{\alpha}, B^{\alpha} - \bar{F}^{\dot{\alpha}} i \nabla_{\dot{\alpha}}^{\alpha} + LiW^{\alpha} \right\} - 2i \bar{F}^{\dot{\alpha}} i \bar{W}_{\dot{\alpha}} + E^{\alpha\dot{\alpha}} i \nabla_{\alpha\dot{\alpha}} - F_{\alpha} i W^{\alpha} \\
&= \left\{ \nabla_{\alpha}, D^{\alpha} \right\} + (\bar{A} - A) - F_{\alpha} i W^{\alpha} \\
&= \left\{ \nabla_{\alpha}, D^{\alpha} \right\} - \frac{1}{2} \left\{ \bar{\nabla}^{\dot{\alpha}}, \bar{\mathcal{C}}_{\dot{\alpha}} - \bar{B}_{\dot{\alpha}} \right\} - F_{\alpha} i W^{\alpha}
\end{aligned} \tag{D.0.22}$$



# Appendix E

## Color structures

In this Appendix we review briefly the color structure associated to each diagram. First of all we remark that we are considering  $SU(N)$  as gauge group in the large  $N$  (planar) limit. This simplifies many relations from the very beginning, since the same definitions of structure constant become easier. Moreover it allows to keep only leading  $N$  terms in the final results.

### E.1 Color conventions

The color conventions we used are defined by the following relations.

(Anti)commutators of color matrices  $T$  define structure constant  $f$  and  $d$ . In the large  $N$  limit we get

$$[T^a, T^b] = if^{abc}T^c \quad (\text{E.1.1})$$

$$\{T^a, T^b\} = d^{abc}T^c \quad (\text{E.1.2})$$

To fix completely the conventions we need only two other relations. They are

$$\text{Tr}(T^a T^b) = \delta^{ab} \quad (\text{E.1.3})$$

$$T_{ij}^a T_{kl}^a = \delta_{il} \delta_{jk} \quad (\text{E.1.4})$$

Structure constants satisfy Jacobi identity

$$f_{abm}f_{cdm} + f_{cbm}f_{dam} + f_{dbm}f_{acm} = 0 \quad (\text{E.1.5})$$

## E.2 Color structure and covariant effective action diagrams

In a theory with just adjoint fields, like in the  $\mathcal{N} = 4$  SYM, the color structure of a diagram involves just structure constants  $f_{abc}$ . In the background field method there are two possible sources of  $f$ 's: The covariant propagators, i.e. the **quantum-background vertices**, and the **pure quantum vertices**. Consistently with this, we can separate the color analysis in two steps, one general and involving just vacuum diagrams (i.e. pure quantum vertices) and one specific for a peculiar scattering process.

When color is considered, two characteristics distinguish covariant propagators from usual propagators: They are not diagonal with respect to color and the color factor associated to them changes with the number of insertions of background fields when they are power expanded. This is a direct consequence of the fact that covariant propagators include interactions between quantum and background fields. In general, one should think at covariant propagators as objects carrying two open color indices

$$\frac{1}{\square_+} \rightarrow \left( \frac{1}{\square_+} \right)_{ab}, \quad \frac{1}{\square_-} \rightarrow \left( \frac{1}{\square_-} \right)_{ab}, \quad \frac{1}{\hat{\square}} \rightarrow \left( \frac{1}{\hat{\square}} \right)_{ab} \quad (\text{E.2.1})$$

More precisely, the two color indices of the propagators refers order by order in the expansion to a different color structure. Diagrammatically we read

$$\begin{array}{c} \text{a} \quad \text{b} \\ \hline \end{array} = \begin{array}{c} \text{a} \quad \text{b} \\ \cdot \quad \cdot \end{array} + \begin{array}{c} \text{a} \quad \text{b} \\ \cdot \quad \cdot \quad \uparrow \text{c} \\ \text{wavy line} \end{array} + \begin{array}{c} \text{a} \quad \text{b} \\ \cdot \quad \cdot \quad \uparrow \text{c} \quad \uparrow \text{d} \\ \text{wavy line} \quad \text{wavy line} \end{array} + \dots \quad (\text{E.2.2})$$

So, at each insertion of external fields  $\begin{array}{c} \text{m} \quad \text{p} \\ \cdot \quad \cdot \quad \uparrow \text{n} \\ \text{wavy line} \end{array}$  it corresponds a color factor  $if_{mnp}$ . Just the first term in the expansion is diagonal in color.

Color factors associated to pure quantum vertices has been extrapolated in Section 6.1. From there we derive the color structure of each vacuum diagram. We find that\*

- Cubic vertices graphs

$$\begin{array}{c} \text{a} \quad \text{d} \\ \text{b} \quad \text{e} \\ \text{c} \quad \text{f} \end{array} \longrightarrow f_{abc} f_{def} \quad (\text{E.2.3})$$

This factor is common to each cubic vertex vacuum diagram.

---

\*See Tab 6.1

- Tadpole graphs

The color factor associated to every quartic vertex is

$$\begin{array}{c} \text{b} \quad \text{c} \\ \diagdown \quad \diagup \\ \cdot \\ \diagup \quad \diagdown \\ \text{a} \quad \text{d} \end{array} \longrightarrow f_{abe} f_{ecd} \quad (\text{E.2.4})$$

As pointed out in Section 6.2.2, when we build up from these vertices tadpole-like diagrams, it is possible to distinguish between three different cases depending on which legs are closed to form loops (see Fig. E.1).

$$\begin{array}{ccc}
 \begin{array}{c} \text{b} \quad \text{c} \\ \cdot \\ \text{a} \quad \text{d} \end{array} &
 \begin{array}{c} \text{c} \quad \text{b} \\ \cdot \\ \text{a} \quad \text{d} \end{array} &
 \begin{array}{c} \text{d} \quad \text{b} \\ \cdot \\ \text{a} \quad \text{c} \end{array} \\
 a) \text{ ab contraction} &
 b) \text{ ac contraction} &
 c) \text{ ad contraction}
 \end{array} \quad (\text{E.2.5})$$

Figure E.1: The three different color contraction for the tadpole vacuum diagrams

Note that all the color indices carried by quantum lines are summed indices. For example, for the cubic vertex diagrams we should write

$$\begin{array}{c} \text{a} \quad \text{d} \\ \cdot \\ \text{b} \quad \text{e} \\ \cdot \\ \text{c} \quad \text{f} \end{array} \longrightarrow f_{abc} f_{def} \left( \frac{1}{\square_1} \right)_{ad} \left( \frac{1}{\square_2} \right)_{be} \left( \frac{1}{\square_3} \right)_{cf} \quad (\text{E.2.6})$$

where  $\frac{1}{\square_{(1,2,3)}}$  represent the covariant propagators of the first, second and third line. So, the only open color indices are the ones carried by the background fields inside the covariant propagators once that they are expanded at the desired order in  $W$ 's. As a consequence, different distributions of the legs along the same vacuum diagram, i.e. cubic vertices or tadpole-like diagrams with different topologies, carry different color structures.

### E.3 Four point color structures

Consider the specific case of the four point planar scattering amplitude in  $\mathcal{N} = 4$  SYM theory. The UV finiteness of the theory allows the presence of two different topologies

in the cubic vertex diagram sector (the doublebox and the pentabox topology (see Fig F.1)) and for only one topology in the tadpole sector. The color structure for the tadpole topology must then be analyzed for each of the different cases of Fig E.1. We summarize the topologies and their associated color structure in Tab E.1<sup>†</sup>

A few remarks are necessary:

- Orientation of the cubic vertex diagrams  
Color structures associated to doublebox and pentabox diagrams induce an orientation on the external legs of the planar diagrams. Color states that cubic vertex diagrams must be read clockwise or counterclockwise. The “closeness” of two scattered particles follows from the choice of this orientation. In particular, looking at all possible helicity–dependent four point topologies (see Fig F.1), it is immediate to see that two plus helicity particles are consecutive in topologies (a), (b), (d) and (e). So, just these four topologies contributes to the MHV ( $1^+2^+3^-4^-$ ) color ordered scattering amplitude. The other helicity configurations contribute to the  $+ - + -$  amplitudes.
- Trianglebox diagrams:  
Consider diagrams like the ones in Fig. E.2. Although they have the same topo-

$$\begin{array}{ccc}
 \begin{array}{c} \frac{1}{\square} W^\alpha \frac{1}{\square} W_\alpha \frac{1}{\square} \\ \text{---} \text{---} \text{---} \\ \text{---} \text{---} \text{---} \\ \frac{1}{\square} \overline{W}^{\dot{\alpha}} \frac{1}{\square} \overline{W}_{\dot{\alpha}} \end{array} & , & \begin{array}{c} \frac{1}{\square} W^\alpha \frac{1}{\square} W_\alpha \frac{1}{\square} \overline{W}^{\dot{\alpha}} \\ \text{---} \text{---} \text{---} \\ \text{---} \text{---} \text{---} \\ \frac{1}{\square} \overline{W}_{\dot{\alpha}} \frac{1}{\square} \end{array} & , & \begin{array}{c} \frac{1}{\square} W^\alpha \frac{1}{\square} W_\alpha \frac{1}{\square} \\ \text{---} \text{---} \text{---} \\ \text{---} \text{---} \text{---} \\ \frac{1}{\square} \overline{W}_{\dot{\alpha}} \frac{1}{\square} \end{array} \\
 \text{1) } \text{---} \text{---} \text{---} & & \text{2) } \text{---} \text{---} \text{---} & & \text{3) } \text{---} \text{---} \text{---} \\
 \text{---} \text{---} \text{---} & & \text{---} \text{---} \text{---} & & \text{---} \text{---} \text{---} \\
 \frac{1}{\square} \overline{W}^{\dot{\alpha}} \frac{1}{\square} \overline{W}_{\dot{\alpha}} & & \frac{1}{\square} \overline{W}_{\dot{\alpha}} \frac{1}{\square} & & \frac{1}{\square} \overline{W}_{\dot{\alpha}} \frac{1}{\square}
 \end{array}
 \tag{E.3.1}$$

Figure E.2: Similar triangleboxes with different color factors

logical structure sketched in Fig E.3 their color structures are respectively the doublebox, the pentabox ones and a structure subleading in color. Note that Jacobi identity (E.1.5) relates these three different diagrams. It is possible to show that this is equivalent to integrate by parts the  $\overline{W}$  at the right vertex: In principle one could write  $\overline{W}^{\dot{\alpha}}$  as the commutator of covariant derivatives

$$\overline{W}_{\dot{\alpha}} = -\frac{1}{2} [\nabla^\alpha, \nabla_{\alpha\dot{\alpha}}] \tag{E.3.2}$$

---

<sup>†</sup> $i$  factors associated to the structure constants are not considered in the table. Along our computation, we considered the  $i$ 's associated to the quantum vertices in the combinatorics of Tab 6.1. The other four  $i$ 's from quantum–background vertices give an innocuous factor 1.

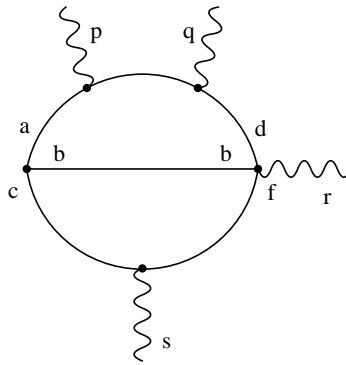


Figure E.3: General topology for a trianglebox

Covariant derivatives can be integrated by parts on the right vertex and we get back  $\overline{W}$  by reconstructing the commutator (E.3.2) on the other two lines with eventually some extra sign. The signs are equivalent to the signs one gets by considering just the color structure of the original diagram and by applying Jacobi identity on it. This is a direct proof of the fact that the integration by parts of derivatives respects the color structure of the diagrams and vice versa.

- Tadpoles and cubic vertex diagrams:

By using the trivial identity  $\frac{1}{\square} \square = 1$  it is possible to write a tadpole-like diagram as a cubic vertex diagram with a  $\square$  on the middle line. Roughly speaking, inserting  $\frac{1}{\square} \square$  inside a tadpole opens it up into a cubic vertex diagram.

Color plays an active role when this kind of manipulation is performed. The relative sign in front of the color structures of tadpoles  $(ac)$  and  $(ad)$  of Fig E.1 causes a relative sign between the “opened” tadpoles. In particular, the opened  $(ac)$  tadpole becomes a doublebox-like topology diagram while the opened tadpole  $(ad)$  pick up a sign when written as a doublebox with a  $\square$  on the middle line. This sign is crucial for the cancellation of UV divergences, as we have seen in Section 6.3.

Note that even if in principle tadpoles  $(ab)$  can be opened in the same way as the other two tadpole topologies, its color structure does not match any one of the cubic vertex diagrams and prevents us from opening it.

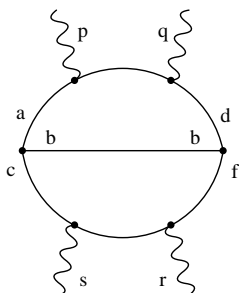
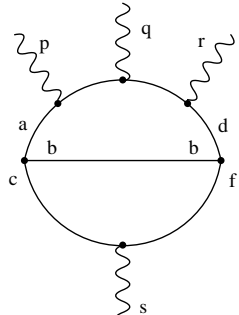
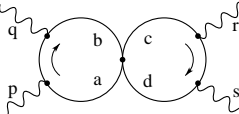
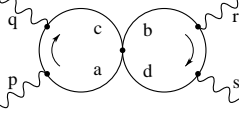
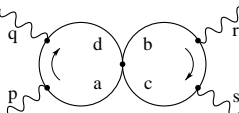
Topology	Color Structure
 <p>(a) Doublebox</p>	$f_{abc}f_{dbf}f_{apm}f_{mqd}f_{csn}f_{nrf}$ $=$ $+N^2 \{Tr(t^p t^s t^r t^q) + Tr(t^p t^q t^r t^s)\}$
 <p>(b) Pentabox</p>	$f_{abc}f_{dbf}f_{apm}f_{mqn}f_{nrd}f_{csf}$ $=$ $-N^2 \{Tr(t^p t^s t^r t^q) + Tr(t^p t^q t^r t^s)\}$
 <p>(c) Tadpole ab</p>	$f_{abe}f_{ecd}f_{apm}f_{mqb}f_{crn}f_{nsd}$ $=$ $+N^2 \{Tr(t^p t^q t^s t^r) + Tr(t^q t^p t^r t^s) - Tr(t^p t^q t^r t^s) - Tr(t^q t^p t^s t^r)\}$
 <p>(a) Tadpole ac</p>	$f_{abe}f_{ecd}f_{apm}f_{mqc}f_{brn}f_{nsd}$ $=$ $+N^2 \{Tr(t^p t^q t^s t^r) + Tr(t^q t^p t^r t^s)\}$
 <p>(a) Tadpole ad</p>	$f_{abe}f_{ecd}f_{apm}f_{mqd}f_{brn}f_{nsc}$ $=$ $-N^2 \{Tr(t^p t^q t^s t^r) + Tr(t^q t^p t^r t^s)\}$

Table E.1: Color factors for four point topologies





this point of view. In fact, to exchange the lower line with the upper one, both these lines has to cross the middle one. This, of course, can produce signs when the middle line is fermionic.

The same exchange can be performed on the lines of tadpole-like diagrams too. In that case Up-Down symmetry consist in exchanging the two loops.

The Up-Down symmetry is actually valid at the more general level of vacuum diagrams, before  $\nabla$ -algebra is performed. When legs of quantum vertices are contracted to form the lines of the vacuum diagrams, there is nothing that forbids to interchange two of them provided that the statistic of the lines interchanged is considered.

## F.2 Left-Right Symmetry

The second geometric symmetry of cubic vertex graphs is connected with the exchange of the left and right vertices. In general, there is no preferred orientation in the graphs that forces to read them from the left to the right. So, one is free to rewrite the graph reading it line by line from the right to the left, i.e. to exchange left and right vertices. Note that this symmetry acts as a reflection with respect to a vertical axis passing in the middle of a graph.

While reflecting left-right a graph, the following sign rules must be respected:

- 1) For each fermionic field exchange the graph picks up a sign;
- 2) Each covariant derivative entering in the graph along a loop line takes a sign;
- 3) Covariant derivatives applied to external fields do not take signs;
- 4) Graphs with an odd number of external  $W$ 's fields pick up a sign when reverted
- 5) Graphs with an even number of external  $W$ 's fields do not pick up signs when reverted
- 6) Covariant propagators do not take signs.

The first three rules, in particular the second one, preserve the momentum structure underlying each graph. On the other hand, the rules (4) and (5) are necessary to preserve color structures. The basic idea, in fact, is that each external  $W$  from the color point of view corresponds to a structure constant insertion  $i f_{abc}$  (see Appendix E for a more detailed analysis). When the graph is reverted, also the order of indexes in  $f$  is reverted and this produce a minus sign for each  $f$ , i. e. for each external  $W$ .

Rule (6) is a consistency check of the other rules:  $\frac{1}{\square}$  is, in fact, a complicated expressions that involves connections  $\Gamma_{\alpha\dot{\alpha}}$  and spacetime derivatives  $\partial_{\alpha\dot{\alpha}}$  (see equation (C.0.37)).

On the other hand, in principle one would expect that all the components of its expansion behave like the lower order term  $\frac{1}{\square_0}$  under Left–Right, i.e. they do not pick up signs. The rules (1)–(5) guarantee this: Higher order terms of  $\frac{1}{\square}$  present always the same number of connections and derivatives so that, under Left–Right, at each sign due to an extra insertion of background fields (rule (4) and (5)) it corresponds another sign due to the presence of a derivative (rule (2)).

One could be a bit puzzled about the consistence of Left–Right symmetry and  $\nabla$ –algebra procedure. In fact, the  $\nabla$ –algebra has been performed pushing from the left to the right vertex all the spinorial derivatives and one could expect that this could give an orientation to the diagrams. Actually, this is not the case. In fact,  $\nabla$ –algebra procedure works fine as well by pushing spinorial derivatives from the right to the left vertex and the results one gets pushing left or right derivatives are the same if they are read the firsts from left to right and the seconds from right to left. Moreover, in principle one could exchange the left and the right vertex even before closing the legs to form the vacuum diagrams and performing the  $\nabla$ –algebra. The results is clearly unaffected if the two vertices are exchange at that level. Thus, they are unaffected if the exchange is done at any stage of the computation.

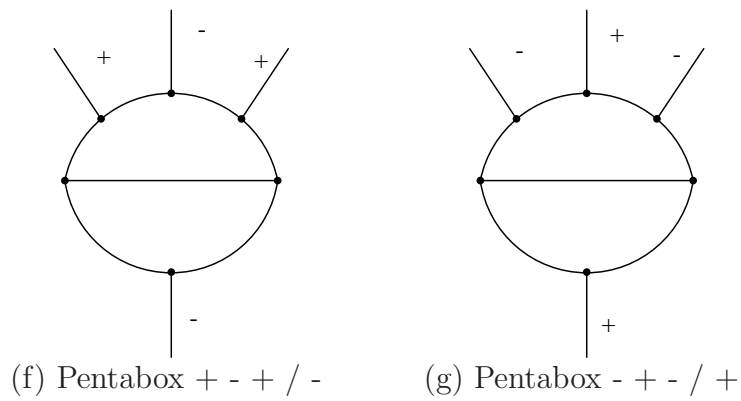
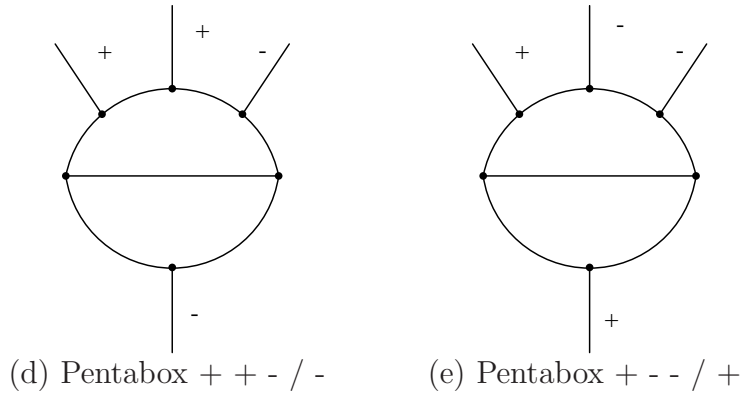
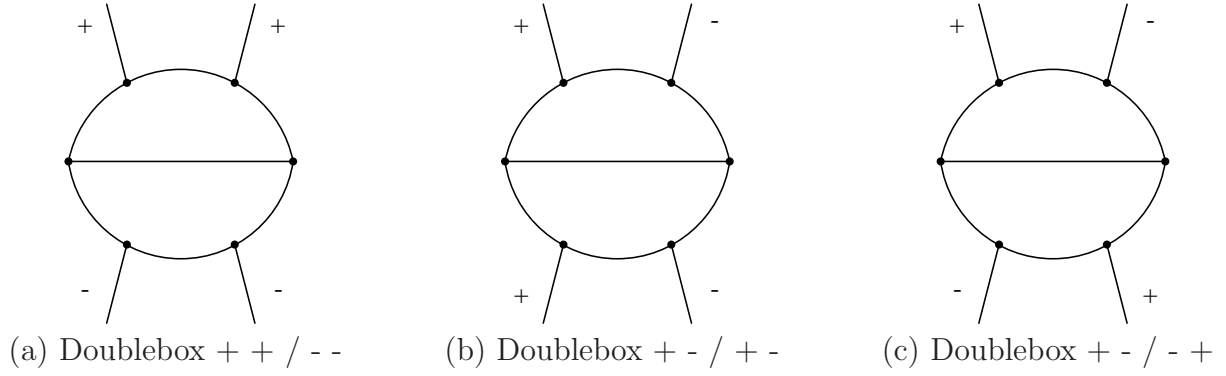
### F.3 Consequences of geometric symmetries

The consequences of Up–Down and Left–Right symmetries go beyond the simple re-summation and simplification of many terms in the computation of the effective action. Actually, there are further important restrictions that geometric symmetries impose on the allowed independent helicity configurations in a scattering process. Moving up–down and left–right the diagrams, different helicity configurations are in fact mapped one into the other.

In the specific case of the four point effective action, with two particles with positive and two with negative helicity, the bunch of independent helicity sectors gets reduced to the ones in Fig F.1.

In these pictures we have separated the doublebox topologies (figures (a)–(c)) from the pentabox topologies (figures (d)–(g)). By using these informations and the color informations it follows that only topologies (a), (b), (d) and (f) give contributions to the color ordered four point amplitude ( $A(1^+, 2^+, 3^-, 4^-)$ ). These are exactly the topologies that we considered along our computation.

Up–Down and Left–Right symmetries of course reduce the number independent helicity configurations for the scattering processes involving any number of particles. The extension of the classification of Fig F.1 to higher points follows the same logic used for the four point case and can be easily reconstructed by using what done here as a road map.



(F.3.1)

Figure F.1: Simplifications in the four point topologies induced by the UD and the LR symmetries

# Appendix G

## Conventions in momentum space

In this Appendix we review the basic conventions we used for Fourier transforming the contributions to the effective action from the configuration representation to the momentum representation. Moreover we give the conventions for the basic scalar integrals in which the color ordered amplitude  $A(1^+, 2^+, 3^-, 4^-)$  turns out to be divided.

### G.1 Fourier transform conventions

After  $\nabla$ -algebra has been performed and all covariant objects have been expanded up to the wanted number of external fields, we are left with diagrams involving background fields and momentum derivatives  $\partial_{\alpha\dot{\alpha}}$  only. In this appendix we describe the conventions we follow to Fourier transforming these derivatives from position representation to momentum representation.

Fourier transform for the propagator is

$$\Delta(x - y) = \int \frac{d^4 p}{(2\pi)^4} \frac{e^{-ip(x-y)}}{p^2} \quad (\text{G.1.1})$$

and for background fields

$$A(x) = \int \frac{d^4 p}{(2\pi)^4} e^{-ipx} \tilde{A}(p) \quad (\text{G.1.2})$$

Diagrammatically, these relations correspond to the pictures in Fig G.1. Note that we always take **external momenta** to be **outgoing**.

We remind that after  $\nabla$ -algebra all the derivatives are thought as acting from left to right. Looking at the position where they enter a diagram, we can distinguish two cases:

- A derivative appears on an **internal line** as  $(\partial_{\square}^1) \rightarrow \partial_x \Delta(x - y)$

$$\begin{array}{ccc} \bullet \text{---} \bullet & \longrightarrow & \bullet \text{---} \bullet \\ \text{x} \quad \text{y} & & \quad \vec{p} \end{array} \quad (\text{G.1.3})$$

$$\begin{array}{ccc} \bullet \text{~~~~~} & \longrightarrow & \bullet \text{~~~~~} \\ \text{x} & & \quad \vec{p} \end{array} \quad (\text{G.1.4})$$

Figure G.1: Fourier transform of derivatives on internal and external lines

In this case we replace it with

$$\partial_{\alpha\dot{\alpha}} \longrightarrow -ip_{\alpha\dot{\alpha}} \quad (\text{G.1.5})$$

where  $p$  is the momentum flowing from left to right on the line corresponding to the propagator. As it is clear from (G.1.1) and the corresponding figure (G.1.3), if the momentum flows from right to left we pick up an extra minus sign on the right hand side of (G.1.5).

- A derivative appears on an **external line**, that is we have  $\partial_x A(x)$   
In this case we replace it with

$$\partial_{\alpha\dot{\alpha}} A(x) \longrightarrow -ip_{\alpha\dot{\alpha}} \tilde{A}(p) \quad (\text{G.1.6})$$

where  $p$  is the external outgoing momentum (see figure (G.1.4)).

The rules here described satisfy conservation of momentum at each vertex and integration by parts relations. For example, consider the diagrammatic of Fig G.2. This relation is the diagrammatic version of the algebraic commutation relation

$$\begin{aligned} \frac{1}{\square} (\partial_{\alpha\dot{\alpha}} A(x)) \frac{1}{\square} &\equiv \frac{1}{\square} [\partial_{\alpha\dot{\alpha}}, A(x)] \frac{1}{\square} = \frac{1}{\square} \partial_{\alpha\dot{\alpha}} (A(x) \frac{1}{\square}) - \frac{1}{\square} A(x) \partial_{\alpha\dot{\alpha}} \frac{1}{\square} \\ &= -\frac{1}{\square} \overleftarrow{\partial}_{\alpha\dot{\alpha}} A(x) \frac{1}{\square} - \frac{1}{\square} A(x) \partial_{\alpha\dot{\alpha}} \frac{1}{\square} \\ &= (\partial_{\alpha\dot{\alpha}} \frac{1}{\square}) A(x) \frac{1}{\square} - \frac{1}{\square} A(x) \partial_{\alpha\dot{\alpha}} \frac{1}{\square} \end{aligned} \quad (\text{G.1.7})$$

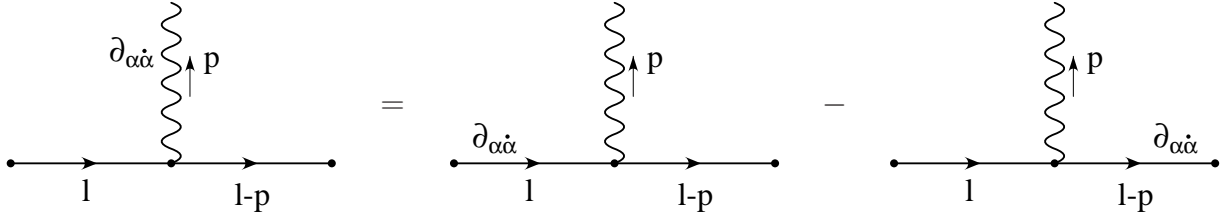


Figure G.2: Diagrammatic expression for the conservation of the momenta at the vertices

where, when not explicitly indicated, the derivatives are thought as acting from left to right and we have integrated by parts from the second to the third line.

Moving (G.1.7) to momentum space with the use of (G.1.5) and (G.1.6), we get the following identity

$$-ip_{\alpha\dot{\alpha}} = -i\ell_{\alpha\dot{\alpha}} - (-i\ell_{\alpha\dot{\alpha}} + ip_{\alpha\dot{\alpha}}) \quad (\text{G.1.8})$$

This is a proof that our momentum conventions are consistent with the algebraic procedures we heavily used during the computation of the effective action.

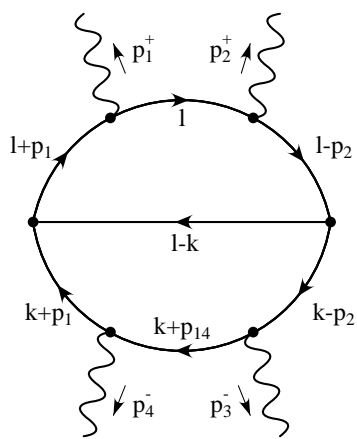
We define Mandelstam variables

$$s = (p_1 + p_2)^2 \quad t = (p_1 + p_4)^2 \quad u = (p_1 + p_3)^2 \quad (\text{G.1.9})$$

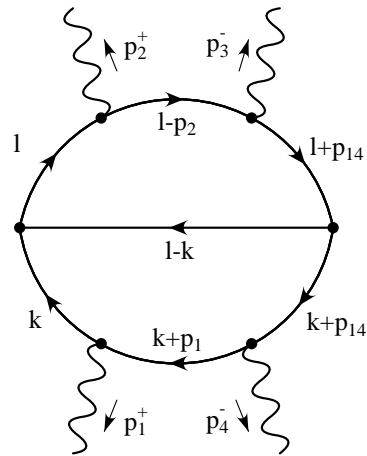
## G.2 Topologies for the scalar integrals

In this Section we summarize the loop integral conventions used for the two doublebox and the two pentabox sectors in which the four point MHV effective action is divided (see Section 7.1). Note that the propagators of these integrals form a set of nine propagators. These propagators are called *irreducible propagators* since they are the smaller set of independent squared objects formed by the momenta that the conservation of external momenta and the massless condition allow to construct at two loops and four points.

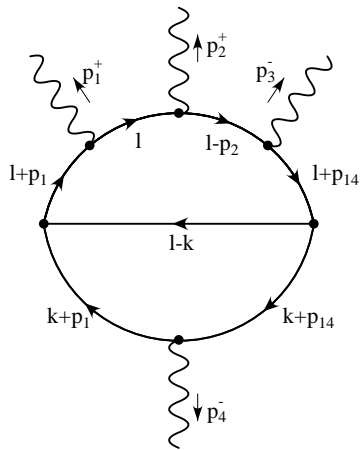
The list of the integrals is the following



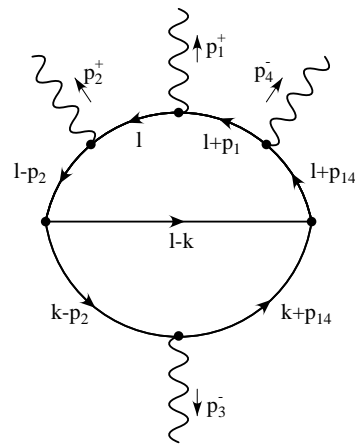
A) Doublebox ++/--



B) Doublebox + -/+ -



C) Pentabox ++ -/-



D) Pentabox + - -/+

Figure G.3: List of two loop scalar integrals



# Appendix H

## Scalar, vector and tensor integrals

The loop integrals we have to deal with along the computation can be divided into three classes according to their Lorentz structure: The scalar integrals, the vector integrals and the tensor integrals. In this Appendix we show many useful relations between these integrals. We focus on two main aspects:

1) **Symmetries of the scalar integrals**

Since a scalar integral is a Lorentz invariant, it must be a function of Mandelstam variables  $s$ ,  $t$  and  $u$  only. Any transformation on the external and loop momenta that leaves Mandelstam variables unchanged maps a scalar integral into another equivalent.

2) **Passarino–Veltman reduction of vector and tensor integrals**

Vector and tensor integrals can be reduced to linear combinations of scalar integrals through the Passarino–Veltman reduction technique [120].

Thus, after PV reduction, the expression we get are written in terms of scalar integrals only and a lot of simplifications follow from the symmetries discussed at point 1).

### H.1 Symmetries of the scalar integrals

A careful inspection of the propagators that enter in the scalar structures presented in Fig G.3 shows that all the denominators of the integrals are functions of just nine propagators, namely

$$\begin{aligned} k^2, & \quad (k + p_1)^2, & \quad (k - p_2)^2, & \quad (k + p_{14})^2, \\ \ell^2, & \quad (\ell + p_1)^2, & \quad (\ell - p_2)^2, & \quad (\ell + p_{14})^2, \\ & & \quad (\ell - k)^2. & \end{aligned} \tag{H.1.1}$$

	Transformation	Permutation
1)	$k \leftrightarrow \ell$	$\{123456789\} \longrightarrow \{567812349\}$
2)	$p_1 \leftrightarrow -p_2$ $p_3 \leftrightarrow -p_4$	$\{123456789\} \longrightarrow \{132457689\}$
3)	$k \rightarrow k_4 - p_{14}$ $\ell \rightarrow \ell - p_{14}$ $p_1 \leftrightarrow -p_4$ $p_2 \leftrightarrow -p_3$	$\{123456789\} \longrightarrow \{423186759\}$

Table H.1: Basic symmetries of the scalar integrals

As we have previously discussed, this set of propagators constitutes the *irreducible propagators*, i.e. the smaller set of independent propagators that can be built up for a process involving four massless particles at two loops.

Propagators, in fact, are squared functions of loop and external momenta. At four points and two loops, when the conservation of external momenta is considered, the set of independent momenta includes the loop momenta  $k$  and  $\ell$  and three combination of the external momenta. In (H.1.1) we choose ( $p_1$ ,  $p_2$  and  $p_{14} = p_1 + p_4$ ) but in principle any other choice of the external momenta would be equivalent.

The nine propagators in (H.1.1) are the only squared structures that is possible to construct with our choice of independent momenta. All other squared structures can be written as combinations of the irreducible ones.

Note that to fix a set of irreducible propagators is equivalent to fix the freedom due to the conservation relation.

This fact has important consequences as far as two loop scalar integrals are concerned. The integrand of a scalar integral is, in fact, a function of the irreducible propagators, since they are the only independent squared structures. On the other hand, since the scalar integrals are invariant under Lorentz transformations, they must be functions of the Mandelstam variables only. As a consequence, any transformation on the momenta  $k$ ,  $\ell$  and  $p_i$  ( $i = 1, \dots, 4$ ) that leaves unchanged the Mandelstam variables and is closed on the set of irreducible propagators allows to map a scalar integral into another equivalent one. In this way a web of connections between integrals can be worked out.

There are three basic transformations that can be found. They are summarized in Tab H.1. Numbers (1, 2,  $\dots$ ) refer to the irreducible propagators ( $k^2, (k + p_1)^2, \dots$ ) as they appear in the sequence (H.1.1).

Moreover, any combination of the exchanges 1), 2) and 3) of the Tab H.1 produces

further transformations between the irreducible propagators that leave the final analytic structure of any scalar integral unchanged. In this way further connections between scalar integrals can be found.

More generally, it is worth noting that any integral of a polynomial function of the squares (H.1.1) is invariant with respect to the transformation of Tab H.1. The fact that the irreducible squares enter in the integrand at denominator (as true Feynman propagators) or at numerator is completely irrelevant.

Although the most part of the loop integrals that contributes to the effective action have vector or tensor Lorentz structures, in the next Section we show that it is always possible to rewrite these integrals as a combination of scalar integrals through the Passarino–Veltman reduction procedure.

Thus, since the final expression for the effective action turns out to be a function of scalar integrals only, the relations between integrals that come from the transformations (H.1) are of primary importance for the derivation of our final results.

## H.2 Passarino–Veltman reduction

In this Section we analyze the Passarino–Veltman reduction for loop integrals that are relevant for the four point effective action. In principle, we have to analyze the reduction of vector and tensor integrals separately for each relevant topology (doubleboxes and pentaboxes). However, PV procedure involves only those parts of the loop integrals that present a non-trivial index structure and is blind with respect to all the Lorentz–scalar terms. Since the topology of the diagrams is related to the propagators and since these are definitely Lorentz invariant, PV reduction works following the same rules for each topological sector.

The main ingredients for the PV reduction an integral are:

- 1) A **basis**  $e_i$  on which expand the integral in terms of unknown scalar coefficients  $A_i$

$$I_{\alpha_1 \dots \alpha_n \dot{\alpha}_1 \dots \dot{\alpha}_n} = \sum_{i=1}^n A_i (e_i)_{\alpha_1 \dots \alpha_n \dot{\alpha}_1 \dots \dot{\alpha}_n} \quad (\text{H.2.1})$$

- 2) A **set of tensor objects** by which saturate open indices of (H.2.1) and build up a linear system that defines the coefficients  $A_i$ .

The objects that can be used at points 1) and 2) are the only ones that can carry the Lorentz structure after that the loop integrals are performed. So, generally they are the independent external momenta  $(p_i)_{\alpha\dot{\alpha}}$ , the Ricci symbols  $c_{\alpha\beta}$ ,  $c_{\dot{\alpha}\dot{\beta}}$  and, eventually, combinations of these elements.

In the following sections we describe the choices we did at points 1) and 2) and we will give the solutions for the scalar coefficients  $A_i$  for the vector and the tensor cases.

## H.2.1 Vector Integrals

Consider a general two loop vector integral with the form

$$T_{\alpha\dot{\alpha}} = \int d^4k d^4\ell \frac{v_{\alpha\dot{\alpha}}}{\text{denominator}} \quad (\text{H.2.2})$$

where  $v_{\alpha\dot{\alpha}}$  can be either  $k_{\alpha\dot{\alpha}}$  or  $\ell_{\alpha\dot{\alpha}}$  and "denominator" stays for any possible topology listed in Fig. G.3. A good basis for this kind of integrals is formed by a set of three independent combination of the external momenta. We choose for convenience  $p_1$ ,  $p_2$  and  $p_4$ . So, we can write

$$T_{\alpha\dot{\alpha}} = A (p_1)_{\alpha\dot{\alpha}} + B (p_2)_{\alpha\dot{\alpha}} + C (p_4)_{\alpha\dot{\alpha}} \quad (\text{H.2.3})$$

We need now to choose a set of three vector-like objects by which saturate open indices in relation (H.2.3) and define a linear system in the unknown coefficients  $A$ ,  $B$  and  $C$ . Coherently with the set of irreducible propagators fixed in (H.1.1) we choose  $p_1$ ,  $p_2$  and  $p_{14}$ .

By multiplying (H.2.3) for these vectors, we find the following relations

$$\begin{cases} x = sB + tC \\ y = sA + uC \\ z = tA - tB + tC \end{cases} \quad (\text{H.2.4})$$

where  $x$ ,  $y$  and  $z$  are defined in the following way

$$\begin{aligned} x &= \int \frac{(p_1)^{\alpha\dot{\alpha}} k_{\alpha\dot{\alpha}}}{\text{denominator}} = \int \frac{(k + p_1)^2 - k^2}{\text{denominator}} \\ y &= \int \frac{(p_2)^{\alpha\dot{\alpha}} k_{\alpha\dot{\alpha}}}{\text{denominator}} = \int \frac{-(k - p_2)^2 + k^2}{\text{denominator}} \\ z &= \int \frac{(p_{14})^{\alpha\dot{\alpha}} k_{\alpha\dot{\alpha}}}{\text{denominator}} = \int \frac{(k + p_{14})^2 - k^2 - t}{\text{denominator}} \end{aligned} \quad (\text{H.2.5})$$

As a consequence, the scalar coefficients  $A$ ,  $B$  and  $C$  depends only on the irreducible propagators both at denominator and at numerator. More precisely, the solutions of the system (H.2.4) are

$$\begin{aligned} A &= \frac{1}{2st} (t(x + y) + sz) \\ B &= -\frac{1}{2su} (2sx + t(x + y) - sz) \\ C &= -\frac{1}{2tu} (t(x - y) + sz) \end{aligned} \quad (\text{H.2.6})$$

## H.2.2 Tensor Integrals

Consider now a general two loop tensor integral whose a structure can be written

$$T_{\alpha\beta\dot{\alpha}\dot{\beta}} = \int \frac{v_{\alpha\dot{\alpha}} w_{\alpha\dot{\alpha}}}{\text{denominator}} \quad (\text{H.2.7})$$

In this expression  $v$  and  $w$  can be either  $\ell$  or  $k$ .

We expand  $T_{\alpha\beta\dot{\alpha}\dot{\beta}}$  on a basis formed by  $p_1$ ,  $p_2$  and  $p_3$  and the Ricci symbol  $c$  in the following way

$$\begin{aligned} T_{\alpha\beta\dot{\alpha}\dot{\beta}} = & A c_{\alpha\beta} c_{\dot{\alpha}\dot{\beta}} \\ & + B (p_1)_{\alpha\dot{\alpha}} (p_1)_{\beta\dot{\beta}} + C (p_2)_{\alpha\dot{\alpha}} (p_2)_{\beta\dot{\beta}} + D (p_3)_{\alpha\dot{\alpha}} (p_3)_{\beta\dot{\beta}} \\ & + E (p_1)_{\alpha\dot{\alpha}} (p_2)_{\beta\dot{\beta}} + F (p_2)_{\alpha\dot{\alpha}} (p_1)_{\beta\dot{\beta}} \\ & + G (p_1)_{\alpha\dot{\alpha}} (p_3)_{\beta\dot{\beta}} + H (p_3)_{\alpha\dot{\alpha}} (p_1)_{\beta\dot{\beta}} \\ & + L (p_2)_{\alpha\dot{\alpha}} (p_3)_{\beta\dot{\beta}} + M (p_3)_{\alpha\dot{\alpha}} (p_2)_{\beta\dot{\beta}} \end{aligned} \quad (\text{H.2.8})$$

Suppose now to multiply (H.2.8) by this set of tensor objects

$$\begin{aligned} & C^{\alpha\beta} C^{\dot{\alpha}\dot{\beta}}, \\ & (p_1)^{\alpha\dot{\alpha}} (p_1)^{\beta\dot{\beta}}, \quad (p_1)^{\alpha\dot{\alpha}} (p_2)^{\beta\dot{\beta}}, \quad (p_1)^{\alpha\dot{\alpha}} (p_3)^{\beta\dot{\beta}}, \\ & (p_2)^{\alpha\dot{\alpha}} (p_1)^{\beta\dot{\beta}}, \quad (p_2)^{\alpha\dot{\alpha}} (p_2)^{\beta\dot{\beta}}, \quad (p_2)^{\alpha\dot{\alpha}} (p_3)^{\beta\dot{\beta}}, \\ & (p_3)^{\alpha\dot{\alpha}} (p_1)^{\beta\dot{\beta}}, \quad (p_3)^{\alpha\dot{\alpha}} (p_2)^{\beta\dot{\beta}}, \quad (p_3)^{\alpha\dot{\alpha}} (p_3)^{\beta\dot{\beta}}. \end{aligned} \quad (\text{H.2.9})$$

The linear system that we produce is

$$\begin{aligned} x_1 &= 4A + s(E + F) + u(G + H) + t(L + M) \\ x_2 &= s^2C + u^2D + su(L + M) \\ x_3 &= sA + tuD + s^2F + suH + stL \\ x_4 &= uA + stC + suF + u^2H + tuM \\ x_5 &= sA + tuD + s^2E + suG + stM \\ x_6 &= s^2B + t^2D + stG + stH \\ x_7 &= tA + suB + stE + tuH + t^2M \\ x_8 &= uA + stC + suE + u^2G + tuL \\ x_9 &= tA + suB + stF + tuG + t^2L \\ x_{10} &= u^2B + t^2C + tuE + tuF \end{aligned} \quad (\text{H.2.10})$$

In this expression,  $x_i$  are given by the product of  $T_{\alpha\beta\dot{\alpha}\dot{\beta}}$  by the  $i$ -th element of (H.2.9). So, for example

$$\begin{aligned} x_1 &= C^{\alpha\beta} C^{\dot{\alpha}\dot{\beta}} T_{\alpha\beta\dot{\alpha}\dot{\beta}} = \int \frac{v^{\alpha\dot{\alpha}} w_{\alpha\dot{\alpha}}}{\text{denominator}} = \int \frac{-(v-w)^2 + v^2 + w^2}{\text{denominator}} \\ x_2 &= (p_1)^{\alpha\dot{\alpha}} (p_1)^{\beta\dot{\beta}} T_{\alpha\beta\dot{\alpha}\dot{\beta}} = \int \frac{(p_1)^{\alpha\dot{\alpha}} v_{\alpha\dot{\alpha}} (p_1)^{\beta\dot{\beta}} w_{\beta\dot{\beta}}}{\text{denominator}} = \int \frac{((v+p_1)^2 - v^2) ((w+p_1)^2 - w^2)}{\text{denominator}} \end{aligned} \quad (\text{H.2.11})$$

Note that scalar products inside the  $x_i$  involving  $p_3$  do not produce irreducible propagators (H.1.1). However it is always possible to use conservation of external momenta and write

$$\begin{aligned} p_3^{\alpha\dot{\alpha}} v_{\alpha\dot{\alpha}} &= -p_{14}^{\alpha\dot{\alpha}} v_{\alpha\dot{\alpha}} - p_2^{\alpha\dot{\alpha}} v_{\alpha\dot{\alpha}} \\ &= -(v+p_{14})^2 + t + (v-p_2)^2 \end{aligned} \quad (\text{H.2.12})$$

Thus the  $x_i$ 's and, as a consequence the coefficients  $A, \dots, L$  of eq. (H.2.8), can be written like in the vector case as functions of the irreducible propagators only.

By using the definitions (H.2.11), the solutions of the system (H.2.10) read

$$\begin{aligned} A &= x_1 + \frac{t}{2su}x_2 - \frac{1}{2s}x_3 - \frac{1}{2u}x_4 - \frac{1}{2s}x_5 + \frac{u}{2st}x_6 - \frac{1}{2t}x_7 - \frac{1}{2u}x_8 - \frac{1}{2t}x_9 + \frac{s}{2tu}x_{10} \\ B &= \frac{t}{2su}x_1 + \frac{t^2}{2s^2u^2}x_2 - \frac{t}{2s^2u}x_3 - \frac{t}{2su^2}x_4 - \frac{t}{2s^2u}x_5 + \frac{1}{2s^2}x_6 - \frac{t}{2su^2}x_8 + \frac{1}{2u^2}x_{10} \\ C &= \frac{u}{2st}x_1 + \frac{1}{2s^2}x_2 - \frac{u}{2s^2t}x_3 - \frac{u}{2s^2t}x_5 + \frac{u^2}{2s^2t^2}x_6 - \frac{u}{2st^2}x_7 - \frac{u}{2st^2}x_9 + \frac{1}{2t^2}x_{10} \\ D &= \frac{s}{2tu}x_1 + \frac{1}{2u^2}x_2 - \frac{s}{2tu^2}x_4 + \frac{1}{2t^2}x_6 - \frac{s}{2t^2u}x_7 - \frac{s}{2tu^2}x_8 - \frac{s}{2t^2u}x_9 + \frac{s^2}{2t^2u^2}x_{10} \\ E &= -\frac{1}{2s}x_1 - \frac{t}{2s^2u}x_2 + \frac{1}{2s^2}x_3 + \frac{1}{2s^2}x_5 - \frac{u}{2s^2t}x_6 + \frac{1}{2st}x_7 + \frac{1}{2su}x_8 \\ F &= -\frac{1}{2s}x_1 - \frac{t}{2s^2u}x_2 + \frac{1}{2s^2}x_3 + \frac{1}{2su}x_4 + \frac{1}{2s^2}x_5 - \frac{u}{2s^2t}x_6 + \frac{1}{2st}x_9 \\ G &= -\frac{1}{2u}x_1 - \frac{t}{2su^2}x_2 + \frac{1}{2u^2}x_4 + \frac{1}{2su}x_5 + \frac{1}{2u^2}x_8 + \frac{1}{2tu}x_9 - \frac{s}{2tu^2}x_{10} \\ H &= -\frac{1}{2u}x_1 - \frac{t}{2su^2}x_2 + \frac{1}{2su}x_3 + \frac{1}{2u^2}x_4 + \frac{1}{2tu}x_7 + \frac{1}{2u^2}x_8 - \frac{s}{2tu^2}x_{10} \\ L &= -\frac{1}{2t}x_1 + \frac{1}{2st}x_3 - \frac{u}{2st^2}x_6 + \frac{1}{2t^2}x_7 + \frac{1}{2tu}x_8 + \frac{1}{2t^2}x_9 - \frac{s}{2t^2u}x_{10} \\ M &= -\frac{1}{2t}x_1 + \frac{1}{2tu}x_4 + \frac{1}{2st}x_5 - \frac{u}{2st^2}x_6 + \frac{1}{2t^2}x_7 + \frac{1}{2t^2}x_9 - \frac{s}{2t^2u}x_{10} \end{aligned} \quad (\text{H.2.13})$$

# Appendix I

## Building up the pure vector diagram

In this Appendix we describe which is the correct way to construct all the vacuum diagrams coming from the three point pure vector vertex. The cubic gauge vertex (see eq. (6.2.19)) is

$$-\frac{g}{2}(if^{abc}) \left( (\nabla^\alpha V)^a V^b (\bar{\nabla}^2 \nabla_\alpha V)^c + \frac{1}{3} (\nabla^\alpha V)^a V^b [iW_\alpha, V]^c \right) \quad (\text{I.0.1})$$

In what follows we analyze in detail what happens for the construction of the vacuum diagrams when the first term of this expression is contracted with itself. The rules so derived at the end of this section are applicable also when the second term of the vertex (I.0.1) is contracted with itself and when the mixed combinations are considered too.

In order to construct all two loop vacuum diagrams from the first part of the vertex (I.0.1) we have to contract in all possible ways two copies of the vertex. There are six possible different contractions, namely

$$f^{abc} f^{def} \times \left( (\nabla^\alpha V)^a V^b (\bar{\nabla}^2 \nabla_\alpha V)^c \right) \times \left( (\nabla^\alpha V)^d V^e (\bar{\nabla}^2 \nabla_\alpha V)^f \right) \quad (\text{I.0.2})$$



$$f^{abc} f^{def} \times \left( (\nabla^\alpha V)^a V^b (\bar{\nabla}^2 \nabla_\alpha V)^c \right) \times \left( (\nabla^\alpha V)^d V^e (\bar{\nabla}^2 \nabla_\alpha V)^f \right) \quad (\text{I.0.3})$$



$$f^{abc} f^{def} \times \left( (\nabla^\alpha V)^a V^b (\bar{\nabla}^2 \nabla_\alpha V)^c \right) \times \left( (\nabla^\alpha V)^d V^e (\bar{\nabla}^2 \nabla_\alpha V)^f \right) \quad (\text{I.0.4})$$



$$f^{abc} f^{def} \times \left( (\nabla^\alpha V)^a V^b (\bar{\nabla}^2 \nabla_\alpha V)^c \right) \times \left( (\nabla^\alpha V)^d V^e (\bar{\nabla}^2 \nabla_\alpha V)^f \right) \quad (\text{I.0.5})$$



$$f^{abc} f^{def} \times \left( (\nabla^\alpha V)^a V^b (\bar{\nabla}^2 \nabla_\alpha V)^c \right) \times \left( (\nabla^\alpha V)^d V^e (\bar{\nabla}^2 \nabla_\alpha V)^f \right) \quad (\text{I.0.6})$$



$$f^{abc} f^{def} \times \left( (\nabla^\alpha V)^a V^b (\bar{\nabla}^2 \nabla_\alpha V)^c \right) \times \left( (\nabla^\alpha V)^d V^e (\bar{\nabla}^2 \nabla_\alpha V)^f \right) \quad (\text{I.0.7})$$



Each contraction produces a different vacuum diagram. A very tricky point are the signs carried by each diagram. There are two sources of signs:

### 1) Color structure

We want to keep fixed the color factor  $f^{abc} f^{def}$  in front of each diagram. At the same time, we want that the legs of the vertices get contracted always in the following ordered way:

$$a \leftrightarrow d, \quad b \leftrightarrow e, \quad c \leftrightarrow f \quad (\text{I.0.8})$$

This optimal configuration can be obtained by relabeling color indices and by using the properties of the structure constants under exchange of indices. Signs can be produced while doing these exchanges.

### 2) Fermion exchanges

While the vacuum diagram is composed it is possible that fermionic legs of the left vertex has to jump across fermionic legs of the right vertex. We get a minus sign for each jump. For example, the contraction (I.0.2) takes a sign for fermion exchanges:

$$f^{abc} f^{def} \times \left( (\nabla^\alpha V)^a V^b (\bar{\nabla}^2 \nabla_\alpha V)^c \right) \times \left( (\nabla^\alpha V)^d V^e (\bar{\nabla}^2 \nabla_\alpha V)^f \right) =$$



$$= -f^{abc} f^{def} \times \left( (\nabla^\alpha V)^a (\nabla^\alpha V)^d \right) \times \left( V^b V^e \right) \times \left( (\bar{\nabla}^2 \nabla_\alpha V)^c (\bar{\nabla}^2 \nabla_\alpha V)^f \right) \quad (\text{I.0.9})$$





Expression (I.0.9) is what we usually represent pictorially in this way

The arrows indicate the sense in which the derivatives act (the left vertex derivatives towards right and vice versa).

Once all the six diagrams from equations (I.0.2)–(I.0.7) are composed following rules 1) and 2), it is convenient to free the middle line of spinorial derivatives by integrating them by parts on the left vertex\*. Note that by construction the middle line is free of spinorial derivatives at its right end. So, this is an operation that involves the left vertex only. While performing this operation carefulness must be used once again to signs: There is a minus for each derivative moved and a minus for each fermionic exchange.

The results, when the second cubic vertex in (I.0.1) is taken into account too, are exactly the vacuum diagrams represented in the “pure vector cubic diagrams” subsection of Section 6.2, the only difference being that the derivatives close to the right vertex operate towards the left and should be turned to be left–pointing derivatives. The rules to revert right–vertex derivatives are described with accuracy in Section 6.2.

The procedure here described is different with respect to what we did following [100]. In this Appendix, in fact, we start by constructing diagrams and then we rearrange them. In [100] and in our computation in Section 6.2 the procedure starts by managing vertices and constructing diagrams just at the final stage. This second procedure is eventually faster, since possible cancellations between various contributions occurs immediately in the vertices, not only in the final stage of the computation. However, in order to follow this second procedure we need a list of rules to keep under control the signs. The procedure is the following

**A) For the left vertex:**

- 1) Consider the vertices as they are written in (I.0.1). Write all possible permutation of the legs of the vertex. In our case, this means to consider six

---

\*The convenience follows from the fact that there is a remarkable cancellations between the diagrams involving the second vertex in (I.0.1) with the diagrams that come out after this reshuffling of vacuum graphs from the first vertex in (I.0.1). Note that in principle one can do  $\nabla$ -algebra even on not-free middle-line diagrams. However the number of vacuum diagrams increases considerably.

different permutations of the vertex. From the color point of view, three of them are cyclic and three anti-cyclic. Signs in front of each term are determined by **fermion exchanges** while permuting the legs of the vertex and by **color** (anti-cyclic permutations get an extra minus sign).

- 2) By integrating by parts spinorial derivatives on each of the various permutations, free out the middle line. For the signs, there is a minus sign for each spinorial derivative moved and an extra minus sign for each fermionic exchange.

At the end of these operations we are left with an expression that can be reduced to equation (6.1.7).

### **B) For the right vertex:**

Use vertex (I.0.1) as it appears there. Remember that the derivatives of this vertex must be thought to operate towards the left. This can in principle produce signs and exchange of reciprocal position of derivatives when they are converted to derivatives pointing to the right. A clear exposition of this operation is in Section 6.2.

### **C) Composing the diagrams:**

Join left vertex legs with right vertex legs. Lines must be closed by looking at their positions: Upper with upper, central with central, lower with lower. Pick up an extra minus sign if a fermionic leg of the right vertex jumps across a fermionic line of the left vertex.

Signs in front of vacuum diagrams at the end of this quick procedure turn out to be the same as the signs at the end of the more pedestrian procedure described in the first part of this Appendix.

# Appendix J

## *Pierre*

*Pierre* is a set of programs that provides an automatization of many passages of the superspace approach to scattering amplitudes.

### J.1 PC can make your life easier

There are three main troubles that one has to deal with when a direct computation of a scattering amplitude is done by hand in superspace:

- 1) There are many contributing diagrams;
- 2) Each diagram is the result of a lot of algebraic passages;
- 3) There are both fermionic and bosonic objects.

The consequences of these problems are that hand made computations take a considerable time. Moreover, the presence of fermionic fields introduce a lot of occasions for sign errors so that to become confident with the results of long computations longer and longer checks are required. It is certainly not impossible to perform a perfect hand made computation. However, every technique that speeds up the computation and makes it safer, can make easier the life of a Ph.D. student and are welcome.

The possibility of make automatic the superspace approach to scattering amplitudes by implementing it on the PC is based on two important aspects of the background field method: 1) There are only a few basic objects, namely the background fields  $W^\alpha$ ,  $\overline{W}^{\dot{\alpha}}$ , the covariant derivatives  $\nabla_\alpha$ ,  $\overline{\nabla}_{\dot{\alpha}}$  and  $\nabla_{\alpha\dot{\alpha}}$  and the covariant propagator  $\frac{1}{\square}$ ; 2) The basic relations between these objects are the algebraic relations of eq. (B.0.1). All the passages along the computation can be reduced to this small core-set of relations.

Algebraic relations are easily implemented on a PC by using symbolic calculus programs. Most parts of *Pierre* have been written in FORM, one of the most efficient symbolic manipulation systems [121, 122]. However, some part of *Pierre* is based on hybrid programs that move from FORM to more common computer algebra systems like Mathematica.

The automatization of the computational procedures requires two elements:

- 1) A dictionary between superspace objects and *Pierre*'s corresponding elements. In particular, this requires the programs to be able to deal with spinorial structures and fermionic objects;
- 2) The segmentation of the full computational procedure in a set of more elementary routines and the definition of a precise sequence in which these routines must be called to reproduce the full computation.

In the next two Sections we give a more detailed description on these aspects of *Pierre*.

A third element, although not necessary, turns out to be useful: *Pierre*'s output data are written in *Pierre*'s language. An interface between its language and L<sup>A</sup>T<sub>E</sub>X textual language makes PC results much more readable. Two different interfaces have been created for translating strings of superfields and superdiagrams. They make use of programming languages like Perl and stream editors like Sed. Unfortunately, *Pierre*'s outputs consist in a larger class of objects, including loop integrals too, for which a translator have not been arranged for the moment.

## J.2 *Pierre*'s dictionary

Each basic object in superspace has a specific name in *Pierre*'s FORM language. The correspondence between what we usually read in papers (T<sub>E</sub>X column) and what we should write for *Pierre* is recorded in the Tab J.1.

It is worth to mention that only the Ricci tensor  $c^{\alpha\beta}$  is defined as a commuting function while all other objects are non-commuting functions. In the Table, the number of empty slots after each function in *Pierre* column corresponds to the number of indexes supported by each field in Superspace. However, we remind that functions in FORM do not have limitations on the number of the indexes.

The control of spinorial structures is extremely important in superspace. Each string of superspace objects carries upper and lower dotted and undotted indices. In *Pierre* upper and lower indices are distinct by the prefix *U* and *L* while a suffix *d* distinguish the dotted indices from the undotted ones. So, we have

$$\begin{array}{ll}
 \text{U}\alpha \equiv \alpha & \text{upper, undotted} & \text{L}\alpha \equiv \alpha & \text{lower, undotted} \\
 \text{U}\alpha\dot{\phantom{\alpha}} \equiv \dot{\alpha} & \text{upper, dotted} & \text{L}\alpha\dot{\phantom{\alpha}} \equiv \dot{\alpha} & \text{lower, dotted}
 \end{array} \quad (\text{J.2.2})$$

$\text{T}_{\text{E}}\text{X}$	<i>Pierre</i>	$\text{T}_{\text{E}}\text{X}$	<i>Pierre</i>
$\nabla^\alpha$	$D( )$	$\overline{\nabla}^\alpha$	$Db( )$
$\nabla^2$	$D2$	$\overline{\nabla}^2$	$Db2$
$\nabla^{\alpha\dot{\alpha}}$	$D( , )$	$\square$	Box
$\frac{1}{\square}$	oBox	$\frac{1}{\square}$	proph
$\frac{1}{\square}_+$	proplus	$\frac{1}{\square}_-$	prominus
$\frac{1}{\square}_0$	oBoxzero	$(\frac{1}{\square} - \frac{1}{\square}_0)$	oBoxprime
$W^\alpha$	$W( )$	$\overline{W}^\alpha$	$Wb( )$
$(\nabla^\alpha W^\beta)$	$DW( , )$	$(\overline{\nabla}^\alpha \overline{W}^\beta)$	$DbWb( , )$
$(\nabla^{\alpha\dot{\alpha}} W^\beta)$	$MW( , , )$	$(\nabla^{\alpha\dot{\alpha}} \overline{W}^\beta)$	$MWb( , , )$
$(\nabla^{\alpha\dot{\alpha}} (\nabla^\beta W^\gamma))$	$MDW( , , , )$	$(\nabla^{\alpha\dot{\alpha}} (\overline{\nabla}^\beta \overline{W}^\gamma))$	$MDbWb( , , , )$
$c^{\alpha\beta}$	$C( , )$		

(J.2.1)

Table J.1: Basic definitions of superspace objects in *Pierre*'s language

Indexes can be contracted or free. Contracted indices, when moved updown, take a sign while free indices can be lowered or uppered when opportunely contracted with a Ricci symbol. *Pierre* supports these two operations too. In particular the first one is accomplished by requiring that in a string of superfields a couple of contracted indices has always the first index up and the second down.

Contracted indices satisfy another important convention, the Einstein summation rule. *Pierre* cannot understand what a mute upper or lower index is\*. In spite of this, it is possible to fix the freedom on the relabeling of indices by imposing a conventional rule for labeling the contracted couples of indices. This standardization in the names gives advantages also for the  $\text{L}^{\text{A}}\text{T}_{\text{E}}\text{X}$  translators.

*Pierre* supports other functions that are not reported in Tab J.1. Two of them are *separe* and *one*: These are not objects with a correspondent in superspace but they have a topological sense. *separe* specifies where a line ends in a Feynman supergraph. Feynman diagrams in *Pierre*'s language are strings of fields separated by the function *separe*. For

---

\*In FORM mute indices exist but they are all lower indices. Thus they are not suitable for computations in superspace

example

$$\begin{array}{c} \frac{1}{\square} W^\alpha \frac{1}{\square} \\ \circlearrowleft \\ \frac{1}{\square_0} \\ \circlearrowright \\ \frac{1}{\square} W_\alpha \frac{1}{\square} \end{array} \equiv \text{oBox}^*W(Ua)^*\text{oBox}^*\text{separe}^*\text{oBoxzero}^*\text{separe}^*\text{oBox}^*W(La)^*\text{oBox}$$

(J.2.3)

On the other hand, a string like

$$\text{separe}^*\text{one}^*\text{separe} \tag{J.2.4}$$

is the result of the product of  $\frac{1}{\square} \square = 1$  on a the middle line. This means that the middle line is free of propagators and has to be interpreted as a point. Tadpole-like diagrams are characterized by the function *one* on the middle line.

Other important functions are *Pierre's* correspondents for the coefficients of the covariant propagators (see Appendices C and D for their definition in superspace). Each coefficient in *Pierre* is identified by a letter  $A, B, \dots, L$  and by the termination **box**. Thus, in general they have the following structure

$$(\text{prefix}) - \mathbf{X} - (\text{suffix}) - \mathbf{box}$$

where  $\mathbf{X}$  stay for a general letter  $A, B, \dots, L$ . There are two possible prefixes: **mc** and **bar** that stay respectively for the calligraphic coefficients  $\mathcal{A}, \mathcal{B}, \dots, \mathcal{L}$  and for barred coefficients  $\overline{A}, \overline{B}, \dots, \overline{L}$ . Barred calligraphic coefficients are identified by the combined prefix **mbar**. A suffix **h** and **t** is used for hatted and tilted coefficients as they have been defined in Section 6.3.1. So, for example we have

$$\begin{aligned} B^\alpha &\equiv \text{Bbox}(\text{La}) \\ \tilde{\mathcal{E}}_{\alpha\beta\dot{\alpha}} &\equiv \text{mbarEtbox}(\text{La}, \text{La1}, \text{Lad}) \end{aligned} \tag{J.2.5}$$

### J.3 Main routines

The computation of the  $n$  point effective action in superspace can be divided in three main parts

- 1) The computation of the master equation valid for a generic number of scattered particles;

- 2) The power series expansion of the coefficients of the covariant propagators up to the wanted number of external fields and with a specific helicity configuration;
- 3) The extraction from the master equation of the  $n$ -point effective action.

*Pierre* provides an automatization of each of these operations with specific routines. A partial concatenation of the routines has been programmed in various executable shell scripts. A full concatenation of these three main steps has not been produced so that, in order to compute a specific amplitude, manual work is still required. However, the segmentation in these three steps is not a negative feature. In fact, a rigid recursive procedure, like a full automatic procedure would be, is unable to find important simplifications in the results that follow from the many identities between the propagator coefficients (see Appendices C and D). The cancellation of the UV divergences in Section 6.3 furnishes a clear example of this fact.

In what follows, we describe in detail which parts of the computation are completely automatic.

### J.3.1 Computing the master equation

As we have described in Chapter 6, the computation of the all- $n$  expression for the effective action can be divided in three steps: 1) Compute the vertices of the theory from the lagrangian; 2) Build up the vacuum diagrams and the combinatorial factors; 3) Compute the  $\nabla$ -algebra on each vacuum diagram.

The heavier and most important part of the computation is the third one. *Pierre* supplies for an automatic computation of the  $\nabla$ -algebra of one loop diagrams and two loop cubic vertices diagrams. Also two loop tadpole like diagrams can be computed by *Pierre* by considering them as products of two one loop diagrams. The inputs are simply the propagators and the covariant derivatives that define a vacuum diagram. Helicity and planarity conditions are optional conditions: In principle, *Pierre* can perform the  $\nabla$ -algebra without using any of these hypothesis.

All the results of Section 6.2 have been computed or checked by *Pierre*. In particular, all the two loop vacuum diagrams of the  $\mathcal{N} = 4$  theory have been collected in a data file. A shell script, *dalgebra.sh*, allows to call them and to process the automatic  $\nabla$ -algebra computation. The economy of time is remarkable: Each vacuum diagram is computed in about  $10^2$  seconds.

We stress that combinatorial factors and eventual signs that come out when a vacuum diagram is constructed<sup>†</sup> are not included in *Pierre* and must be computed separately.

---

<sup>†</sup>See Appendix I

### J.3.2 Computing the coefficients

The coefficients of the covariant propagators can be divided in two classes by looking at their origin. The coefficients of  $\frac{1}{\square_+}$ ,  $\frac{1}{\square_-}$  and  $\frac{1}{\square}$  can be considered as primary coefficients. All the other coefficients can be derived from them through the identities (C.0.29)–(C.0.34) and (D.0.19)–(D.0.21). *Pierre* can compute this second class of coefficients from the first one: The computation of the primary coefficients must be performed separately by hand. An improvement to include an automatic computation of the primary coefficients is in progress.

We have expanded most of the coefficients (although not all of them) up to six external fields and requiring at most two consecutive  $\overline{W}$ . The results have been stored in a database in *Pierre*'s language. In principle, these data are sufficient to compute MHV amplitudes involving up to six particles in any SYM theory.

It is important to remark that the computation of the non-primary coefficients can be performed by hand without using the identities between the coefficients. This alternative derivation can be used as a check of *Pierre*'s results. We have performed this check up to three external fields finding a perfect agreement between *Pierre*'s and hand made results. We remind that the expansion up to three external fields is required for the computation of the four points effective action in  $\mathcal{N} = 4$  SYM theory.

### J.3.3 Computing the $n$ -point effective action

The extraction of a fixed  $n$ -point effective action from an all- $n$  master equation is a complicated operation. As it has been described in Chapter 7 for the easiest four point case, it is not sufficient to expand the coefficients up to the required order and to replace this expansion in the master equation but a lot of other operations are necessary. Just to mention the principal ones we remember the imposition of the Up-Down and Left-Right symmetries, the integration by parts of the spinorial derivatives, the Fourier transform to momentum space, the Passarino-Veltman reduction of vector and tensor integrals.

All these operations have been implemented in *Pierre* in distinct shell scripts. The programs have been optimized in order to extrapolate the four point MHV effective action in  $\mathcal{N} = 4$  SYM theory. However, they can be easily expanded to more general cases.

The names of the main shell scripts written and their functions have been summarized in Tab J.2.

The extraction of the four point effective action in configuration space is done automatically from the all- $n$  effective action through a concatenation of many of these simpler scripts. The concatenation is performed through another shell script, *legoland.sh*. The output of this program are two data files that include respectively the two point contributions and the sum of the four and the three point contributions enhanced to four point



through the integration by parts of spinorial derivatives (see Section 7.1.2). In order to get the full four point effective action it is necessary to elaborate the two point contributions manually as it has been described in Section 7.1.1.

The passage from configuration space to momentum space is done by using more scripts: After the Fourier transformation (*reading.sh*) it is possible to implement a lot of simplifications due to on-shell conditions (*simply.sh*) and to the resummation of antisymmetric structures through the Ricci symbol (*antisym.sh*)

$$\Phi_\alpha \Psi_\beta - \Phi_\beta \Psi_\alpha = c_{\beta\alpha} \Phi^\gamma \Psi_\gamma$$

After these operations, the result presents scalar loop integrals as well as tensor and vector integrals. The PV reduction of these last two kinds of integrals is performed through the scripts *PVtens.sh* and *PVvet.sh* respectively. These scripts are written part in **FORM** and part in **Mathematica**.

All the operations in momentum space require the control of both the loop integral structures and the spinorial structures. The denominator of the loop integrals is easily handled in *Pierre* by assign to each of the topologies of Fig G.3 a different name. Unfortunately this notation has not permitted to construct a program to implement the symmetries of scalar integrals.

A general scheme of *Pierre* is given in Fig J.1. We have put in boxes the main steps of the computation and in ovals the automatic passages performed by *Pierre*. Rhombuses highlight the part of the computation that, unfortunately, still need manual work.

It is worth to mention that beyond *Pierre* other programs have been useful in the computation scattered along the second part of this thesis. In particular, they are *FIRE* [123] and *FIESTA* [124], **Mathematica** based tools for the reduction of loop integrals to master integrals and for their numerical evaluation.

Shell script	Operation
<i>updown.sh</i>	Up–Down symmetry
<i>leftright.sh</i>	Left–Right symmetry
<i>renameforlego.sh</i>	Relabeling of superdiagrams
<i>spinorial.sh</i>	Integration by parts of spinorial derivatives
<i>colino.sh</i>	Selector of 4 pts MHV diagrams only
<i>MHVselector4.sh</i>	Selector of up to 4 pts MHV diagrams
<i>selector3.sh</i>	Selector of 3 pts diagrams
<i>selector2.sh</i>	Selector of 2 pts diagrams
<i>reading.sh</i>	Fourier transform to momentum space
<i>plus.sh</i>	To sum various stuff
<i>simply.sh</i>	On–shell conditions in momentum space
<i>antisym.sh</i>	Antisymmetrization conditions in momentum space
<i>PVvet.sh</i>	PV reduction of vector integrals
<i>PVtens.sh</i>	PV reduction of tensor integrals
<i>toprint.sh</i>	L <sup>A</sup> T <sub>E</sub> X translator for strings of superfields
<i>topaint.sh</i>	L <sup>A</sup> T <sub>E</sub> X translator for superfields

Table J.2: List of shell scripts for the extraction of a specific amplitude from a master equation.

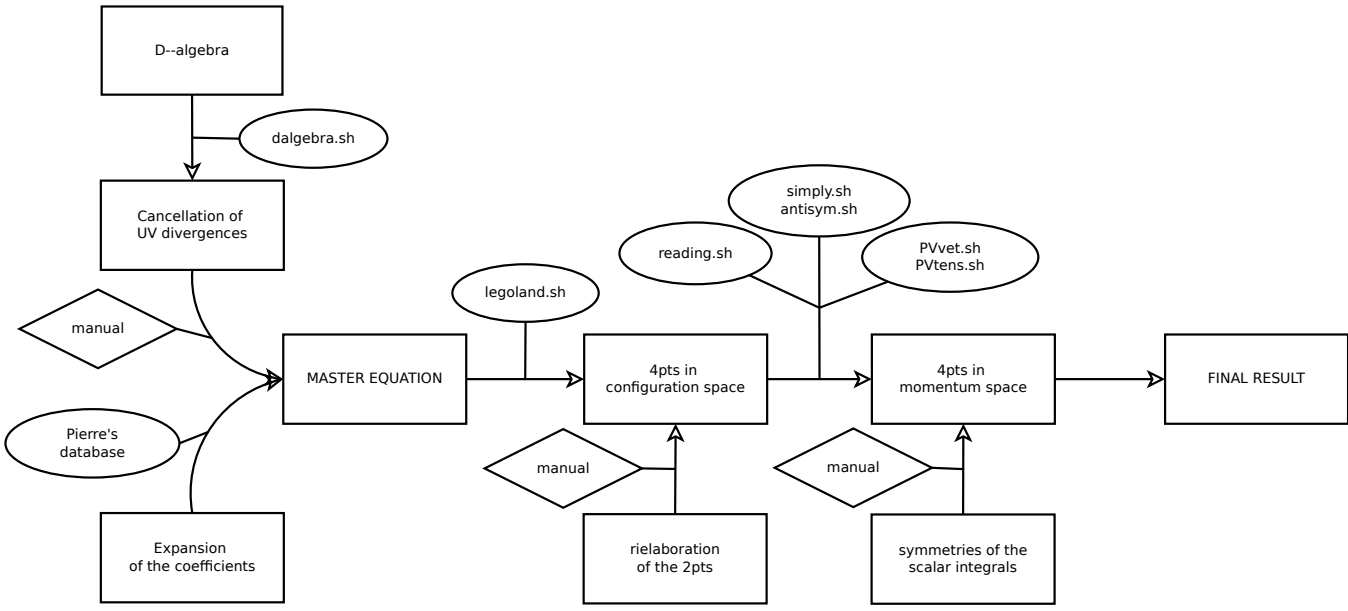


Figure J.1: Scheme of *Pierre*



# Bibliography

- [1] S. J. Gates, M. T. Grisaru, M. Rocek and W. Siegel, “Superspace, or one thousand and one lessons in supersymmetry,” *Front. Phys.* **58** (1983) 1 [arXiv:hep-th/0108200].
- [2] J. M. Maldacena, *Adv. Theor. Math. Phys.* **2** (1998) 231 [*Int. J. Theor. Phys.* **38** (1999) 1113] [arXiv:hep-th/9711200];  
S. S. Gubser, I. R. Klebanov and A. M. Polyakov, *Phys. Lett. B* **428** (1998) 105 [arXiv:hep-th/9802109];  
E. Witten, *Adv. Theor. Math. Phys.* **2** (1998) 253 [arXiv:hep-th/9802150].
- [3] G. 't Hooft, *Nucl. Phys. B* **72**, 461 (1974).
- [4] L. Brink, J. H. Schwarz and J. Scherk, *Nucl. Phys. B* **121**, 77 (1977).
- [5] F. Gliozzi, J. Scherk and D. I. Olive, *Nucl. Phys. B* **122**, 253 (1977).
- [6] P. Fayet, *Nucl. Phys. B* **149**, 137 (1979).
- [7] M. T. Grisaru, M. Roček and W. Siegel, *Nucl. Phys. B* **159** (1979) 429.
- [8] M. T. Grisaru, M. Rocek and W. Siegel, *Phys. Rev. Lett.* **45**, 1063 (1980).
- [9] M. T. Grisaru, M. Rocek and W. Siegel, *Nucl. Phys. B* **183**, 141 (1981).
- [10] S. Mandelstam, *Nucl. Phys. B* **213**, 149 (1983).
- [11] L. Brink, O. Lindgren and B. E. W. Nilsson, *Phys. Lett. B* **123**, 323 (1983).
- [12] M. T. Grisaru and W. Siegel, *Nucl. Phys. B* **201**, 292 (1982) [Erratum-ibid. *B* **206**, 496 (1982)].
- [13] N. Marcus and A. Sagnotti, *Phys. Lett. B* **135**, 85 (1984).
- [14] N. Marcus and A. Sagnotti, *Nucl. Phys. B* **256**, 77 (1985).
- [15] J. Polchinski, *Phys. Rev. Lett.* **75**, 4724 (1995) [arXiv:hep-th/9510017].
- [16] J. Polchinski, arXiv:hep-th/9611050.

- [17] G. T. Horowitz and A. Strominger, Nucl. Phys. B **360**, 197 (1991).
- [18] O. Aharony, S. S. Gubser, J. M. Maldacena, H. Ooguri and Y. Oz, Phys. Rept. **323**, 183 (2000) [arXiv:hep-th/9905111].
- [19] O. Lunin and J. Maldacena, JHEP **0505** (2005) 033 [arXiv:hep-th/0502086].
- [20] S. Frolov, JHEP **0505** (2005) 069 [arXiv:hep-th/0503201].
- [21] I. R. Klebanov and E. Witten, Nucl. Phys. B **536**, 199 (1998) [arXiv:hep-th/9807080].
- [22] D. Martelli and J. Sparks, Commun. Math. Phys. **262**, 51 (2006) [arXiv:hep-th/0411238].
- [23] S. Benvenuti, S. Franco, A. Hanany, D. Martelli and J. Sparks, JHEP **0506**, 064 (2005) [arXiv:hep-th/0411264].
- [24] D. Martelli and J. Sparks, Phys. Lett. B **621**, 208 (2005) [arXiv:hep-th/0505027]; M. Cvetič, H. Lu, D. N. Page and C. N. Pope, Phys. Rev. Lett. **95**, 071101 (2005) [arXiv:hep-th/0504225].
- [25] A. Butti, D. Forcella and A. Zaffaroni, JHEP **0509**, 018 (2005) [arXiv:hep-th/0505220].
- [26] I. R. Klebanov and M. J. Strassler, JHEP **0008**, 052 (2000) [arXiv:hep-th/0007191].
- [27] J. M. Maldacena and C. Nunez, Phys. Rev. Lett. **86**, 588 (2001) [arXiv:hep-th/0008001].
- [28] J. Polchinski and M. J. Strassler, arXiv:hep-th/0003136.
- [29] E. Witten, Adv. Theor. Math. Phys. **2**, 505 (1998) [arXiv:hep-th/9803131].
- [30] A. Karch and E. Katz, JHEP **0206**, 043 (2002) [arXiv:hep-th/0205236].
- [31] A. Karch, E. Katz and N. Weiner, Phys. Rev. Lett. **90**, 091601 (2003) [arXiv:hep-th/0211107].
- [32] J. Erdmenger, N. Evans, I. Kirsch and E. Threlfall, Eur. Phys. J. A **35**, 81 (2008) [arXiv:0711.4467 [hep-th]].
- [33] E. Bergshoeff, M. de Roo, E. Eyras, B. Janssen and J. P. van der Schaar, Nucl. Phys. B **494**, 119 (1997) [arXiv:hep-th/9612095].
- [34] D. Arean and A. V. Ramallo, JHEP **0604**, 037 (2006) [arXiv:hep-th/0602174].
- [35] O. Aharony, A. Fayyazuddin and J. M. Maldacena, JHEP **9807**, 013 (1998) [arXiv:hep-th/9806159].

- [36] M. Kruczenski, D. Mateos, R. C. Myers and D. J. Winters, JHEP **0307**, 049 (2003) [arXiv:hep-th/0304032].
- [37] T. Sakai and J. Sonnenschein, JHEP **0309**, 047 (2003) [arXiv:hep-th/0305049];  
P. Ouyang, Nucl. Phys. B **699**, 207 (2004) [arXiv:hep-th/0311084];  
D. Arean, D. E. Crooks and A. V. Ramallo, JHEP **0411**, 035 (2004) [arXiv:hep-th/0408210];  
S. Kuperstein, JHEP **0503**, 014 (2005) [arXiv:hep-th/0411097];  
T. S. Levi and P. Ouyang, arXiv:hep-th/0506021.
- [38] X. J. Wang and S. Hu, JHEP **0309**, 017 (2003) [arXiv:hep-th/0307218];  
C. Nunez, A. Paredes and A. V. Ramallo, JHEP **0312**, 024 (2003) [arXiv:hep-th/0311201];  
F. Canoura, A. Paredes and A. V. Ramallo, JHEP **0509**, 032 (2005) [arXiv:hep-th/0507155].
- [39] F. Canoura, J. D. Edelstein, L. A. P. Zayas, A. V. Ramallo and D. Vaman, JHEP **0603**, 101 (2006) [arXiv:hep-th/0512087];  
F. Canoura, J. D. Edelstein and A. V. Ramallo, JHEP **0609**, 038 (2006) [arXiv:hep-th/0605260].
- [40] R. Apreda, J. Erdmenger, D. Lust and C. Sieg, JHEP **0701**, 079 (2007) [arXiv:hep-th/0610276];  
C. Sieg, JHEP **0708**, 031 (2007) [arXiv:0704.3544 [hep-th]].
- [41] D. Arean, A. Paredes and A. V. Ramallo, JHEP **0508**, 017 (2005) [arXiv:hep-th/0505181].
- [42] N. R. Constable, J. Erdmenger, Z. Guralnik and I. Kirsch, Phys. Rev. D **68**, 106007 (2003) [arXiv:hep-th/0211222];  
M. Kruczenski, D. Mateos, R. C. Myers and D. J. Winters, JHEP **0405**, 041 (2004) [arXiv:hep-th/0311270];  
R. C. Myers and R. M. Thomson, JHEP **0609**, 066 (2006) [arXiv:hep-th/0605017].
- [43] D. Arean and A. V. Ramallo, JHEP **0604**, 037 (2006) [arXiv:hep-th/0602174].
- [44] J. Babington, J. Erdmenger, N. J. Evans, Z. Guralnik and I. Kirsch, Phys. Rev. D **69**, 066007 (2004) [arXiv:hep-th/0306018].
- [45] N. J. Evans and J. P. Shock, Phys. Rev. D **70**, 046002 (2004) [arXiv:hep-th/0403279];  
N. Evans, J. P. Shock and T. Waterson, JHEP **0503**, 005 (2005) [arXiv:hep-th/0502091].
- [46] S. A. Cherkis and A. Hashimoto, JHEP **0211**, 036 (2002) [arXiv:hep-th/0210105];  
H. Nastase, arXiv:hep-th/0305069;  
B. A. Burrington, J. T. Liu, L. A. Pando Zayas and D. Vaman, JHEP **0502**, 022

- (2005) [arXiv:hep-th/0406207];  
 J. Erdmenger and I. Kirsch, JHEP **0412**, 025 (2004) [arXiv:hep-th/0408113];  
 I. Kirsch and D. Vaman, Phys. Rev. D **72**, 026007 (2005) [arXiv:hep-th/0505164];  
 R. Casero, C. Nunez and A. Paredes, Phys. Rev. D **73**, 086005 (2006) [arXiv:hep-th/0602027];  
 A. Paredes, JHEP **0612**, 032 (2006) [arXiv:hep-th/0610270];  
 F. Benini, F. Canoura, S. Cremonesi, C. Nunez and A. V. Ramallo, JHEP **0702**, 090 (2007) [arXiv:hep-th/0612118];  
 R. Casero and A. Paredes, Fortsch. Phys. **55**, 678 (2007) [arXiv:hep-th/0701059];  
 F. Benini, F. Canoura, S. Cremonesi, C. Nunez and A. V. Ramallo, JHEP **0709**, 109 (2007) [arXiv:0706.1238 [hep-th]];  
 B. A. Burrington, V. S. Kaplunovsky and J. Sonnenschein, arXiv:0708.1234 [hep-th];  
 F. Benini, arXiv:0710.0374 [hep-th];  
 R. Casero, C. Nunez and A. Paredes, arXiv:0709.3421 [hep-th].
- [47] I. Kirsch, JHEP **0609**, 052 (2006) [arXiv:hep-th/0607205].
- [48] D. Arean, A. V. Ramallo and D. Rodriguez-Gomez, Phys. Lett. B **641**, 393 (2006) [arXiv:hep-th/0609010];  
 D. Arean, A. V. Ramallo and D. Rodriguez-Gomez, JHEP **0705**, 044 (2007) [arXiv:hep-th/0703094].
- [49] V. G. Filev, C. V. Johnson, R. C. Rashkov and K. S. Viswanathan, arXiv:hep-th/0701001;  
 V. G. Filev, arXiv:0706.3811 [hep-th].
- [50] D. Mateos, R. C. Myers and R. M. Thomson, JHEP **0705**, 067 (2007) [arXiv:hep-th/0701132];  
 R. C. Myers, A. O. Starinets and R. M. Thomson, arXiv:0706.0162 [hep-th].
- [51] J. Erdmenger, M. Kaminski and F. Rust, Phys. Rev. D **76**, 046001 (2007) [arXiv:0704.1290 [hep-th]];  
 J. Erdmenger, K. Ghoroku and I. Kirsch, JHEP **0709**, 111 (2007) [arXiv:0706.3978 [hep-th]].
- [52] R. de Mello Koch, N. Ives, J. Smolic and M. Smolic, Phys. Rev. D **73**, 064007 (2006) [arXiv:hep-th/0509007];  
 A. Hamilton and J. Murugan, JHEP **0706**, 036 (2007) [arXiv:hep-th/0609135].
- [53] R. Hernandez, K. Sfetsos and D. Zoakos, JHEP **0603**, 069 (2006) [arXiv:hep-th/0510132].
- [54] M. Spradlin, T. Takayanagi and A. Volovich, JHEP **0511**, 039 (2005) [arXiv:hep-th/0509036].



- [55] M. Pirrone, JHEP **0612**, 064 (2006) [arXiv:hep-th/0609173];  
M. Pirrone, JHEP **0803**, 034 (2008) [arXiv:0801.2540 [hep-th]].
- [56] E. Imeroni and A. Naqvi, JHEP **0703**, 034 (2007) [arXiv:hep-th/0612032].
- [57] A. Mariotti, JHEP **0709**, 123 (2007) [arXiv:0705.2563 [hep-th]].
- [58] S. D. Avramis, K. Sfetsos and D. Zoakos, arXiv:0704.2067 [hep-th];  
J. Kluson and K. L. Panigrahi, arXiv:0710.0148 [hep-th].
- [59] A. A. Tseytlin, Nucl. Phys. B **487**, 141 (1997) [arXiv:hep-th/9609212].
- [60] J. P. Gauntlett, D. Martelli, S. Pakis and D. Waldram, Commun. Math. Phys. **247**  
(2004) 421 [arXiv:hep-th/0205050].
- [61] M. Grana, R. Minasian, M. Petrini and A. Tomasiello, JHEP **0408**, 046 (2004)  
[arXiv:hep-th/0406137];  
M. Grana, R. Minasian, M. Petrini and A. Tomasiello, JHEP **0511**, 020 (2005)  
[arXiv:hep-th/0505212];  
R. Minasian, M. Petrini and A. Zaffaroni, JHEP **0612**, 055 (2006) [arXiv:hep-  
th/0606257];  
L. Martucci and P. Smyth, JHEP **0511**, 048 (2005) [arXiv:hep-th/0507099].
- [62] P. Breitenlohner and D. Z. Freedman, Phys. Lett. B **115**, 197 (1982); Annals Phys.  
**144**, 249 (1982).
- [63] R. Lehoucq, J. Uzan and J. Weeks, Kodai Math. J. **26**, 119 (2003)  
[arXiv:math/0202072].
- [64] T. Albash, V. Filev, C. V. Johnson and A. Kundu, arXiv:0709.1547 [hep-th];  
J. Erdmenger, R. Meyer and J. P. Shock, arXiv:0709.1551 [hep-th];  
T. Albash, V. Filev, C. V. Johnson and A. Kundu, arXiv:0709.1554 [hep-th].
- [65] S. Hong, S. Yoon and M. J. Strassler, JHEP **0404**, 046 (2004) [arXiv:hep-  
th/0312071].
- [66] N. Beisert and R. Roiban, JHEP **0508**, 039 (2005) [arXiv:hep-th/0505187];  
S. A. Frolov, R. Roiban and A. A. Tseytlin, Nucl. Phys. B **731**, 1 (2005) [arXiv:hep-  
th/0507021].
- [67] A. Mauri, S. Penati, A. Santambrogio and D. Zanon, JHEP **0511**, 024 (2005)  
[arXiv:hep-th/0507282].
- [68] F. Cachazo, P. Svrcek and E. Witten, JHEP **0409**, 006 (2004) [arXiv:hep-  
th/0403047].
- [69] V. A. Smirnov and O. L. Veretin, Nucl. Phys. B **566**, 469 (2000) [arXiv:hep-  
ph/9907385].

- [70] H. Lehmann, K. Symanzik and W. Zimmermann, *Nuovo Cim.* **1**, 205 (1955).
- [71] M. T. Grisaru and H. N. Pendleton, *Nucl. Phys. B* **124**, 81 (1977).
- [72] F. A. Berends and W. T. Giele, *Nucl. Phys. B* **306**, 759 (1988).
- [73] F. Cachazo, P. Svrcek and E. Witten, *JHEP* **0409**, 006 (2004) [arXiv:hep-th/0403047];  
G. Georgiou and V. V. Khoze, *JHEP* **0405**, 070 (2004) [arXiv:hep-th/0404072];  
G. Georgiou, E. W. N. Glover and V. V. Khoze, *JHEP* **0407**, 048 (2004) [arXiv:hep-th/0407027].
- [74] R. Britto, F. Cachazo, B. Feng and E. Witten, *Phys. Rev. Lett.* **94**, 181602 (2005) [arXiv:hep-th/0501052].
- [75] S. J. Parke and T. R. Taylor, *Phys. Rev. Lett.* **56**, 2459 (1986).
- [76] Z. Bern and A. G. Morgan, *Nucl. Phys. B* **467**, 479 (1996) [arXiv:hep-ph/9511336].
- [77] C. Anastasiou, R. Britto, B. Feng, Z. Kunszt and P. Mastrolia, *JHEP* **0703**, 111 (2007) [arXiv:hep-ph/0612277].
- [78] Z. Bern, L. J. Dixon, D. C. Dunbar and D. A. Kosower, *Nucl. Phys. B* **425**, 217 (1994) [arXiv:hep-ph/9403226].
- [79] K. G. Chetyrkin, A. L. Kataev and F. V. Tkachov, *Nucl. Phys. B* **174** (1980) 345;
- [80] K. G. Chetyrkin and F. V. Tkachov, *Nucl. Phys. B* **192** (1981) 159.
- [81] T. Gehrmann and E. Remiddi, *Nucl. Phys. B* **580**, 485 (2000) [arXiv:hep-ph/9912329].
- [82] V. A. Smirnov and O. L. Veretin, *Nucl. Phys. B* **566**, 469 (2000) [arXiv:hep-ph/9907385].
- [83] T. Gehrmann and E. Remiddi, *Nucl. Phys. B* **601**, 248 (2001) [arXiv:hep-ph/0008287].
- [84] Z. Bern, L. J. Dixon and D. A. Kosower, *JHEP* **0408**, 012 (2004) [arXiv:hep-ph/0404293].
- [85] Z. Bern, J. S. Rozowsky and B. Yan, *Phys. Lett. B* **401**, 273 (1997) [arXiv:hep-ph/9702424].
- [86] Z. Bern, J. J. M. Carrasco, H. Johansson and D. A. Kosower, *Phys. Rev. D* **76**, 125020 (2007) [arXiv:0705.1864 [hep-th]].

- [87] Z. Bern, M. Czakon, D. A. Kosower, R. Roiban and V. A. Smirnov, Phys. Rev. Lett. **97**, 181601 (2006) [arXiv:hep-th/0604074].
- [88] Z. Bern, L. J. Dixon, D. A. Kosower, R. Roiban, M. Spradlin, C. Vergu and A. Volovich, Phys. Rev. D **78**, 045007 (2008) [arXiv:0803.1465 [hep-th]].
- [89] F. Cachazo, M. Spradlin and A. Volovich, Phys. Rev. D **78**, 105022 (2008) [arXiv:0805.4832 [hep-th]].
- [90] C. Anastasiou, Z. Bern, L. J. Dixon and D. A. Kosower, Phys. Rev. Lett. **91**, 251602 (2003) [arXiv:hep-th/0309040].
- [91] S. Catani, Phys. Lett. B **427**, 161 (1998) [arXiv:hep-ph/9802439].
- [92] Z. Bern, L. J. Dixon and V. A. Smirnov, Phys. Rev. D **72**, 085001 (2005) [arXiv:hep-th/0505205].
- [93] L. F. Alday and J. M. Maldacena, JHEP **0706**, 064 (2007) [arXiv:0705.0303 [hep-th]].
- [94] D. J. Gross and P. F. Mende, Phys. Lett. B **197**, 129 (1987).
- [95] L. F. Alday and J. Maldacena, JHEP **0711**, 068 (2007) [arXiv:0710.1060 [hep-th]].
- [96] J. M. Maldacena, Phys. Rev. Lett. **80**, 4859 (1998) [arXiv:hep-th/9803002];  
S. J. Rey and J. T. Yee, Eur. Phys. J. C **22**, 379 (2001) [arXiv:hep-th/9803001].
- [97] L. F. Alday and R. Roiban, Phys. Rept. **468**, 153 (2008) [arXiv:0807.1889 [hep-th]].
- [98] L. F. Abbott, Nucl. Phys. B **185** (1981) 189; Acta Phys. Polon. B **13** (1982) 33.
- [99] L. F. Abbott, M. T. Grisaru and R. K. Schaefer, Nucl. Phys. B **229** (1983) 372.
- [100] M. T. Grisaru and D. Zanon, Nucl. Phys. B **252**, 578 (1985).
- [101] Z. Bern, L. J. Dixon, D. C. Dunbar and D. A. Kosower, Nucl. Phys. B **435**, 59 (1995) [arXiv:hep-ph/9409265].
- [102] J. M. Drummond, G. P. Korchemsky and E. Sokatchev, Nucl. Phys. B **795**, 385 (2008) [arXiv:0707.0243 [hep-th]].
- [103] A. Brandhuber, P. Heslop and G. Travaglini, Nucl. Phys. B **794**, 231 (2008) [arXiv:0707.1153 [hep-th]].
- [104] C. Anastasiou, A. Brandhuber, P. Heslop, V. V. Khoze, B. Spence and G. Travaglini, JHEP **0905**, 115 (2009) [arXiv:0902.2245 [hep-th]].
- [105] J. M. Drummond, J. Henn, G. P. Korchemsky and E. Sokatchev, Phys. Lett. B **662**, 456 (2008) [arXiv:0712.4138 [hep-th]].

- [106] Z. Bern, L. J. Dixon, D. A. Kosower, R. Roiban, M. Spradlin, C. Vergu and A. Volovich, Phys. Rev. D **78**, 045007 (2008) [arXiv:0803.1465 [hep-th]]; J. M. Drummond, J. Henn, G. P. Korchemsky and E. Sokatchev, Nucl. Phys. B **815**, 142 (2009) [arXiv:0803.1466 [hep-th]].
- [107] J. M. Drummond, J. Henn, G. P. Korchemsky and E. Sokatchev, Nucl. Phys. B **826**, 337 (2010) [arXiv:0712.1223 [hep-th]].
- [108] J. M. Drummond, J. Henn, V. A. Smirnov and E. Sokatchev, JHEP **0701**, 064 (2007) [arXiv:hep-th/0607160].
- [109] Z. Bern, M. Czakon, L. J. Dixon, D. A. Kosower and V. A. Smirnov, Phys. Rev. D **75**, 085010 (2007) [arXiv:hep-th/0610248].
- [110] Z. Bern, J. J. M. Carrasco, H. Johansson and D. A. Kosower, Phys. Rev. D **76**, 125020 (2007) [arXiv:0705.1864 [hep-th]].
- [111] J. M. Drummond, J. Henn, G. P. Korchemsky and E. Sokatchev, Nucl. Phys. B **828**, 317 (2010) [arXiv:0807.1095 [hep-th]].
- [112] N. Berkovits and J. Maldacena, JHEP **0809**, 062 (2008) [arXiv:0807.3196 [hep-th]]; N. Beisert, R. Ricci, A. A. Tseytlin and M. Wolf, Phys. Rev. D **78**, 126004 (2008) [arXiv:0807.3228 [hep-th]].
- [113] A. Brandhuber, P. Heslop and G. Travaglini, Phys. Rev. D **78**, 125005 (2008) [arXiv:0807.4097 [hep-th]].
- [114] J. M. Drummond, J. Henn, G. P. Korchemsky and E. Sokatchev, arXiv:0808.0491 [hep-th]; A. Brandhuber, P. Heslop and G. Travaglini, JHEP **0908**, 095 (2009) [arXiv:0905.4377 [hep-th]]; H. Elvang, D. Z. Freedman and M. Kiermaier, JHEP **1003**, 075 (2010) [arXiv:0905.4379 [hep-th]].
- [115] A. Brandhuber, P. Heslop and G. Travaglini, JHEP **0910**, 063 (2009) [arXiv:0906.3552 [hep-th]].
- [116] M. T. Grisaru, S. Penati, A. Romagnoni, JHEP **0602**, 043 (2006) [arxiv:hep-th/0510175].
- [117] R. E. Cutkosky, J. Math. Phys. **1**, 429 (1960).
- [118] Z. Bern, L. J. Dixon and D. A. Kosower, Annals Phys. **322**, 1587 (2007) [arXiv:0704.2798 [hep-ph]].

- [119] Z. Bern, L. J. Dixon, D. C. Dunbar, M. Perelstein and J. S. Rozowsky, Nucl. Phys. B **530**, 401 (1998) [arXiv:hep-th/9802162];  
Z. Bern, J. J. Carrasco, D. Forde, H. Ita and H. Johansson, Phys. Rev. D **77**, 025010 (2008) [arXiv:0707.1035 [hep-th]].
- [120] G. Passarino and M. J. G. Veltman, Nucl. Phys. B **160**, 151 (1979).
- [121] J. A. M. Vermaseren, arXiv:math-ph/0010025.
- [122] J. A. M. Vermaseren, Nucl. Phys. Proc. Suppl. **183**, 19 (2008) [arXiv:0806.4080 [hep-ph]].
- [123] A. V. Smirnov, JHEP **0810**, 107 (2008) [arxiv:0807.3243 [hep-ph]].
- [124] A. V. Smirnov and M. N. Tentyukov, Comput. Phys. Commun. **180**, 735 (2009) [arxiv:0807.4129 [hep-ph]];  
A. V. Smirnov, V. A. Smirnov and M. N. Tentyukov, arxiv:0912.0158 [hep-ph].
- [125] S. Penati, M. Pirrone and C. Ratti, JHEP **0804**, 037 (2008) [arXiv:0710.4292 [hep-th]].
- [126] S. Penati, M. Pirrone and C. Ratti, Fortsch. Phys. **56**, 876 (2008).